Steel Design Guide 20

Steel Plate Shear Walls

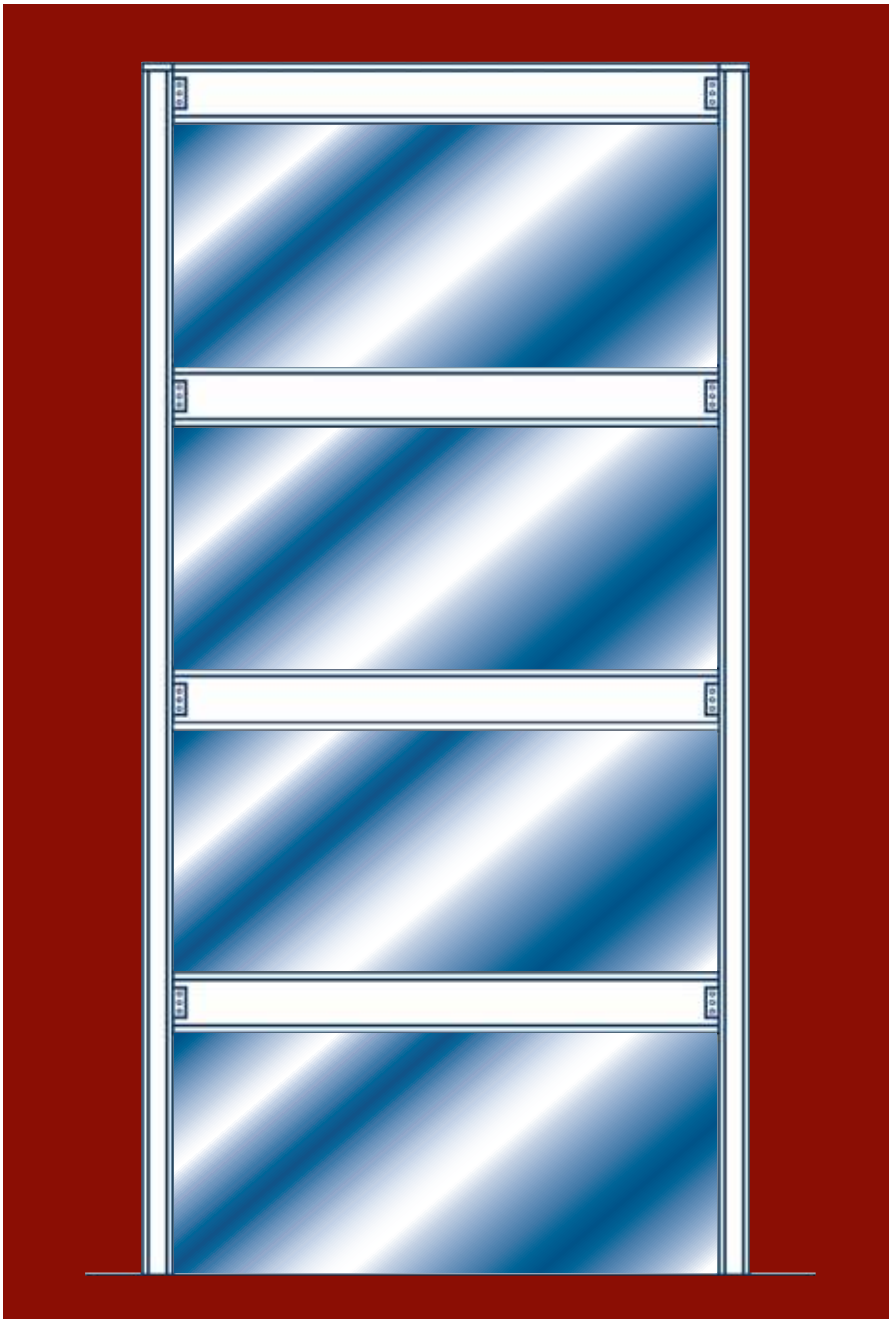

Steel Plate Shear Walls

RAFAEL SABELLI, S.E.
DASSE Design
San Franciso, CA
and

MICHEL BRUNEAU, Ph.D.
Multidisciplinary Center for
Earthquake Engineering Research
University of Buffalo, Buffalo, NY

AMERICAN INSTITUTE OF STEEL CONSTRUCTION, INC.

The information presented in this publication has been prepared in accordance with recognized engineering principles and is for general information only. While it is believed to be accurate, this information should not be used or relied upon for any specific application without competent professional examination and verification of its accuracy, suitability, and applicability by a licensed professional engineer, designer, or architect. The publication of the material contained herein is not intended as a representation or warranty on the part of the American Institute of Steel Construction or of any other person named herein, that this information is suitable for any general or particular use or of freedom from infringement of any patent or patents. Anyone making use of this information assumes all liability arising from such use.

Caution must be exercised when relying upon other specifications and codes developed by other bodies and incorporated by reference herein since such material may be modified or amended from time to time subsequent to the printing of this edition. The Institute bears no responsibility for such material other than to refer to it and incorporate it by reference at the time of the initial publication of this edition.

Printed in the United States of America

First Printing: May 2007

Authors

Rafael Sabelli, S.E., is the Director of Technical Development of DASSE Design in San Francisco. He is a member of the AISC Task Committee on the Seismic Provisions for Structural Steel Buildings and is the former Chair of the Seismology Committee of the Structural Engineers Association of California. He was the 2000 NEHRP Professional Fellow in Earthquake Hazard Reduction. He is the author of numerous publications on concentrically braced frames, including analytical studies and design guides on buckling-restrained braced frames.

Michel Bruneau, Ph.D., is Director of the Multidisciplinary Center for Earthquake Engineering Research (MCEER) headquartered at the University of Buffalo. Bruneau also is a professor of civil, structural, and environmental engineering within the University of Buffalo's School of Engineering and Applied Sciences. He is the author of numerous research articles on steel plate shear walls and other topics in seismic engineering and is coauthor of "Ductile Design of Steel Structures." He has participated in several reconnaissance visits to assess structural damage caused by earthquakes and other disasters around the world.

Acknowledgements

The authors express their gratitude to several people who made significant contributions to this Design Guide.

Warren Pottebaum helped develop the capacity-design relationships used in the design examples and tested them using various analytical methodologies. Lisa Cassedy helped develop the methodology for low-seismic applications, as well as for openings in shear walls. Both are engineers at DASSE Design Inc.

The contributions of Darren Vian, Jeff Berman, and Diego López-García in the study of the system have proved valuable in the writing of this document. Additionally, Jeff Berman's development of the preferred design method for Vertical Boundary Elements in time for its inclusion in Chapter 3 is appreciated. Assistance with translation was provided by Ramiro Vargas and Shuichi Fujikura, both doctoral students at the University at Buffalo. Their help is greatly appreciated.

Numerous researchers and design engineers have contributed photographs and descriptions of tests and buildings with steel plate shear walls. These contributions provide a valuable context for the design methods described in this guide. In particular, John Hooper was very generous in providing insight from his experiences with the system, including both analytical methodologies and insight from construction of buildings with steel plate shear walls.

The authors also thank AISC for the opportunity to work on this project and for mobilizing its volunteers to provide a thorough and insightful review. In particular, the thorough review by Charles Carter and Christopher Hewitt was indispensable in improving the quality and clarity of the design examples, and in improving the consistency of the design method developed by the authors. Reviewers included:

Abolhassan Astaneh-Asl
Charles J. Carter
D. Brad Davis
Jason Ericksen
Christopher Hewitt
William D. Liddy
Walterio López
James O. Malley
Brett Manning
Davis G. Parsons II
John Rolfes
Ignasius Seilie

Table of Contents

Chapter 1

History of Steel Plate Shear Walls

1.1. INTRODUCTION

Steel plate shear walls (SPW) have been used in a significant number of buildings, beginning decades ago, before the existence of design requirements specifically addressing this structural system. Implementation has accelerated significantly since the recent publication of various design standards, specifications, and other guidelines providing design requirements in both high-seismic applications and wind and low-seismic applications (as will be reviewed in subsequent chapters).

1.1.1. Overview

This introduction provides a general description of steel plate shear walls (SPW) and the Special Plate Shear Wall (SPSW) system. This introduction also describes the format and organization of the Design Guide.

This Design Guide has been developed using:

- ASCE 7-05 *Minimum Design Loads for Buildings and Other Structures*, including Supplement No. 1
- AISC 360-05 *Specification for Structural Steel Buildings*
- AISC 341-05 *Seismic Provisions for Structural Steel Buildings*, including Supplement No. 1

Analytical and capacity-design methods presented in this Design Guide typically establish the seismic load effect on a member or connection; this load effect can be utilized in either LRFD or ASD load combinations. The design examples in this Design Guide illustrate the LRFD method.

The Design Guide addresses design for both high-seismic applications and wind and low-seismic applications. Certain provisions of AISC 341 are used regardless of the Seismic Design Category.

Throughout this Design Guide, standards are referred to by their number (e.g., ASCE 7, AISC 360, AISC 341, etc.). The document titles are listed in the bibliography.

1.1.2. Wall Types

Steel plate shear walls in building construction are of various types. By far the most popular in the United States is the unstiffened, slender-web steel plate shear wall. This type is the basis for the SPSW system, which is included as a "Basic Seismic Force Resisting System" in ASCE 7 and AISC 341. This type of web plate has negligible compression strength and thus, shear buckling occurs at low levels of loading. Lateral loads are resisted through diagonal tension in the web plate[1] (akin to tension-field action in a plate girder), rather than in shear. Boundary elements are designed to permit the web plates to develop significant diagonal tension; for high-seismic design, they are designed to permit the web plates to reach their expected yield stress across the entire panel.

Stiffened web plates may also be used. Stiffening increases the shear-buckling strength of the web plate. Sufficient stiffening to permit the web plate to develop its shear yield strength may be added, or the stiffening may be partial. For partially stiffened web plates, the strength is a combination of the shear buckling strength and the additional strength gained from tension-field action. This available strength is calculated using methods developed for plate girders, as discussed in Chapter 3.

Composite steel plate shear walls have also been used in building design. In this system, steel web plates are stiffened by adding concrete on one or both sides of the web plate. Sufficient stiffening is typically provided to permit shear yielding of the web plate. Chapter 3 contains a treatment of composite steel plate shear walls, including the requirements of AISC 341.

Stiffening of the web plate has a moderate effect on the strength and stiffness of the wall. Additionally, it tends to reduce the flexural strength and stiffness required of the boundary elements. Stiffening of the web plates also results in hysteretic behavior that is significantly less pinched. However, it also substantially increases the cost of the construction and increases the thickness of the wall. It is generally preferred to achieve the required strength and stiffness by utilizing an unstiffened, slender web plate, rather than a stiffened web plate. Very high strength and stiffness can be provided by unstiffened steel web plates of moderate thickness. In high-seismic design, the hysteretic behavior can be improved with the use of rigid beam-to-column connections in the frame of the shear wall.

Steel plate shear walls with unstiffened, slender web plates are the focus of this Design Guide. Chapter 3 contains a design method for this type of steel plate shear wall.

[1]The term *web plate* is used to refer to the steel plate that resists the horizontal shear in the wall. A web plate connects to columns, called Vertical Boundary Elements (VBE), on either side, and beams, called Horizontal Boundary Elements (HBE), above and below.

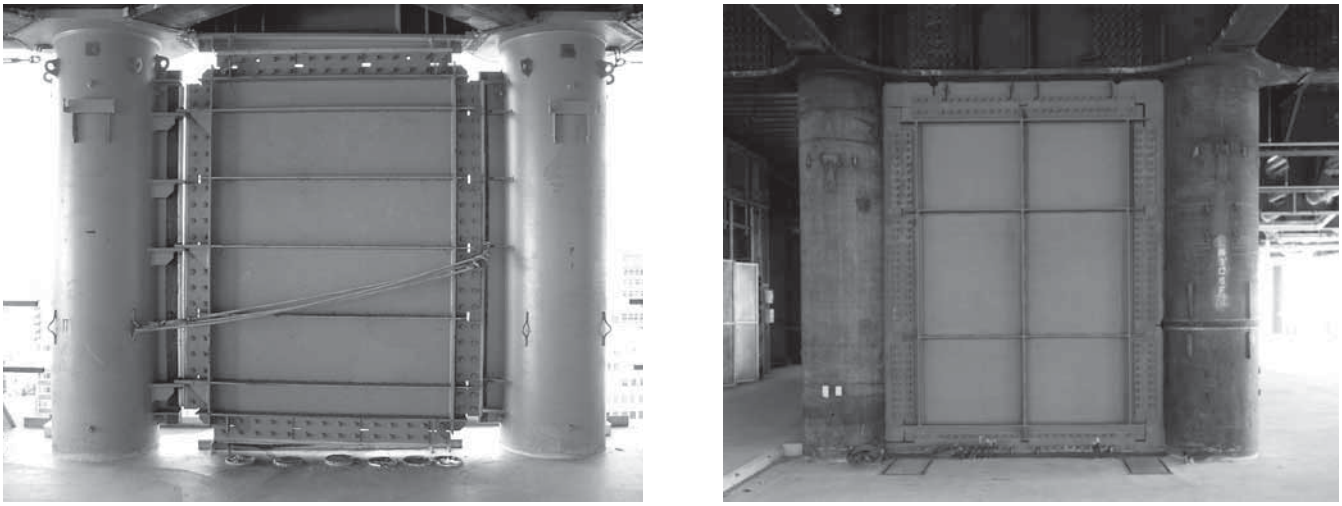

(a) (b)

Fig. 1–1. SPW panel in Japan: (a) wall with horizontal panel stiffeners (courtesy of Takanaka); (b) wall with horizontal and vertical stiffeners (courtesy of Nippon Steel).

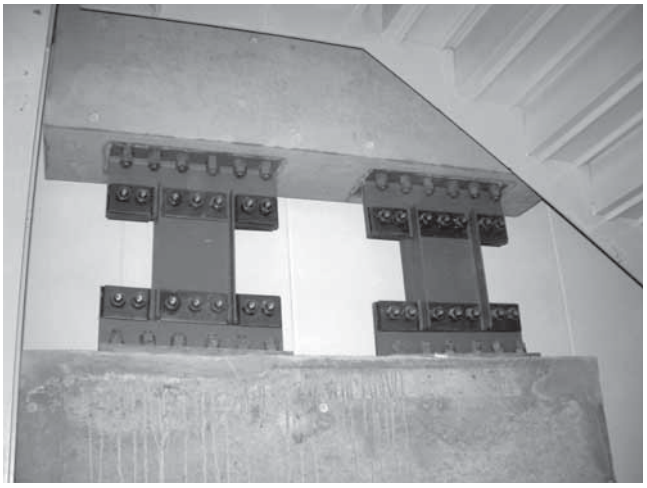

Fig. 1–2. Small shear yielding elements in Japan (courtesy of Shimizu).

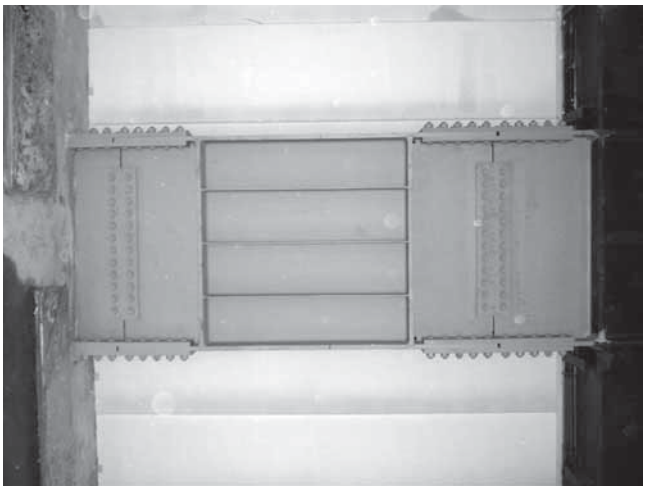

Fig. 1–3. Shear link connected between closely spaced columns (courtesy of Nippon Steel).

Chapter 4 uses this system in a design example for wind and low-seismic application, and Chapter 5 uses this system in a design example for high-seismic application. Chapter 6 addresses the design of openings in steel plate shear walls with unstiffened, slender web plates.

1.1.3. Applications

Steel plate shear walls have been used in a large number of buildings, including in the United States, Canada, Mexico, and Japan. Building types have ranged from single-family residential to high-rise construction. In addition to new construction, steel web plates have been added to retrofit existing frame buildings requiring additional strength and stiffness.

SPSW may be used wherever the building function permits walls of moderate length. Mid-rise and high-rise construction, with their repetitive floor plans and continuous building core, are especially well suited for SPSW.

Chapter 1 contains an extensive list of buildings utilizing steel plate shear walls.

1.1.4. Advantages

Steel plate shear walls, and SPSW in particular, offer significant advantages over many other systems in terms of cost, performance, and ease of design.

Compared to concrete shear walls, the reduced thickness (and thus plan area devoted to them) represents a substantial benefit. The reduced mass can also be significant in the design of the foundation. Most importantly, however, steel plate shear walls can be erected in significantly less time than concrete shear wall structures.

SPSW may be considered as an alternative to braced frames. They can provide equivalent strength and stiffness and require the same or less plan area.

The speed of construction of SPSW is comparable to that of braced frames as well. While there is typically a significant amount of field welding, most if not all web-plate field welding can be selected as single-pass fillet welds, and thus erection typically proceeds at a rapid pace.

The strength and stiffness of the system ensure good performance under moderate lateral loads. The ductility of steel web plates in SPSW results in good performance under severe seismic loading.

Because SPSW can provide significant strength and stiffness, shorter bays can be used. This results in greater flexibility for use of the space.

SPSW are relatively easy to design—the capacity-design calculations for the design examples in Chapters 4 and 5 were performed on a simple spreadsheet. As is discussed in Chapter 3, SPSW can be modeled with either membrane elements or truss elements using many of the structural engineering programs typically employed by design offices.

1.1.5. Limitations

SPSW may be used for structures ranging from one or two-story residential structures to the tallest high rise.[2] However, while the system is viable for both small and large structures, aspects of the design vary with building size.

Compliance with some requirements of AISC 341 for seismic design may prove to be more difficult or at least more tedious than typical detailing practice for smaller structures. The provisions that require the beams and columns of SPSW to form a moment frame (and comply with certain requirements for Special Moment Frames) may be especially onerous in structures that combine SPSW with light-frame construction.

For taller structures, drift control is much more difficult. While providing a steel plate with sufficient strength does not pose a problem, building drift may require longer bays of SPSW to reduce forces in columns. However, because SPSW bays with long horizontal proportions have not been studied, their use is restricted. Building drift control may require that SPSW be supplemented in some way, such as by coupling two SPSW to reduce the axial forces in columns, or by providing outrigger beams to deliver some of the overturning force to adjacent columns.

1.1.6. Design Guide Structure

This Design Guide is divided into seven chapters. Chapter 1 includes an extensive survey of buildings that employ the system. New construction and retrofits in Japan, Canada, Mexico, and the United States are presented, showing the extensive use of the system and a wide range of applications.

Chapter 2 includes a survey of the research (both analytical and experimental) into the system behavior. Chapter 2 also provides a brief treatment and comparison of the design provisions that have been developed for this system in Canada and the United States.

Chapter 3 includes a treatment of the mechanics of unstiffened, slender-web-plate shear walls. It also provides a discussion of stiffened and composite steel plate shear walls. Chapter 3 discusses methods of analysis, and both general requirements and seismic design methods are presented. For seismic design, the requirements of AISC 341 are illustrated, and equations for determining the required strength of elements are developed.

[2]ASCE 7 limits SPSW to 160 ft in Seismic Design Categories D, E, and F, unless a dual system is used.

Fig. 1–4. Intermediate column approach used in Japan (courtesy of Takanaka).

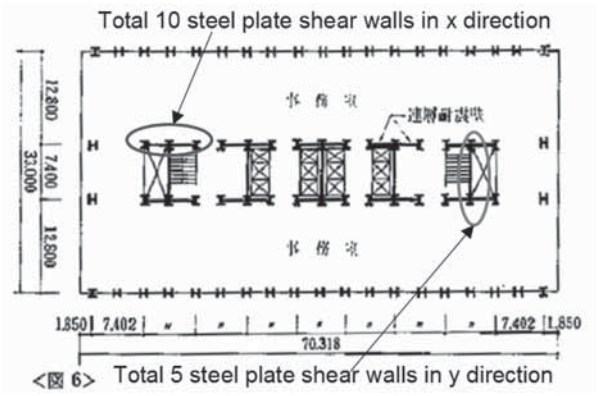

Fig. 1–6. Plan layout of SPW for Nippon Steel Building (Yokoyama et al., 1978).

Fig. 1–5. Shinjuku Nomura Building (top) and Nippon Steel Building (bottom).

Fig. 1–7. Kobe City Hall (photo by M. Bruneau).

Chapter 4 includes a design example of a building in an area of low seismicity (i.e., when R can be taken equal to 3). A nine-story building is designed utilizing the SPSW system designed for normal ductility (without the application of the ductile detailing requirements of AISC 341).

Chapter 5 includes a design example of a building in an area of high seismicity (i.e., when R is taken greater than 3). The same nine-story building as was designed in Chapter 4 is redesigned for high ductility in full conformance with AISC 341.

Chapter 6 addresses the design of openings in SPSW. Equations are developed for sizing the web plates around the opening and for computing the required strength of local boundary elements. A design example is included to illustrate the procedure.

Chapter 7 includes discussion of various other topics related to the design of SPSW, such as available and appropriate steel materials, serviceability considerations, configuration issues, types of construction, and fire protection.

Appendix A includes a list of symbols defined in the Design Guide. Other symbols used in the Design Guide are defined in AISC 341, AISC 360, or ASCE 7. Appendix A also contains a glossary of the terms that are used in the text, such as horizontal boundary element, local boundary element, and vertical boundary element.

An extensive bibliography is included. This bibliography includes all references made in the Design Guide, as well as other publications concerning the system. Additionally, several papers on shear buckling of plates and the design of plate girders are listed.

1.2. USAGE IN JAPAN

Japanese design practice requires that the design of any building over 60 m (200 ft) in height, or any building implementing special devices irrespective of height, be the object of a peer review. Traditionally, the Building Center of Japan has overseen the peer-review process, and steel plate shear wall buildings are referred to its Special Steel Structures committee. As a result, a variety of approaches have been taken to design these systems. However, one common denominator is that peer-review committees typically require that some level of non linear dynamic time-history analysis be conducted to verify the design of these systems, although the complexity of these analyses can vary from project to project.

In most cases, one of three different types of steel plate shear wall approaches have been used in Japan. The first implementations consisted of walls with steel plates filling the entire bay width between columns and between girders, much like the North American practice. These walls were always stiffened (sometimes heavily) as buckling is not permitted for members providing lateral load resistance in Japan (Figure 1–1). More recently, and partly as a result of the requirement that plates be able to achieve their full plastic shear strength, many other types of structural configurations have emerged in which shear yielding elements are introduced, without being SPW in the sense considered in North America. In one such configuration, braces designed to remain elastic are connected to a specially detailed shear plate, which is itself connected to beams at mid-span, as shown in Figure 1–2, or connected between closely spaced columns, as shown in Figure 1–3. A more popular configuration recently has been the intermediate column design, in which a similar special ductile steel plate is inserted at mid-span of a column; the top and bottom parts of the column serve the same role as the braces or concrete walls used to support the shear plates in the previous concept, but being vertical elements, they are more accommodating for architectural purposes (Figure 1–4). These two more recent configurations have somewhat eclipsed the conventional SPW in popularity (Nakashima, 2005). In all cases, the shear yielding plate systems are treated as hysteretic dampers during the design process and are not designed to resist gravity loads.

Examples of early SPW buildings in Japan include the Nippon Steel Building and the Shinjuku Nomura Building, both in Tokyo and built in the 1970s (Figure 1–5). Plan layout of the SPW in the Nippon Steel Building is shown in Figure 1–6 (Yokoyama et al., 1978). The SPW were used at and above the fourth story, while SPW embedded in concrete were used for the lower stories. Wall panels were typically 9 ft × 12.2 ft, stiffened horizontally and vertically, and either 3⁄16 in., 1⁄4 in., 11⁄32 in., or 15⁄32 in. (4.5 mm, 6.0 mm, 9.0 mm, or 12.0 mm) thick. The Shinjuku Nomura Building, Tokyo's third tallest building at the time at 693 ft and 51 stories, is an example of early SPW construction in Japan (ENR 1978). Steel panels 10 ft high by 16.5 ft long were reinforced with vertical stiffeners on one side and horizontal stiffeners on the other, and each panel was reportedly connected to its surrounding steel frame with 200 to 500 bolts. The precision required for such bolting operations proved challenging, and the project manager for the contractor (Kumagai-Gumi) expressed a strong determination to weld the plates in future such projects, as apparently was done in another Tokyo high-rise at the time. A total of eight T-shaped steel walls were located around elevator cores and service shafts. Other Japanese buildings at the time were designed with patented precast concrete seismic wall cores. The motivation to use a steel plate wall stemmed from the desire to use an innovative and nonpatented construction system.

The 35-story Kobe City Hall Tower (Figure 1–7) has stiffened SPW from the third floor and above (reinforced concrete walls were used in the basement levels, and composite walls over two stories were used as a transition between the steel and reinforced concrete walls, as shown in Figure 1–8). The structure was subjected to the 1995 Kobe earthquake. Fujitani et al. (1996) reported minor local buckling of the

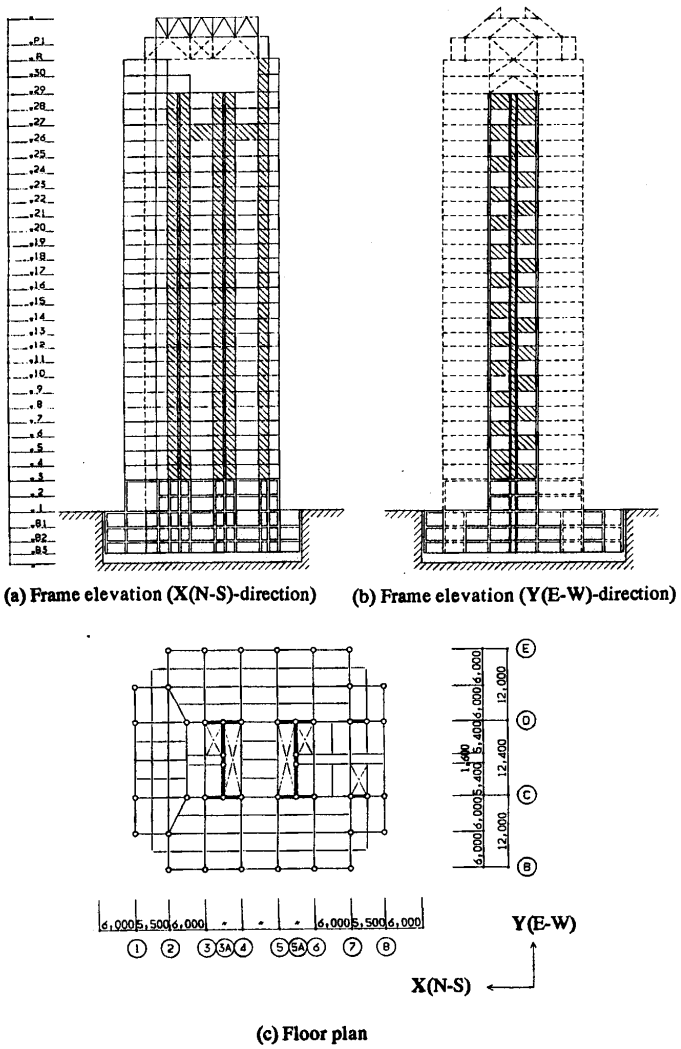

Fig. 1–8. Plan and elevation of Kobe City Hall Building (Fujitana et al., 1996).

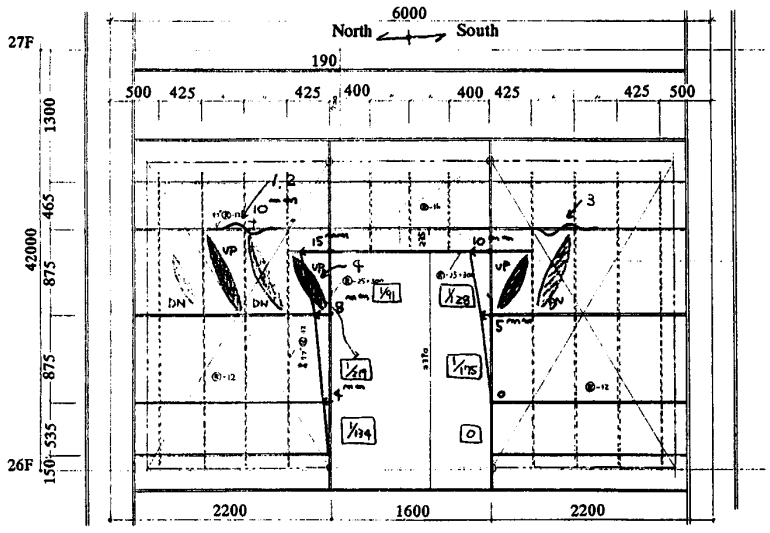

Fig. 1–9. Sketch of plate buckling at 26th story of Kobe City Hall Building (Fujitana et al., 1996).

stiffened steel plate shear walls on the 26th story (Figure 1–9) and residual building drifts (roof offsets of 8.9 in. [225 mm] and 1.4 in. [35 mm] from the vertical in the north and west directions, respectively).

Note that an upper story of the lower-rise building of the Kobe City Hall complex (seen in the foreground of Figure 1–7) collapsed in a soft-story mechanism—more specifically, this failure occurred at the level where a moment-resisting frame system having steel sections embedded in reinforced concrete transitioned into a regular moment-resisting reinforced concrete frame (Nakashima et al., 1995); however, this building had a significantly lower period than the adjacent tower, which attracted greater seismic forces, precluding comparison of the seismic performance between the two structures.

Following the development of special Low-Yield Steel (LYS) by Nippon Steel, some SPW projects have included LYS plates to dissipate energy (Yamaguchi et al., 1998). These special steels start to yield at relatively low steel strength, namely, between 80 and 120 MPa (12 and 18 ksi) for LYS100 (calculated by the 2 percent offset method) and between 215 and 235 MPa (31 and 34 ksi) for LYS 235; strain harden significantly up to 200 to 300 MPa (29 to 44 ksi) and 300 to 400 MPa (44 to 58 ksi), respectively; and exhibit more than 40 percent elongation before fracture. Their large ductility is advantageous for seismic design. Furthermore, because of their lower strength, thicker plates are required to resist a given lateral load than with conventional steel, resulting in fewer stiffeners required to prevent buckling. The Saitama Wide-Area Joint Agency Buildings, 31 and 26 stories, provide an example of implementation of a stiffened SPW with LYS 100 (Figure 1–10). Plates vary from 1 in. to ¼ in. (25 mm to 6 mm) thick along the height of the building, with panels of up to 15 ft × 10 ft (4.5 m × 3 m) in size. The walls are positioned around the stairwells in somewhat of a checkerboard pattern to minimize the effect of bending in the walls. Note that LYS steels are not yet produced in North America.

In reviewing the Japanese experience with SPW, it is important to recognize that the traditional structural engineering practice in Japan has been to make all the beam-to-column connections in the building fully restrained moment connections, even when braces or walls are introduced in parts of the structural systems. In that context, SPW are treated as hysteretic dampers with the primary function to reduce maximum building response during an earthquake. The presence of SPW and complete moment resisting frames nonetheless provides significant redundancy compared with North American practice.

1.3. USAGE IN THE UNITED STATES

Originally, in the absence of codified design provisions for SPW, engineers relied on engineering principles to size and detail these walls. The following examples illustrate a sample of approaches adopted to satisfy different project constraints.

For a new 16-story building that expanded the existing H.C. Moffitt Hospital at the University of California San Francisco Medical Center (Dean et al., 1977; Wosser and Poland, 2003), various types of structural systems were considered. Shear walls were determined to be the best structural system to accommodate the constraints of high design seismic forces and high stiffness (assumed adequate at the time to protect essential hospital systems from damage so they could stay in service after a severe earthquake), and limited available story height to match the floor levels of the adjacent existing building and thus accommodate the many ducts, pipes, and other mechanical and electrical items in the ceiling space. Wosser and Poland (2003) report that reinforced concrete shear walls more than 4 ft thick would have been required to resist the substantial specified design forces, which was deemed architecturally unacceptable, and steel plate walls were used instead. Static analyses as well as response-spectrum modal analysis were conducted for the structural system. Finite-element analysis was used to model the shear walls having irregular shapes and openings. Wosser and Poland report:

As a result of the stringent design criteria, the configuration of the structure, and the chosen structural solution, a number of unusual structural details were required and developed. Among these were special foundation details to handle high overturning forces and offset shear wall footings, the creation and presentation of an entire detailing system for the steel plated shear walls, and special diaphragm details to handle the high shear transfers inherent in the structural configuration. The wall plates of the steel-plated shear walls were sized to take the total shear forces in the wall. The concrete cover provided stiffness to the structure and was reinforced to the extent that it would be compatible with the steel in terms of strain. The concrete was also used to stiffen the steel plate. Number 3 ties at 2 feet on center each way were used to tie together the concrete walls at each side of the plate. Each steel plated wall is composed of several elements including columns, girders, wall plates, and trim members as shown on the diagrammatic elevation (Figure 1–11). The columns are either heavy standard 14 WF sections or special built-up H columns. Plate girders are generally 49 inches deep, with either 9- or 14-inch flanges. Wall plates are structural steel plates extending vertically between plate girders and horizontally between columns, trim member, etc. (Figure 1–12).

Typical wall details are shown in Figures 1–11 and 1–12. Design of this project was completed in 1977 and construction spanned over 5 years.

SPW designed in the 1970s were stiffened to prevent

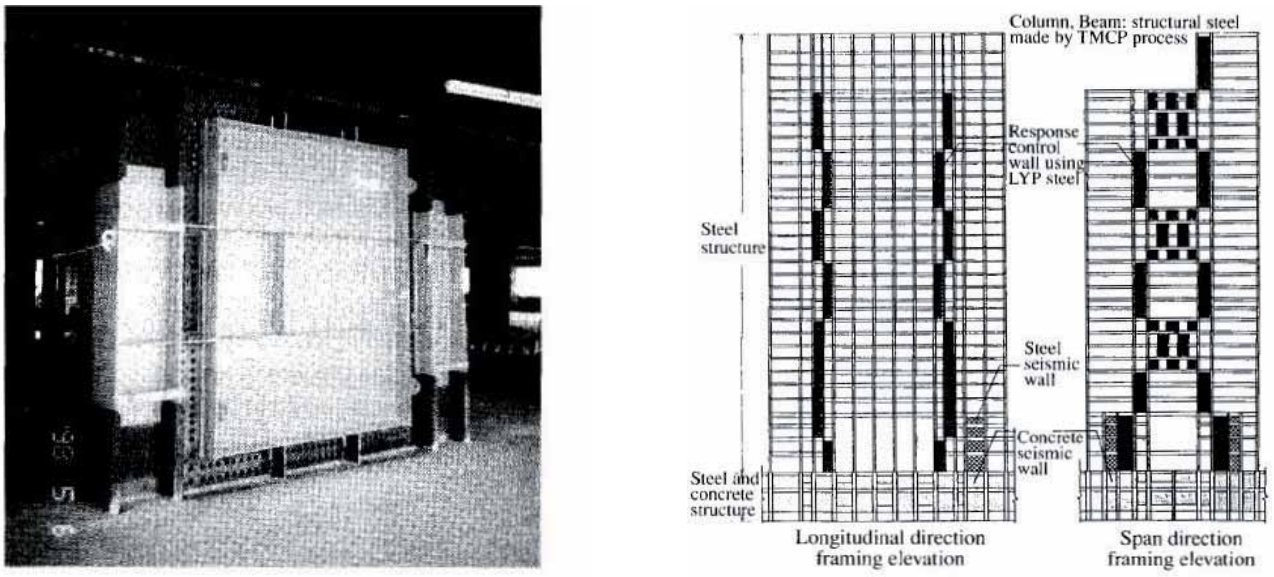

Fig. 1–10. Concept for building with SPW of LYS (Yamaguchi et al., 1998).

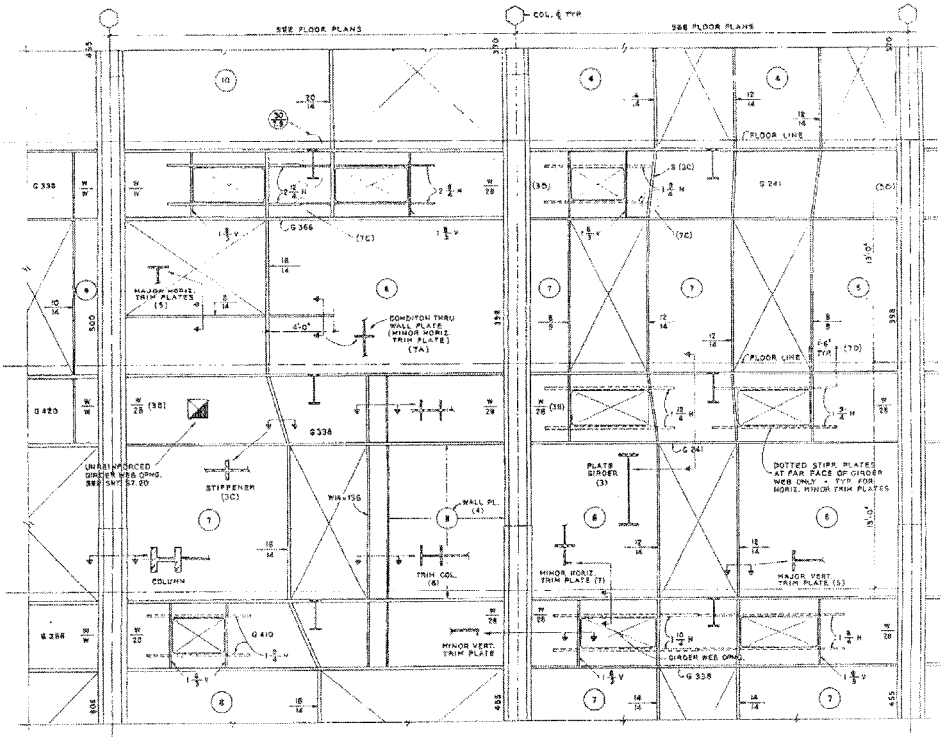

Fig. 1–11. H. C. Moffitt Hospital Addition, typical steel shear wall detail (Wosser and Poland, 2003).

buckling of the wall plate. For example, SPW were used for the wind-controlled design of the Hyatt Regency Hotel in Dallas (*ENR*, 1977; 1978a), shown in Figure 1–13. In the narrow direction of the tower, steel plate walls were used because bracing would have encroached on interior space, and concrete shear walls would have slowed down the pace of construction. Steel plates 10 ft × 25.5 ft, 1 in. thick, were used throughout. It is reported that the gravity support provided by the 1-in.-thick plates was taken into account to reduce the column and beam sizes, providing savings in construction cost.

SPW were also used for the Olive View Medical Center at Sylmar in California's San Fernando Valley (*Architectural Record*, 1978; *ENR*, 1978b). This facility was constructed to replace the reinforced concrete hospital built in 1964 at that same location that had to be demolished due to the extensive damage it suffered during the 1971 San Fernando earthquake. A combination of perimeter and interior shear walls was used, with reinforced concrete walls in the lower two stories and SPW in the upper four stories. Wall plates varied in thickness from ⅝ in. to ¾ in., with various window openings, and were erected in 15.5 ft × 25 ft modules (Figure 1–14) with bolted splices. The wall design was considered less costly than moment resisting frames, and steel walls were used in the upper stories as a measure to reduce the weight of the structure.

It is worth noting that this hospital was severely shaken by the 1994 Northridge earthquake. Accelerometers at the site recorded peak ground accelerations of 0.91g, and instruments at the roof recorded peak values of 2.31g (Celebi, 1997).[3]

No structural damage was reported, but substantial water damage occurred. A number of unbraced sprinkler branch lines broke or leaked at threaded joints, sprinkler heads were broken off when struck by suspended ceiling systems, various pipes broke at their connection to equipments, and valves to chilled water lines fractured at the penthouse level. Upper stories were contaminated with water flowing down and forcing evacuation (OSHPD, 1995). Extensive nonstructural damage such as failure of suspended ceiling systems, storage racks, book racks, and ductwork was also reported (Naeim and Lobo, 1997), as shown in Figure 1–15. This highlighted the importance of proper design and detailing for nonstructural systems, which is true for all structural systems.

Stiffened SPW were also used for the seismic retrofit of the Veterans Administration Medical Center in Charleston, South Carolina (Baldelli, 1983). The decision to use steel walls instead of concrete walls was based on the need to minimize disruption of service in the hospital (which remained in operation during the retrofit) and to allow for future expansion. The steel walls were deemed more expensive than their concrete counterparts, but uninterrupted use of the medical facility provided savings exceeding the cost difference. The walls consisted of 5⁄16-in.-thick plates connected to a ⅜ in. × 7½ in. perimeter plate, itself connected to the existing concrete floors using drilled-in epoxy anchors spaced 6 in. to 18 in. (Figure 1–16). Plate and channel stiffeners were designed to prevent the subpanels from buckling by limiting compression and shear stresses to one-fourth of the buckling stresses. It was recognized that a thinner plate and smaller stiffeners would have been theoretically possible by considering the strength provided by diagonal tension-field action within each subpanel, but no actual such reductions would have been possible since the wall stiffness requirements were found to govern in this particular case.

SPW have been used in the seismic retrofits of other types of facilities. For example, the 1937 Oregon State Library, a reinforced concrete frame structure, was reinforced with SPW to allow the structure to remain open during renovation and to preserve existing historical finishes (Robinson and Ames, 2000). Steel walls were also advantageous in this case because the moisture and humidity generated during concrete placement would have required relocating the historical book collection to protect it against possible damage. Steel plates were also designed in small panels that could be installed by hand to avoid using heavy machinery (Figures 1–17 and 1-18). Bolted splices using structural WT-shapes were used as much as possible, to minimize the risk of fire from welding in the library. Finite-element analysis and site-specific response spectrum analysis were used to determine building response. The existing structure was assumed to provide no resistance to lateral loads, and stiffness requirements often controlled design as many of the existing structural elements were assessed to be sensitive to excessive deflections. Steel members with drilled-in expansion-type or adhesive-type anchors were used to deliver the seismic loads to the new walls (Figure 1–19). The footings also required retrofitting to resist the overturning forces from the new SPW.

Implementation of unstiffened SPW in the United States is more recent and is indirectly influenced by the recognition of SPW systems in the *National Building Code of Canada* (NBCC) and *Canadian Steel Design Standard CAN/CSA S16.1* since 1994. Similar provisions were included in FEMA 450 (*NEHRP Recommended Provisions for Seismic Regulations for New Buildings and Other Structures*) in 2004 and AISC 341 in 2005.

[3]More information is available at the USGS web site: **http://pubs.usgs.gov/fs/2003/fs068-03/perf.html** (USGS fact sheet 068-03).

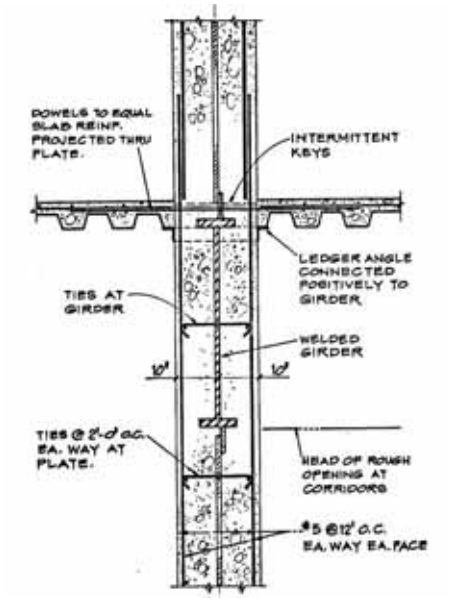

Fig. 1–12. H.C. Moffit Hospital Addition, typical steel shear wall, and example cross-section (Dean et al., 1977; Wosser and Poland, 2003).

(a)

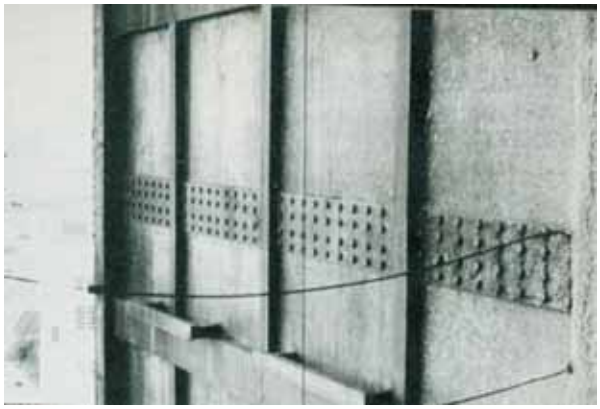

(b)

(c)

*Fig. 1–13. Hyatt Regency Dallas: (a) completed building (from http://dallasregency.hyatt.com); (b) stiffened steel plate wall detail (*Architectural Record, *1978); (c) during construction (*Architectural Record, *1978).*

A significant project for a 46-story high-rise in San Francisco (The Century) proposed to use a core wall system having unstiffened SPW and large composite (concrete-filled) steel pipe columns as boundary elements. The composite columns contribute substantially to the flexural stiffness and resistance to overturning in the system (Figure 1–20b). Although that project was eventually cancelled (after its design was completed and building permits obtained), the same concept was reused in the narrow North-South direction of the core for the U.S. Federal Courthouse, a 23-story building in Seattle (Figures 1–20a, 1–21, and 1–22); braced frames were used in the East-West direction. Selection of SPW for these projects was based on four advantages associated with this system. First, the SPW system required walls thinner than those needed for an equivalent concrete shear wall (18 in., including the furring for the SPSW, versus 28 in. for the concrete shear wall), resulting in savings of approximately 2 percent in gross square footage. Second, the system was lighter than concrete shear walls (approximately 18 percent less than using an equivalent concrete shear wall core system), with a corresponding reduction in foundation loads due to gravity and overall building seismic loads. The third advantage was the reduced construction time as the wall was fast to erect, did not require a curing period, and was (according to the steel erector for that project) easier to assemble than equivalent special concentrically braced frames. The fourth advantage of this system was its excellent post-buckling strength and ductility (experiments conducted to validate the system used for this particular project are described in Chapter 2).

SPW have been used to strengthen buildings having moment resisting frames that were damaged by the 1994 Northridge earthquake. The two-story plus basement structure shown in Figure 1–23, located in the San Fernando Valley near the epicenter, experienced damage to nearly one-half of its moment frame connections in the North-South direction of the building. The lateral system for the building consisted of two moment resisting frames in each direction of the building. Each frame consisted of three bays (four columns interconnected by three girders).

Due to the essential facility occupancy, the performance criterion for strengthening this building was to meet immediate occupancy requirements for the 475-year event at that site, which was deemed possible using a SPW system to limit horizontal drift and therefore, rotational demand, on the existing moment connections. Steel plates ¼ in. thick (made with material with F_y from 36 to 40 ksi) were added to each of the two moment frame lines in each direction, welded to a 1 in. continuous fish plate without special corner reinforcement. The walls were spliced with groove welds.

The existing steel moment frame columns and girders were used to provide the vertical and horizontal boundary elements of the SPW panels. The design was validated by both nonlinear static pushover methods using the FEMA 356 (FEMA, 2000b) target displacement method to estimate rooftop displacements. The nonlinear pushover model consisted of unidirectional equivalent diagonal "strips" to model the tensile field behavior of shear panel and the force transfers in the boundary elements (Figure 1–23). This analysis was further validated by nonlinear time-history analysis using tension-only diagonal strips in both directions to model the tensile field behavior in both directions during the time-history responses. The strips possessed tensile stiffness and strength with no compression strength or stiffness (see Chapters 2 and 3 for a detailed discussion of this method of analysis).

The SPW system provided significant stiffness to the original moment frame and did not take up as much space as a comparable concrete shear wall or steel braced frame. The concept also allowed the building to remain occupied during construction.

SPW have recently found applications in low-rise residential buildings that have sizeable open floor plans and are required to be built with an engineered framing system (Eatherton, 2005). These were designed using SPW as this system was deemed less expensive than the moment frame alternative and faster to construct by having the SPW shop fabricated. Walls were designed in accordance with the Canadian SPW requirements (CAN/CSA S16-01 contained the only codified SPW seismic design requirements available at the time). As such, a pushover analysis was performed with the plate in each panel modeled as 10 tension strips. Boundary members were designed to remain elastic up to the expected yield strength of the plate.

For a 17,000-ft^2 residence in Atherton, California (Figure 1–24), the SPW columns are 2.5 ft center-to-center, and the web plate is 14 gage, ASTM A1011 material specified with yield strength of 33 ksi. Coupon tests were conducted on the plate material to verify actual yield strength and elongation.

SPW were also used for a 9,000-ft^2 residence in San Mateo County (Eatherton and Johnson, 2004) to meet the owner-specified requirement that no significant structural damage be suffered in a probable earthquake (Figure 1–25). For the given open floor plan with few solid lengths of walls, moment frames would have required thicker walls to accommodate large columns. The SPW lateral system was designed to remain elastic and capable of resisting several times the code-specified level of base shear. Typical wall length is 4.5 ft center-to-center of columns, sometimes with wall panels side-by-side where it was possible. Plate was typically 12 gage, with the same material specifications and coupon tests as the residence in Atherton.

Figure 1–26 shows a 23,000-ft^2 two-story structure in Los Altos, California, with significantly open floor plan, where SPW were deemed to be a superior and more economical alternative over moment frames.

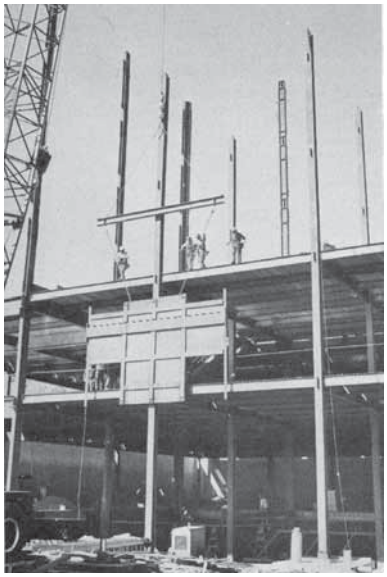

(a)

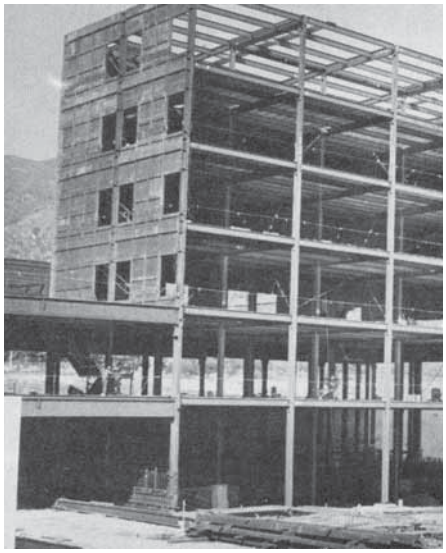

(b)

*Fig. 1–14. Olive View Hospital steel plate assembly (*ENR, *1978).*

Fig. 1–15. Nonstructural damage in Olive View Hospital due to 1994 Northridge earthquake (Naeim and Lobo, 1997).

Figure 1–27 shows a four-story residence in San Francisco in which SPW were used. The lateral-force-resisting elements were selected to fit within the restrictive architectural geometry. SPW were the only solution that allowed deep architectural recesses in the wall surface while still providing adequate stiffness in a modest length. The plate was welded directly to the beams and columns in the shop; bolted solutions were considered too difficult to fit up, and welding the plate to another piece welded to the beam or column would have been more expensive. The steel plate shear wall proved more economical than braces for the taller, more slender frames.

In addition to providing in-plane resistance to wind or seismic loads, SPW are also finding applications in blast-resistant design (Innovation, 2002) on the basis of their out-of-plane strength. As one example, the new U.S. Federal Aviation Administration security protocols call for blast- and impact-resistant air traffic control towers and prevention of tower collapse in the event of major structural damage (such as loss of a column). Relying on SPW's ability to inelastically dissipate energy, a tower concept built from stacked panels 20 ft long by 10 ft wide with ⅛-in.-thick plates was proposed to satisfy the new requirement (Figure 1–28). Nonlinear time-history finite-element analysis of the system was conducted using plate and membrane elements and large deflection capabilities, under blast impulse loading conditions.

1.4. USAGE IN CANADA

Since the early 1980s, unstiffened steel plate shear walls have been constructed in Canada, as these were the types of SPW on which Canadian research focused. An eight-story building was constructed in Vancouver, British Columbia, to provide adequate seismic performance in the narrow building direction where the only locations available for lateral-load-resisting structural elements were adjacent to elevator shafts and staircases; eccentrically braced frames were used in the other direction (Glotman, 2005).

With the publication of SPW seismic design requirements in the Canadian Steel Design Standard (CAN/CSA S16-01), implementation accelerated significantly. A series of SPW located around elevator shafts was found to be the best solution to resist lateral load on a six-story building with an irregular floor plan (Figure 1–29) that provided a 39,830 ft^2 expansion to the Canam Manac Group headquarters in St. Georges, Quebec (Driver, 2001). Simplicity in construction details contributed to the cost effectiveness of the SPW system. Walls were 8.5 ft wide (center-to-center of columns) and 75 ft tall, delimited by the dimensions of the elevator cores. Infill plates were 0.19 in. thick throughout (Figure 1–30). Two-story tiers were shop fabricated and assembled in the field with slip-critical bolted splices.

A SPW system was also selected for the seven-story ING building in Ste-Hyacinthe, Quebec, on the basis of faster construction time and gain of usable floor space, compared to the other structural systems considered (reinforced concrete walls and steel braced frames, among many). The design concept relied on a core of walls located in the middle of the building (Figure 1–31). Full-height (80 ft) walls were prefabricated in the shop; some of the walls were fabricated in half-width segments and joined together on site with a vertical welded seam spanning from top to bottom, except for the beam splices that were bolted (Figure 1–32). The base of the wall was continuously anchored to the foundation (Figure 1–33).

SPW were also used for a two-story addition to an existing single-story building of the Institut de Recherches Cliniques de Montréal (ICRM) in Montreal (Figure 1–34). One of the SPW spanned two stories, from the top of the existing one-story steel frame to the roof; another spanned three stories, with respective dimensions of 10 ft × 11.5 ft (3 m × 3.5 m) and 10 ft × 15.7 ft (3m by 4.8m), with 0.268-in.-thick (6.8-mm) plates. Each wall was shipped as a unit to the site.

1.5. USAGE IN MEXICO

A 22-story condominium building located on a hillside was originally planned in reinforced concrete with story heights of 10 ft (3 m) and total height of 225 ft (68.5 m). However, a steel alternative was designed for cost comparison at the owners' request. Preliminary calculations showed that ductile steel frames combined with concrete shear walls located around the elevator cores were more economical, and this structural system was selected for construction. Savings were mostly obtained in the lower floor weight and in faster construction time. However, the construction schedule could not be met because the contractor couldn't keep the concrete shear wall construction on pace with that of the steel frame—the walls were needed to stabilize the steel frame laterally but, typically, the steel columns were erected over three stories and then had to wait for the concrete shear walls to catch up.

The same owners subsequently built a nearly identical building on an adjacent site (Figures 1–35 to 1–37). Based on their prior experience, it was decided to replace the concrete shear walls with SPW. These walls were designed following the design criteria and recommendations of Canadian Standard CAN/CSA S16.1 because this system was not yet covered by the applicable Mexican design code (Reglamento de Construcciones del Distrito Federal, i.e., Policies for Construction in the Federal District), although the system was contemplated for inclusion in future editions of the Mexican code at that time. That building was constructed as scheduled, significantly faster and at a lower cost than the previous one.

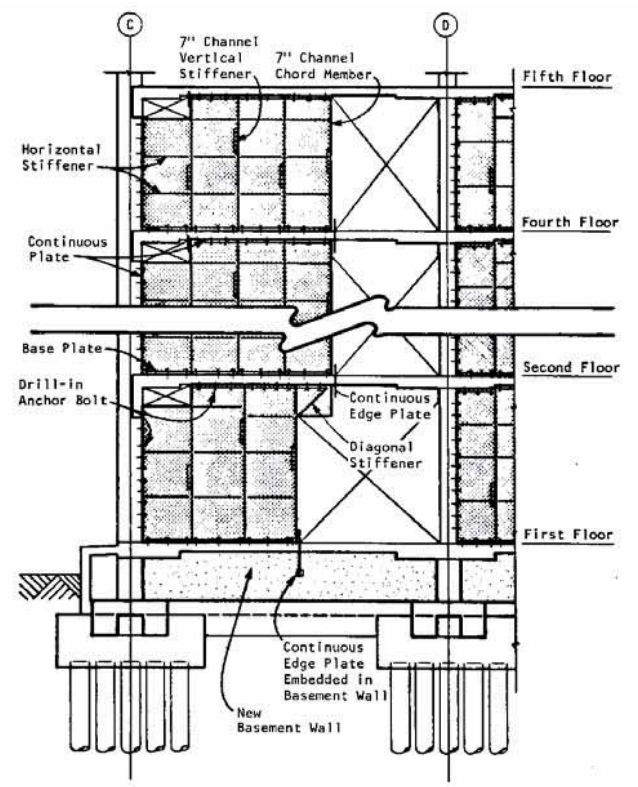

Fig. 1–16. Elevations of steel plate panels in Veterans Administration Medical Center in Charleston, SC (Baldelli, 1983).

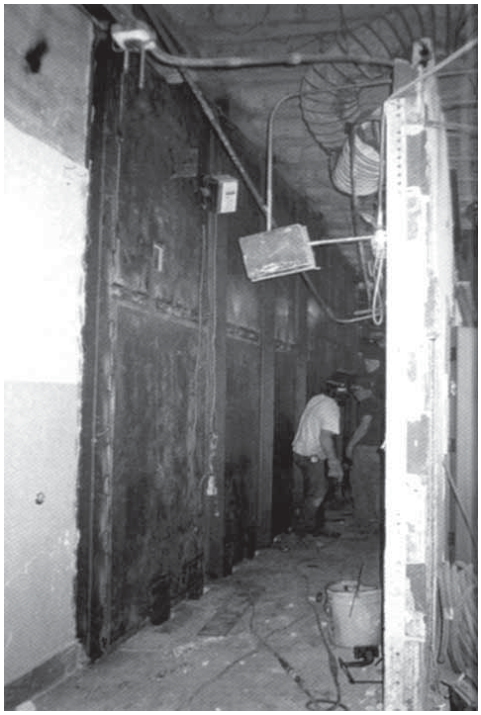

Fig. 1–17. Installation of new steel plate shear walls (courtesy of KPFF Consulting Engineers, Portland, OR).

Fig. 1–18. New steel plate shear walls (courtesy of KPFF Consulting Engineers, Portland, OR).

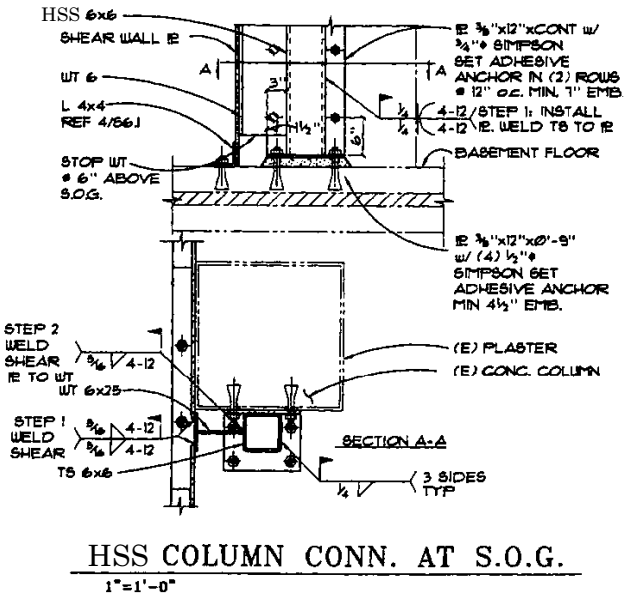

Fig. 1–19. Connection of SPW to existing R/C frame (courtesy of KPFF Consulting Engineers, Portland, OR).

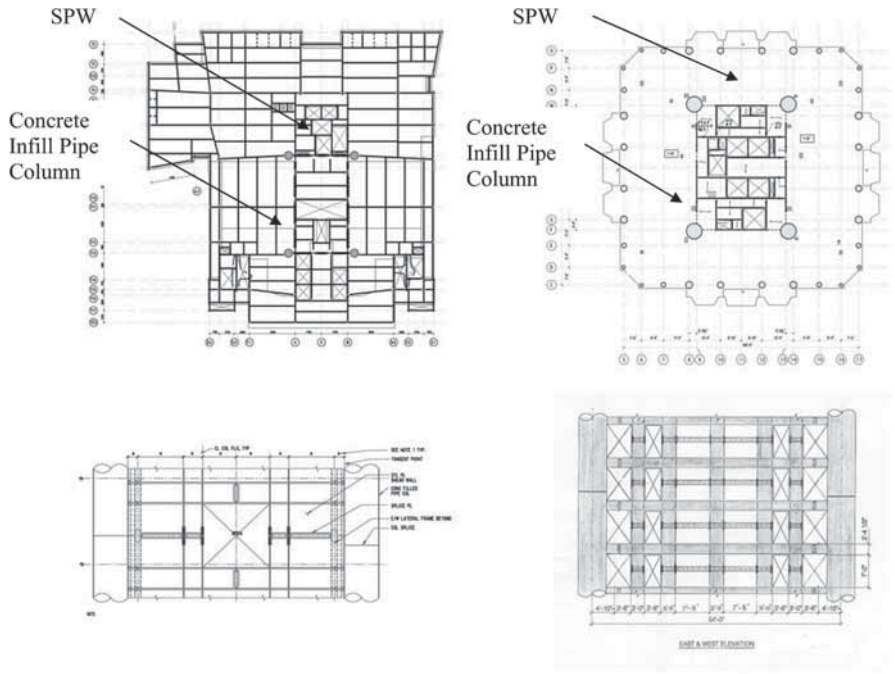

Fig. 1–20. Core walls with composite concrete infill steel pipe columns (Seilie and Hooper, 2005).

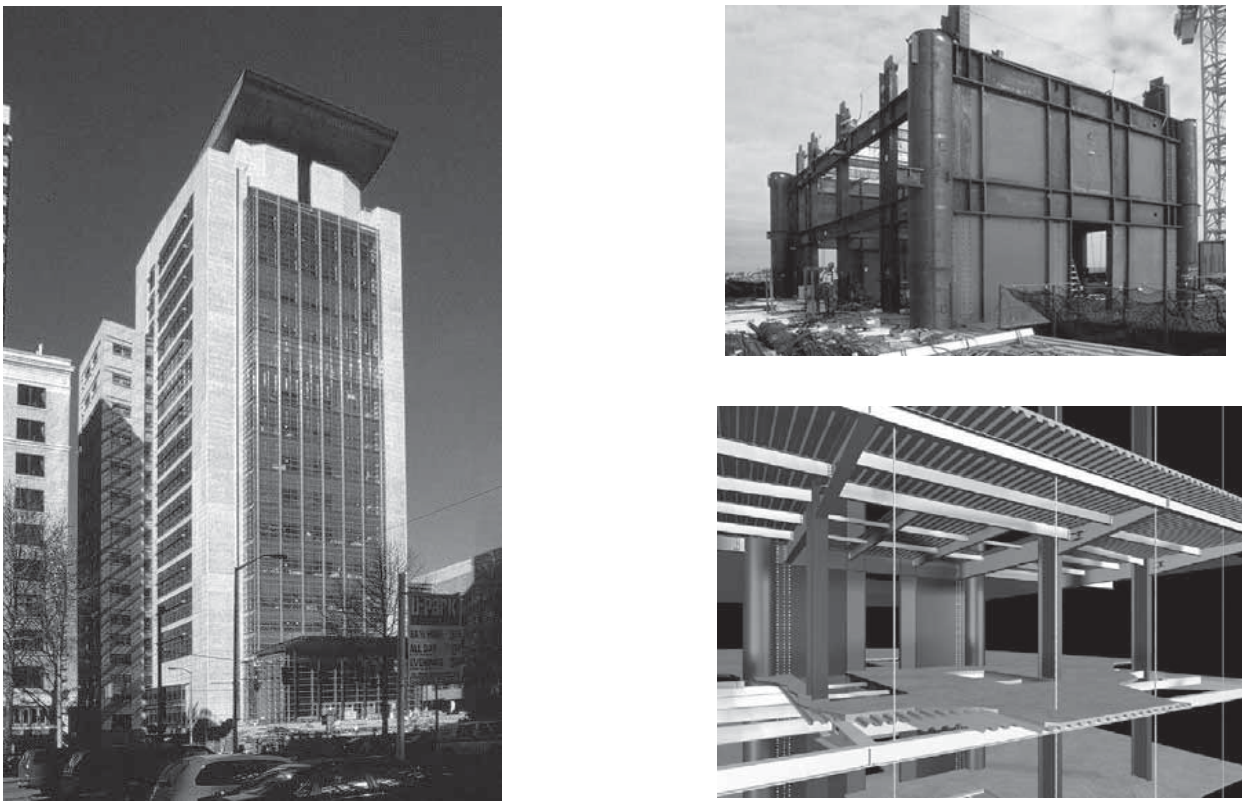

Fig. 1–21. U.S. Federal Courthouse, Seattle (courtesy of John Hooper, Magnusson Klemencic Associates, Seattle, WA).

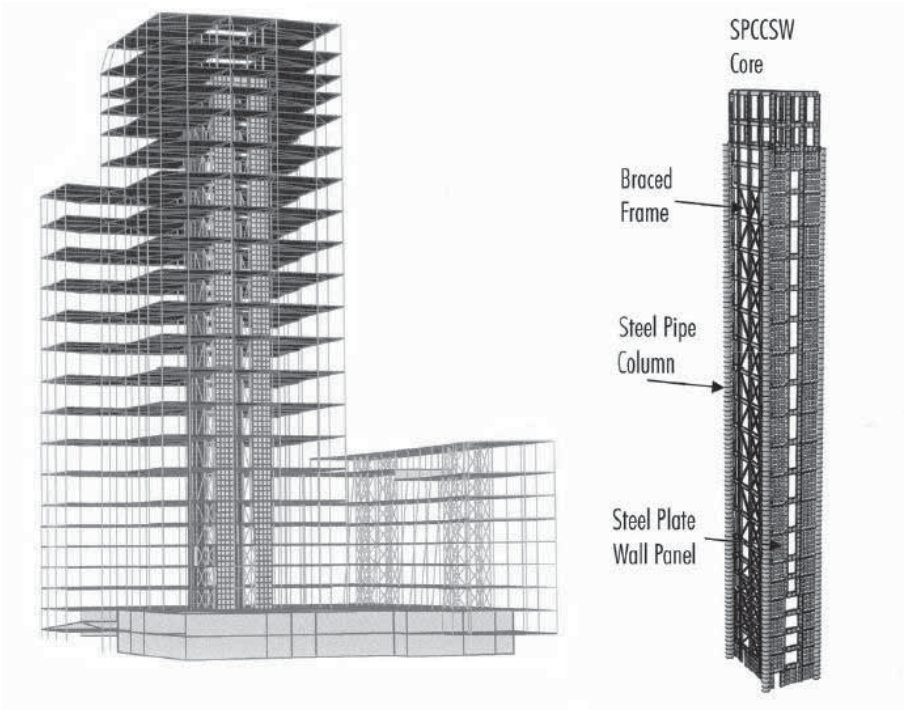

Fig. 1–22. Structural system for U.S. Federal Courthouse, Seattle (courtesy of John Hooper, Magnusson Klemencic Associates, Seattle, WA).

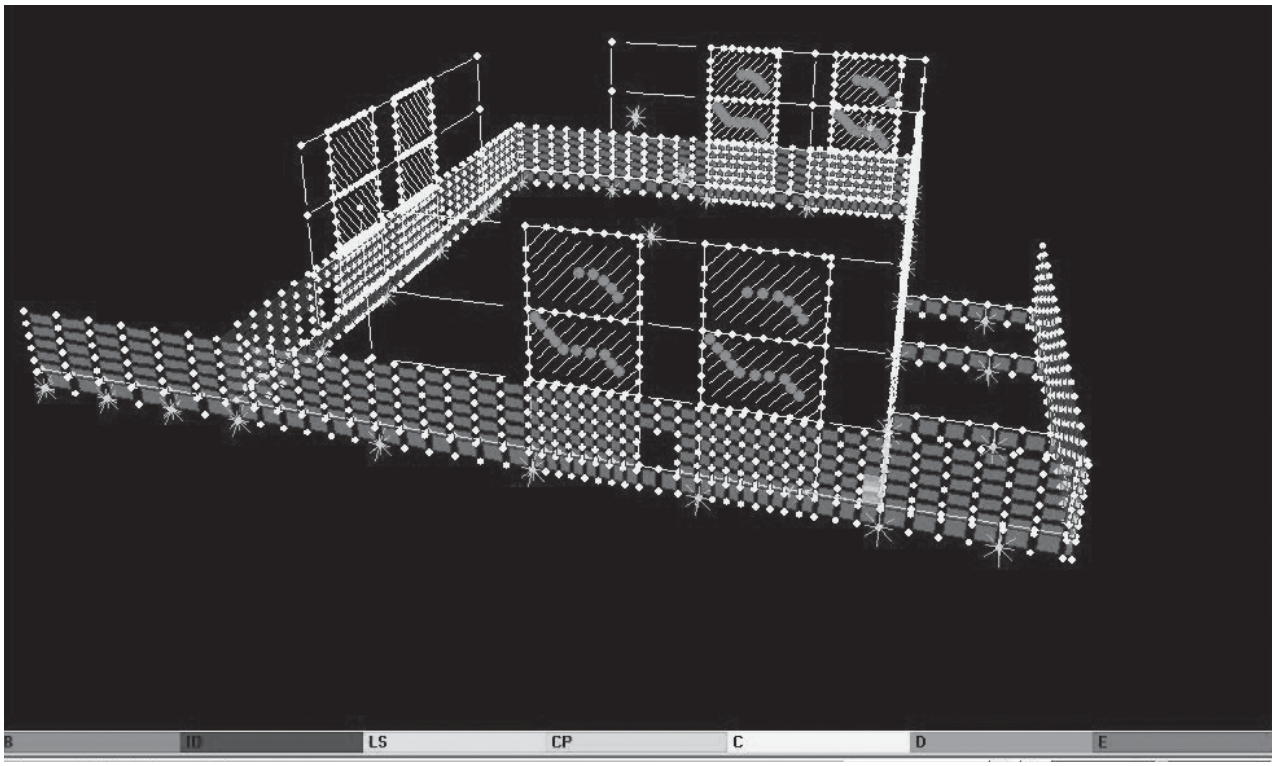

Fig. 1–23. Strip models used in project using SPW for strengthening (courtesy of Jay Love, Degenkolb Engineers, Oakland, CA).

Fig. 1–24. Residential building with SPW in Atherton, CA (courtesy of M. Eatherton, GFDS Engineers, San Francisco).

Fig. 1–25. Residential building with SPW in San Mateo County, CA (courtesy of M. Eatherton, GFDS Engineers, San Francisco).

Fig. 1–26. Residential building with SPW in Los Altos, CA (courtesy of M. Eatherton, GFDS Engineers, San Francisco).

Fig. 1–27. SPW in four-story residence in San Francisco (courtesy of Jon Brody, Jon Brody Structural Engineers, San Francisco).

(a)

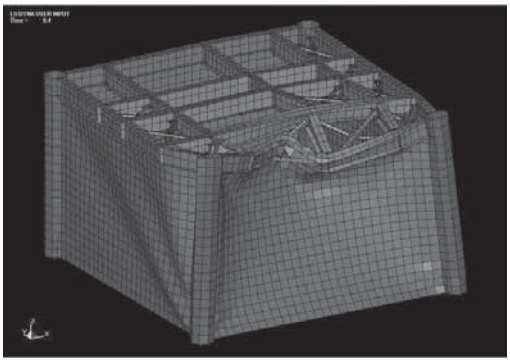

(b)

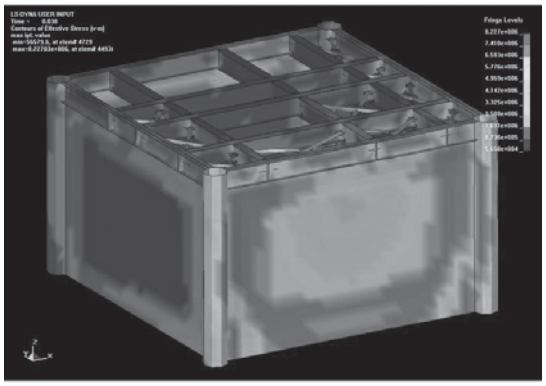

(c)

Fig. 1–28. Proposed blast- and impact-resistant air traffic control towers using SPW in Medford, OR: (a) elevation; (b) deflected shape; and (c) effective stress contours from finite element analysis (courtesy of John Pao, BPA Group, Structural Engineers, Bellevue, WA).

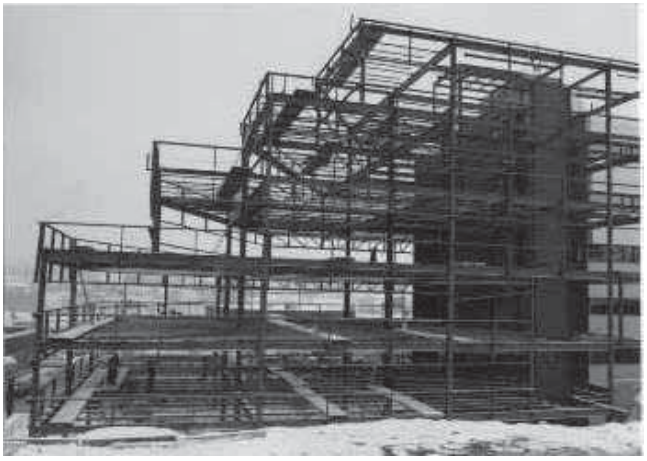

Fig. 1–29. Canam Manac Group headquarters expansion (courtesy of Richard Vincent, Canam Manac Group, St. George, Quebec, Canada).

Fig. 1–31. Core wall at middle of ING building (courtesy of Louis Crepeau and Jean-Benoit Ducharme, Groupe Teknika, Montreal, Canada).

Fig. 1–30. SPW in Canam Manac Group headquarters expansion (courtesy of Richard Vincent, Canam Manac Group, St. George, Quebec, Canada).

Fig. 1–32. Close-up view of wall at mid-span splice location, ING building (courtesy of Louis Crepeau and Jean-Benoit Ducharme, Groupe Teknika, Montreal, Canada).

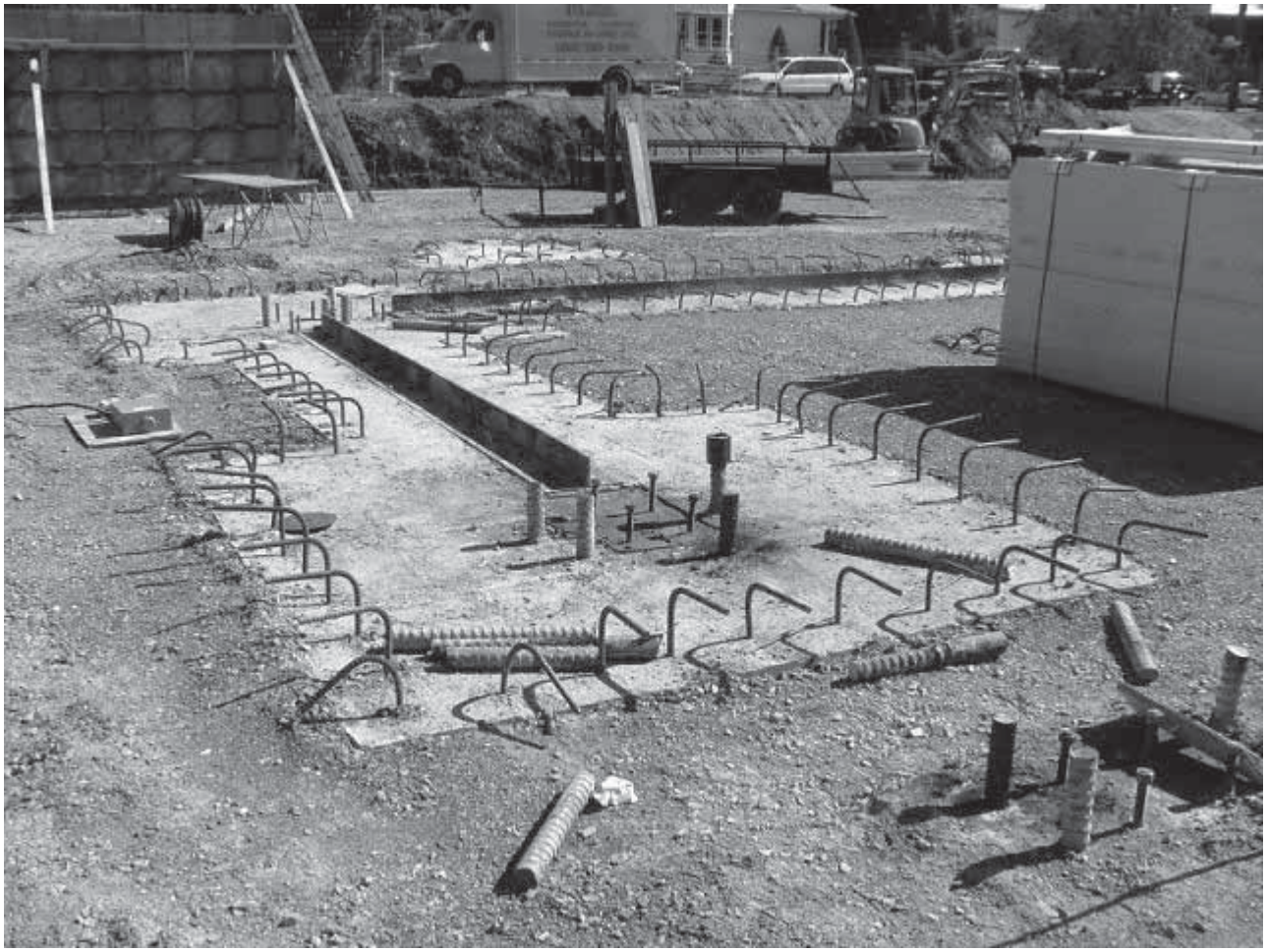

Fig. 1–33. SPW and details at base of SPW, ING building (courtesy of Louis Crepeau and Jean-Benoit Ducharme, Groupe Teknika, Montreal, Canada).

Fig. 1–34. SPW details for ICRM building (courtesy of Louis Crepeau and Jean-Benoit Ducharme, Groupe Teknika, Montreal, Canada).

Fig. 1–35. SPW building in Mexico—outside view of walls around elevator core (Martinez-Romero, 2003).

Fig. 1–36. SPW building in Mexico—inside view of walls around elevator core (Martinez-Romero, 2003).

Fig. 1–37. SPW building in Mexico (Martinez-Romero, 2003).

Chapter 2

Literature Survey

2.1. LITERATURE SURVEY

A steel plate shear wall (SPW) is a lateral-load-resisting system consisting of vertical steel plate infills connected to the surrounding beams and columns and installed in one or more bays along the full height of the structure to form a cantilevered wall (Figure 2–1). SPW subjected to cyclic inelastic deformations exhibit high initial stiffness, behave in a very ductile manner, and dissipate significant amounts of energy. These characteristics make them suitable to resist seismic loading. SPW can be used not only for the design of new buildings but also for the retrofit of existing construction. Beam-to-column connections in SPW may, in principle, be either of the simple type or moment-resisting type. Note that only the latter are allowed by AISC 341 for high-seismic applications.

Prior to key research performed in the 1980s, the design limit state for SPW was considered to be out-of-plane buckling of the infill panel. To prevent buckling, engineers designed SPW with heavily stiffened infill plates. However, several experimental and analytical studies using both quasi-static and dynamic loading showed that the post-buckling strength and ductility of slender-web SPW can be substantial (Thorburn et al., 1983; Timler and Kulak, 1983; Tromposch and Kulak, 1987; Roberts and Sabouri-Ghomi, 1992; Sabouri-Ghomi and Roberts, 1992; Cassese et al., 1993; Elgaaly et al., 1993; Driver et al., 1998; Elgaaly and Liu, 1997; Elgaaly 1998; Rezai, 1999; Lubell et al., 2000; Berman and Bruneau, 2003a; Vian and Bruneau, 2004, Berman and Bruneau, 2004). Based on some of this research, Canadian Standards Association steel design standard CAN/CSA S16-01 provided design clauses for SPW with the wall allowed to buckle in shear and develop tension-field action (CSA, 2001). Similar behavior is now also allowed in the 2003 *NEHRP Recommended Provisions* (FEMA 450) and AISC 341.

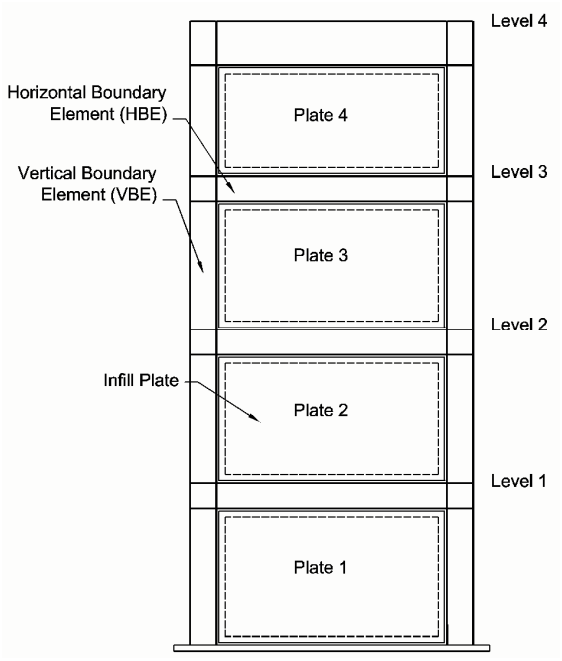

Fig. 2–1. Typical steel plate shear wall (Bruneau et al., 2005).

The post-buckling strength and tension-field action mechanism of unstiffened plates can be described as follows. It is assumed that the steel panels of SPW do not carry gravity loads and experience only shear deformations when the structure is subjected to lateral loads, and that each panel is bounded by rigid beam and column elements. At the center of the shear wall panel (away from the boundary restraints), the plate is then subject to essentially pure shear, with principal stresses oriented at a 45° angle to the direction of load, and the principal stresses being both compression and tension. The buckling strength of the plate in compression is dependent upon the slenderness of the plate (depth-to-thickness ratio and width-to-thickness ratio). These ratios are typically relatively high for normal building geometries and reasonable wall thicknesses, and buckling strength is correspondingly very low. In addition, it is inevitable that the plate will not be straight or flat due to fabrication and erection tolerances, potentially resulting in reduced compression strength. When the lateral load applied to the wall generates principal compressive stresses that exceed the compression strength of the plate, the plate buckles, generating fold lines in the plate perpendicular to these compressive stresses (and parallel to the principal tensile stresses). At this point, lateral loads are transferred through the plate by the principal tension stresses. This post-buckling behavior is typically referred to as "tension-field action." This is illustrated in Figure 2–2.

This mechanism has been recognized as early as in the 1930s in aerospace engineering (Wagner, 1931), and as early as in the 1960s in steel building construction, when it was

incorporated into the design process of plate girders (Basler, 1961). The appropriateness of post-buckling stiffness and strength characteristics of SPW to resist *service* lateral loads was analytically predicted by Thorburn et al. (1983) and experimentally confirmed by Timler and Kulak (1983).

Research on unstiffened steel plate shear walls has investigated the effect of simple versus rigid beam-to-column connections on the overall behavior (Caccese et al., 1993), the dynamic response of steel plate shear walls (Sabouri-Ghomi and Roberts, 1992; Rezai, 1999), the effects of holes in the infill plates (Roberts and Sabouri-Ghomi, 1992; Vian and Bruneau, 2004), the use of low-yield-point steel and light-gauge steel (Vian and Bruneau, 2004; Berman and Bruneau, 2005), and infill connections (Elgaaly 1998; Schumacher et al., 1999). Furthermore, finite-element modeling of unstiffened steel plate shear walls has been investigated in some of the aforementioned papers, as well as by Elgaaly et al. (1993) and Driver et al. (1997). Some of the above research is reviewed in the following sections. Note that this chapter focuses on unstiffened SPW and that, in the following, the acronym SPW refers to an unstiffened steel plate shear wall.

2.2. ANALYTICAL STUDIES

A typical SPW (Figure 2–1) consists of horizontal and vertical boundary elements that may or may not carry gravity loads and thin infill plates that buckle in shear and form a diagonal tension field to resist lateral loads. Based on an elastic strain energy formulation, Timler and Kulak (1983) derived the following equation for the inclination angle of the tension field, α, in a SPW infill plate, as measured by the angle between the direction of the strips and the vertical direction:

$$\alpha = \arctan \sqrt[4]{\frac{1+\dfrac{tL}{2A_c}}{1+th\left(\dfrac{1}{A_b}+\dfrac{h^3}{360I_cL}\right)}} \qquad (2\text{–}1)$$

where t is the thickness of the infill plate, h is the story height, L is the bay width, I_c is the moment of inertia of the vertical boundary element, A_c is the cross-sectional area of the vertical boundary element, and A_b is the cross-sectional area of the horizontal boundary element. The flexural stiffness of the horizontal boundary elements was excluded in the derivation because the opposing tension fields that develop above and below these intermediate horizontal members approximately cancel out and induce little significant flexure there.

Using the inclination angle given by Equation 2–1, an analytical model, known as a strip model, in which the infill plates are represented by a series of pin-ended, tension-only strips, was developed by Thorburn et al. (1983) and subsequently refined by Timler and Kulak (1983). A typical strip model representation of a SPW is shown in Figure 2–3, and the accuracy of the strip model has been verified through comparisons with experimental results such as in Figure 2–4, which has been adapted from Driver et al. (1998). Note

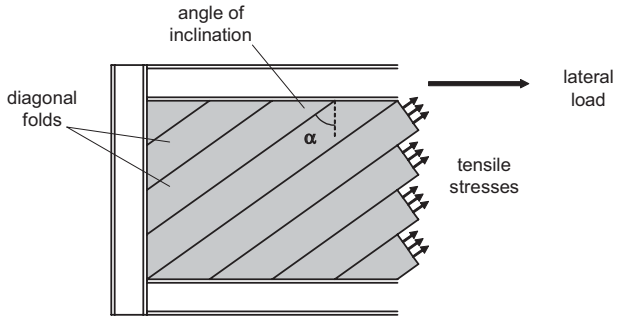

Fig. 2–2. Idealized tension-field action in a typical SPW (courtesy of Diego López-García, Pontificia Universidad Católica de Chile, Chile).

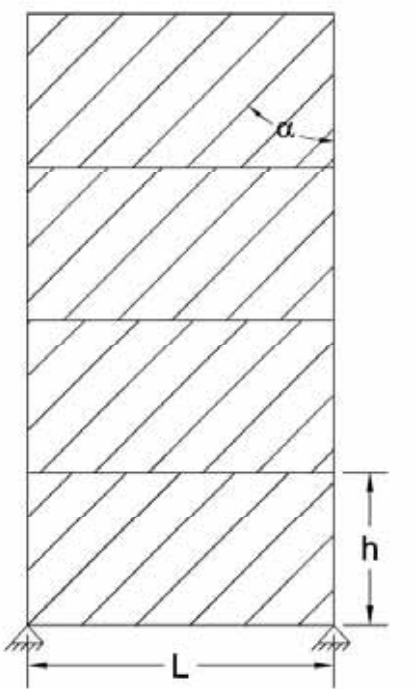

Fig. 2–3. Strip model representation of a SPW (Berman and Bruneau, 2003a).

that each strip has a cross-sectional area equal to the tributary width of the strip times the infill thickness. Parametric studies (Thornburn et al., 1983) recommended using at least 10 strips per panel to ensure accuracy of results and noted that little gain in accuracy is achieved when a larger number of strips is used.

Other analytical studies of interest are summarized as follows.

Elgaaly, Caccese, and Du (1993)

Elgaaly et al. (1993) used finite-element models, and models based on the revised multi-strip method proposed by Timler and Kulak (1983), to replicate results experimentally achieved by Caccese et al. (1993). The finite element model used nonlinear material properties and geometry, a 6 × 6 mesh to represent the plates on each story, and six beam elements for each frame member. The 0.075 in. and 0.106 in. (1.9 mm and 2.7 mm) plate thicknesses used in the finite-element models were identical to those from the experimental work. Moment-resisting beam-to-column connections were assumed. Lateral load was monotonically applied until loss of stability developed due to column plastic hinging and flange local buckling. It was found that the wall with thicker plates was not significantly stronger because column yielding was the governing factor for both cases. The finite-element models using shell elements significantly overpredicted both capacity and stiffness compared with the experimental results. These discrepancies were attributed to difficulty in modeling initial imperfections in the plates and the inability to model out-of-plane deformations of the frame members.

The specimen using moment-resisting beam-to-column connections and the 0.075-in. (1.9-mm)-thick plate was also modeled using the multi-strip method. Twelve strips were used to represent the plate at each story. The angle of inclination of the strips was found to be 42.8°, which agreed well with the results of the finite element model that predicted the principal strains in the middle of the plates oriented between 40° and 50° with the vertical. Using an elastic perfectly plastic stress-strain curve for the strips, the model was found to produce results in reasonable agreement with the experimental results with respect to initial stiffness, ultimate strength, and displacement at the ultimate strength. Using an empirically obtained trilinear stress-strain relationship for the strips, even better agreement with the experimental results was obtained. This model also proved to provide equally good results for the specimens having 0.03 in. and 0.105 in. (0.76 mm and 2.66 mm) plate thicknesses.

An analytical model for predicting the hysteretic cyclic behavior of thin steel plate shear walls was also developed. This model was based on the strip model but incorporated strips in both directions (see Figure 2–5), which is necessary to capture cyclic behavior. The hysteretic model involved the use of an empirically derived, hysteretic, stress-strain relationship for the strips, and good agreement with experimental results was reported.

Xue and Lu (1994)

Xue and Lu (1994) performed an analytical study on a three-bay, 12-story, moment-resisting frame structure, which had the middle bay infilled with a steel plate shear wall. The

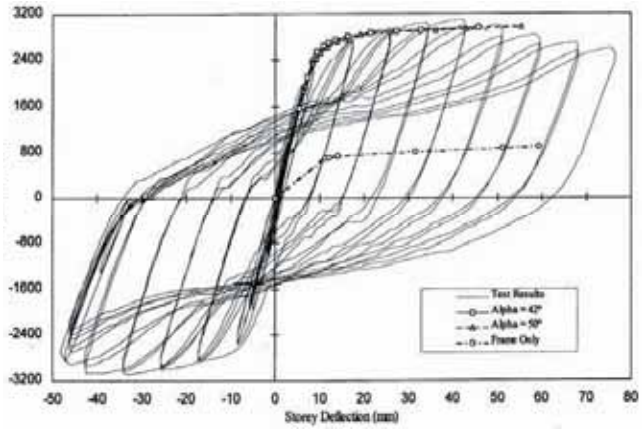

Fig. 2–4. Comparison of strip model and experimental results (Driver et al., 1998).

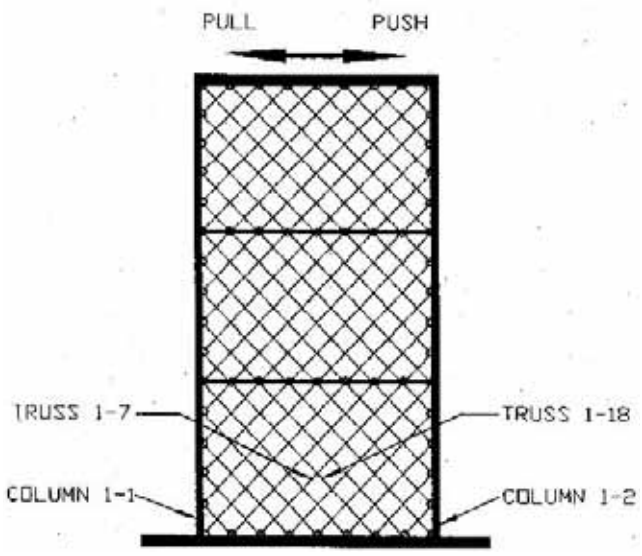

Fig. 2–5. Cyclic strip model (Elgaaly et al., 1993).

effect of beam-to-column and plate connections was the focus of this study. Four scenarios were considered:

1. Moment-resisting beam-to-column connections and infill plates fully connected to the surrounding frame.

2. Moment-resisting beam-to-column connections and the infill plates attached to only the beams.

3. Simple beam-to-column connections and fully-connected infill plates.

4. Simple beam-to-column connections with infill plates connected only to the beams.

Plate thicknesses were the same for each configuration but varied along the height. Stories 1 to 4, 5 to 8, and 9 to 12, respectively, had 0.11-in., 0.094-in., and 0.087-in. (2.8-mm, 2.4-mm, and 2.2-mm)-thick plates. The exterior bays were 360 in. (9,144 mm) wide, the interior (infilled) bay was 144 in. (3,658 mm) wide, and all stories were 144 in (3,658 mm) tall, except the first story, which was 180 in. (4,572 mm) tall.

The finite-element analysis considered beams and columns modeled using elastic beam elements and plates modeled using elasto-plastic shell elements. Initial imperfections in the infill plates were modeled to conservatively match the shape of the buckling modes of the plates. Each model was subjected to pushover analysis with forces applied at each story.

It was found that the type of beam-to-column connection in the infilled bay had an insignificant effect on the global force-displacement behavior of the system and that connecting the infill panels to the columns provided only a modest increase in the ultimate capacity of the system. Xue and Lu (1994) concluded that connecting the infill plates to only the beams and using simple beam-to-column connections in the interior bay was the optimal configuration because this drastically reduced the shear forces in the interior columns and helped avoid premature column failure. However, because the small number of cases considered does not allow generalization of this observation, this recommendation has not been implemented in the NEHRP Provisions or AISC 341.

Bruneau and Bhagwagar (2002)

Bruneau and Bhagwagar conducted nonlinear inelastic dynamic analyses to investigate how structural behavior is affected when thin infills of steel, low-yield steel, and other nonmetallic materials are used to seismically retrofit steel frames located in regions of low and high seismicity, namely, New York City and Memphis. A typical three-bay frame extracted from an actual 20-story hospital building in New York City was considered for this purpose. Fully rigid and perfectly flexible frame connection rigidities were considered to capture the extremes of frame behavior. Thin steel infill panels were found to reduce story drifts without significant increases in floor accelerations, and low-yield steel was found to lead to slightly better seismic behavior than A572 Grade 50 steel under extreme seismic conditions, but at the cost of some extra material.

The study also illustrated that, theoretically, with infinitely elastic boundary elements, undesirable behavior could be developed in SPW having high width-to-height aspect ratio of the panel and low stiffness in the boundary elements. In one such theoretical case (Figure 2–6), truss members 1 to 8 are in compression as a result of the beam and column deflections induced by the other strips in tension. In this case, the entire tension field is taken by the last four truss members. Behavior would be worse if the bottom beam were also free to deflect. While this extreme example is not practical, it illustrates that the infill plate yields progressively across its width, as a function of the stiffness of its surrounding beams and columns; simultaneous yielding across the entire infill plate width would require rigid columns and beams as well as pinned beam-to-column connections.

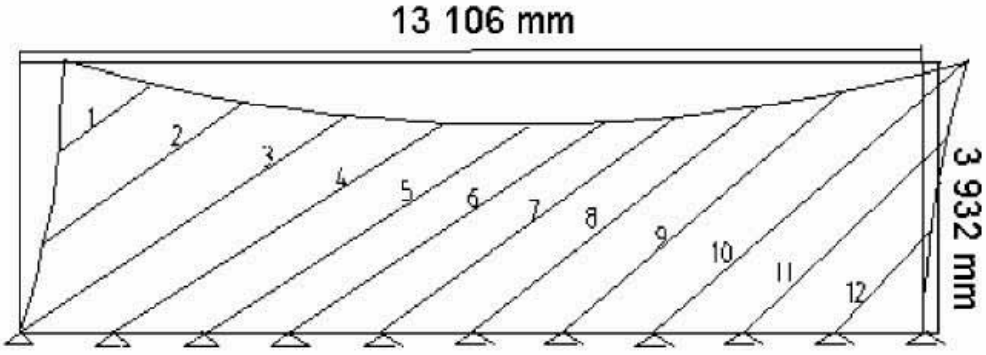

Fig. 2–6. Deflection of elastic, excessively flexible SPW panel (Bruneau and Bhagwagar, 2002).

Kharrazi, Ventura, Prion, and Sabouri-Ghomi (2004)

Kharrazi et al. (2004) investigated the design of SPW systems in terms of the separate shear and bending deformations occurring in a multi-story frame. They proposed a modified plate-frame interaction model for the analysis of shear and bending deformations and resulting forces in SPW. The objective was to describe the interaction between those components and characterize the respective contributions to deformations and strength.

A trilinear shear load-displacement diagram is developed by considering the behavior of the panel up to the points of shear buckling and perfectly plastic yielding of the tension field in the plate. Critical strength and displacement values are derived for both shear buckling and tension-field yielding, then combined into a bilinear model. It should be noted that, if the critical shear buckling strength is assumed negligible (i.e., a very thin panel), the derived equations for panel strength, stiffness, and yield displacement reduce to those of Thorburn et al. (1983).

The bending component of plate wall behavior was investigated. Equations for moment and displacement were derived for a single-story panel at the critical point at which panel buckling occurs, assuming a linear strain distribution across the wall cross-section. The procedure assumes that, after panel bucking, the neutral axis will move toward the column in tension, since compressive stresses in the web will be released, similar to the neutral axis migration in a reinforced concrete beam following section cracking on the tension side. Expressions were developed for behavior of the panel after this event. Equations for shear behavior and bending behavior are combined using interaction equations to complete the proposed method.

2.3. TESTING

Experimental research (Tromposch and Kulak, 1987; Roberts and Sabouri-Ghomi, 1991; Caccese et al., 1993; Elgaaly and Liu, 1997; Driver et al., 1998a; Lubell et al., 2000) suggests that, when subjected to cyclic deformation levels well beyond the elastic limit, SPW possess adequate hysteretic response characteristics. In these experiments, single- and multi-story SPW models of various scale levels were subjected to quasi-static cyclic loads. In all cases, resulting experimental hysteresis loops are stable up to relatively large ductility ratios, and indicate that a significant amount of energy is dissipated through inelastic deformations. Hysteresis loops, however, are invariably "pinched" because, when a SPW is loaded in a given direction, tensile stresses do not develop diagonally until the deformation level is equal to the magnitude of residual deformations left by former inelastic incursions in the same direction. Experimental evidence, however, indicates that pinching effects are less pronounced in SPW having moment-resisting beam-to-column connections than in those having simple connections. Some of these tests are reviewed in the following text. Tests on nonconventional wall configurations, such as walls with specially detailed vertical slits (Hitaka and Matsui, 2003) and walls with corrugated panels (Mo and Perng, 2000; Berman and Bruneau, 2003b), are beyond the scope of this Design Guide.

2.3.1. COMPONENT TESTS

Timler and Kulak (1983)

Timler and Kulak (1983) tested a single-story, large-scale SPW specimen to verify the analytical work of Thorburn et al. (1983) briefly summarized in the previous section. A specimen consisting of two SPW panels, with centerline bay width of 148 in. by a story height of 98 in. (3,750 mm by 2,500 mm), as shown in Figure 2–7, was tested under monotonically increasing loading to the serviceability drift limit, followed by loading to failure. Simple beam-to-column con-

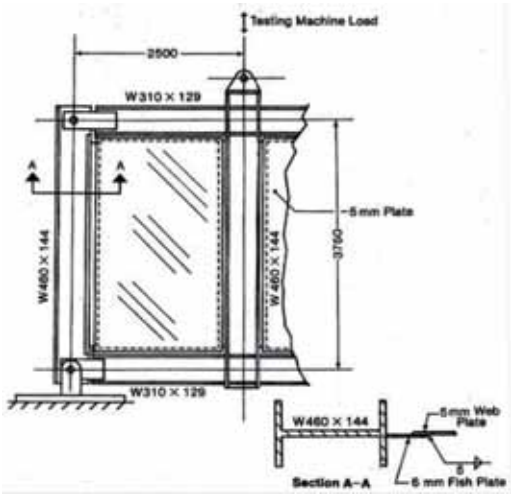

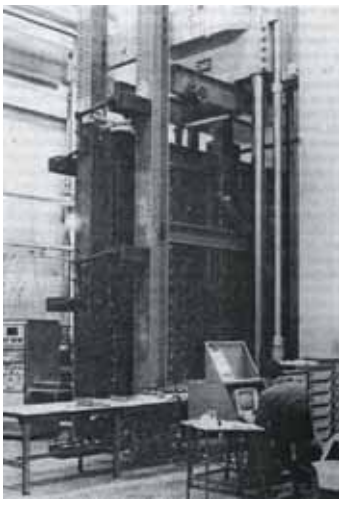

Fig. 2–7. Specimen tested by Timler and Kulak (1983).

nections were used to connect the W18×97 (W460×144) beams to the W12×87 (W310×129) column sections. The 0.197 in. (5 mm) infill panel was welded to the boundary frame by means of a 0.236-in. (6-mm)-thick "fish plate." No effective gravity loads were applied to the system. At the serviceability limit, the angle of inclination of the tension field along the centerline of the panel was found to vary from 44° to 56°. The maximum load attained was 1,213 kips (5,395 kN). Failure of the specimen resulted from tearing of the weld used to connect the infill plate to the fish plate, and it was concluded that had this been avoided the specimen could have resisted a larger ultimate load.

Tromposch and Kulak (1987)

Tromposch and Kulak (1987) tested a large-scale steel plate shear wall (Figure 2–8) similar to that tested by Timler and Kulak (1983). The major differences between the two were a change in the bay dimensions to 108 in. (2,750 mm) width by 87 in. (2,200 mm) story height; the use of bolted rather than welded beam-to-column connections; thinner plates, 0.118 in. (3 mm), made of hot-rolled steel; stiffer beams, W24×162 (W610×241); prestressing of columns to simulate the effect of gravity load; and a more comprehensive cyclic and monotonic loading regimen. Stiffer beams were used in order to simulate the effect of a tension field above and below the panel being tested so that the results could be applied to multi-story steel plate shear walls.

Twenty-eight fully reversed quasi-static load cycles were applied up to a load level of 67 percent of the ultimate strength. The maximum displacement reached during this loading stage was 0.67 in. (17 mm) or h_s/129 (0.8 percent drift).

After that sequence, the prestressing rods were removed from the columns and loading increased monotonically to determine the failure loads and associated deformations (Figure 2–9). The final displacement reached was 2.80 in. (71 mm) or h_s/31 (3.2 percent drift). Failure of the specimen was attributed to bolt slippage at the beam-to-column connections and tearing of the welds attaching the infill plate to the fish plate. However, testing was stopped because the actuator reached its maximum capacity while the test specimen could have taken more load. Hysteretic loops obtained from the experiment were pinched but stable and showed stable energy dissipation.

The multi-strip model was used to predict the test results and was found to be adequate in predicting the ultimate strength of the wall and in predicting the envelope of cyclic response. In order to achieve this result, it was necessary to treat the frame connections as rigid at low load levels and pinned after bolt slippage had occurred.

Roberts and Sabouri-Ghomi (1992)

Roberts and Sabouri-Ghomi (1992) conducted a series of 16 quasi-static cyclic loading tests on unstiffened steel plate shear panels with centrally placed circular openings. The test setup consisted of a plate clamped between pairs of stiff, pin-ended frame members. Two diagonally opposite pinned corners were connected to the hydraulic grips of a 56.2 kip (250 kN) servo-hydraulic testing machine, which applied the loading.

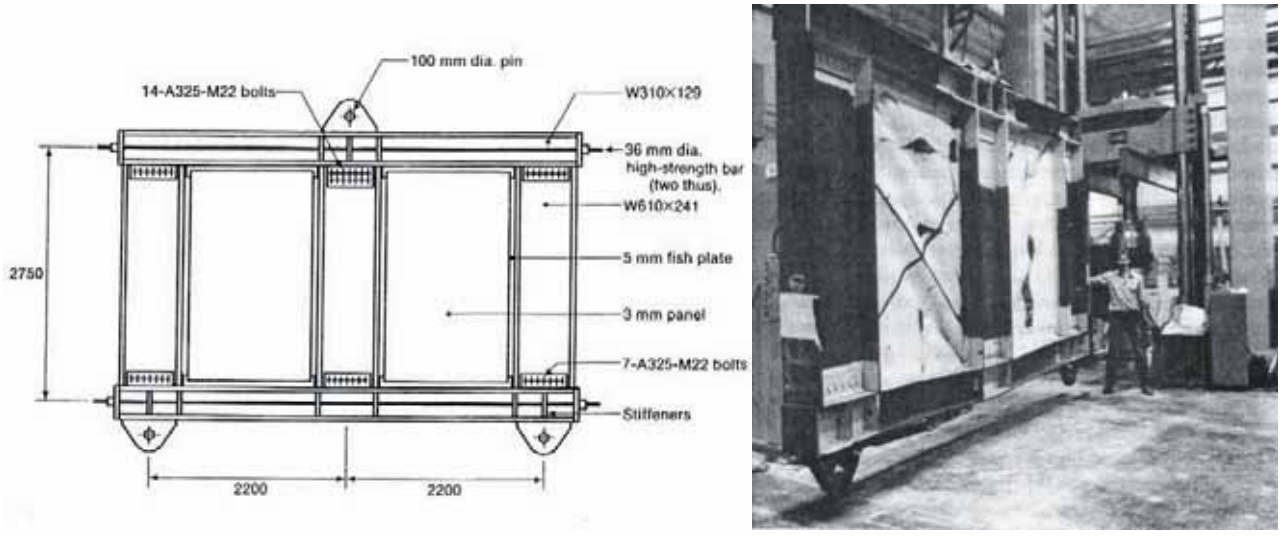

Fig. 2–8. Specimen tested by Tromposch and Kulak (1987): (a) geometry and specimen details; (b) specimen damage state after testing.

Specimen panel depth, d, was 11.8 in. (300 mm) for all specimens; panel width, b, was either 11.8 in. or 17.7 in. (300 mm or 450 mm); panel thickness, h, was either 0.033 in. or 0.048 in. (0.83 mm or 1.23 mm), with the panels having 0.2 percent offset yield stress values of 32 ksi (219 MPa) and 22 ksi (152MPa), respectively; and four values were selected for the diameter of the central circular opening, D: 0 in., 2.4 in., 4.1 in., and 6.0 in. (0 mm, 60 mm, 105 mm, and 150 mm). A schematic of a specimen and hinge detail are shown in Figure 2–10.

On the basis of experimental results, the approximate strength and stiffness reduction factor proposed in Equation 2–2 for a perforated panel with a single hole was found to give conservative results:

$$\frac{V_{yp\ perf}}{V_{yp}} = \frac{K_{perf}}{K_{panel}} = \left[1 - \frac{D}{d}\right] \qquad (2\text{–}2)$$

In Equation 2–2, $V_{yp.perf}/V_{yp}$ and K_{perf}/K_{panel} are the ratios of strength and elastic stiffness, respectively, of a perforated panel specimen with a single hole to an identical solid panel specimen, and the remaining parameters are defined above. Equations for panels having multiple holes are presented in a later section.

Schumacher, Grondin, and Kulak (1999)

Schumacher et al. (1999) investigated the cyclic inelastic behavior of the connection of SPW plate to boundary beams and columns using full-sized panel corner details and finite-element analysis. The four infill panel connection details considered are shown in Figure 2–11. In Detail A, the infill plate is welded directly to the boundary members, which is a more difficult detail to implement in practice; Detail B has fish plates welded to each of the boundary members and the infill plate lapped and welded over the fish plates (Modified B is a variation with a corner cut out to reduce concentration of stresses); Detail C has the infill plate welded to boundary members on one side of each corner and to a fish plate on the other side. Note that Tromposch and Kulak (1987) developed an earlier version of Detail B that includes a supplemental strap plate bridging the gap, and that was used by Driver et al. (1997). Cyclic inelastic response and energy dissipation capacity of all specimens was comparable. Tears ultimately developed in all specimens except the one with Detail A, but the tears had negligible impact on behavior and did not result in structural failure.

Berman and Bruneau (2003b) and Vian and Bruneau (2005)

One difficulty in the selection of SPW systems is that the available panel material may be stronger or thicker than needed for a given design situation. This will increase the necessary sizes of horizontal and vertical boundary members as well as foundation demands, since these members are generally designed for the strength of the plate. To alleviate this concern, recent work has focused on the use of light-gauge, cold-rolled (Berman and Bruneau, 2003b) and low-yield strength (LYS) steel for the infill panel (Vian and Bruneau, 2005), and on the placement of a pattern of

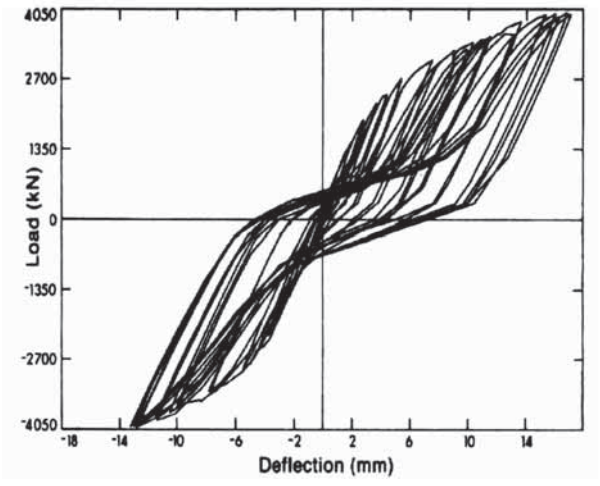

Fig. 2–9. Cyclic response of SPW tested by Tromposch and Kulak (1987).

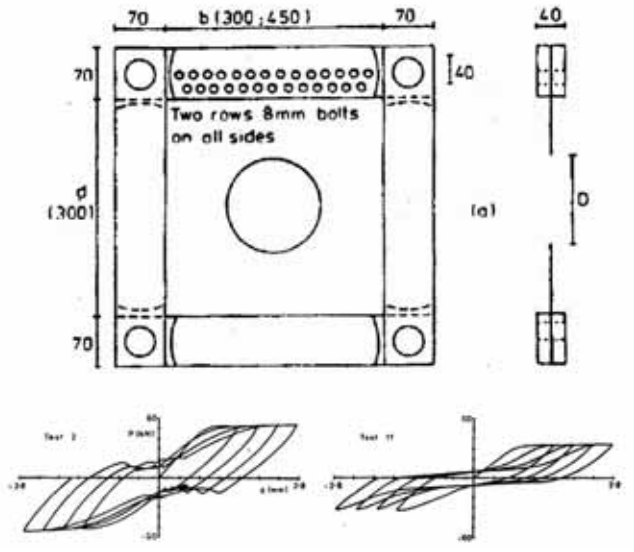

Fig. 2–10. Test setup and quasi-static cyclic response of solid (left) and perforated (right) SPW tested by Roberts and Sabouri-Ghomi (1992).

perforations to decrease the strength and stiffness of the panel (Vian and Bruneau, 2005). In addition, the use of reduced beam sections at the ends of the horizontal boundary members was investigated as a means of reducing the overall system demand on the vertical boundary members (Vian and Bruneau, 2005).

A SPW test specimen utilizing a light-gauge infill panel with 0.0396 in. (1.0 mm) thickness is shown in Figure 2–12 (Berman and Bruneau, 2003b). The specimen used W12×96 (W310×143) columns and W12×86 (W460×128) beams. This test was performed using quasi-static cyclic loading conforming to the recommended loading protocol of ATC 24 (ATC, 1992). Results are shown in Figure 2–13 along with the boundary frame contribution. After subtracting the boundary frame contribution, the hysteresis of Figure 2–14 is obtained.

This specimen reached a ductility ratio of 12 and drift of 3.7 percent, and the infill panel was found to provide approximately 90 percent of the initial stiffness of the system. The limit state of the specimen was due to fractures in the infill panel propagating from the corners. Figures 2–15 and 2–16 show the buckling of the infill plate at the peak displacement of cycle 20 (ductility ratio of 6, 1.82 percent drift) and the fracture at the infill panel corner during cycle 26 (ductility ratio of 10, 3.07 percent drift).

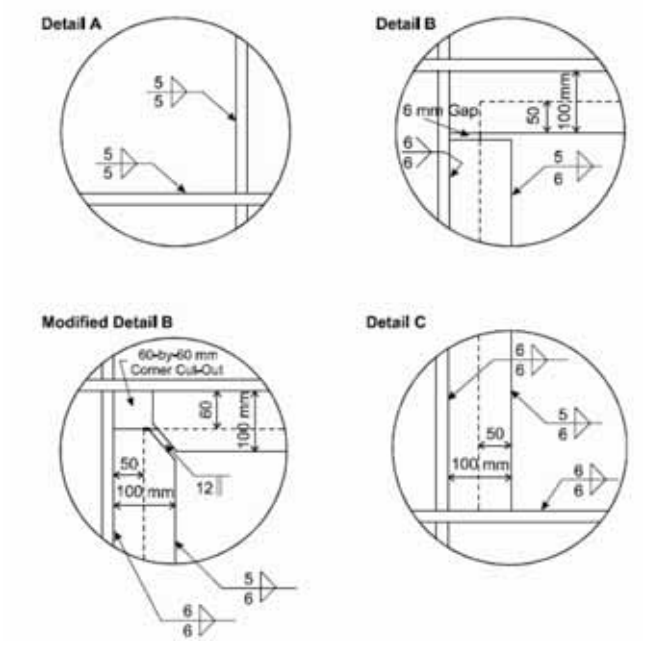

Fig. 2–11. Infill plate connection details tested by Schumacher et al. (1999). Dimensions shown are in millimeters.

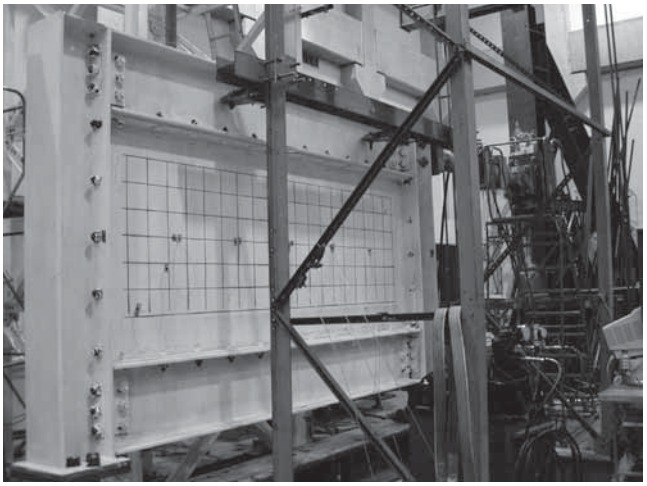

Fig. 2–12. Light-gauge SPW prior to testing (Berman and Bruneau, 2003b).

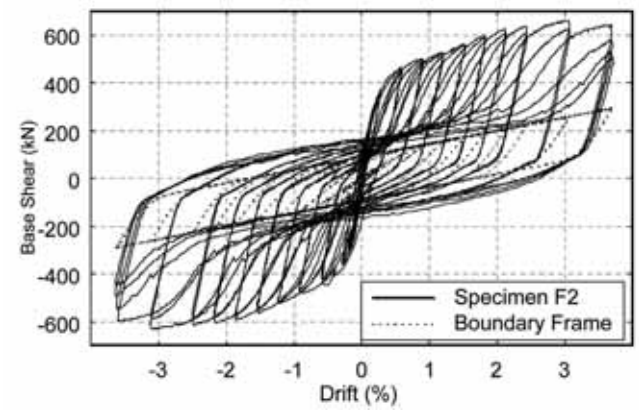

Fig. 2–13. Light-gauge SPW and boundary frame hysteresis (Berman and Bruneau, 2003b).

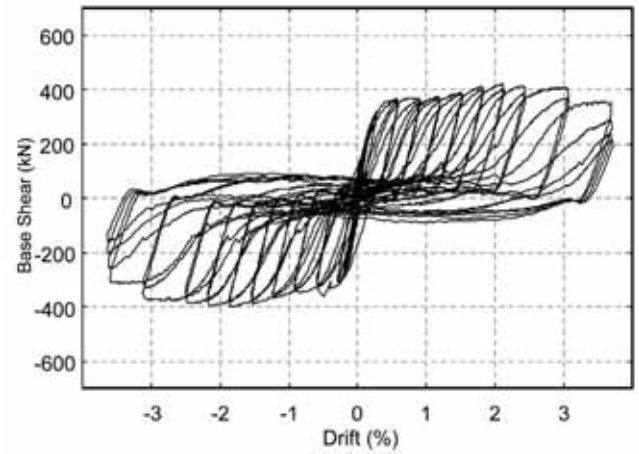

Fig. 2–14. Light-gauge SPW hysteresis—infill only (Berman and Bruneau, 2003b).

Other possible alternatives to a SPW with oversized plates have been considered by Vian and Bruneau (2005). These alternatives are (a) LYS panels (Figure 2–17), (b) perforated steel panels (Figure 2–18), and (c) steel panels with reinforced cut-out corners (Figure 2–19). The reduced yield stress of LYS panels reduces forces imposed on frame members. Perforated steel panels reach the same objective while allowing wires, pipes, and plumbing to pass through the panel, a convenient feature when disruption of building functionality must be kept to a minimum. In other situations, panels with reinforced cut-out corners provide the same strength as a solid panel while allowing some through access for utilities. Perforations through the wall may help expand the range of implementation of SPW while also serving as a method of reducing the panel strength and therefore the demand on the surrounding framing. This latter characteristic may prove beneficial in markets that do not have LYS readily available for structural applications.

Three SPW specimens of similar size and dimension, but utilizing LYS infill panels, were designed, built, and subjected to quasi-static cyclic loading (Vian and Bruneau, 2004). The frames consisted of 50 ksi (345 MPa) steel members, while the infill panels were 0.102 in. (2.6 mm) thick, LYS steel plates with an initial yield strength of 24 ksi (165 MPa), and tensile strength of 44 ksi (300 MPa). All specimens also had beam-to-column connection details that included reduced beam sections (RBS) at each end, introduced only for the purpose of reducing the size of the top and bottom beams while preventing mid-span hinges (Vian and Bruneau, 2005).

Experimental results indicate that these alternative SPW assemblies possess adequate hysteretic characteristics, although these specimens could not be subjected to deformations levels beyond a 3 percent drift ratio due to experimental setup problems.

All specimens tested in this experimental program exhibited stable force-displacement behavior, with very little pinching of hysteresis loops until significant accumulation of damage at large drifts. The specimens with perforated plate performed well, exhibiting stable hysteretic behavior. The stiffness and strength were both reduced, as anticipated, from the solid panel specimen (S2) values, as shown in Figure 2–20.

Vian and Bruneau (2005) developed equations for estimating the reduction in panel stiffness due to the presence of perforations. For a panel with multiple perforations, arranged in diagonal strips, such as the tested specimen shown in Figure 2–18, a stiffness reduction factor can be derived assuming that the elastic behavior of a typical perforated strip, as shown in Figure 2–21, can represent the strips in the entire panel, as a group of parallel axially loaded members. Five variables define the panel perforation layout geometry: the perforation diameter, D; the diagonal strip spacing, S_{diag}; the number of horizontal rows of perforations, N_r; the panel height, H_{panel}; and the diagonal strip angle, θ. Using these parameters, the total displacement of the perforated strip can be calculated, and the resulting stiffness is set equal to the stiffness of a tension member of uniform effective width. This effective width, divided by the gross width of the perforated strip, is the stiffness reduction factor proposed in Equation 2–3:

$$\frac{K_{perf}}{K_{panel}} = \frac{1-\frac{\pi}{4}\left(\frac{D}{S_{diag}}\right)}{1-\frac{\pi}{4}\left(\frac{D}{S_{diag}}\right)\left(1-\frac{N_r D\ \sin\theta}{H_{panel}}\right)} \qquad (2\text{–}3)$$

Fig. 2–15. Buckling of infill panel at 1.82 percent drift (Berman and Bruneau, 2003b).

Fig. 2–16. Fracture of infill panel corner at 3.07 percent drift (Berman and Bruneau, 2003b).

to be used only when $D/S_{diag} \leq 0.5$. This equation provided very good agreement with the experimental results observed during the specimen P tests described above, differing by approximately 5 percent.

Equation 2–3 was recommended (with d substituted for S_{diag}) for estimating strength reduction in similar systems. This panel strength reduction factor showed very good agreement (within 5 percent) with the observed behavior of specimen P as compared with solid panel specimen S2.

Vian and Bruneau (2005) also proposed geometric constraints to ensure ductile performance of the perforated infill panels. It was recommended that the ratio of perforation diameter to spacing, D/S_{diag}, be such that

$$\frac{D}{S_{diag}} \leq \left(1 - Y_t \frac{F_y}{F_u}\right) \qquad (2\text{–}4)$$

where F_y and F_u are the yield and tensile strength, respectively, of the infill panel material, and it is recommended to use values of Y_t equal to 1.0 for $F_y/F_u \leq 0.8$, or 1.1 otherwise, as suggested by Dexter et al. (2002) and specified for design of tension flanges with holes by AISC (2005b). It was also recommended that the steel moment frames with perforated SPSW be designed for maximum inter-story drifts of 1.5 percent. For simplicity, it was suggested that the perforation layout angle, θ, be adopted as a constant 45° angle.

2.3.2. MULTI-STORY TESTS

Caccese, Elgaaly, and Chen (1993)

An experimental investigation into the effects of panel slenderness ratio and type of beam-to-column connection was performed by Caccese et al. (1993). They tested five one-fourth scale models of three-story steel plate shear walls with varying plate thicknesses and beam-to-column connection types (see Figure 2–22). Plate thicknesses used were 0.03 in., 0.075 in., and 0.105 in. (0.76 mm, 1.9 mm, and 2.66 mm) with moment-resisting connections and 0.03 in. and 0.075 in. (0.76 mm and 1.9 mm) simple shear beam-to-column

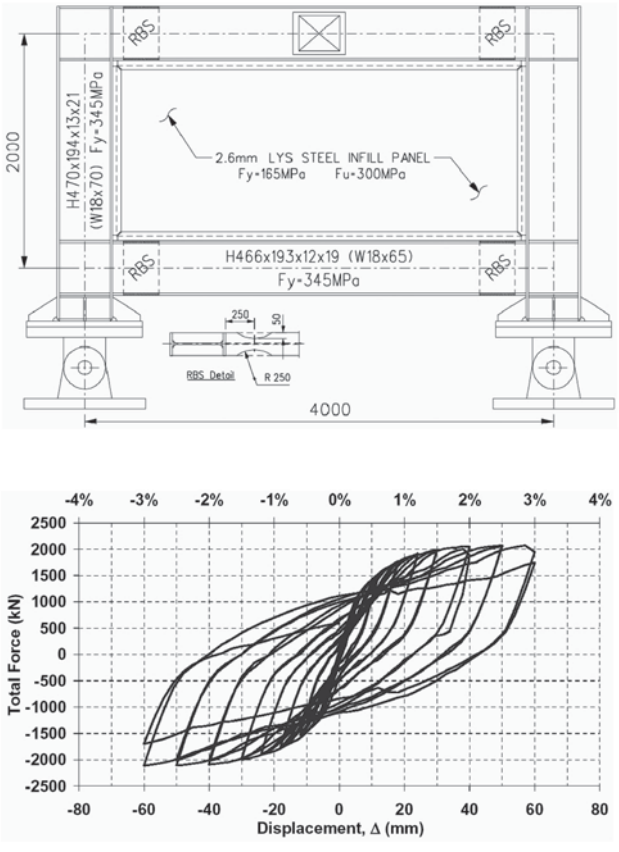

Fig. 2–17. Test setup and quasi-static cyclic response of the flat LYS SPW tested by Vian and Bruneau (2005).

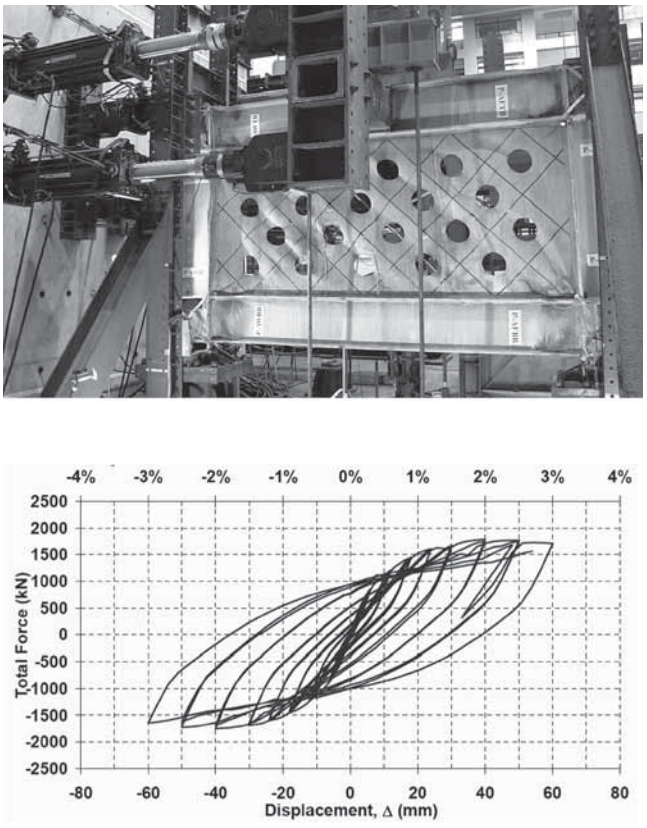

Fig. 2–18. Perforated panel specimen (P) at 3 percent drift (Vian and Bruneau, 2005).

connections. The wall height was 9 ft 5 in. (2,870 mm) with 2 ft 9 in. (838 mm) stories and a 9-in. (229-mm)-deep stiff structural member at the top of the third story to anchor the tension field. Bays were 4 ft 1 in. (1,245 mm) wide, and infill panels were continuously welded to the boundary frame.

Loading was applied at the top of the third story only. Columns were not preloaded axially, and the effects of gravity load were not considered. The loading program consisted of three cycles at each of eight displacement levels incremented by ¼ in. (6.35 mm). The maximum displacement reached was 2 in. (50.8 mm) or 2 percent drift. After these 24 cycles were complete, the same cyclic displacement program was reapplied. If the specimen was still intact at this point, it was pushed monotonically to the displacement limit of the actuator.

This test series revealed a transition in failure modes depending on the plate thickness used. When slender plates were used, the plates buckled and yielded in the tension field before any boundary members, and failure of the system was governed by the formation of plastic hinges in the columns. As the plate thickness increased, the failure mode was governed by column instability. Once instability governed, further increases in the plate thickness were found to have only a negligible effect on the strength of the system. Caccese et al. concluded that the use of slender plates will therefore result in more stable systems because they will not be governed by column buckling prior to the plate reaching a fully yielded state. Kennedy et al. (1994), commenting on those results, argued that the columns in a steel plate shear wall system can be designed to support the load induced by the infill panel and that column buckling prior to plate yielding can therefore be avoided.

Caccese et al., also reported that the difference between using simple and moment-resisting beam-to-column connections was small. This was attributed to the fact that the infill plate was fully welded all around to the frame, which in essence creates a moment-resisting connection. This point was later addressed by Kulak et al. (1994), who argued that the differences in the material properties, plate thicknesses, and the failure of a weld in one of the specimens precluded

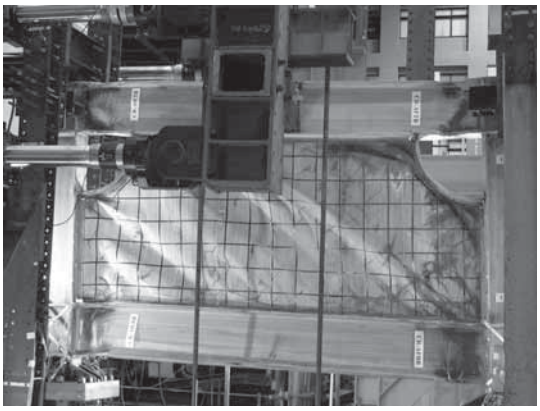

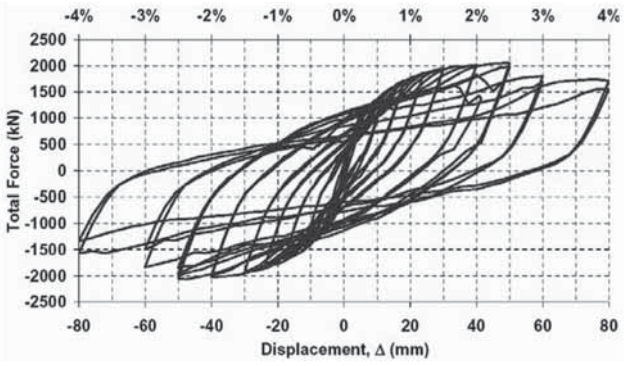

Fig. 2–19. Specimen condition at 4 percent drift and quasi-static cyclic response of the LYS SPW with reinforced cut-out corners tested by Vian and Bruneau (2005).

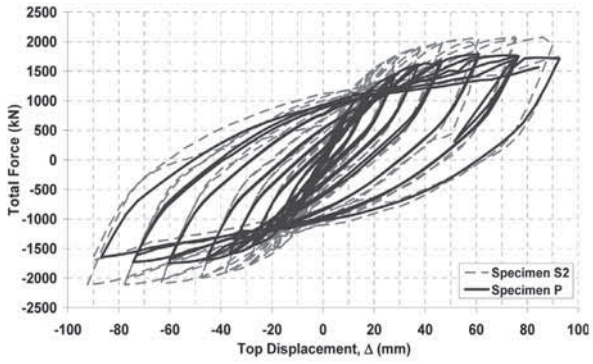

Fig. 2–20. Solid panel (S2) and perforated panel (P) specimen hysteresis curves (Vian and Bruneau, 2005).

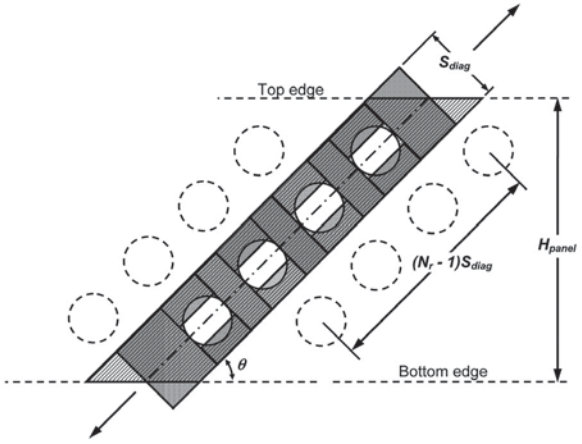

Fig. 2–21. Details of typical diagonal strip—segment lengths and widths (Vian and Bruneau, 2005).

a direct comparison in the context of connection type. They also pointed out that Tromposch and Kulak (1987) showed analytically that greater energy dissipation could be achieved with the use of moment connections.

Driver, Kulak, Kennedy, and Elwi (1997)

Driver et al. (1997) tested a large-scale multi-story SPW to better identify the elastic stiffness, the first yield, ductility and energy absorption capacity, cyclic stability, and failure mode of the wall. The test specimen was constructed with moment-resisting beam-to-column connections and a better understanding of the interaction between the plates and moment frame was sought.

The specimen (Figure 2–23) was four stories tall, with a first story height of 6 ft 4 in. (1,927 mm), a height of 6 ft (1829 mm) for the other stories, and a bay width of 10 ft (3050 mm). The plate thicknesses were 0.19 in. (4.8 mm) and 0.13 in. (3.4 mm) for the lower two and upper two stories, respectively. A relatively large and stiff beam was used at the roof level to anchor the tension field forces that would develop. A fish plate connection was used to connect the infill plates to the frame, as shown in Figure 2–24.

Actuators were mounted at each story to provide a distributed force over the height of the structure. Gravity loading was also applied. Cyclic quasi-static loading was applied for 35 cycles of increasing lateral displacement. The yield displacement and corresponding base shear of the specimen were, respectively, found to be 0.33 in. (8.5 mm) and 540 kips (2,400 kN), based on observation of the experimental load versus deformation curve. At three times the yield displacement, tearing of a first-story plate weld occurred, and yielding of the column panel zone at the top of the first story was observed. At this point the base shear was 675 kips (3,000 kN). Local buckling of the column flange below the first-story was observed at four times the yield displacement. Several tears in the first story plate and severe local buckling of the same column were observed at six times the yield displacement (Figure 2–25). At this point, the structure was still holding 95 percent of the ultimate strength reached. Failure occurred at nine times the yield displacement when the complete joint penetration groove weld at the base of a column fractured (Figures 2–26 and 2-27). Even at this point, the structure was holding 85 percent of the ultimate strength reached.

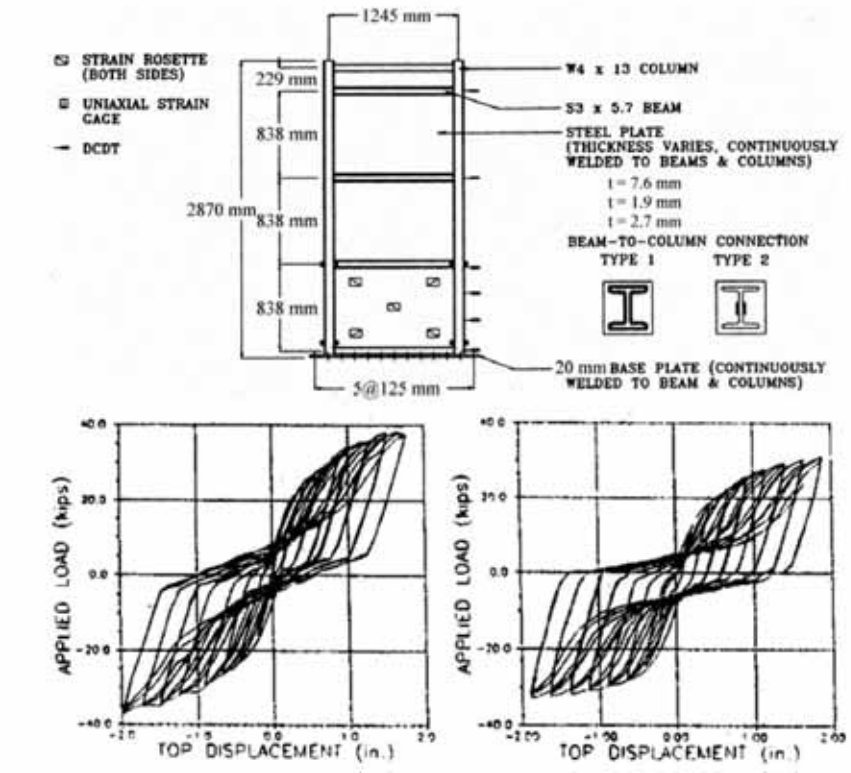

Fig. 2–22. Test setup and global quasi-static cyclic response of Type 1 (left) and Type 2 (right) SPW tested by Caccese et al. (1993).

Observation of the specimen following the test revealed minimal whitewash flaking in the beam-to-column connections, leading the researchers to conclude that most of the energy dissipation was achieved through yielding of the plates. Additionally, it was found by investigating the hysteresis loops for each story, that the first-story plate absorbed the majority of the damage (Figure 2–23—note that unsymmetrical loops were recorded after one of the actuators reached its maximum stroke in one direction). It was concluded that the steel plate shear wall tested, with moment-resisting connections, exhibited excellent ductility and stable behavior.

The specimen was then modeled analytically considering both finite-element and strip-model approaches. The finite-element simulation predicted the ultimate strength and initial stiffness well for all stories (see earlier Figure 2–4). However, at displacements larger than the yield displacement, the simulation overestimated the stiffness of the steel plate shear wall. It was concluded that this discrepancy was due to the inability to include second-order geometric effects. The strip model also gave good overall agreement with experimental results, with the exception of underestimating the initial stiffness. At loads of 55 percent of the ultimate strength and above, the tangent stiffness of the strip model became approximately equal to that of the experiment.

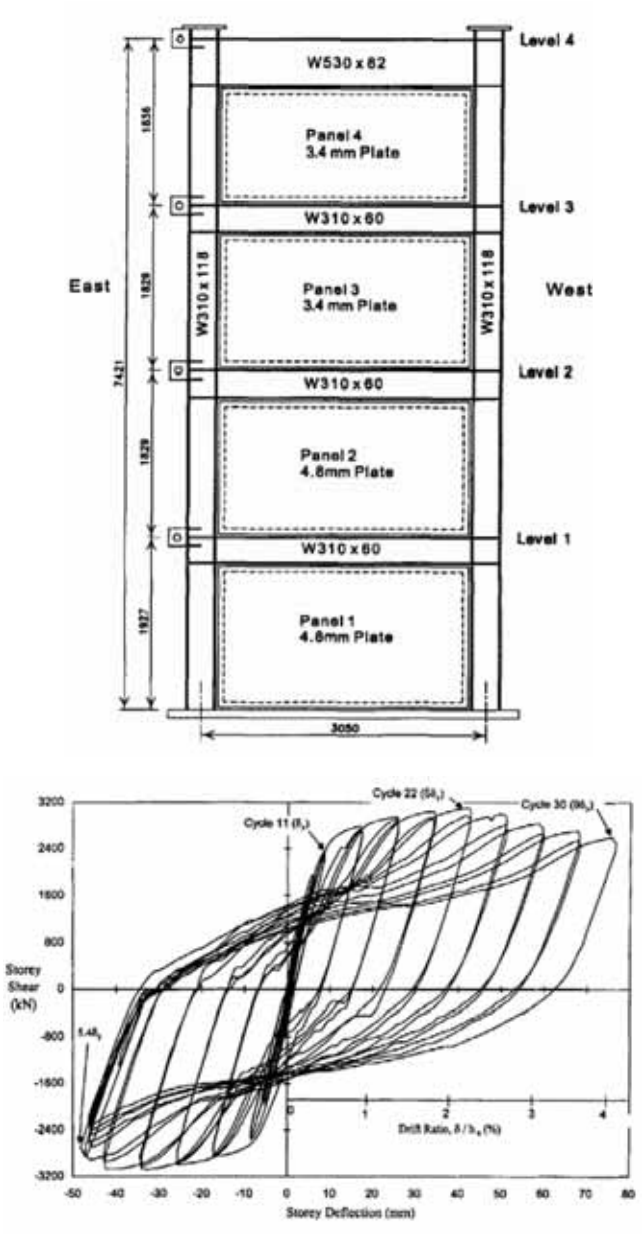

Fig. 2–23. Test setup and quasi-static cyclic response (panel 1) of the SPW tested by Driver et al. (1998a).

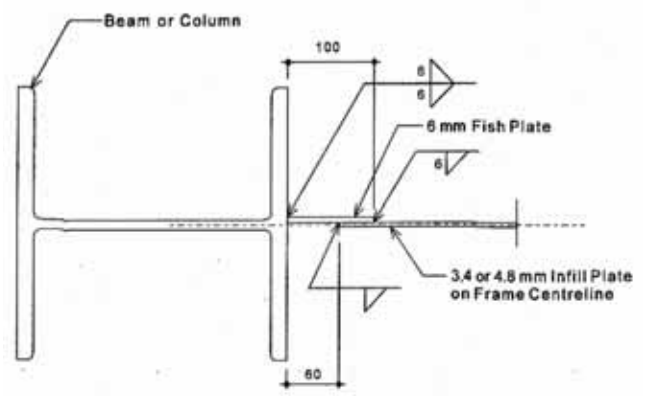

Fig. 2–24. Fish plate connections detail (Driver et al., 1997).

Fig. 2–25. Tears at top corner of first-story panel (courtesy of Robert Driver, University of Alberta, Edmonton, Canada).

Also included in this investigation was a revision of the hysteretic model proposed by Tromposch and Kulak (1987). The model was revised by explicitly separating the contributions from the moment-resisting frame and infill panel. The two components were assigned empirically derived bilinear hysteretic behavior, which when combined, resulted in a trilinear behavior of the system and further improved agreement with experimental results.

Behbahanifard, Grondin, and Elwi (2003)

Behbahanifard et al. (2003) conducted quasi-static lateral cyclic testing, with simulated gravity loads, on a three-story frame structure, consisting of the upper three stories in the four-story SPW structure tested during an earlier study by Driver et al. (1997). Although the infill panel in the first story buckled and underwent some plastic deformations during that previous test, it is reported that there was no significant noticeable permanent damage in the upper three stories. The beam at the top of level 1 was removed and the remainder of the specimen welded to a 90-mm-thick base plate. The tested wall reached a strength of 787 kips (3,500 kN) at a roof displacement of 2 in. (50 mm), after 24 cycles of loading (including 14 cycles after first yielding). The resulting hysteretic behavior measured at each story is shown in Figure 2–28. A tear developed in the first-story panel at a drift of 1.1 in. (28 mm) as a result of low-cycle fatigue from re-

Fig. 2–26. Local buckling and fracture of column at end of test (courtesy of Robert Driver, University of Alberta, Edmonton, Canada).

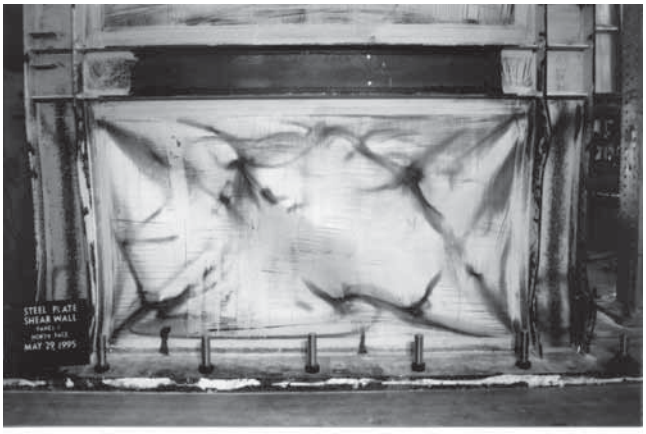

Fig. 2–27. First-story panel deformation at end of test (courtesy of Robert Driver, University of Alberta, Edmonton, Canada).

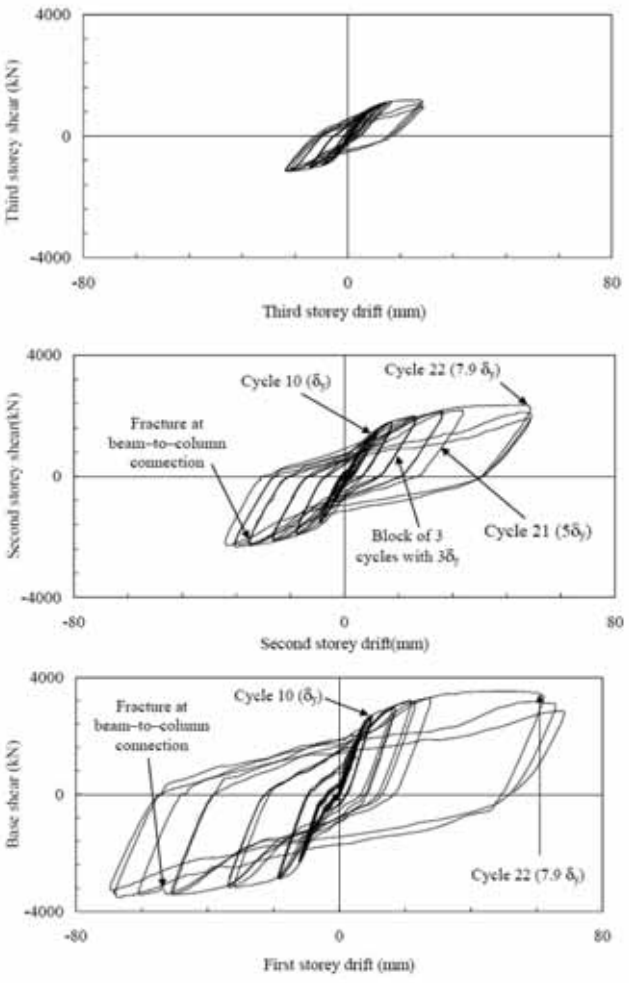

Fig. 2–28. Hysteretic behavior at each story (Behbahanifard et al., 2003).

peated kinking under cyclic plate buckling. Flange buckling at the column base and in the beam at the first level started to develop at a drift of 1.1 in. (28 mm) and beam flange fracture occurred at a drift of 1.4 in. (35 mm). Column buckling also initiated. The beam was rewelded and testing resumed until the actuator maximum stroke of 2 in. (50 mm) was reached. Final state of the specimen is shown in Figure 2–29.

A finite-element model was developed based on the nonlinear dynamic explicit formulation, implementing a kinematic hardening material model to simulate the Bauschinger effect, after experiencing convergence problems analyzing the model using the implicit finite-element model formulation. After validating this model against the experimental results, it was used within a parametric study to identify parameters affecting the stiffness and strength of SPW systems. An interior SPW panel was idealized for this analysis by modeling a single SPW with rigid floor beams and subjected to shear force and constant gravity loading. It was found that a decrease in the aspect ratio produced an increase in the strength and non-dimensional stiffness of SPW. This increase is negligible within the aspect ratio range of 1.0 to 2.0 but noticeable for aspect ratios less than 1.0. Panel out-of-plane imperfections were found to be of no significant consequence, provided they were limited to 1 percent of $\sqrt{L \times h}$ based on this study, which is within normal fabrication tolerances. It was also found that increases in gravity loads and overturning moments on SPW reduces the elastic stiffness and strength of the shear wall panel, as well as the drift at which the peak strength is reached.

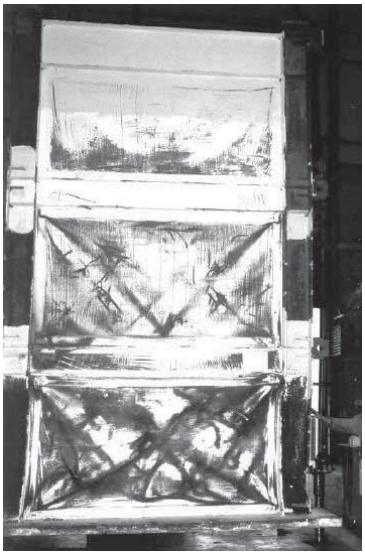

(a)

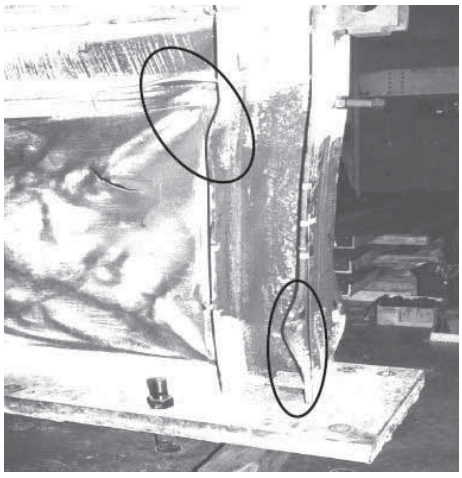

(b)

Fig. 2–29. Specimen at end of test: (a) global view; (b) local column buckling and tear in panel (Behbahanifard et al., 2003).

Rezai (1999)

One four-story, 1:4 scale SPW specimen was subjected to shake-table tests (Rezai, 1999). The shake-table test specimen was one bay wide and four stories high, with a bay width of 3 ft (918 mm) and a story height of 3 ft 11 in. (900 mm). Plates were 0.06 in. (1.5 mm) thick and were welded to a 0.10-in. (2.5-mm)-thick fish plate, which in turn was welded to the members of the boundary frame. Figure 2–30 shows the test specimen along with the instrumentation layout.

Due to limitations in the shake-table capability, the plates remained mostly elastic for all ground motions applied. Some limited energy dissipation was observed in the first two stories. Some yielding was reported to have developed in a first-story column and its base plate.

Finite-element and strip models of the test specimen of Lubell et al. (2000), which are reviewed in the following section, were generated. In both cases, the models overpredicted the initial stiffness. The strip model was able to adequately predict the first yield and ultimate strengths when compared with the experimental results of Lubell et al. (2000). However, it was found that the influence of overturning moment on the base shear versus roof displacement behavior is significant in the accuracy of the strip model. For tall slender walls, large overturning moments result in high flexural and axial columns forces that decrease the overall system stiffness. For tall and narrow panels, the strip model also less accurately predicts the wall stiffness. For shorter and wider walls, such as the Driver et al. (1997) test, the strip model was reported to give more satisfactory results. It was also found that modeling individual stories instead of the entire wall (as suggested at that time in Appendix M of CAN/CSA-S16.1-94) does not accurately represent the wall because it neglects the effects of global overturning moment on the base shear versus roof displacement behavior.

An alternative strip model was proposed in which the strips are reorganized to capture the variation in the inclination of the tension field across the plate, using five strips to model each web plate, and using only the corner nodes of the frame and the mid-points of the columns and beams (Figure 2–31). Rezai gives equations for the areas to be used for these tension elements. Additionally, an effective width concept was employed so that incomplete tension-field action could be accounted for. This effective width depends on the stiffness of the boundary members. The proposed model was able to better represent the initial stiffness of the wall but did not accurately capture its yield and ultimate strengths.

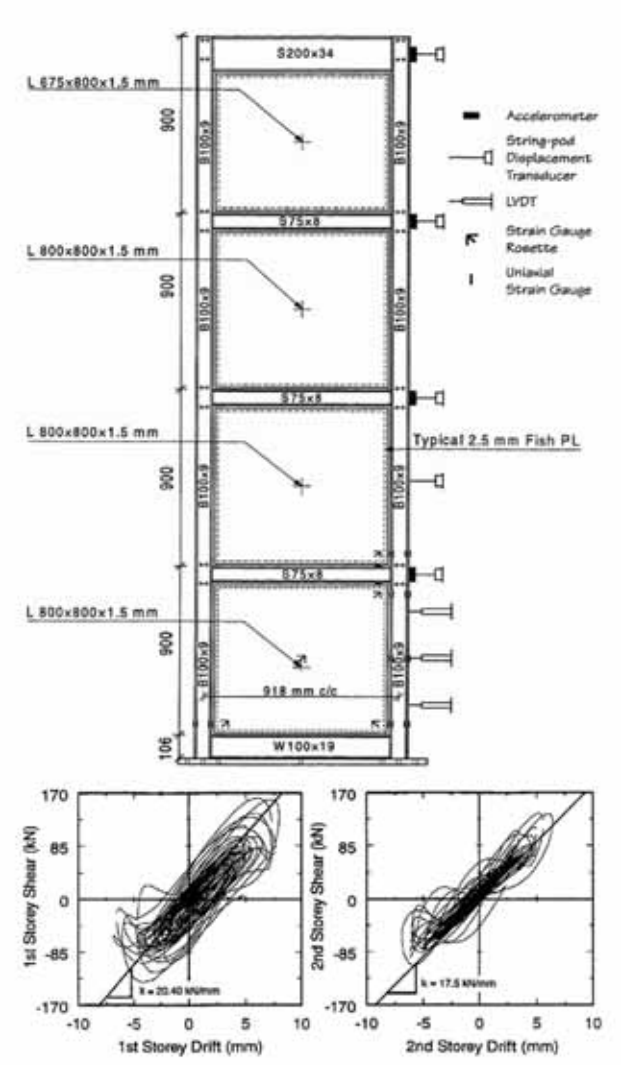

Fig. 2–30. Experimental setup and dynamic response of the SPW tested on a shaking table (Rezai, 1999).

Lubell, Prion, Ventura, and Rezai (2000)

Lubell et al. (2000) tested one four-story and two single-story steel plate shear walls. All specimens had aspect ratios of 1:1 with bay widths and story heights equal to 2 ft 11 in. (900 mm). All infill panels used 0.06-in. (1.5-mm)-thick plates with a yield stress of 46 ksi (320 MPa), and the boundary frames used moment connections. The loading was applied in a cyclic, quasi-static manner following the ATC-24 protocol (ATC, 1992).

The first single-story specimen was pushed to seven times the yield displacement of the structure. This test was terminated because of the failure of a lateral brace due to excessive out-of-plane deflection of the top of the specimen. As a result, the top beam of the second test was stiffened to prevent out-of-plane displacement of the frame. The ultimate strength of the first single-story specimen was found to be 45 kips (200 kN) with a yield strength of 40.5 kips (180 kN) and yield displacement of 0.35 in. (9 mm) (Figure 2–32). In the second test, the yield strength was found to be 42.7 kips (190 kN) at a displacement of 0.12 in. (3 mm) with a ultimate strength of 58.5 kips (260 kN) at four times the yield displacement. Failure of the second specimen occurred when a column fractured after significant plastic hinging at a load of 42.7 kips (190 kN) and displacement of six times the yield displacement (Figure 2–33). The significant increase in the ultimate strength and stiffness of the second test was attributed to the stiffened upper beam. Anchorage of the tension field by use of a substantially stiff top beam was found to be of paramount importance in the performance of steel plate shear walls and is necessary to achieve optimal performance.

The four-story steel plate shear wall specimen was subjected to equal lateral loads applied at each floor level. Grav-

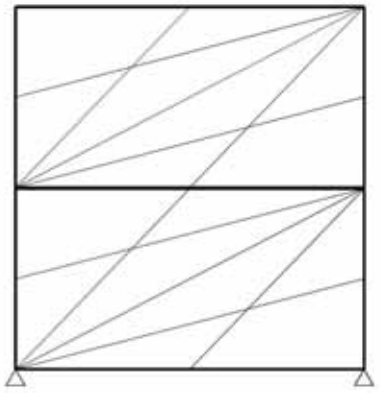

Fig. 2–31. Rezai's tension-strip model (Rezai, 1999).

ity loads were applied using steel plates stacked at each story. This specimen was found to yield at a base shear of 33.7 kips (150 kN) and a first floor displacement of 0.35 in. (9 mm). Failure from global instability due to column yielding occurred at 1.5 times the yield displacement (Figure 2–34). It was observed from the hysteresis loops of the individual stories that the first story absorbed most of the inelastic action and damage. This trend was consistent with what Driver et al. (1997) and Rezai (1999) found in their multi-story steel plate shear wall experiments. In all experiments by Lubell et al. (2000), significant pull-in of the columns was observed. It was reported that all walls ended up in an "hour-glass" shape after significant lateral cyclic displacements were applied (Figure 2–35). This led to the conclusion that a capacity design of the bounding columns in a steel plate shear wall is necessary to ensure that the infill panels yield prior to column hinging and to minimize pull-in of the columns.

Strip models of the specimen were also developed to evaluate the accuracy of the modeling technique. It was found that the strip model overpredicted the elastic stiffness of the first single-story test and the four-story test, but accurately predicted the yield and ultimate strengths as well as the post-yield stiffness. When a stiffer upper beam was present, as in the second single-story test, the strip model was found to give better results for the elastic stiffness. It was concluded that the strip model can accurately represent panels that are dominated by inelastic behavior in shear. When flexural inelastic behavior governs, it was recommended that other more advanced modeling techniques be employed.

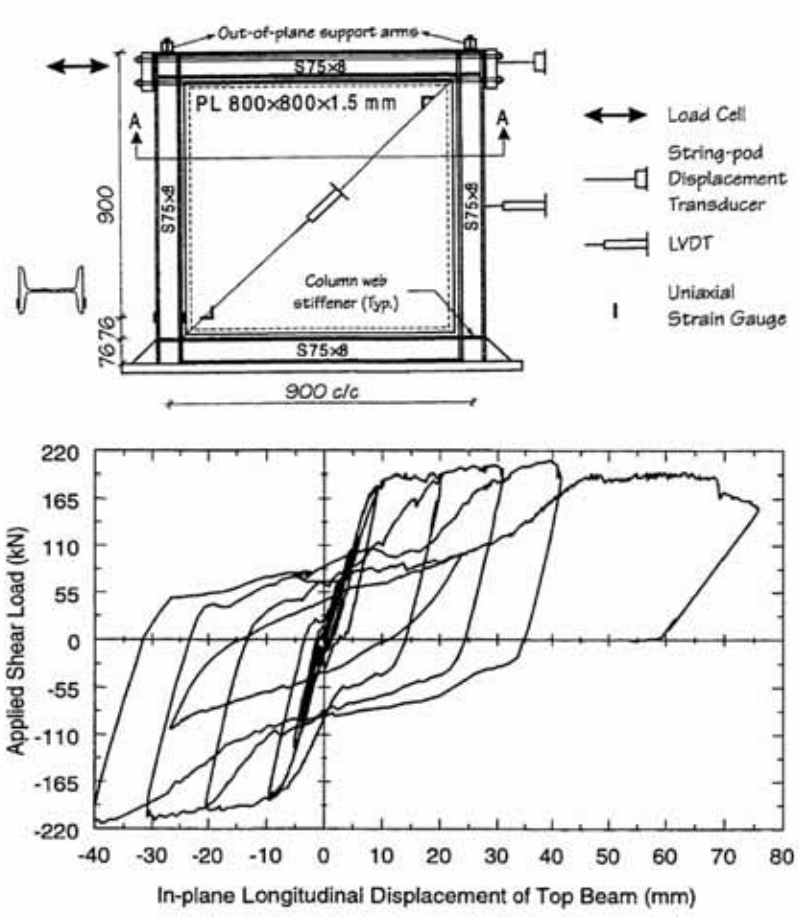

Fig. 2–32. Test setup (taken from Rezai, 1999) and quasi-static cyclic response of specimen SPW1 tested by Lubell et al. (2000).

Astaneh-Asl and Zhao (2001)

In support of the Century Tower project (described in Chapter 1), half-scale three-story SPW test specimens were tested, subjected to a uniform shear force (Figure 2–36). The specimen behaved elastically up to inter-story drifts of 0.6 percent, when first-yield lines were observed on the wall plate and W-shape column (the nongravity column of the system that serves to frame an opening in the wall). Beyond that point, the compression diagonal and tension-field action developed in the wall panels. At 2.2 percent drift, the W-shape column developed flange local buckling. The specimen was subjected to 40 elastic cycles and 39 inelastic cycles, up to an inter-story drift of 3.3 percent and maximum shear strength of 917 kips. At that point, the upper floor-coupling beam completely fractured at the face of the column. A second specimen behaved similarly. It was subjected to 14 elastic cycles up to 0.7 percent drift, and 15 subsequent inelastic cycles, up to an inter-story drift of 2.2 percent and maximum shear force of 1,225 kips, when the upper floor-coupling beam fractured at the face of the column. Figure 2–37 shows the resulting hysteresis loops for the walls in first floor and second floor of the second specimen. Note that the concrete-filled pipe columns resisted approximately 20 percent of the total lateral load, and that beams that connected to the columns transferred their load using reinforcing bars extended into the pipe column and welded to the beam flanges (Hooper, 2005).

2.4. ANALYSIS ISSUES

While past research has shown that the behavior of SPW can be adequately predicted by inelastic finite-element analysis, accurate estimates of response quantities are obtained only when steel panels are modeled using a large number of shell elements (Elgaaly et al., 1993) capable of realistically accounting for material and geometric nonlinearities (Driver et al., 1998b). These limitations lead to sophisticated, time-consuming models that, while suitable for research purposes, are generally not appropriate for practical applications.

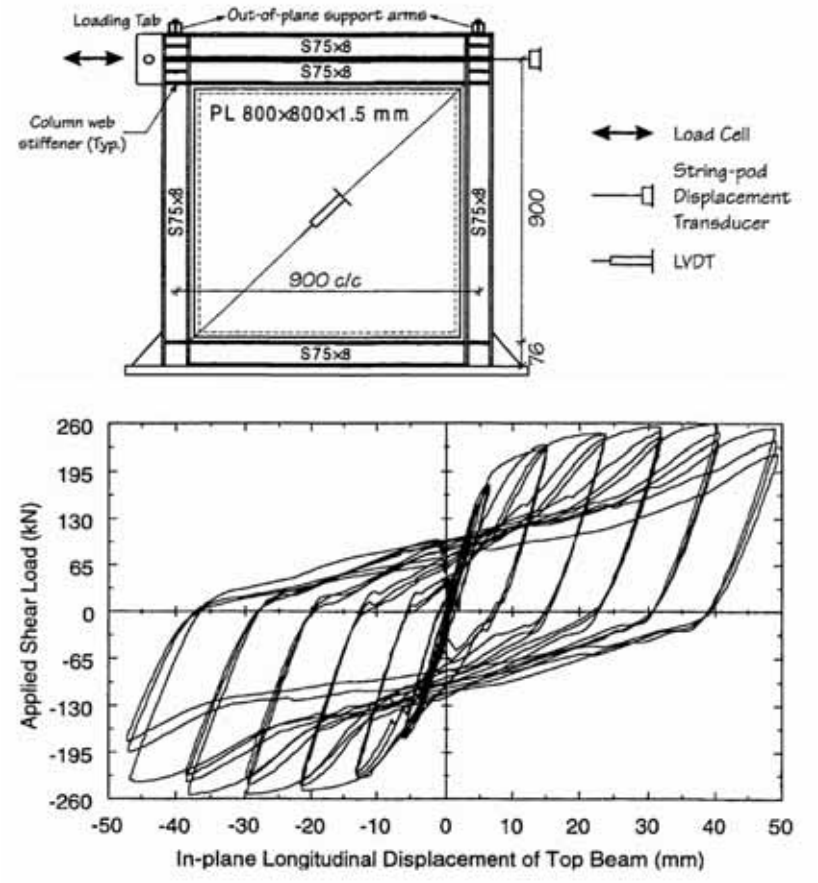

Fig. 2–33. Test setup (taken from Rezai, 1999) and quasi-static cyclic response of specimen SPW2 tested by Lubell et al. (2000).

Fig. 2–34. Near and far view of local instability of columns at first story of SPW (courtesy of Carlos Ventura, University of British Columbia, Vancouver, Canada).

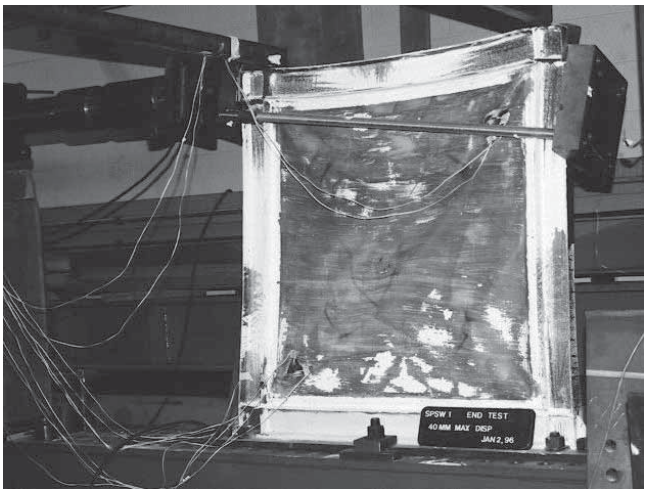

Fig. 2–35. Hour-glass shape of specimen due to "pull-in" of columns and beams (courtesy of Carlos Ventura, University of British Columbia, Vancouver, Canada).

Unfortunately, usage of simpler elements results in models that are not capable of providing reliable estimates of stiffness, strength, and hysteretic characteristics (Elgaaly et al., 1993). In particular, models using "standard" (i.e., elastic and isotropic) shell elements do not provide meaningful information because they do not capture transverse forces on boundary elements. Since steel panels of typical SPW buckle at very low deformation levels and tension-field action develops well before any yielding occurs, the pre-buckling stiffness predicted by elastic, isotropic shell elements overestimates the actual rigidity of SPW. Elastic finite-element analyses can also be misleading as they may consider the wall plate as contributing to resist gravity loads and overturning moments in ways not actually possible with thin infill plates.

A more practical and convenient analytical tool is the strip model, originally proposed by Thorburn et al. (1983). As described earlier, this approach consists of modeling the steel panel as a set of parallel, uniformly spaced, tension-only strips pinned at both ends (i.e., elements capable of resisting

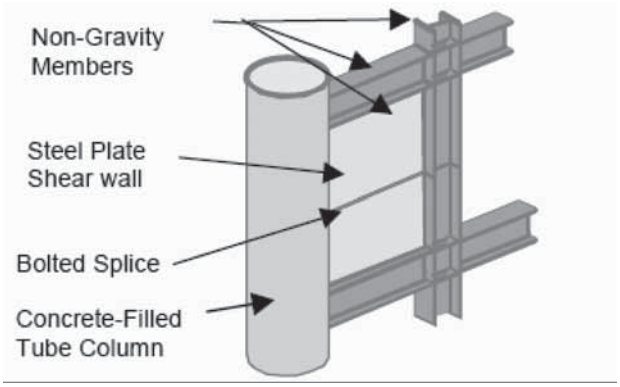

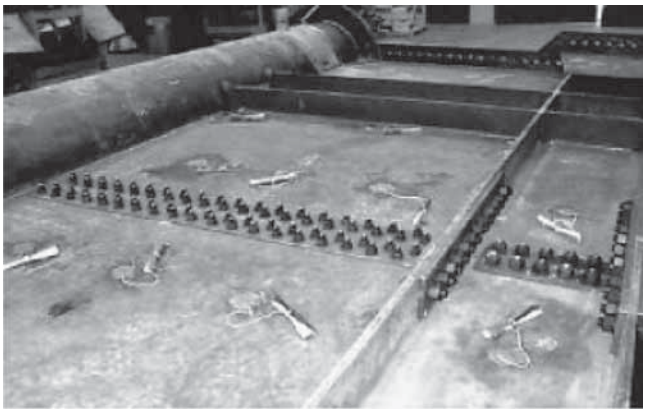

Fig. 2–36. Specimen tested by Astaneh-Asl and Zhao (2001).

tensile axial forces only), while the beams and columns are modeled with conventional beam elements (Figure 2–38). In a way, the strips represent the post-buckling diagonal folds described in Section 2.1. The modulus of elasticity of the strips is set equal to that of steel, and the area of each strip is set equal to the steel panel thickness multiplied by the distance between the strips (measured along a direction perpendicular to that of the strips).

It has been shown that the strip model can adequately predict the initial, pre-yielding stiffness of a SPW and forces in frame members under service loads (Timler and Kulak, 1983). It can also be used in nonlinear (pushover) analysis to obtain the full force-displacement relationship for the wall and ultimate forces in the system elements. For static nonlinear analysis, it is suggested that an elasto-plastic (i.e., zero post-yielding stiffness) axial force versus axial deformation relationship be used for each strip. Additionally, beam elements capable of accounting for inelastic deformations in frame members, which are likely to occur at large deformations levels, should be used. This approach has successfully been used to reasonably predict monotonic force-displacement relationships of complete SPW, as well as those of individual stories (Figure 2-4) (Driver et al., 1998).

The strip model has also been shown to be capable of successfully predicting the quasi-static cyclic response of SPW (Elgaaly et al., 1993; Elgaaly and Liu, 1997; Lubell et al., 2000). This kind of analysis requires models that have a symmetric layout of strip elements to account for tension-field action in both loading directions (Figure 2–39). It must be noted that, since the strips are tension-only elements, the strip force versus strip deformation relationship should have the characteristics schematically described in Figure 2–39b. Since, when unloaded after an incursion into the inelastic range (point "a"), a strip exhibits residual deformations (point "b"), tensile stresses will not develop in the next cycle in the same direction until point "b" is reached (these hysteretic characteristics cause the "pinching" behavior described earlier). A comparison between experimental and analytical results can be seen in Figure 2–40, which shows a case where a trilinear hysteretic model was used. Similar models

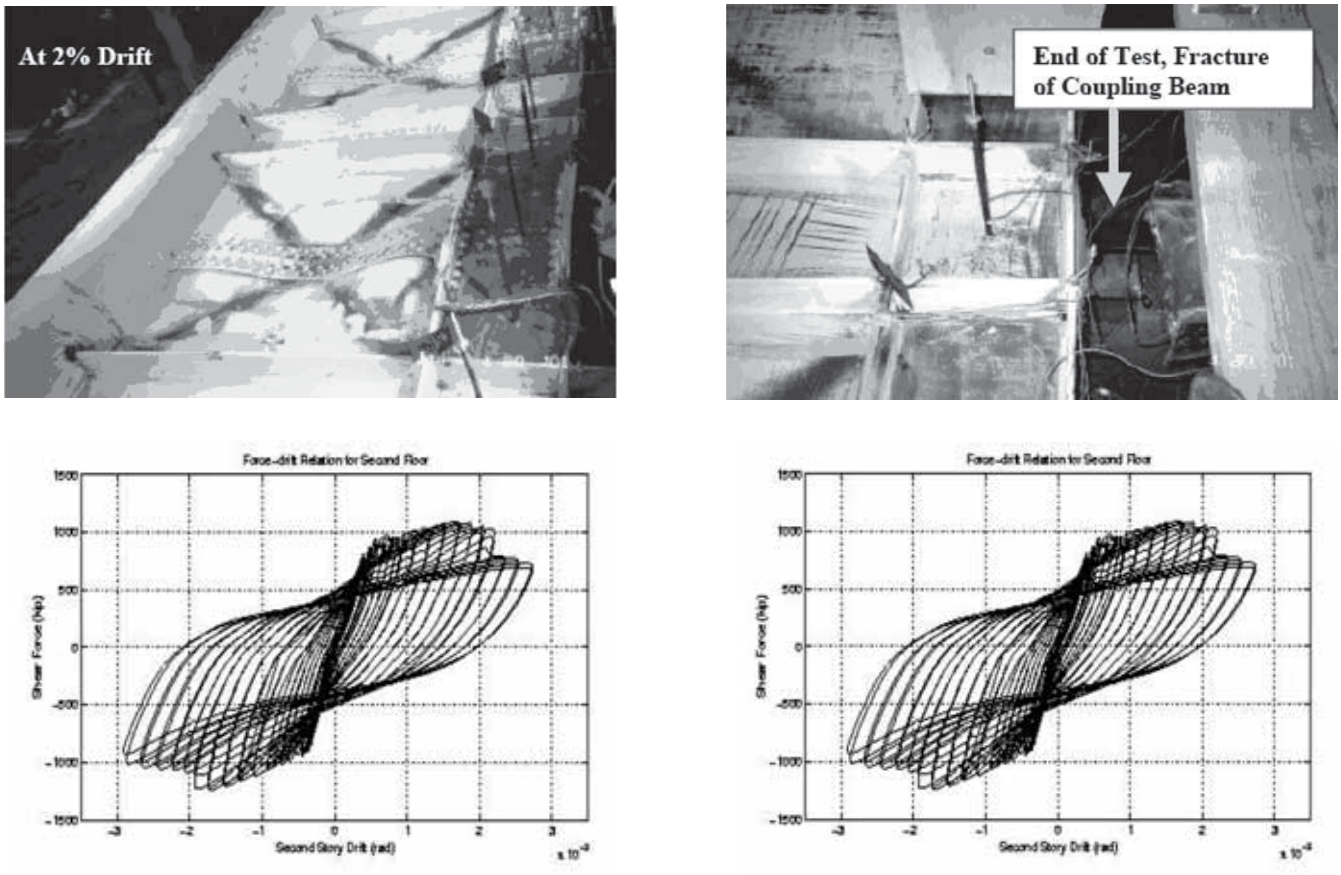

Fig. 2–37. Inelastic deformation of SPW and hysteretic response (Astaneh-Asl and Zhao, 2001).

have also been used to perform nonlinear dynamic analysis (Bruneau and Bhagwagar, 2002).

In the case of multi-story SPW, equally spaced strips oriented at all stories as indicated by Equation 2–2 result in models having staggered node points at the beams (Timler et al., 1998; Bruneau and Bhagwagar, 2002). An example can be seen in Figure 2–41a. Such models are unnecessarily complicated and are likely to indicate artificial bending in beams due to differential pulling forces. The strip inclination angles at different stories are typically similar. For practical purposes, it is then preferable to use models where the strips have the same inclination at all stories and common nodes at the beams (Figure 2–41b). The inclination angle can be calculated as the average of the values calculated at each story. It has been shown that this simplification has little effect on analytical results (Timler et al., 1998). This recommendation also applies for models having a symmetric array of strip elements.

2.5. DESIGN METHODS

Design methods prescribed in various Specifications are reviewed in the subsequent section and chapter. However, plastic analysis can be a useful complementary tool for design. Using the collapse mechanism of a single-story SPW in a frame with simple connections represented by the strip model, as shown in Figure 2–42, results in the following equation for maximum shear strength (Berman and Bruneau, 2003a):

$$V = \frac{1}{2} F_y t L \sin 2\alpha \tag{2–5}$$

where F_y is the infill panel yield stress and other terms are as previously defined.

For a single-story SPW in a frame with rigid beam-to-column connections, plastic analysis can again be used to find the maximum shear strength as

$$V = \frac{1}{2} F_y t L \sin 2\alpha + \frac{4M_p}{h} \tag{2–6}$$

which considers flexural hinging in beams or columns in addition to plate yielding, and where M_p is the smaller of the beam and column plastic moments. It also assumes that this strength can be attained prior to the development of undesirable limit states, such as plate fracture.

While this approach does not provide information about the magnitude of the displacement response, it gives equations to estimate the ultimate shear strength of a SPW by hand calculations. These expressions can also be used to gain insight into the most probable collapse mechanism, i.e.,

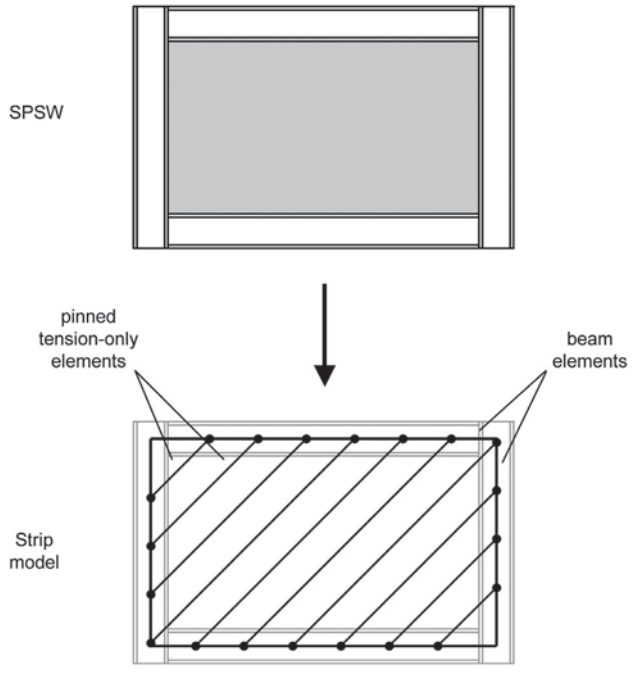

Fig. 2–38. Strip model for static (linear and nonlinear) analysis of SPW (courtesy of Diego López-García, Pontificia Universidad Católica de Chile, Chile).

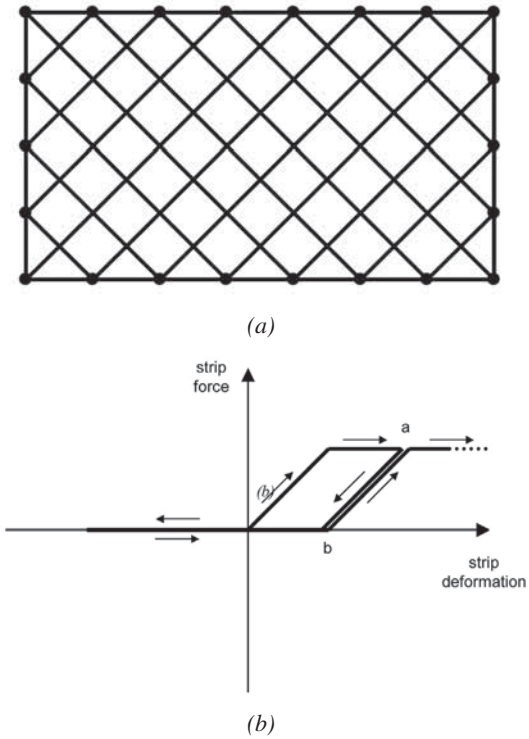

(a)

(b)

Fig. 2–39. Strip model for cyclic static and dynamic nonlinear analysis: (a) diagram of panel model; (b) hysteretic strip force vs. strip deformation relationship (courtesy of Diego López-Garcia, Pontificia Universidad Católica de Chile, Chile).

the one for which the corresponding ultimate shear strength is a minimum. For instance, the shear strength at story "*i*" developing an undesirable soft-story mechanism (i.e., plastic hinges at the ends of the columns in a given story) in a multistory SPW with moment-resisting connections is given by

$$\sum_{j=i}^{n} V_j = \frac{1}{2} F_y\, t_{wi}\, L \sin\left(2\alpha\right) + \frac{4M_{pci}}{h_i} \qquad (2\text{–}7)$$

where V_j = lateral loads applied above story i and t_{wi}, M_{pci}, and h_i are thickness of the steel panel, plastic moment capacity of columns, and height of story i, respectively. Similar expressions for other possible collapse mechanisms are presented in Berman and Bruneau (2003a). These equations can be used to determine an infill panel thickness for use in development of the strip model.

Ideally, a SPW used in seismic applications should be designed in such a way that all its steel panels dissipate energy through inelastic deformations when the structure is subjected to the expected seismic actions. Hence, for a given frame geometry (which is often dictated by architectural/functional considerations), the thickness of the steel panel at a given story should be determined as a function of the corresponding story shear demand. A practical approach consists of solving Equation 2–5 for t_w, which gives

$$t_{wi} = \frac{2V_i}{F_y L \sin\left(2\alpha_i\right)} \qquad (2\text{–}8)$$

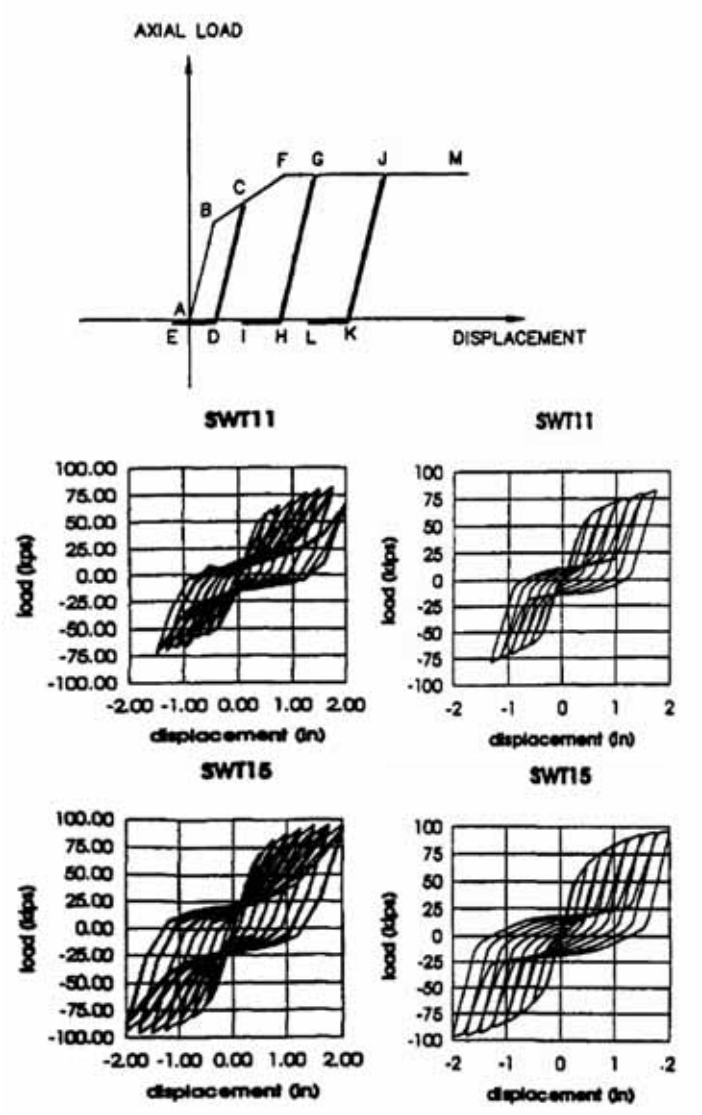

Fig. 2–40. Trilinear hysteretic model for strip elements proposed by Elgaaly and Liu (1997) and comparison between experimental (left) and analytical (right) quasi-static cyclic response of SPW specimens.

where subscript "*i*" refers to story *i*. Equation 2–8 is slightly conservative for simple beam-to-column connections and somewhat conservative for moment-resistant connections, since the contribution of this type of connection to the lateral resistance of the SPW is neglected in Equation 2–5. It must be noted that Equation 2–8 indicates that steel panels should have different thickness at different stories, a condition that is sometimes difficult to achieve in practice due to the availability of steel plates.

As mentioned before, the ultimate strength of a steel panel is fully developed only when the corresponding frame members are sufficiently stiff and strong to "anchor" the tension diagonals. Furthermore, for vertical boundary elements (VBE), it has been recommended (Montgomery and Medhekar, 2001) that the moment of inertia, I_c, should be such that

$$0.70\,h\left(\frac{t_w}{2\,L\,I_c}\right)^{0.25} \leq 2.5 \qquad (2\text{–}9)$$

which leads to

$$I_c \geq \frac{0.00307 t_w h^4}{L} \qquad (2\text{–}10)$$

While no practical expressions similar to Equation 2–10 have been proposed for the horizontal boundary elements (HBE) at the roof and foundation levels, it is possible to modify the same equation to be applicable to HBE. However, sections providing the strength necessary to satisfy the corresponding flexural demands are likely to provide an adequate stiffness. It must be remembered that the HBE at the roof and foundation levels must anchor the pulling action from a yielding steel panel, which generally results in substantial sizes.

It has been argued that, since the behavior of SPW is similar to that of vertically cantilevered plate girders (VBE are analogous to the plate-girder flanges, HBE to the plate-girder stiffeners, and steel panels to the plate-girder web), the former could be designed using well-established procedures suitable for the latter (Astaneh-Asl, 2001). However, while the plate girder analogy is conceptually valid and useful, it is quantitatively inadequate and leads to overly conservative designs. Detailed explanations, including quantitative comparisons, are presented in Berman and Bruneau (2004).

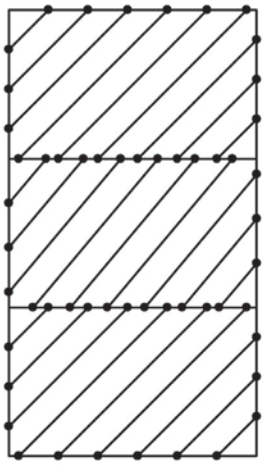

(a)

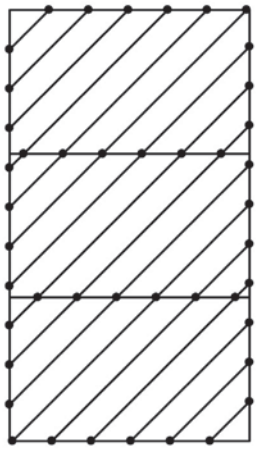

(b)

Fig. 2–41. Strip models having (a) staggered and (b) common strip nodes at the beams (courtesy of Diego López-García, Pontificia Universidad Católica de Chile, Chile).

2.6. CODE DEVELOPMENT

2.6.1. CSA S16-01

Canadian standard CAN/CSA-S16, *Limit States Design of Steel Structures* (CSA, 2001), has included specifications for the design of SPW since 1994. In this document, the equiva-

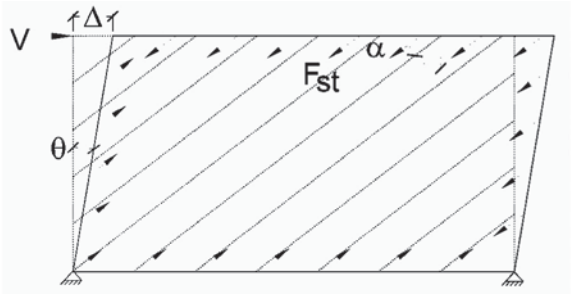

Fig. 2–42. Single-story collapse mechanism (Berman and Bruneau, 2003a).

lent truss model (Thorburn et al., 1983) is recommended for preliminary design purposes. The approach consists of first designing a tension-only braced frame, by using diagonal steel truss members where steel panels would be otherwise be used in the SPW. The areas of the diagonal steel truss members are designed to resist the specified lateral loads, and to meet drift requirements. The truss members are then converted into steel panels. The thickness, t_{wi}, of the steel panel at story i, is given by

$$t_{wi} = \frac{2 A_i \sin\theta_i \sin 2\theta_i}{L \sin^2 2\alpha_i} \qquad (2\text{–}11)$$

where A_i and θ_i are the area and the angle of inclination (measured with respect to a vertical axis) of the equivalent truss member at story i, respectively. While this approach is useful at the preliminary design stage, the resulting strength of the steel panels can be somewhat unconservative when the width-to-height ratio is not equal to unity (Berman and Bruneau, 2003a). The plate is then divided into strips (per the approach described earlier) and analyzed for the specified loads.

The CAN/CSA-S16-01 standard recognizes limited ductility plate walls (i.e., SPW with no special requirements for beam-to-column connections and assigned a force modification factor R = 2) and ductile plate walls (i.e., SPW with moment-resisting beam-to-column connections and a force modification factor R = 5, the largest R value assigned to the most ductile systems in this standard). Ductile walls are designed according to capacity design principles, with plate yielding providing the "fuse." For limited ductility plate walls, there are no special seismic requirements.

For ductile SPW, horizontal and vertical boundary elements are required to be designed to elastically resist development of the full expected yield strength of the infill plates. This ensures that the infill plate can yield in tension prior to plastic hinging of the boundary elements (providing for substantial energy dissipation in seismic applications). Such capacity design can be achieved by designing the boundary elements for the forces found from pushover analysis of the strip model or indirectly from a procedure in CAN/CSA S16-01. The connection of the infill plate to the boundary elements should also be designed for the expected yield strength of the infill plate, and can use either a welded or bolted configuration. Furthermore, the vertical boundary elements should satisfy a minimum stiffness requirement to prevent excessive deformations under the tension-field action of the web plate (Equation 2–8). Finally, horizontal boundary elements should be provided at the top and bottom of a SPW to anchor the tension field.

Most features of CAN/CSA-S16-01 have been implemented in the United States seismic design provisions, either in specifications or in commentary, and are therefore not presented in detail in this section. However, an important difference between the United States and Canadian practice is that analysis methods for obtaining forces to be used in capacity design of SPSW are not included in the requirements of United States specifications, but rather presented in their commentaries. In that case, the CAN/CSA-S16-01 requires capacity design of the columns in ductile plate walls and specifies that this can be achieved indirectly by the use of a factor B, defined as the ratio of probable shear resistance, V_{re}, at the base of the wall to the calculated factored design base shear. The probable shear resistance at the base of the wall is given by $V_{re} = 0.5R_yF_ytL \sin 2\alpha$, where R_y is the ratio of the expected (mean) steel yield stress to the specified minimum yield stress (specified as 1.1 for A572 Gr. 50 steel), F_y is the specified minimum yield stress of the plate, L is the bay width, and α has been defined earlier. The design axial forces and local moments in the columns are then amplified by this factor. More specifically, the column axial forces determined from the factored design overturning moment at the base of the wall are amplified by B and kept constant for a height of either two stories or L (the bay width), whichever is greater. The axial forces then are assumed to linearly decrease to B times the axial forces found from the actual factored overturning moment at one story below the top of the wall. The maximum value of B (which is meant to ensure a ductile failure mode) can be limited to the value of the ductility factor R_μ assigned by CAN/CSA-S16-01.

2.6.2. 2003 NEHRP Recommended Provisions (FEMA 450) and AISC 2005 Seismic Provisions

The NEHRP *Recommended Provisions for Seismic Regulations for New Buildings and Other Structures* (FEMA, 2004; referred to here as FEMA 450) and the 2005 *Seismic Provisions for Structural Steel Buildings* (AISC, 2005; referred to here as AISC 360) include minimum design requirements for SPW. It must be noted that SPW are denoted as Special Steel Plate Walls in FEMA 450 and as Special Plate Shear Walls in AISC 341. In both documents, columns are designated as Vertical Boundary Elements (VBE), beams are referred to as Horizontal Boundary Elements (HBE), steel panels are denoted simply as webs, and a web and its surrounding HBE and VBE constitute a panel (this last definition is not explicit in AISC 341).

In these documents, the nominal strength of a web is set equal to

$$V_n = 0.42\, F_y t_w L_{cf} \sin(2\alpha) \qquad (2\text{–}12)$$

where L_{cf} is the clear distance between VBE flanges. In Equation 2–12, α is to be calculated using Equation 2–1. It must be noted that Equation 2–12 is identical to Equation 2–5 except that L (distance between VBE centerlines) is

replaced by L_{cf} and the 0.50 factor is replaced by 0.42, which is simply 0.50 divided by an overstrength factor equal to 1.2 (for consistency with other lateral-load resisting structural systems that are designed to resist the specified loads without considering their overstrength). The available shear strength of a web is determined as ϕV_n or V_n/Ω, where $\phi = 0.90$ and $\Omega = 1.67$. According to these regulations, HBE and VBE are to remain essentially elastic under forces generated by fully yielded webs, but flexural hinges are allowed at the ends of HBE. Both documents require that VBE satisfy Equation 2–9 and that $0.80 < L/h \leq 2.50$. In addition, several details are specified for HBE-VBE connections. Finally, FEMA 450 imposes a limit on the slenderness of the web, quantitatively expressed by

$$\frac{\min(L, h)}{t_w} \leq 25\sqrt{\frac{E}{F_y}} \qquad (2\text{–}13)$$

This limit is well into the elastic shear-buckling range. It is based on the tested range of slenderness, rather than on separating modes of behavior.

Chapter 3

System Behavior and Design Methods

3.1. OVERVIEW

This chapter provides a general discussion of the behavior and design of Special Plate Shear Walls (SPSW) and other types of steel plate shear walls.

The fundamental mechanics of steel plate shear walls are discussed here as they pertain to the design of the system. Likewise, the analytical methods discussed herein are intended to be used to derive design forces for members of SPSW and to estimate the displacement of SPSW in a manner that is consistent with building code requirements. More precise modeling of the behavior of SPSW is beyond the scope of this Design Guide.

Methods of analysis are presented in this chapter. The application of the recommended methods is more fully illustrated in Chapters 4 and 5.

3.2. MECHANICS

Steel plate shear walls typically resist lateral loads primarily through diagonal tension in the web plate and overturning forces in the adjoining columns. This behavior is idealized in Figure 3–1. As is explained later, this is a simplification of steel plate shear wall behavior, and the internal forces of slender-web steel plate shear walls (such as SPSW) must be examined more closely.

Web plates in steel plate shear walls can be categorized according to their ability to resist buckling. Typical web plates are unstiffened and very slender, and their compression strength is negligible. Subsequent to compression buckling of the web plate on one diagonal, a tension field will develop in the plate along the opposite diagonal. In this way, frames with slender webs can resist very large forces and are thus an economical means to provide lateral strength and stiffness. The effects of web-plate tension on the adjoining frame elements constitute a central part of the understanding of walls with this type of web plate.

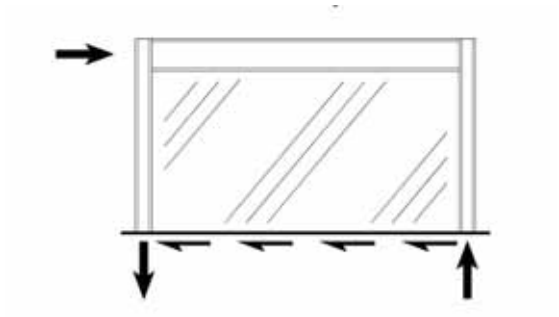

Fig. 3–1. Idealized shear wall behavior.

As discussed in Chapter 1, stiffened steel plate shear walls have also been used to resist seismic forces, primarily in Japan. As is the case with plate girders, the reduction of web-plate slenderness by the introduction of stiffeners increases its strength. Stiffening typically consists of plates welded to one or both sides of the steel web plate. Concrete can also be used to stiffen web plates; typically, walls stiffened in this manner qualify as composite plate shear walls (discussed below). While stiffening increases the effectiveness of the web plate, it is not typically as economical as the unstiffened web plate. For this reason, the SPSW system is based on unstiffened, slender webs.

Composite steel plate shear walls (C-SPW) similarly provide stiffening of the steel web plate, permitting utilization of the full yield strength of the steel material. Additionally, the shear strength of the concrete is effective to some degree in the resistance to lateral loads (although AISC 341 does not permit it to be utilized in design). As is the case for stiffened shear walls, C-SPW are typically less economical than walls with slender, unstiffened webs.

The SPSW system, as listed by ASCE 7 and treated by AISC 341, is based on the use of slender web plates. Neither stiffened-web steel plate shear walls nor composite steel plate shear walls should be considered SPSW, and the design provisions in Part I of AISC 341 are not applicable to such walls. C-SPW should be designed in accordance with Part II of AISC 341; there is no equivalent set of seismic design provisions applicable to stiffened-web steel plate shear walls.

The design of both stiffened-web steel plate shear walls and C-SPW is outside of the scope of this Design Guide. Nonetheless, this chapter provides a brief discussion of their behavior. The design examples that follow in Chapters 4 and 5 are limited to unstiffened, slender-web SPSW.

3.2.1. Unstiffened Steel Plate Shear Walls

Unstiffened steel plate shear walls are typically designed as Special Plate Shear Walls (SPSW). AISC 341 includes high-seismic design provisions for SPSW (Part I, Section 17); no low-seismic design provisions for the system exist. Both design examples in this Design Guide use unstiffened, slender steel plate shear walls. Design Example 1 (Chapter 4) illustrates the use of the system for low-seismic design (e.g., Seismic Design Category B); Design Example 2 (Chapter 5)

illustrates the use of the system for high-seismic design (e.g., Seismic Design Category D).

Typical SPSW have slender webs that are capable of resisting large tension forces but little or no compression. This behavior is analogous to tension-only bracing, which relies on beams in compression to transmit the horizontal component of a brace force to the brace at the level below, and in which overturning forces are imposed on columns.

Figure 3–2 shows the internal forces in a braced frame in which the braces only resist tension. Overturning forces are resisted by the columns and are delivered by the vertical component of the brace forces. The beams serve to transfer the horizontal component of the force in the brace above across the frame to the connection point of the brace below. Where braces only resist tension, the beams are typically subject to large compression forces.

This behavior is also analogous to that of the transverse stiffeners in plate girders. Tension-field action in the webs requires a transverse compression strut in order to be transmitted along the length of the member. Figure 3–3 shows the role of transverse stiffeners in a plate girder.

While both of these analogies are useful in the basic understanding of SPSW behavior, they are insufficient for capturing many of the aspects of SPSW behavior that must be understood in order to design the system. The mechanics of SPSW behavior are distinct from both tension-only bracing and plate girders. While the web plates work almost entirely in tension, the beams and columns that constitute the frame around the web plate are designed differently from the frame members of tension-only bracing, and from the flanges and stiffeners of plate girders. Columns in SPSW are referred to as Vertical Boundary Elements, or VBE; beams are referred to as Horizontal Boundary Elements, or HBE.

The tension in the web plate acts along the length of the boundary elements, rather than only at the intersection of beams and columns, as is the case for tension-only bracing. As such, large inward forces can be exerted on the boundary elements.

While flanges in plate girders are not expected to provide sufficient stiffness to permit the webs to develop their full tension strength along their entire depth, VBE of SPSW are designed to provide such stiffness, and the full tension strength of the web plate is realized. Both HBE and VBE are designed to resist web-plate tension forces acting inward on the SPSW at an angle determined from the frame geometry and member section properties. VBE and HBE resist these inward forces through flexure. Figure 3–4 illustrates the resulting flexural deformation of the boundary elements due to these inward forces schematically.

It should be noted that the effect of these inward forces acting directly on the HBE is typically counteracted to a large degree by similar tensile forces in the web plate of the adjacent story, although these are often of different magnitudes. Such counteracting tensile forces are not, of course, present at the top beam of a SPSW, nor at the foundation, and the design of those elements must include consideration of the inward forces. The beam at the top story of a SPSW is typically quite deep. At the foundation, a steel or concrete

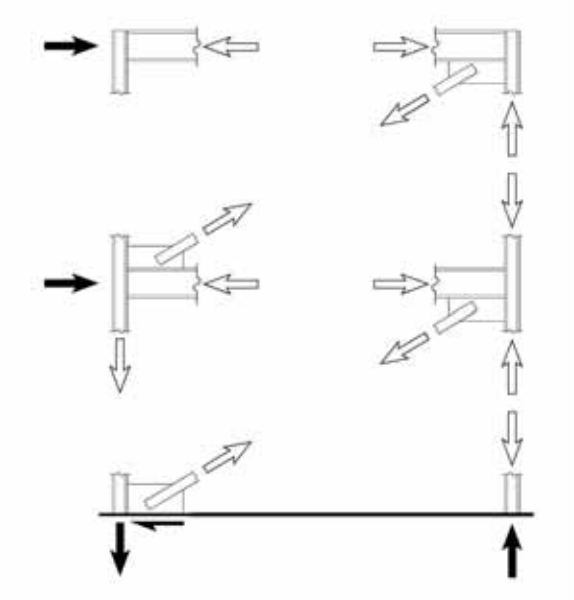

Fig. 3–2. Beam and column forces in tension-only bracing configurations.

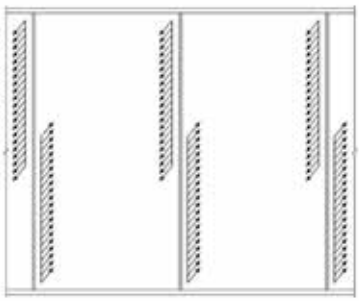

Fig. 3–3. Plate-girder transverse stiffener behavior.

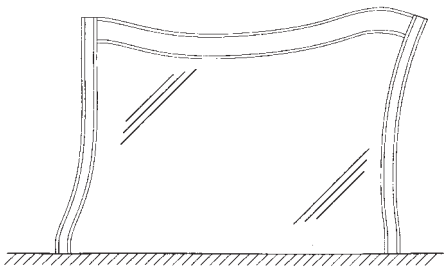

Fig. 3–4. Inward flexure of SPSW boundary elements.

grade beam with sufficient strength to anchor the tension in the web plate is typically provided.

These inward forces, and the resistance provided by the boundary elements, are fundamental to the understanding of SPSW behavior. Figure 3–5 shows free-body diagrams of the web plate, boundary elements, and SPSW. No end moments are shown, as though the HBE-to-VBE connections are pinned. In high-seismic design these connections are required to be rigid, and end moments result from both the inward flexure shown in Figure 3–4 and from frame behavior. For purposes of illustrating the effects of web-plate tension, the figure does not include fixity of the beam-to-column connection.

As Figure 3–5 indicates, the tensile forces in the web plate induce flexure in the VBE, in addition to the axial forces due to overturning of the wall. If the transverse stiffness (moment of inertia with respect to in-plane flexure) of the VBE is small, uniform tension cannot be developed across the web plate and the strength of the system is significantly reduced. (Such behavior is similar to that of plate girders.) If the transverse stiffness of VBE is high, web plates can develop their full tension strength at the vertical interfaces with the VBE. The shear due to web-plate tension is in opposite directions in the VBE on either side of the web plate, and the horizontal reaction at the column base of the VBE in compression is opposite the horizontal reaction of the web plate.

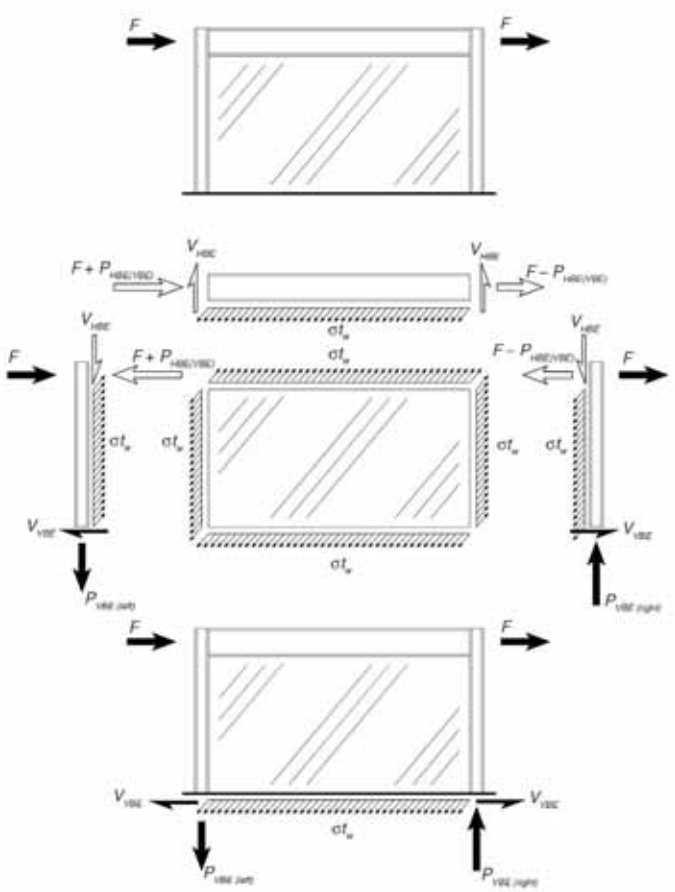

Fig. 3–5. Free-body diagrams of the web plate, boundary elements, and SPSW.

Figure 3–5 also shows that the inward flexure of the VBE is resisted by the HBE at the top and bottom of the VBE segment (typically at each floor). Thus, the HBE are required to resist significant compression in conjunction with the flexural forces induced by tension in the web plates.

Additionally, the figure shows that the compression under the VBE on the right ($P_{VBE\ (right)}$) is balanced by both tension in the left-hand VBE ($P_{VBE\ (left)}$) and in the web plate (σt_w). This results in increased compression in the right-hand VBE (as compared to the simplistic model illustated in Figure 3–1) due to the decreased distance between the centroids of the compression and tension forces. It also results in a somewhat reduced tension force in the left-hand VBE due to the assistance provided by the web plate.

The restraint provided by HBE enables the VBE to resist the flexure caused by web-plate tension. HBE typically occur at floor levels, where they also serve as the beams or girders supporting the deck. In some cases, designers have introduced additional horizontal struts in between story levels to reduce the flexural forces in, and flexibility of, the VBE (Eatherton, 2004). This is especially effective at tall stories, where the flexural forces in VBE are large, and where the required flexural stiffness governs the design of VBE. The seismic provisions for SPSW do not anticipate such intermediate struts, although their use is consistent with methods for design of intermediate HBE at openings. Additional requirements for such intermediate struts are discussed later in this chapter.

Note that in Figure 3–5, the force at the upper-right connection (between the HBE and the VBE in compression) is the difference between two components: the collector force (F), and the inward reaction from the VBE ($P_{HBE(VBE)}$). In some conditions this will be in tension, in others it will be in compression. It is typically in tension at the top story and at levels at which the web-plate thickness is reduced by a large percentage; it is typically in compression elsewhere. At the VBE in tension, the connection is in compression and the two components are additive.

The symbols in Figure 3–5 are as follows:

F = the applied lateral force on the wall

$P_{HBE(VBE)}$ = the axial force applied at the end of the HBE due to the web-plate tension on the VBE

P_{VBE} = the axial force reaction of the VBE

V_{HBE} = the shear reaction of the HBE due to the web-plate tension

V_{VBE} = the shear reaction of the VBE due to the web-plate tension

t_w = web-plate thickness

σ = web-plate tension stress

In high-seismic design of SPSW, it is assumed that lateral loads will be sufficient to cause full tension yielding of the web plate, and thus the web-plate forces are uniform, as shown in the figure (in the elastic range, the web-plate tension stress is far from uniform). This condition of full tension yielding is used to define the required strength of the connections of the web plate to the boundary elements.

The tension stress in the web plate is used, in conjunction with gravity loads, to define the required strength of the boundary elements themselves. For this use it is convenient to decompose the diagonal tension stress in the web plate. Figure 3–6 shows the stresses acting on the vertical and horizontal interfaces of the web plate. In this analysis of stresses, it is assumed that the web plate is in pure tension and that no shear or compression stresses exist on sections cut in the direction of the tension stress.

The following symbols are used in Figure 3–6:

α = angle of tension stress (measured from vertical)

Δ = width of web-plate segment under consideration

σ_{11} = principal stress at horizontal boundary

σ_{12} = shear stress at horizontal boundary

σ_{22} = principal stress at vertical boundary

σ_{21} = shear stress at vertical boundary

σ = web-plate tension stress

The interface stresses are functions of both the web-plate stress and the angle of tension in the web plate. Equations for these stresses are derived from statics using trigonometric functions:

$$\sigma_{11} = \sigma \cos^2(\alpha)$$

$$\sigma_{12} = \sigma \sin(\alpha) \cos(\alpha) = \tfrac{1}{2} \sigma \sin(2\alpha)$$

$$\sigma_{22} = \sigma \sin^2(\alpha)$$

$$\sigma_{21} = \sigma \sin(\alpha) \cos(\alpha) = \tfrac{1}{2} \sigma \sin(2\alpha)$$

In order to apply these equations, it is necessary to establish the angle of tension stress in the web plate. This is done using AISC 341 Equation 17–2 (Equation 3–1):

$$\tan^4 \alpha = \frac{1 + \dfrac{t_w L}{2A_c}}{1 + t_w h\left[\dfrac{1}{A_b} + \dfrac{h^3}{360 I_c L}\right]} \qquad (3\text{–}1)$$

where

h = distance between HBE centerlines

A_b = cross-sectional area of a HBE

A_c = cross-sectional area of a VBE

I_c = moment of inertia of a VBE taken perpendicular to the direction of the web-plate line

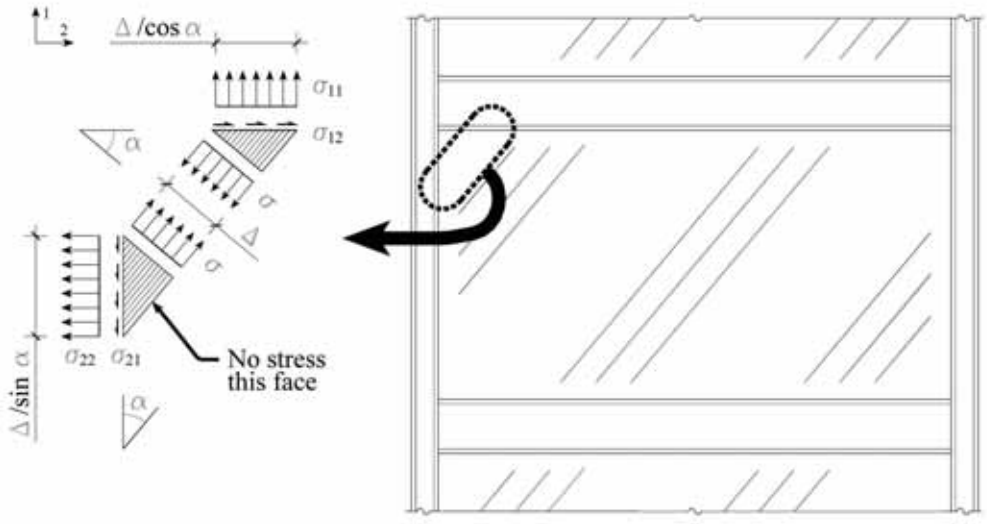

Fig. 3–6. Detail of stresses imposed on SPSW boundary elements by web-plate yielding.

L = distance between VBE centerlines

t_w = thickness of the web plate

This equation is based on a derivation by Thorburn et al. (1983), which considered a frame with simple beam-to-column connections. The derivation was subsequently modified by Timler et al. (1988) into the form shown above. The equation is based on the assumption that the web plate has no compression strength. The tension field is assumed to be a constant stress at a constant angle.

Thorburn also derived an expression of the angle of tension stress based on rigid beam-to-column connections

$$\tan^4 \alpha = \frac{1 + t_w L\left[\frac{1}{2A_c} + \frac{L^3}{120 I_b h}\right]}{1 + t_w h\left[\frac{1}{A_b} + \frac{h^3}{360 I_c L}\right]} \qquad (3\text{–}2)$$

where

I_c = moment of inertia of a HBE taken perpendicular to the direction of the web-plate line

and all other variables are as previously defined.

The values of the angle of tension stress in the web plate have been found to be sufficiently consistent between the two equations to permit use of the simpler one (Rezai, 1999). It should be noted that neither wall strength nor interface stresses are markedly sensitive to the angle of tension stress. The stiffness of the system is sensitive to moderate changes in the angle α on the order of 10° (Rezai, 1999). Thus AISC 341, which requires rigid beam-to-column connections in SPSW, does not require consideration of the beam flexural stiffness in determining α.

The use of rigid beam-to-column connections introduces additional flexural forces in the boundary elements. These flexural forces should be accounted for in the design of the HBE and VBE; methods for accounting for this are discussed later in this chapter and illustrated in Chapters 4 and 5.

3.2.2. Stiffened Steel Plate Shear Walls

Stiffened steel plate shear walls are able to develop significant compression forces in the web plate, in addition to the tension forces that can be developed in unstiffened SPSW. Because of this, the design of boundary elements does not include such large flexural forces. In fact, walls can be sufficiently stiffened so that no inward forces are exerted on the boundary elements and the interfaces of the web plates can be designed for pure shear. In cases where walls are stiffened to a lesser degree, a combination of shear buckling and tension-field action can be used.

The limiting slenderness of the web plate for which full shear yielding can be achieved can be calculated by setting the shear buckling strength equal to the shear yielding strength. Using relationships developed by Timoshenko (1959) the limiting plate thickness is

$$t_{\text{lim}} = \sqrt{\frac{12(1-\upsilon^2)\frac{F_y}{\sqrt{3}}}{\pi^2 E\left[\frac{5.34}{s_1^2} + \frac{4.0}{s_2^2}\right]}} \qquad (3\text{-}3)$$

where

s_1 = the smaller spacing between stiffeners

s_2 = the larger spacing between stiffeners

t_{lim} = the web-plate thickness below which shear buckling will occur prior to shear yielding

υ = Poisson's ratio

Where the spacing of stiffeners is equal in each direction, the limiting web slenderness ratio below which shear buckling is precluded is

$$\frac{s}{t_w} \le 3.82\sqrt{\frac{E}{F_y}} \qquad (3\text{–}4)$$

where

s = the spacing between stiffeners

t_w = the web-plate thickness

Where stiffeners are used in one direction only, the limiting web slenderness ratio is

$$\frac{s}{t_w} \le 2.88\sqrt{\frac{E}{F_y}} \qquad (3\text{–}5)$$

If the web plate is sufficiently stiffened to meet this criterion, its nominal strength is

$$V_n = 0.6 F_y t_w L_{cf} \qquad (3\text{–}6)$$

where

L_{cf} = the clear length of the web panel between VBE flanges

Stiffeners provided to reduce the web-plate slenderness would have to meet the requirements of Chapter G of AISC 360, including the required transverse stiffness

$$I_{st} \ge a t_w^3 j \qquad (3\text{–}7)$$

where

$j = 2.5(h/a)^2 - 2 \ge 0.5$

Where the limiting web-plate slenderness ratio is exceeded, procedures must be used to determine the shear-buckling strength of the web plate must be determined. As is the case with plate girders, the shear-buckling strength can be supplemented by tension-field action. Procedures derived for plate girder design can be applied to the design of such stiffened steel plate shear walls. These procedures are given in Chapter G of AISC 360. Slenderness limits separating modes of shear limit states (shear yielding from shear buckling with tension-field action) are based on the ratio of the distance between flanges, h in the AISC 360 equations, to the web-plate thickness, t_w.

Because the VBE of steel plate shear walls act like the flanges of plate girders, the dimensions and elements that are vertical in plate girders are horizontal in steel plate shear walls. The distance between vertical stiffeners, s_x, is used for h in the equations for shear strength. Vertical stiffeners are added to reduce the web-plate slenderness. Where the spacing is very large, greater wall strength can be calculated using the procedures for SPSW.

The procedure also utilizes the spacing between transverse stiffeners, a. Where the only transverse stiffeners are the beams at each story, the dimension a, as well as the ratio a/s_x (a/h in the AISC 360 equation) is very large, and tension-field action cannot be used in the design of the steel plate shear wall. Only shear buckling, represented by the symbol C_v, is permitted for such walls. Horizontal stiffeners are typically added on the wall face opposite the vertical stiffeners. Figure 3–7 shows a steel plate shear wall with vertical and horizontal stiffeners.

Plate-girder procedures do not permit tension-field action in the end panel of the girder. This is because it is assumed that the stiffener at the end of the girder has little flexural stiffness and cannot anchor the tension-field action. For steel plate shear walls, a steel or concrete grade beam designed to resist the tension-field action can be provided at the base, and a strong beam can be provided at the roof, thus permitting the inclusion of tension-field action in the calculation of the available strength.

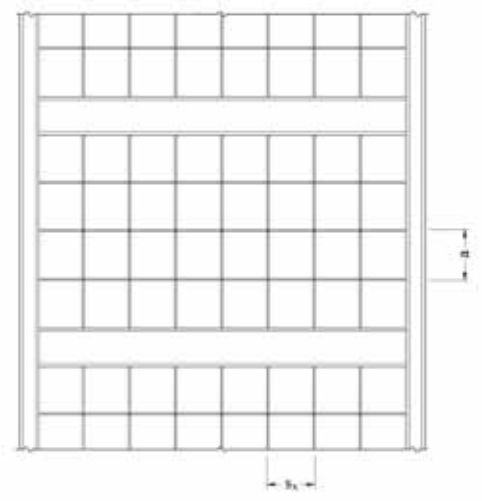

Fig. 3–7. Steel plate shear wall with vertical and horizontal stiffeners.

Beams anchoring the tension field in the web plate should be designed for transverse loading corresponding to the diagonal tension stress calculated in the same way as for unstiffened shear walls. For high-seismic design, a liberal estimate of the tension stress acting on the diagonal should be used for the design of beams (thus resulting in a conservative design):

$$\sigma_{tf} = R_y F_y (1 - C_v) \tag{3–8}$$

where

C_v = the ratio of shear buckling stress to shear yield stress, as given in AISC 360 Equations G2–3, G2–4, and G2–5

$R_y F_y$ = the expected yield stress of the web-plate material

σ_{tf} = the tension stress in the web plate

This stress is used to compute the required strength of the web plate resulting from seismic load effects and is combined with stresses resulting from other loads, according to the appropriate load combinations (ASD or LRFD).

The angle at which this tension-field stress acts in stiffened steel plate shear walls has not been well established. It is therefore recommended that two angles be considered and the larger forces be used in design. The first angle is that derived for unstiffened SPSW from AISC 341 Equation 17–2 (Equation 3–1). The second is based on plate girder design (Berman and Bruneau, 2000):

$$\tan(\gamma) = \frac{s_x}{a} \tag{3–9}$$

where

a = the vertical dimension of the web plate between horizontal stiffeners

s_x = distance between vertical stiffeners

γ = the angle of the tension field, measured from the member axis (vertical in the case of steel plate shear walls)

The transverse load can thus be expressed by two equations:

$$\sigma_{11} \le R_y F_y (1 - C_v) \cos^2(\alpha) \tag{3–10}$$

$$\sigma_{11} \le R_y F_y (1 - C_v) \cos^2(\gamma) \tag{3–11}$$

The horizontal force transmitted to the beams should be estimated liberally to avoid failure of these elements (thus resulting in a conservative design). Rather than using the sum of the shear-buckling strength and the horizontal component of the tension-field action, the full expected shear yield stress of the web plate should be used:

$$\sigma_{12} = 0.6 R_y F_y \qquad (3\text{–}12)$$

Again, this stress is used to compute the required strength of the web plate resulting from seismic load effects and is combined with stresses resulting from other loads, according to the appropriate load combinations (ASD or LRFD).

Plate-girder procedures will underestimate the strength of steel plate shear walls. Where tension-field action is neglected, the calculated strength of the web plate is based only on shear buckling; the additional strength provided by tension-field action can be significant, even in webs that do not conform to the limiting *a/h* (*a/s*$_x$) ratios in AISC 360. Even where tension-field action is utilized, the plate-girder methods will underestimate the shear strength of walls due to the assumption of negligible flexural stiffness of the flanges (which, in the case of steel plate shear walls, are the columns at wall boundaries).

Because of this underestimation, plate-girder procedures must be used with caution for steel-plate shear walls in high-seismic applications. Underestimating web-panel shear strength will lead to underestimation of the maximum overturning moments that the wall can resist and thus of axial forces in the columns.

Furthermore, plate-girder procedures do not account for VBE flexural forces resulting from tension-field action in the web plate. Thus columns could be subjected to larger-than-calculated axial forces in conjunction with significant transverse forces not used in their design. Consideration of these effects is warranted where partially stiffened steel plate shear walls are used.

To address these issues, estimates of column forces in stiffened steel plate shear walls should be based on upper-bound web-plate strengths, rather than the conservative design values in Chapter G of AISC 360. The web shear strength should be taken as the full expected shear yield stress. The resulting stress causing axial force in the column is

$$\sigma_{21} = 0.6\, R_y F_y \qquad (3\text{–}13)$$

A similar liberal estimate should be made of the transverse seismic load effect on the columns in order to ensure that the resulting design is conservative. The same range of angle considered in determining the transverse stresses acting on beams should be applied to columns:

$$\sigma_{22} \le R_y F_y (1 - C_v) \sin^2(\alpha) \qquad (3\text{–}14)$$

$$\sigma_{22} \le R_y F_y (1 - C_v) \sin^2(\gamma) \qquad (3\text{–}15)$$

The design of the connection of the web plate to the boundary elements should also be based on the expected tension strength of the web plate. Again, the angle of tension can be assumed to fall between α (which is calculated using equations for unstiffened SPSW) and γ (which is calculated based on stiffened plate-girder behavior). Both angles should be considered, and the design should satisfy forces from both conditions.

As is the case for unstiffened SPSW, stiffened steel plate shear wall web plates in which shear buckling is anticipated should be provided with perimeter connections that will not be adversely affected by buckling of the web plate.

For more information on the design of stiffened steel plate shear walls, see Berman and Bruneau (2004), Lee and Yoo (1998), and Sugii and Yamada (1996).

3.2.3. Composite Steel Plate Shear Walls

Composite Steel Plate Shear Walls (C-SPW) are able to develop the full shear yield strength of the steel web plate. This is due to the transverse restraint provided by concrete portions of the wall. The design of C-SPW is governed by Section 17 of Part II of AISC 341, which provides specific requirements for the concrete stiffening elements and their connection to the steel plate.

In addition to stiffening the steel plate, the concrete portions of the wall can provide supplementary shear strength. However, AISC 341 does not permit using the concrete strength in determining the wall shear strength; only the steel plate shear strength is considered. This is due to the limited basis for establishing design equations for the transfer of forces between the steel and concrete elements of the system. Thus, the nominal shear strength of C-SPW is based solely on the steel strength:

$$V_{ns} = 0.6\, F_y t_w L_{cf} \qquad (3\text{–}16)$$

Although the concrete elements of the C-SPW are not considered in the calculation of the wall shear strength, they nevertheless contribute both in-plane strength and in-plane stiffness to the wall. For purposes of design to resist drift, it is generally acceptable to ignore the increased stiffness due to the presence of the concrete in determining seismic loads from a response spectrum as long as the seismic response (drift) is calculated using the same stiffness used in determining the seismic loads.

As the concrete elements are not designed for their contribution to the wall shear strength, their primary structural design criterion is providing sufficient stiffening for the steel plate to preclude shear buckling. AISC 341 requires an elastic plate buckling analysis to demonstrate sufficient stiffening. This can be done using a transformed section that includes the flexural contribution of the concrete and using the required transverse stiffness from Equation 3–7 (adapting for the lower modulus of elasticity of concrete). In addition,

AISC 341 gives prescriptive minimum concrete thicknesses: 4 in. on each side where the concrete occurs on both sides of the web plate (as shown in Figure 3–8), and 8 in. where the concrete occurs on one side only of the web plate (as shown in Figure 3–9).

AISC 341 also contains minimum concrete reinforcement requirements. Concrete elements must comply with ACI 318 Section 14.3 (which gives certain minimum reinforcement requirements for concrete walls), must have a reinforcement ratio in each direction of at least 0.0025, and must have a maximum spacing of reinforcement of 18 in.

In order for the concrete elements to provide the required stiffening of the steel web plate, significant interconnection is necessary. This can be accomplished by headed or hooked studs for cast-in-place concrete elements (using provisions for these in AISC 341) or bolts for precast concrete elements. Figure 3–10 shows these types of connectors.

As is the case for other types of steel plate shear walls, boundary elements in C-SPW must be designed considering the upper bound of the web shear strength. For the steel web plate, the upper bound strength is the same as for stiffened steel plate shear walls:

$$V_{ns} = 0.6\, R_y F_y\, t_w L_{cf} \qquad (3\text{–}17)$$

In both cases, the strength is the full shear strength calculated using the expected yield stress. This shear value must be used in the design of the connection of the web plate to the adjoining beams and columns.

However, this value by itself will lead to underestimation of boundary element forces due to the omission of any concrete contribution. For purposes of boundary-element design, the contribution of the concrete is required to be estimated at the design story drift. For typical conditions where the concrete encases steel boundary elements or is cast directly against them, the full concrete strength as defined by ACI 318 Chapter 11 is appropriate. The limitation of usable wall strength in Section 11.10.3 can be neglected for purposes of establishing the upper-bound wall strength (reinforcement levels high enough to exceed this limit would be unusual in concrete elements designed only to provide stiffening). Note that this concrete strength is completely neglected for purposes of calculating the required steel web-plate strength.

It has been proposed that leaving a small gap around the concrete elements can provide more reliable seismic performance (Astaneh-Asl, 2001). Such a gap will ensure that the concrete elements are not active until a determined level of story shear deformation. Upon further deformation, the story shear strength and stiffness would increase. Figure 3–11 shows a detail of a C-SPW with such a gap (adapted from Astaneh-Asl, 2001). In such a design, detailing that ensures the concrete is not composite with the steel is required in

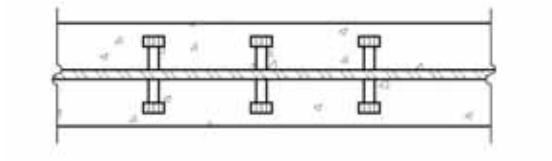

Fig. 3–8. C-SPW with concrete on both sides of the web plate.

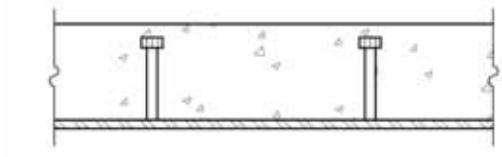

Fig. 3–9. C-SPW with concrete on one side of the web plate.

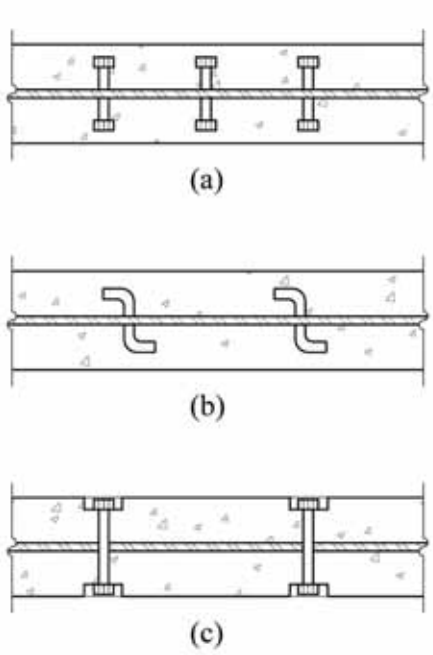

Fig. 3–10. Types of connectors of concrete to steel web plate in C-SPW.

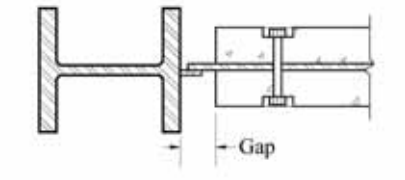

Fig. 3–11. Detail of a C-SPW with a gap between the concrete elements and the boundary elements.

order to avoid limiting the inelastic strain to the gap region of the plate.

In addition to the in-plane design of C-SPW, the high weight of C-SPW necessitates that out-of-plane seismic forces be considered. For such loading, the flexural strength of the concrete may be utilized. If a gap is provided, the flexural and shear strength of the unstiffened web plate may be critical.

3.3. ANALYSIS

This section addresses the analysis of SPSW for lateral loading, including both general ($R = 3$) and high-seismic ($R > 3$) use of the system.

The purpose of modeling the system is twofold. First, the model serves to determine forces in the elements of the system in order to permit their design. Flexural and axial forces in the boundary elements, as well as tension in the web plate, must be known in order to size those elements.

For seismic design, the forces in HBE and VBE must be determined for the condition with the web plate fully yielded in tension. This is typically done using capacity design procedures discussed later in this chapter. Nevertheless, all elements must have sufficient available strength to resist the forces determined by analysis, regardless of other calculations performed.

The second purpose of analyzing the SPSW is to estimate the lateral displacement of the frame. Excessive drift may constitute unacceptable performance, and frame stiffness may be the governing design criterion in some cases.

A variety of modeling techniques have been proposed. This Design Guide is limited to the two approaches that are most suitable for use by practicing structural engineers. These include strip models, in which the web plate is replaced by a series of diagonal tension members, and orthotropic membrane models, which utilize nonisotropic membrane elements to model the differing compression and tension resistance of the web plate.

Orthotropic membrane modeling is used in the design examples. This method is recommended for typical applications when software with this capability is available.

3.3.1. Strip Models

Another modeling technique used for analyzing SPSW is the use of a series of parallel, diagonal tension-only members. As is discussed in Chapter 2, the tension-strip method shows reasonable conformance to tested SPSW assemblies.

This method is included in the Canadian design provisions for SPSW (CSA, 2001). The method is also outlined in the Commentary to AISC 341. The CSA provisions require that a minimum of 10 strips be used to model the web plate in order to approximate the effects of a distributed load on the boundary elements of the frame. Under lateral loads, the tension in these diagonals results in the axial and flexural forces as shown in Figure 3–5.

Figure 3–12 shows a typical tension-strip model. The intersection of the tension strips from the panels above and below the beam do not necessarily coincide, and thus the beam must be divided into many segments if the exact angle of tension stress is to be modeled at each level. For a simplifying method of analysis based on averaging of angles of tension stress over the height of the wall see Chapter 2.

The length of the beam segments required for n strips (considering only a single web plate) is

$$\Delta_x = {}^1/_n \, [L + h \tan(\alpha)] \tag{3–18}$$

where

Δ_x = the length of beam segment between nodes

L = width of panel

h = height of panel

n = number of strips

The location of the nodes on the columns must be calculated from the resulting locations of nodes on the beams.

The area of the equivalent strip is given by

$$A_s = \frac{\left[L\cos(\alpha) + h\sin(\alpha)\right]t_w}{n} \tag{3–19}$$

where

A_s = area of a strip

Because of the dependence of strip models on the angle α, they are prone to somewhat tedious alteration of the model

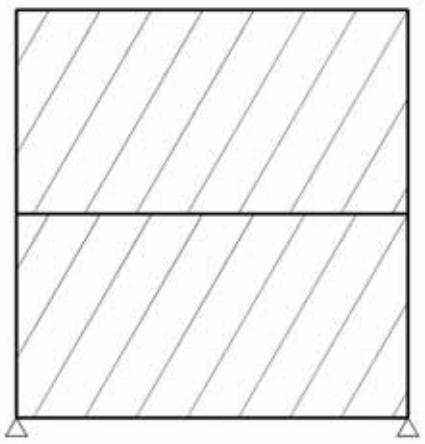

Fig. 3–12. A typical tension-strip model.

during design iterations. Modification of the VBE section could lead to a change in the angle α, which would require modification of the strip element properties and the node locations in the VBE in the model. Chapter 2 gives a method of simplifying the strip-model method by averaging the angle of tension stress over the height of the building. This is typically accurate when the same bay width is used and story heights are similar. The authors recommend that this approach be used wherever the calculated angle of tension stress is within 5° of the average angle. Where the angle at a story deviates by more than this from the average, the difference in angles may have a significant effect.

3.3.2. Orthotropic Membrane Model

Membrane elements can also be used to model the behavior of web plates.

In order to properly model the difference between tension and compression resistance of these slender elements, orthotropic elements are required. Because the tension is oriented in a diagonal direction, the local axes of the membrane element must be set to match the calculated angle of tension stress α. The material properties in the axis aligned with α are the true material properties. The stiffness in the orthogonal direction should be assumed as zero (or a negligible value) in order that the stresses calculated in the compression diagonal are essentially zero.

In addition, it is advisable that the in-plane shear stiffness of the membrane elements be assumed as zero (or a negligible value). Otherwise, it is possible that the analysis will assign a portion of the overturning moment to vertical stress in the web plate, which in reality cannot participate in resisting these forces to any great degree. That is, a small portion adjacent to the column can be considered sufficiently stiffened, but elsewhere buckling of the web plate will occur at very low levels of compressive stress. This modeling inaccuracy will reduce the demands on the columns slightly and increase the wall flexural stiffness to a small degree. For high-seismic design, column demands are calculated using capacity-design methods, so the effect on column required strength is irrelevant. For multi-story walls in which the wall flexibility due to column axial flexibility is comparable to the shear flexibility, the artificially elevated flexural stiffness may be of minor concern.

In the design examples in this Design Guide, the contribution of the web plate (with shear stiffness included) reduced the flexural component of the wall flexibility less than 5 percent, and the effect on the overall flexibility was substantially less. For flanged walls (orthogonal web plates sharing a common VBE) this effect may be substantial.

The membrane-element model is in essence a tension-strip model, and pure tension is calculated in the web plate. The meshing of the membrane should be sufficient to capture flexural forces in the boundary elements. Astaneh-Asl (2001) recommended at least four divisions in each direction (making 16 elements per panel). Figure 3–13 shows an orthotropic membrane model of a SPSW in which each panel has been subdivided into five equal spaces in each direction and the element local axes have been rotated to align with the calculated angle of stress.

This method also has advantages over the conventional strip-modeling method. Design iterations require only recalculation of the angle of tension stress α, and reorientation of the membrane element local axes—a simple procedure in several structural modeling programs with orthotropic membrane elements.

3.3.3. Nonlinear Analysis

Nonlinear analysis can be very advantageous in the design of SPSW. Nonlinear truss elements can be used in a strip model to capture the effects of uniform web tension yielding on HBE and VBE. Nonlinear membrane elements can be used similarly, but these are not available in the most widely used structural analysis programs. The same methods of preventing diagonal and vertical compression described for linear membrane elements are applicable to nonlinear ones.

If nonlinear modeling is used, HBE and VBE can be checked against unfavorable modes of inelastic behavior, such as buckling, by imposing displacements on the frame. These displacements may be those that cause full yielding of the web plate in tension, or they may be determined by other means. FEMA 356 (FEMA, 2000b) provides information on estimating displacement.

This type of pushover analysis is the best means of determining realistic design forces for boundary elements. The flexural and axial forces calculated in this way are often substantially less than those calculated using capacity design.

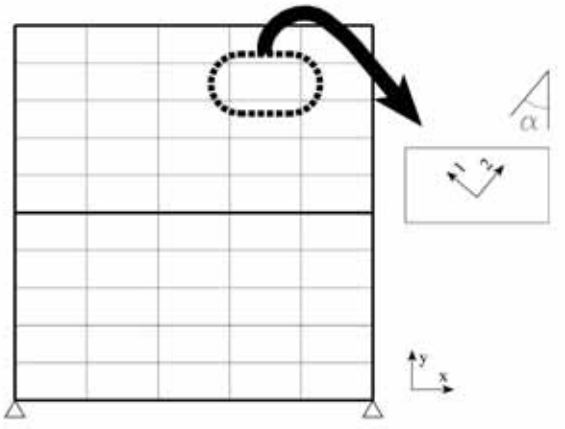

Fig. 3–13. An orthotropic membrane model of a SPSW.

3.4. GENERAL DESIGN REQUIREMENTS

This section addresses the basic design of SPW for strength. As such, it applies to the high-seismic design ($R > 3$) of SPSW as well as low-seismic design ($R = 3$). Proportioning and detailing requirements necessary for system ductility in the seismic design of SPSW are addressed in the next section. As AISC 360 does not address SPSW, some general requirements of the system from AISC 341 are also used in low-seismic design.

3.4.1. Preliminary Design

Before any analysis can be conducted, preliminary sizes of web plates, VBE, and HBE must be selected. This can be done by making assumptions about the distribution of forces in the members. Alternatively, an equivalent braced frame can be used, as described at the end of this section.

For preliminary design, the web plates can be assumed to resist the entire shear in the frame. The angle of tension stress in the web plate must be assumed for preliminary design because it is dependent on the section properties of the HBE and VBE, as well as on the web-plate thickness and the frame dimensions. Typical designs show that the angle of tension stress ranges from 30° to 55°. For preliminary design, the required web-plate thickness is calculated based on an assumed angle (α); it is convenient to assume an angle of 45° (though 30° is used as the assumption in examples in this design guide).

With this assumption, the nominal strength of web plates can be calculated using AISC 341 Equation 17–1 (Equation 3–20):

$$V_n = 0.42F_y t_w L_{cf} \sin(2\alpha) \qquad (3\text{–}20)$$

The nominal strength predicted by this equation is somewhat lower than the theoretical strength corresponding to uniform tension yielding at the determined angle α. This reflects the difference between first significant yield and full yield of the web plate due to uneven elastic distribution of stress (Berman and Bruneau, 2003a).

The equation can then be rearranged to determine the required web-plate thickness:

$$t_w \geq \frac{V_u}{\phi 0.42F_y L_{cf} \sin(2\alpha)} \qquad (3\text{-}21)$$

For LRFD:
where

V_u = the required shear strength (LRFD)

ϕ = the resistance factor given in AISC 341 (0.9)

For ASD:

$$t_w \geq \frac{\Omega V_a}{0.42F_y L_{cf} \sin(2\alpha)}$$

where

V_a = the required shear strength (ASD)

Ω = the safety factor given in AISC 341 (1.67)

Web plates thinner than ¼ in. typically require additional care and effort on the parts of fabricators and erectors in some applications. However, the advantages of using thinner material in SPSW usually justify the additional effort of fabricating and handling the thinner web plates.

Once web plates are selected, preliminary selection of VBE can be made based on the stiffness requirement given in AISC 341 Section 17.4g (Equation 3–22):

$$I_c \geq 0.00307 \frac{t_w h^4}{L} \qquad (3\text{–}22)$$

For low-seismic design, the required moment of inertia may be the governing criterion in the selection of the VBE. Where this criterion is difficult to satisfy, the introduction of an intermediate strut between stories may be considered in order to provide web plates with the necessary VBE stiffness. Such an intermediate strut must have sufficient out-of-plane stiffness to preclude its participation in web-plate buckling. That is, it must be rigid enough to force the web plate to form a buckling node immediately adjacent to the strut. Thus the out-of-plane moment of inertia must meet that required by Equation 3–7. Because this configuration has not been the focus of testing, it is recommended that designs be well above this theoretical minimum. For typical sections selected to resist out-of-plane buckling, this requirement may be easily met.

The angle α should be calculated based on the proportions of the individual web plates above and below the intermediate strut. Figure 3–14 shows a SPSW with such an inter-

Fig. 3–14. SPSW with an intermediate horizontal strut.

mediate strut. Also, the proportions of the panel above and below the strut should comply with the limitations discussed below.

It is not recommended that such intermediate struts be rigidly connected to the VBE, as the formation of a plastic hinge without lateral support (and in conjunction with moderate or high axial force) may not be stable. Instead, a connection with some rotational flexibility should be considered.

SPSW are limited to frames with an aspect ratio of length to height between 0.8 and 2.5, as discussed in the commentary to Section 17.2b of AISC 341. Web plates with lower aspect ratios have been found to have behavior significantly different from that predicted analytically (Rezai, 1999). The aspect ratios of such web plates can be increased by the introduction of intermediate struts, as discussed above.

Web plates with higher aspect ratios have not been studied thoroughly, and the applicability of design recommendations developed for more typical proportions to such web plates is not clear. Of particular concern is the effect of the flexibility of long HBE (see AISC 341).

For preliminary design of HBE, the forces imposed by the web plate can be derived from the same angle α as was assumed for the selection of the web plate. The forces imposed by the web plates above and below the beam are proportional to the web-plate stress and thickness. In low-seismic design, the stress in each web plate can be assumed proportional to the applied load, and the resulting vertical loading on the beam can be derived from the trigonometric relationships shown in Figure 3–6. The load on the HBE due to lateral loading of the frame is the difference in the effects caused by the tension in the web plates above and below the HBE

$$w_r = \left[\frac{V}{L_{cf}\tan(\alpha)}\right]_i - \left[\frac{V}{L_{cf}\tan(\alpha)}\right]_{i+1} \qquad (3\text{–}23)$$

where

w_r = the required strength, w_u (LRFD) or w_a (ASD), as a distributed load on the beam due to web-plate tension

V = the required strength, V_u (LRFD) or V_a (ASD), as appropriate

$[\,]_i$ = the effect due to the web plate at level i

$[\,]_{i+1}$ = the effect due to the web plate at level $i + 1$

This is a seismic load effect and is combined with other loads according to the appropriate load combinations (ASD or LRFD).

If the value of α is assumed to be 45° at all levels in preliminary design, and L_{cf} is typically the same, the load on the HBE due to lateral loading of the frame can be simplified to

$$w_r = \frac{V_{(i)} - V_{(i+1)}}{L_{cf}} \qquad (3\text{–}24)$$

Current design requirements imply that the design of the HBE for this unbalanced loading, in conjunction with the presence of another web plate, will indirectly confer them an adequate stiffness to achieve the intended behavior; that is, that the effective stiffness of the HBE above the web plate will be sufficient to permit full yielding of the plate due this design loading and the web plate above, if present. However, the effectiveness of plate yielding at the desired response level may not be assured and should be verified as part of the design process. Toward that end, it is recommended to provide HBE meeting a minimum stiffness requirement similar to that for VBE

$$I_{HBE} \geq 0.003\frac{(\Delta t_w)L^4}{h} \qquad (3\text{–}25)$$

where

Δt_w = the difference in web plate thickness above and below the HBE

Selection of HBE sections to resist the loading from Equation 3–24, in conjunction with gravity loads, and to meet the stiffness requirement above (Equation 3–25), is sufficient for preliminary design. However, this criterion is fairly stringent, as research is needed to determine the effect of HBE and VBE flexibility on required stiffness. As an alternative, designers may use nonlinear analysis to demonstrate that the required web-plate strength can be achieved within the design story drift with more flexible members.

Gravity loading on HBE may tend to cause vertical tension in the web plate if it is not equal from floor to floor. However, the shear strength of the web plate is not significantly reduced as long as the angle of tension stress is not changed by more than a few degrees. While the effect of such forces on the angle of tension stress has not been studied thoroughly, it is expected that HBE meeting the requirements of Equation 3–25 will perform as expected neglecting this effect for typical conditions.

For long spans, transverse loading due to web-plate tension may be difficult to resist at the top and bottom HBE (where only one web plate connects so there is no counterbalancing distributed load). The loading at the bottom HBE is typically more severe, as the web plate is often thicker there (particularly for taller SPSW). Where piers or piles are used in the foundation system, one or two of these may be located between columns to reduce the required flexural strength of the bottom HBE.

Another alternative that reduces the required strength of not only the bottom but all HBE is a series of vertical struts at mid-span at every level of the SPSW. These struts permit

the top HBE to be supported at mid-span, and its reaction at this location combines with the reactions of all the HBE at intermediate levels, accumulating in the series of struts until the bottom level, where the accumulated force offsets the upward mid-span reaction from the bottom HBE. Figure 3–15 shows a SPSW with such a series of struts. Similar to the intermediate strut discussed above, the out-of-plane moment of inertia of these intermediate vertical struts must meet that required by Equation 3–7 in order to force the individual web-plate panels on either side to buckle independently. As with the horizontal struts, it is recommended that designs be well above the theoretical minimum of Equation 3–7. The angle of tension stress, α, may be calculated based on the geometry of the overall panel from VBE to VBE, as the flexibility of the HBE is not considered in Equation 3–1. The panel aspect ratio should be calculated based on the proportions on either side of the vertical strut.

Where these struts are not continuous from roof beam to anchor beam, they are effective in sharing the unbalanced load on the beams that they connect. Such an approach may be useful in providing more uniform beam sizes in the SPSW frame.

These vertical struts should be designed for axial forces corresponding to the HBE reactions based on the transverse loading w_r defined above. The same fraction of the bay length should be used at each level to calculate this reaction. In this way the force required at the top of the wall to resist the downward pull of the top web plate, plus the downward forces at each intermediate level based on the differential web-plate tension above and below the beam, will equal the upward force required to resist the pull of the bottom web plate. Assuming fixed-fixed HBE, the resulting equation for the required axial strength of the strut is

$$P_{(i)} = \sum_{i}^{n} \frac{1}{2} w_{r(i)} L_{cf} \tag{3–26}$$

This equation, combined with Equation 3–24, results in the following expression:

$$P_{(i)} = \frac{V_{(i)}}{2\tan(\alpha)} \tag{3–27}$$

This is a seismic load effect and is combined with other loads according to the appropriate load combinations (ASD or LRFD).

The use of these vertical struts is especially convenient for wide bays, where the beam span may otherwise preclude the economical use of SPSW by necessitating a very strong HBE, which in turn necessitates a stronger VBE if strong-column/weak-beam proportioning is to be maintained (as is required in high-seismic design). The additional cost of these struts should be weighed against the beam and column costs.

A simplified preliminary design method has been proposed by Thorburn et al. (1983). This method involves designing a tension brace to resist the frame story shear and converting that brace design into an equivalent web-plate design. The relationship between the web-plate thickness and the tension brace area varies with the stiffness of the boundary elements. This method is detailed in Chapter 2.

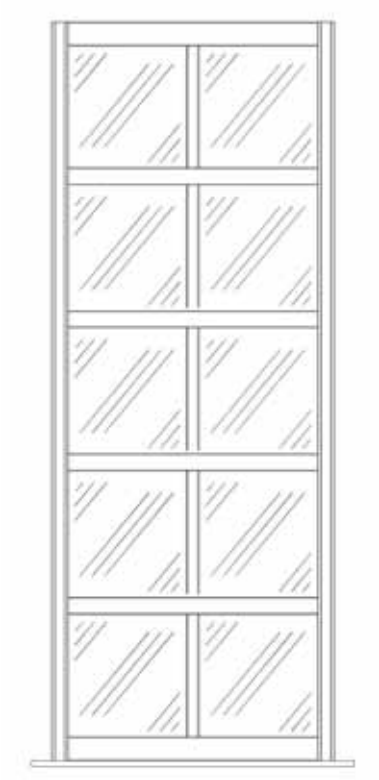

Fig. 3–15. SPSW with an intermediate vertical strut.

3.4.2. Final Design

Once the preliminary selections of web plates and boundary elements have been made, the model of the frame can be constructed. Member design forces can then be obtained for the specified lateral loads. If optimization of the structure is desired, some iteration may be required, as changes in web-plate thickness can have a significant impact on the required stiffness and strength of the VBE and HBE.

For low-seismic design, the designer has two choices: forces from the model can be used directly for sizing web plates, HBE, and VBE, or design of those elements can be done assuming a uniform distribution of the average stress in the web plate.

If the former approach is used, it is important that the web plate is of sufficient thickness so that local yielding is not

required to achieve the web-plate strength. If the web plate must rely on inelastic distribution of stress to resist the design shear, elastic methods of computing the bending stresses in boundary elements are not valid.

The design of connections of the web plate to the boundary elements is based on the stresses in the plate. These forces cannot exceed the expected yield strength of the plate; if this stress is assumed (as is required for seismic design) the resulting design will be conservative. Alternatively, results from the structural model can be used to establish the required strength of these connections.

For the conventional strip model, the stress in the tension strip is simply the calculated tensile force divided by the strip area. Orthotropic models of the web plate will report the tension stress directly.

The effective force (acting at the angle α) per unit length on the connection of the web plate to the HBE is

$$r_{HBE} = \sigma \cos(\alpha)\, t_w \tag{3–28}$$

where

r = r_u (LRFD) or r_a (ASD) = force per unit length of the connection

The effective force per unit length on the connection of the web plate to the VBE is

$$r_{VBE} = \sigma \sin(\alpha)\, t_w \tag{3–29}$$

Bolted connections can be designed using this force times the bolt spacing

$$r_{bolt} = r \times s \tag{3–30}$$

where

s = the space between bolts

Typically the bolt size and spacing will be the same for the web-plate connections to the HBE and VBE, and the larger of the two computed stresses is used. Where stresses approach the yield strength of the plate, more than one row of bolts may be required.

For fillet-welded connections, Chapter J of AISC 360 gives the following expression for fillet weld strength as a function of angle of loading to the longitudinal axis:

$$R_n = F_w A_w \tag{3–31}$$

$$F_w = 0.6F_{EXX}\ [1 + 0.5 \sin^{1.5}(\theta)] \tag{3–32}$$

where

A_w = the area of the weld

F_{EXX} = the electrode classification number

θ = the angle of loading with respect to the fillet-weld axis

In calculating the fillet-weld strength per unit length, the weld size, w, times $\sqrt{2}/2$ should be substituted for the weld area, A_w. The resulting expression of fillet-weld nominal strength per unit length is

$$r_n = 0.6F_{EXX}[1 + 0.5 \sin^{1.5}(\theta)]\frac{\sqrt{2}}{2} w \tag{3–33}$$

where

w = the weld size

For the web-plate connection to the HBE:

$$\theta = 90° - \alpha \tag{3–34}$$

For the web-plate connection to the VBE:

$$\theta = \alpha$$

Thus, the required fillet-weld size for the connection of the web plate to the HBE for LRFD is

$$w_{HBE} = \frac{\sigma \cos(\alpha) t_w \sqrt{2}}{\phi 0.6F_{EXX}\left[1 + 0.5\ \cos^{1.5}(\alpha)\right]} \tag{3–35}$$

and for ASD

$$w_{HBE} = \frac{\Omega\sigma \cos(\alpha) t_w \sqrt{2}}{0.6F_{EXX}\left[1 + 0.5\ \cos^{1.5}(\alpha)\right]}$$

The required fillet-weld size for the connection of the web plate to the VBE for LRFD is

$$w_{VBE} = \frac{\sigma \sin(\alpha) t_w \sqrt{2}}{\phi 0.6F_{EXX}\left[1 + 0.5\ \sin^{1.5}(\alpha)\right]} \tag{3–36}$$

and for ASD

$$w_{VBE} = \frac{\Omega\sigma \sin(\alpha) t_w \sqrt{2}}{0.6F_{EXX}\left[1 + 0.5\ \sin^{1.5}(\alpha)\right]}$$

Fillet-welded connections of web plates are typically made in the field to a "fish plate," which is welded in the shop to the VBE and HBE. The fish plate may be thicker than the web plate in order to permit a larger fillet weld to be deposited against its edge. Figure 3–16 shows such a connection. For usual conditions, the diagonal tension force is shared equally between Welds "A" and "B". When the distance between the two welds is large or the fish plate is much thicker than the web plate, it may not be reasonable to assume that the two welds share the force equally, and the required strength of each of the two welds should be proportioned for a percentage of the tension force equal to

the ratio of the thickness of the plate end it abuts to the total thickness. It is the opinion of the authors that if the fish plate is less than twice the thickness of the web plate, and if the lap length is less than four times the size of the fillet weld, minimal deformation demands are necessary to permit the two fillets to share the force equally.

Because web plates in SPSW are extremely slender, they should be expected to buckle under very small lateral loads or even under their own weight prior to loading. On the tension edge, the offset plate centerlines also tend to cause rotation that would open the root of a joint with only Weld "A" or Weld "B". Thus, either welds must be present on both edges as shown in Figure 3–16, or the tendency to open must otherwise be restrained. If Weld "A" is designed to resist the entire force by itself, Weld "B" may be intermittent.

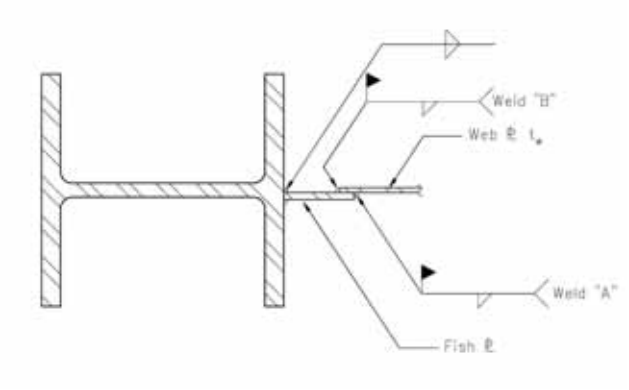

Fig. 3–16. Detail of a fillet-welded web-plate connection.

For thinner plates (less than ⅛ in.), Weld "A" may not be practical to perform, due to the possibility of burning through the base metal. In those cases, Weld "B" must develop the full web-plate strength; such a weld will likely be larger than the largest possible fillet weld.

Openings in SPSW require local boundary elements. These elements are designed to resist forces resulting from the stress in the web plate. Figure 3–17 shows a free-body diagram of a local boundary element at an opening. For clarity, free-body diagrams of the web plates are not shown, nor are end moments that would result from rigid connections due to web-plate tension and frame behavior.

Local boundary elements should meet the stiffness criterion of AISC 341 Section 17.4g. Flexible boundary elements may not permit the angle of stress in the web to reach the predicted value α, and the shear strength of the web plate may be compromised.

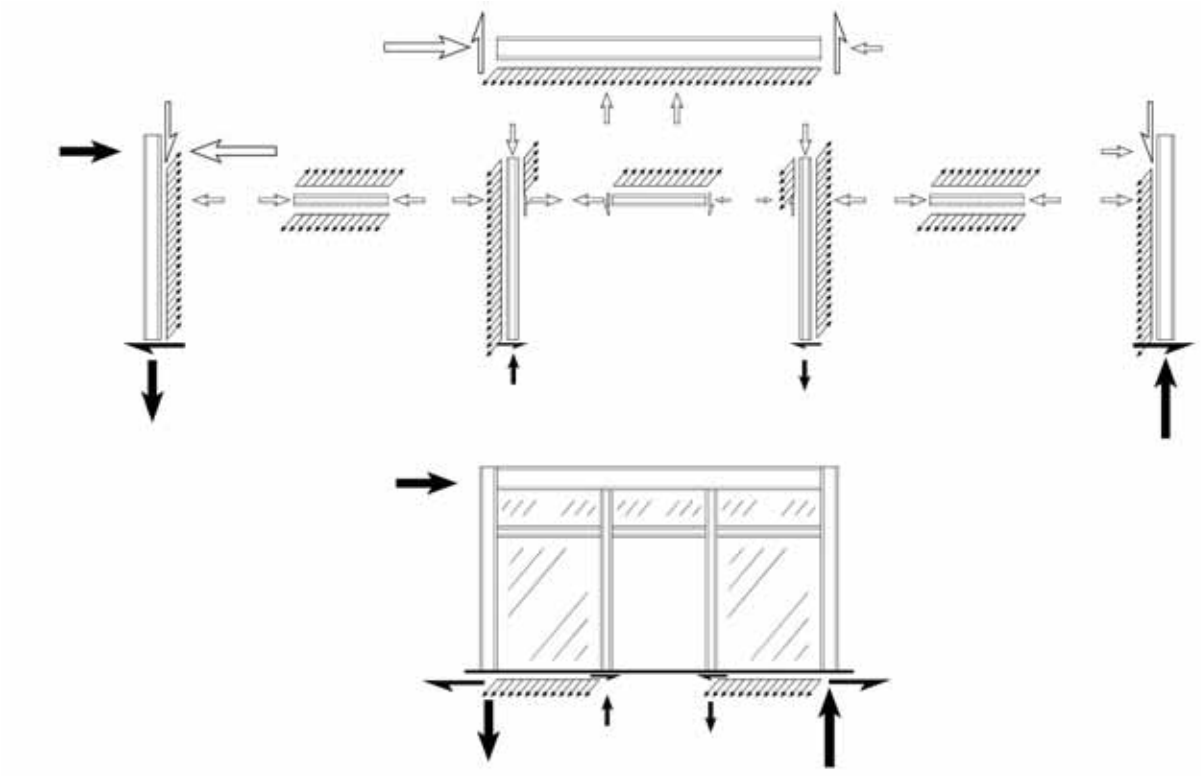

Fig. 3–17. Free-body diagrams of internal and external boundary elements of a SPSW with an opening.

Connections of local boundary elements to each other and to the HBE and VBE need not meet the requirements for HBE-to-VBE connections (i.e., they need not be designed as rigid connections), and horizontal local boundary elements need not be braced in conformance with AISC 341 Section 17.4d. Requirements for rigid connections of HBE to VBE are intended to provide more stable hysteretic performance of the frame through the addition of a moment frame. Such a frame, consisting of the VBE and HBE at diaphragm levels, will be present regardless of the connection type of local boundary elements, which are difficult to stabilize due to the absence of a diaphragm at local boundary elements.

Limited testing of small openings without boundary elements has been performed (Vian and Bruneau, 2004), and designers may consider utilizing such configurations. It is recommended that designs with openings without local boundary elements not be extrapolated beyond tested configurations in terms of size of openings, proportion of horizontal wall length eliminated, or shape of opening.

Chapter 6 provides a more thorough treatment of the design of openings in SPSW.

3.5. HIGH-SEISMIC DESIGN

This section addresses the additional requirements that apply to the use of SPSW to resist high-seismic loads. The general design requirements described in the previous section apply to high-seismic design of SPSW as well.

Expected Performance

Systems designed for high-seismic loading (with a response modification coefficient, R, greater than 3) are expected to undergo multiple cycles of loading into the inelastic range—with controlled damage accepted as a means of dissipating the energy of the earthquake. The use of a response modification coefficient, R, greater than 3 represents the ability of the system to withstand such loading and maintain its integrity to support gravity loads and limit drift. The ability of a system to withstand such loading is termed "system ductility."

Loading of a system beyond its elastic limit necessitates inelastic behavior in the material in one or more locations. As steel is a ductile material, steel systems are well suited to providing the required ductility, as long as the inelastic demands on the steel material occur in appropriate portions of the structure. In the case of SPSW, the web plate is the location where inelastic strain demands are expected to occur. This element is ductile, tough, and relatively easier to replace after damage occurs in a strong earthquake.

The steel materials appropriate for designated yielding elements of steel seismic systems are limited by Section 6.1 of AISC 341. Materials listed in that section can be considered ductile for purposes of high-seismic design.

Web plates in SPSW provide a large area of steel to resist lateral forces. As the conventional strip model suggests, a single web plate provides multiple paths to resist seismic loading. Even the development of cracks in the web plate does not signal the end of its resistance, and such cracks propagate slowly (Driver et al., 1998; Berman and Bruneau, 2003b). These characteristics indicate a tough element.

Because they are not required for the resistance of gravity loads, damage in the web plates is preferable to damage in the boundary elements, which also comprise part of the frame that supports the building weight.

For these reasons, the high-seismic design of SPSW is based on confining ductility demands to the web plates (and, as discussed later, to plastic hinges in the HBE at the VBE face). This is achieved by means of a capacity-design method, in which boundary elements are designed for forces corresponding to the expected strength of the web plate. In this manner, failure of the boundary elements (due to flexural buckling, lateral-torsional buckling, etc.) is precluded, and the more ductile web-plate-yielding behavior is favored.

In order to ensure that web-plate yielding can take place, high-seismic design of SPSW also requires that web-plate connections be designed for the expected strength of the web plate itself. While rupture of the web-plate attachments to the boundary elements is not as undesirable a mode of behavior as failure of a VBE, it nevertheless is inconsistent with the expected system ductility and the use of a high response modification coefficient R.

For multi-story systems, the desired behavior remains tension yielding of the web plates. Thus, the distribution of inelastic demand between floors requires that web plates be designed with similar overstrength (i.e., with similar ratios of calculated required to design strengths). If web plates at some levels are designed with overstrength much greater than those at other levels, the high-overstrength web plates will not participate in providing system ductility, and the seismic drift demands on the other levels will be greater. Uneven drift distribution between stories can cause large flexural demands in the VBE, perhaps leading to their yielding and the formation of a story mechanism. This should be considered carefully when the design of web plates is controlled by using a minimum web-plate thickness selected for ease of construction.

The upper bound of overturning forces on VBE can be calculated based on the expected strength of connecting web plates and beams. This force corresponds to the desired mechanism of web-plate tension yielding at all levels. For systems with more than three or four stories, the likelihood of yielding all stories simultaneously in the same direction is fairly remote, as higher-mode response becomes more significant. Where high overstrength exists at certain levels, the likelihood is even less. The expected mechanisms for taller structures include some concentrations of drift at certain lev-

els and corresponding rotational demands at VBE at these levels.

Berman and Bruneau (2003a) provide a comparison of the work required to achieve two mechanisms: the yielding of the web plates over the entire height of the structure and a story mechanism. Their study indicates that to ensure the former mechanism, the thickness of the web plate must change at each story to match the story shear. Otherwise, a mechanism that to some degree concentrates inelastic deformation in some stories will form. Thus, it is recommended to proportion the web plates to the story shear as closely as possible and not to provide unnecessary overstrength.

In some cases, foundation uplift or diaphragm deformation can be the predominant mode of seismic response of SPSW structures (as is also the case for other stiff systems). ASCE 7 does not fully address these as modes of seismic response. Design of systems based on that mode of behavior is beyond the scope of this Design Guide.

3.5.1. REQUIREMENTS OF THE AISC SEISMIC PROVISIONS (ANSI/AISC 341-05)

AISC 341 addresses the high-seismic design of SPSW. As AISC 360 does not address SPSW, some of the basic requirements of the system contained in AISC 341 are also applied in low-seismic design as well.

The general SPSW requirements applicable to both high-seismic and low-seismic design pertain to the analysis of the system and certain member requirements. Foremost of these is the calculation of the angle of tension stress in the web plate (AISC 341 Equation 17–2, Equation 3–1), and the corresponding expression for web-plate shear strength as a function of the angle (AISC 341 Equation 17–1, Equation 3–20).

Equally important are limitations on the systems to which these equations are applicable. These include the panel aspect ratio (*L/h*) in AISC 341 Section 17.2.b (to the range between 0.8 and 2.5, as discussed under the previous section) and the required VBE stiffness given in Section 17.4.g (Equation 3–22).

Additionally, AISC 341 Section 17.2.c, requires that boundary elements be included adjacent to all openings "unless otherwise justified by testing and analysis". This requirement is applicable to both high-seismic and low-seismic design of SPSW.

In addition to these general design requirements, AISC 341 contains many requirements that are only applicable to high-seismic design. These include requirements for the web-plate connection and for the frame.

As discussed earlier, the high-seismic design of SPSW is based on yielding of the web plate. Thus, AISC 341 requires that the web-plate connection be designed to resist the expected yield strength of the web plate ($R_y F_y t_w$). Connections of web plates must have sufficient strength to permit the plate to develop this force across the entire connection, considering the angle of the tension α as discussed in the previous section.

Likewise, the design of HBE and VBE must be based on forces corresponding to full tension yielding of the web plate. In this way, AISC 341 ensures that web-plate tension yielding is the primary yield mechanism of SPSW.

AISC 341 also requires that a SPSW be designed as a moment frame with a web-plate infill. Specifically, a number of the provisions require that boundary elements and their connections conform to requirements for Special Moment Frames (SMF) or Ordinary Moment Frames (OMF).

Connections of HBE to VBE must be designed as OMF connections; Section 17.4b gives the requirement for SPSW, referring to the OMF Section 11.2 of AISC 341. Additionally, the required shear strength of the HBE-to-VBE connection must be based on the development and strain-hardening of plastic hinges at each end of the HBE (rather than allowing use of the amplified seismic load, as is allowed for a typical OMF). The seismic portion of the required shear strength is given by AISC 341 Equation 9–1 (Equation 3–37):

$$E_m = 2M_{pr}/L_h \tag{3–37}$$

where

E_m = The maximum seismic load effect to be used in ASCE load combinations

L_h = the distance between plastic hinges

$$= L - 2s_h \tag{3–38}$$

where

L = the distance between column centerlines

s_h = the distance from the column centerline to the plastic hinge, as given in AISC 358

For unreinforced connections, such as Reduced Beam Section (RBS) and Welded Unreinforced Flange-Welded Web (WUF-W) connections, s_h can be determined as

$$s_h = ½ (d_c + d_b) \tag{3–39}$$

AISC 358 gives limitations for this distance for the RBS connection; the value above is a reasonable preliminary estimate.

Note that the beam plastic moment strength in Equation 3–37 is typically calculated in the absence of any axial force:

$$M_{pr} = 1.1R_yF_yZ \tag{3–40}$$

Designers may wish to consider the axial force present at the HBE-to-VBE connection in order to reduce the calculated flexural strength and thus required shear strength of the connection. While not explicitly described in AISC

341, this method is consistent with the underlying capacity-design methodology in which the yield mechanism of the frame is considered. Reduction of the calculated HBE flexural strength can be done adapting the interaction equations from Chapter H of AISC 360.

For LRFD the resulting modified beam strength when $P_u/P_y < 0.2$ is

$$M_{pr}^{*} = \left(1.1R_yF_yZ\right)\left[1-\frac{1}{2}\left(\frac{P_{u\ HBE}}{P_y}\right)\right] \qquad (3\text{–}41)$$

and otherwise is

$$M_{pr}^{*} = \frac{9}{8}\left(1.1R_yF_yZ\right)\left[1-\frac{P_{u\ HBE}}{P_y}\right] \qquad (3\text{–}42)$$

For ASD the resulting modified beam strength when $P_u/P_y < 0.2$ is

$$M_{pr}^{*} = \left(1.1R_yF_yZ\right)\left[1-\frac{1}{2}\left(\frac{1.5P_{a\ HBE}}{P_y}\right)\right]$$

and otherwise is

$$M_{pr}^{*} = \frac{9}{8}\left(1.1R_yF_yZ\right)\left[1-\frac{1.5P_{a\ HBE}}{P_y}\right]$$

For SPSW, the additional beam shear due to web-plate tension must be considered. The total beam shear is thus

For LRFD

$$V_u = \frac{2M_{pr}}{L_h} + \frac{P_u}{2} + \frac{w_g + w_u}{2}L_{cf} \qquad (3\text{–}43)$$

For ASD

$$V_a = \frac{2M_{pr}}{L_h} + \frac{P_a}{2} + \frac{w_g + w_a}{2}L_{cf}$$

where

P = concentrated gravity load on the beam (assumed to be centered on the span) based on LRFD or ASD load combinations

w_g = distributed gravity load on the beam (assumed to be uniform) based on LRFD or ASD load combinations

$w_u = R_yF_y\,(t_i - t_{i+1})\cos^2(\alpha)$ (3–44)

$w_a = w_u/1.5$

Note that the appropriate load factors from LRFD or ASD load combinations must be applied to gravity forces in the above equations.

Figure 3–18 shows the free-body diagrams for the condition under which V_p is calculated.

For fully restrained connections, AISC 341 Section 11.2a requires that the connection have the strength to resist the formation of a plastic hinge in the beam (including strain hardening): $1.1R_y\,M_p$ (the "maximum force that can be delivered by the system" is a limitation that is not applicable to the OMF connection in a SPSW). Additionally, the section gives prescriptive requirements for continuity plates, welds, and weld access holes. The required weld-access hole configuration is shown in Figure 11–1 of AISC 341. Single-sided partial-joint-penetration groove welds or fillet welds are not allowed. For partially restrained connections, Section 11.2b requires the same strength as does Section 11.2a.

Welds of flanges in these connections must comply with the requirements in Section 7.3b for demand-critical welds. These include a Charpy V-notch toughness of 20 ft-lb at –20 °F as determined by the appropriate AWS classification test method or manufacturer certification, and 40 ft-lb at 70 °F (but not more than 20 °F above the lowest anticipated service temperature) as determined by Appendix X of AISC 341, or another method approved by the engineer.

In addition, Section 17.4a requires that boundary elements comply with the requirements for SMF in Section 9.6. That is, boundary elements must be proportioned so that the strong-column/weak-beam requirements of Equation 9–3 (Equation 3–45) are met:

$$\frac{\sum M_{pc}^{*}}{\sum M_{pb}} \geq 1.0 \qquad (3\text{–}45)$$

where

$\sum M_{pc}^{*}$ = sum of column plastic moment strengths at a connection (reduced for axial force and computed at the beam centerline)

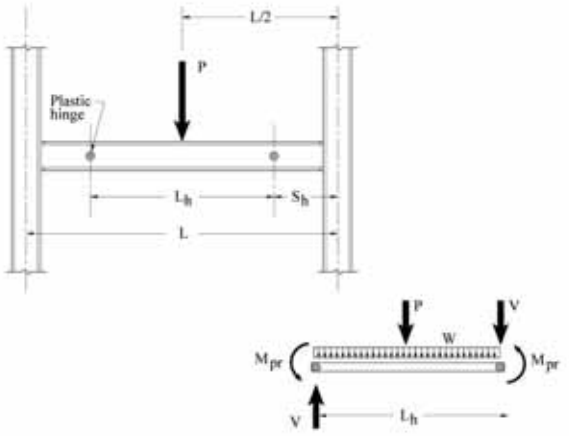

Fig. 3–18. Free-body diagram of SMF beam.

$\sum M_{pb}$ = sum of beam plastic moment strengths at a connection (computed at the column centerline)

Figure 3–19 shows this method for computing beam strength at the column centerline. The beam strength projected to the column centerline is

$$M_{pb} = M_{pr} + V_u s_h \tag{3–46}$$

Panel zones of HBE-to-VBE connections at the top and bottom of the SPSW must also comply with SMF requirements. Section 17.4.f requires compliance with Section 9.3. This section requires that the panel-zone shear strength be computed by calculating the moment at the column face due to the formation of a plastic hinge in the beam at a determined location. Figure 3–20 shows this method for computing beam strength at the column face. The authors recommend that the requirements of AISC 341 Section 17.4 be applied to panel zones at all levels.

The minimum panel-zone thickness is given in AISC Equation 9–3 (Equation 3–47):

$$t \geq \frac{d_z + w_z}{90} \tag{3–47}$$

where

t = the sum thickness of the column web and any doubler plates used

d_z = the panel-zone depth between beam flanges or continuity plates (if present)

w_z = the panel-zone width between column flanges

If doubler plate(s) are required, Section 9.3.c gives prescriptive detailing requirements. Doublers are welded along their vertical edges to develop their full shear strength.

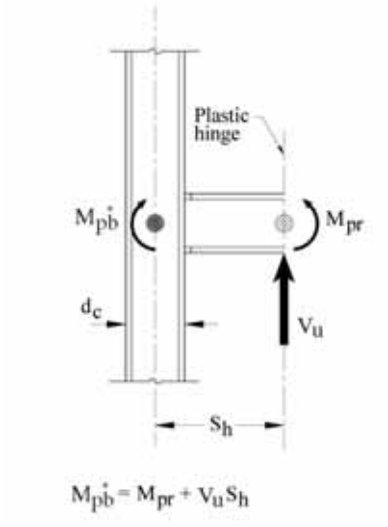

Fig. 3–19. Forces at column centerline from beam plastic hinge.

As boundary elements are configured to comprise a moment frame, the formation of plastic hinges in boundary elements (typically the HBE) under the design seismic loading is considered possible. AISC 341 therefore places certain compactness requirements on them (Section 17.4c). For flanges, the limit is

$$\frac{b_f}{2t_f} \leq 0.30\sqrt{\frac{E}{F_y}} \tag{3–48}$$

For webs, the limits are based on the axial force in the member. The axial force ratio C_a is

For LRFD

$$C_a = \frac{P_u}{\phi_b P_y} \tag{3–49}$$

For ASD

$$C_a = \frac{\Omega_b P_a}{P_y}$$

ϕ_b and Ω_b are as defined in AISC 341 Table I–8–1.

The limiting web slenderness ratios are

$$\text{for } C_a \leq \frac{1}{8}$$

$$\frac{h}{t_w} \leq 3.14\sqrt{\frac{E}{F_y}}\left[1 - 1.54C_a\right] \tag{3–50}$$

$$\text{for } C_a > \frac{1}{8}$$

$$\frac{h}{t_w} \leq 1.12\sqrt{\frac{E}{F_y}}\left[2.33 - C_a\right] \tag{3–51}$$

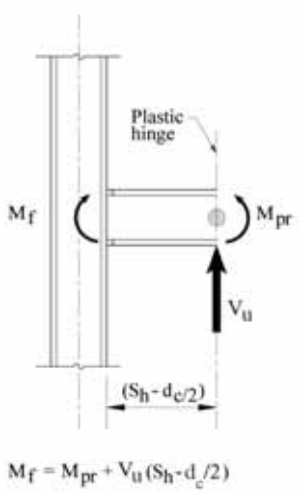

Fig. 3–20. Forces at column face from beam plastic hinge.

Using C_a of 1.0, one can see that a ratio of h/t_w of 36 will always satisfy the requirement for F_y = 50 ksi.

In keeping with the expected moment-frame behavior, Section 17.4.d gives lateral bracing requirements. The maximum brace spacing is the same as for SMF:

$$L_b \leq 0.086 r_y \left(\frac{E}{F_y}\right) \tag{3–52}$$

HBE bracing force requirements are based on the section expected plastic moment:

$$P_{br} = 0.02 F_y b_f t_f \tag{3–53}$$

The brace stiffness required to satisfy AISC 360 Equation A–6–8, using the section expected plastic moment and C_d of 1.0, is

$$\beta_{br} = \frac{13.3 R_y F_y Z}{L_b \left(d - t_f\right)} \tag{3–54}$$

Finally, AISC 341 has specific requirements for VBE splices (Section 17.4e, which refers to Section 8.4). Such splices must be capable of resisting the same forces as are required for the column. For columns subject to net tension, two additional requirements apply. First, if partial-joint-penetration groove welds are used, splice required strengths must be doubled. Second, flange splices must be able to resist forces corresponding to one-half of the expected strength of the smaller flange:

$$R_u = \frac{1}{2} R_y F_y A_f \tag{3–55}$$

Splices are required to be at least four ft from the nearest HBE, or at the midpoint of the clear height of the VBE.

3.5.2. DESIGN

The application of these provisions in order to achieve the expected performance is discussed below. Designers must be aware that conformance to AISC 341 cannot by itself guarantee ductile system behavior for all configurations and applications. Attention must be given to the specifics of each design.

3.5.2.1. Web-Plate Design

The high-seismic design of web plates is the same as the low-seismic design of these elements. The design strength is computed using the calculated angle of tension stress (AISC 341 Equation 17–2, Equation 3–1) and the design shear strength based on that angle (AISC 341 Equation 17–1, Equation 3–20). This strength is compared to the required strength of the web plate as determined from analysis. This required strength is based on the horizontal shear resisted by the SPSW, some of which is resisted by the VBE.

3.5.2.2. HBE Design

Horizontal boundary elements are designed for forces corresponding to yielding of the web plate. Axial forces in HBE are largely due to the effects of web-plate tension on the VBE. Flexural forces are due in part to web-plate tension (where plates of differing thickness are used above and below the beam, or where only one web plate connects to the beam, such as at the top of the SPSW).

The required flexural strength of the HBE at the top and bottom of the SPSW can be quite large. At other levels, the required flexural strength due to web-plate yielding is limited to the difference in web-plate strength above and below and to any difference in the angle of the tension stress α. The load that the web plates are expected to exert on the HBE can be estimated using Equation 3–44.

Where the same web plate thickness is provided both above and below the HBE, Equation 3–44 will result in no flexural requirement for the beam. While this is consistent with achieving the full yielding of the web plates, use of a very flexible beam will result in the contribution of the moment frame being negligible, which is not consistent with the assumed system behavior. At a minimum, the beam must be designed to resist the differential forces due to the calculated story shears tributary to the frame (Equation 3–24). Providing beams of radically different strengths from one level to the next is not recommended.

At the base, a steel beam in the foundation may be provided. Alternatively, a concrete foundation may be designed to resist these forces, typically by acting as a beam spanning between column footings. Strong-column/weak-beam proportioning is not addressed by the provisions at this location. While flexural yielding in the grade beam is preferable to flexural yielding at the base of the column, this may not be feasible for beams designed to span from column to column resisting the tension yielding of the web plate.

While the web local yielding limit state in the HBE is only required to resist the stress σ_{11} (Figure 3–6), this stress combines in the web with the shear stress σ_{12}. It is therefore advisable to use sections with webs that are at least as strong as the expected strength of the web plate. For sections of a different material grade, the recommended minimum thickness of the HBE web is

$$t_{w\,HBE} \geq \frac{t_w R_y F_y}{F_{y\,HBE}} \tag{3–56}$$

where

$F_{y\,HBE}$ = the yield stress of the HBE material

$R_y F_y$ = the expected yield stress of the web-plate material

t_w = the thickness of the web plate

$t_{w\,HBE}$ = the thickness of the HBE web

Flexural forces from frame deformation must also be resisted by the HBE. These flexural forces can be assumed to cause plastic hinges to form at the ends of the beam. Thus, the flexural forces from frame deformation can be ignored if the HBE are designed to have sufficient strength to resist web-plate tension assuming a simple span. Thus, the required midspan flexural strength of the HBE is

For LRFD

$$M_u = \frac{\left(w_u + w_g\right)L_h^2}{8} + \frac{P_u L_h}{4}$$

For ASD (3–57)

$$M_a = \frac{\left(w_a + w_g\right)L_h^2}{8} + \frac{P_a L_h}{4}$$

The *PL*/4 terms above can be modified appropriately when the arrangement of framing beam(s) is not one beam at midspan of the HBE.

This flexural force is combined with the axial force, which has two sources. The first is VBE reactions due to the inward force from the web plate. The second is a difference in the effects of the webs above and below, due to any difference in thickness and angle α and possibly material.

Figure 3–21 shows the assumed yield mechanism of a two-story SPSW, with internal forces due to (a) web-plate tension and (b) flexural deformation.

The axial force from VBE can be estimated by assuming that VBE deliver forces equally to the top and bottom of each story. Thus the axial force from this source is

$$P_{HBE\ (VBE)} = \sum \frac{1}{2} R_y F_y \sin^2(\alpha) t_w h_c \qquad (3–58)$$

From the web plates, the axial force (assuming equal collector conditions on each side of the SPSW) is the additional collector force required to cause web-plate yielding at that level

$$P_{HBE(web)} = \frac{1}{2} R_y F_y \left[t_i \sin(2\alpha_i) - t_{i+1} \sin(2\alpha_{i+1})\right] L_{cf} \qquad (3–59)$$

This force should not be less than the required strength of the collector.

At the VBE in tension, both the collector and the VBE tend to cause compression in the HBE-to-VBE connection. At the VBE in compression, the collector tends to cause tension while the VBE tends to cause compression in the HBE-to-VBE connection.

Equations 3–58 and 3–59 give seismic load effects, which are combined with other loads according to the appropriate load combinations (LRFD or ASD).

The required shear strength of HBE was previously established in the discussion of the AISC 341 requirements (Equation 3–43). As hinging is expected in the HBE, the web connection should be designed to resist both the shear and axial forces.

As noted earlier, the probable beam moment may be reduced considering the axial force present in the HBE-to-VBE connections.

3.5.2.3. VBE Design

The high-seismic design of SPSW requires that web-plate tension yielding be the primary source of system inelasticity. Failure of VBE under overturning forces must be precluded at forces corresponding to yielding of the web plate.

The most direct method of achieving this is to design the web plates for the calculated forces with as little overstrength as possible (i.e., with demand-to-capacity ratios as close to unity as possible), and to design the VBE for the sum of the shear strengths of the connected web plates (plus the gravity load). The seismic axial compressive force is thus limited to the sum of the web-plate strengths plus the sum of the HBE shears derived above

$$E_m = \sum \frac{1}{2} R_y F_y \sin(2\alpha) t_w h + \sum V_u \qquad (3–60)$$

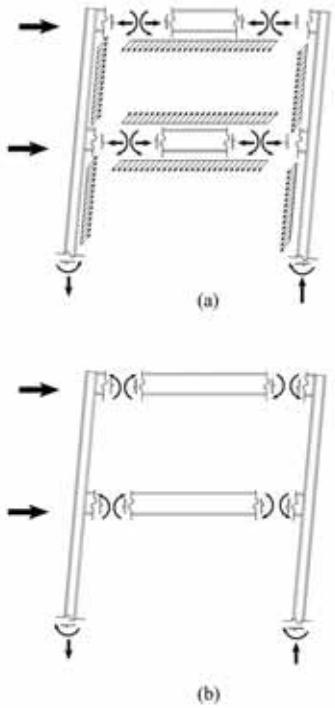

Fig. 3–21. Internal SPSW forces due to (a) web-plate tension (b) flexural deformation.

where

$\sum V_p$ = the sum of beam shears from Equation 3–43.

This force should not be amplified by the overstrength factor Ω_0, as it represents the capacity of the SPSW. The final term is especially important for shorter buildings, as the compression delivered to the column by the top HBE can be significant. For simplicity of calculation, $\sum V_p$ can be bounded by the sum of the beam shear strengths.

Column tension forces can be established similarly. However, across any horizontal section of the SPSW, the seismic tension is shared between the web plate and the VBE, and thus seismic tensile forces in VBE are significantly lower than the corresponding compressive seismic forces in the opposite VBE. In the context of Equation 3–60, the term $\sum V_p$ must be separated into the part that acts upward (the beam shear due to plastic-hinge formation) and the part that acts downward (the force from web-plate tension on the HBE). The expression for seismic axial tension force is

$$E_m = \sum \frac{1}{2} R_y F_y \sin(2\alpha) t_w h_c + \sum \left[\frac{2M_{pr}}{L_h} - \frac{w_u}{2} L_{cf} \right] \quad (3\text{–}61)$$

Note that the forces from web-plate tension on the HBE reduce the tension in the column.

The most accurate method of establishing VBE flexural forces (shears and moments), outside a nonlinear analysis, is to model the VBE as a continuous member on multiple supports (Berman, 2005). Applied to this VBE model are the inward forces due to web-plate tension and the moments from beam plastic hinging (computed at the column centerline as shown in Figure 3–19 and Equation 3–46). Beam supports may be calculated as rigid or as a spring with axial stiffness equivalent to the HBE axial stiffness calculated based on a length equal to ½ L_{cf}. Figure 3–22 shows such a model. HBE axial flexibility is neglected in the figure.

Alternatively, the shears and moments in VBE may be approximated considering the conditions at each story individually. VBE shear is due to both the web-plate tension and the portion of the story shear not resisted by the web plate. The shear due to web-plate tension is

$$V_{VBE(web)} = \frac{1}{2} R_y F_y \sin^2(\alpha) t_w h_c \quad (3\text{–}62)$$

The shear due to hinging of the HBE is

$$V_{VBE(HBE)} = \sum \frac{\frac{1}{2} M_{pb}^*}{h_c} \quad (3\text{–}63)$$

This shear should be at least equal to the portion of the story shear not resisted by the web plate. This force is determined by frame analysis and can be assumed as being shared equally by the two VBE. The total shear is

$$V_u = V_{VBE(web)} + V_{VBE(HBE)} \quad (3\text{–}64)$$

Similarly, VBE moments are due to both the web-plate tension and hinging of the HBE. For a fixed-fixed condition, the moment from web-plate tension at the connection is

$$M_{VBE(web)} = \frac{R_y F_y \sin^2(\alpha) t_w h_c^2}{12} \quad (3\text{–}65)$$

The moment due to hinging of the HBE can be determined from analysis, or, conservatively, one-half of the flexural strengths of the beams can be applied to each column segment at a connection, as indicated by AISC 341 Section 9.6.

It should be noted that Section 17.4a (which invokes Section 9.6, the SMF strong-column/weak-beam check) specifically excludes "consideration of the effects of the webs," and thus Equation 3–64 is not required. It is the opinion of the authors, however, that the flexure from web-plate tension should be considered in conjunction with the forces corresponding to beam hinging. Thus, under this method, this design check is similar to the strong-column/weak-beam check of Section 17.4a.

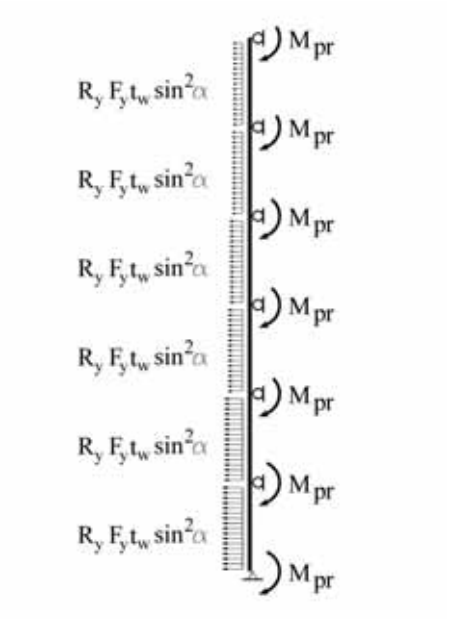

Fig. 3–22. Model of a VBE for computing flexural forces.

The procedure recommended here is twofold. In the VBE design, the moments applied from HBE hinging are not amplified by the factor R_y, nor by the strain-hardening factor of 1.1. The resulting design is therefore likely to result in HBE hinging prior to VBE hinging, although it is not assured that inelastic rotational demands will be precluded in VBE as the HBE strain hardens. In this design check, the critical VBE is the one in compression for three reasons. First, the VBE axial compression force is substantially larger than the tension force. Second, the compression force is additive to gravity forces. Finally, the HBE axial force is less at this connection (due to the collector force and the VBE inward reaction being in opposite directions). Thus, the moment resulting from HBE hinging is larger.

In order to help prevent any VBE hinging from leading to a weak-story condition, a strong-column/weak-beam check is performed. In this case, the factors R_y and 1.1 are used (but the resistance factor on the VBE strength is not). The strong-column/weak-beam check is modified to address the entire SPSW. The greater flexural strength that can be utilized from the VBE in tension is used to supplement that of the VBE in compression, and thus a weak-story condition is avoided. This is presented under "Connection Design."

The moment from HBE hinging is

$$M_{VBE(HBE)} \leq \frac{\frac{1}{2}\sum M^*_{pb}}{1.1R_y} \qquad (3\text{–}66)$$

where

M^*_{pb} = the moment at the column centerline due to beam plastic hinging (see "Connection Design")

If the VBE flexural forces are taken from the analysis instead of from capacity design, they should be amplified to reflect the condition at yielding of the web plate or evaluated at the expected displacement. Where a nonlinear analysis is used to model web-plate yielding, the VBE flexural forces from the analysis at the expected drift may be used directly.

The VBE flexure due to beam hinging is typically greater than that due to web-plate tension. In such cases, the flexure away from the connection does not govern the design.

As the required HBE flexural strength is governed by flexure in the span due to web-plate tension, it is convenient to use a Reduced Beam Section (RBS) connection in the HBE to limit the required flexural strength of the VBE. See AISC 358 for a detailed treatment of the design of RBS connections.

The RBS connection is thus proposed for economy in the design of the VBE. Alternatively, the connection may be a more typical welded connection (WUF-W). Such a connection will not reduce the required flexural strength of the HBE, as this is based on resisting web-plate tension after formation of plastic hinges; it will, however, require a greater VBE flexural strength to maintain strong-column/weak-beam proportioning. This should be considered in weighing the economy of the two connections.

It should be noted that in neither case are the quality requirements of SMF applicable to the connection, as these connections are not expected to undergo the large rotations expected for SMF.

3.5.2.4. Axial Force Reduction in VBE

Axial forces corresponding to web-plate yielding at all levels simultaneously can be extremely high. For this reason, alternative methods for estimating maximum forces corresponding to the expected mechanism have been proposed. Three of these are outlined in the Commentary to AISC 341.

The first method is "nonlinear push-over analysis" (POA). This method involves an analysis with incrementally increasing load and element stiffness properties correspondingly modified as yielding occurs. The force distribution selected should favor high overturning moments for purposes of design of the VBE. POA methods are outlined in detail in FEMA 356.

The second method is the "combined linear-elastic computer programs and capacity design concept" (LE+CD). This method involves the design of the VBE at a given level by applying loads from the expected strength of the connecting web plate and adding the overturning loads from levels above using the amplified seismic load:

$$E_m = \frac{1}{2} R_y F_y \sin(2\alpha)\, t_w h_c + \Omega_0 E_{(above)} \qquad (3\text{–}67)$$

For SPSW, the overstrength factor Ω_0 is 2.0 for the basic system and 2.5 for SPSW in a dual system. Figure 3–23 shows a free-body diagram of the VBE under these seismic loads.

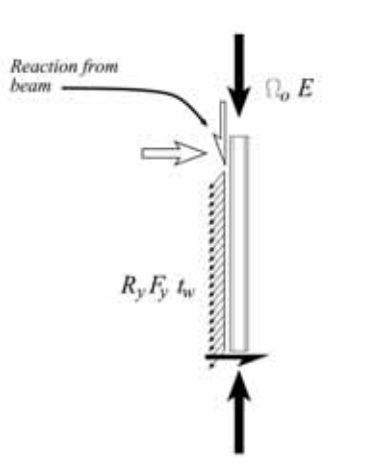

Fig. 3–23. Free-body-diagram of column under LE+CD loading.

To be a true capacity design, the reaction from the beam above should include the effect of web-plate tension.

The third method described is the "indirect capacity design approach" (ICD); this method is based on the CSA-S16-01 code used in Canada (CSA, 2001). In this method, an overstrength factor B is calculated based on the web-plate at the first level.

For LRFD

$$B = \frac{[0.5R_y F_y \sin(2\alpha) t_w L]_1}{(V_u)_1} \tag{3–68}$$

For ASD

$$B = \frac{[0.5R_y F_y \sin(2\alpha) t_w L]_1}{(1.5V_a)_1}$$

where the subscript "1" denotes that values are taken at the first level of the SPSW.

The base overturning is then calculated as B times the overturning moment due to the design seismic forces. This overturning moment is used for the first two levels. Above that, the overturning moment is taken as a linear function between that value and B times the overturning moment due to the design seismic forces at the bottom of the top web plate. The overstrength of the web plates at levels other than the first is not considered in this method. Figure 3–24 shows this diagrammatically.

This moment profile corresponds to a force distribution that is fairly severe with respect to overturning moment. The corresponding loading profile is shown in Figure 3–25.

For convenience, designers may wish to use a computer model to obtain axial forces corresponding to the ICD method. The value of the force can be calculated as

$$F = \frac{B[M_1 - M_n]}{H_{n-1} - H_2} \tag{3–69}$$

where

M_1 = the calculated moment at the bottom of the first level

M_n = the calculated moment at the bottom of the top level

$H_{n\text{-}1}$ = the height above the base of level $(n - 1)$

H_2 = the height above the base of the second level

The height at which this force acts can be calculated as

$$H = [H_{n-1} - H_2]\left[\frac{1}{1 - \frac{M_n}{M_1}}\right] + H_2 \tag{3–70}$$

where

H = the height above the base at which the force acts

Figure 3–26 shows the different overturning column compression and tension forces for the design example in Chapter 5 using the sum of web-plate capacities (CAP), the combined linear-elastic computer programs and capacity design concept (LE+CD), the indirect capacity design approach (ICD), and push-over analysis (POA). Tension forces are shown on the left, and compression forces on the right.

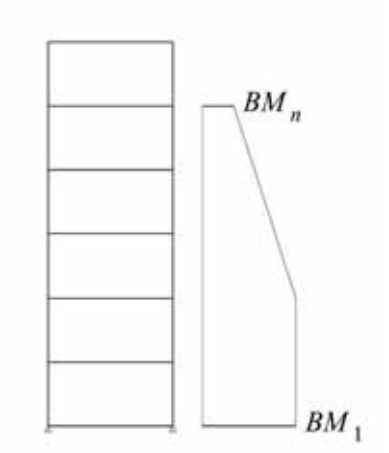

Fig. 3–24. Schematic of ICD overturning moment.

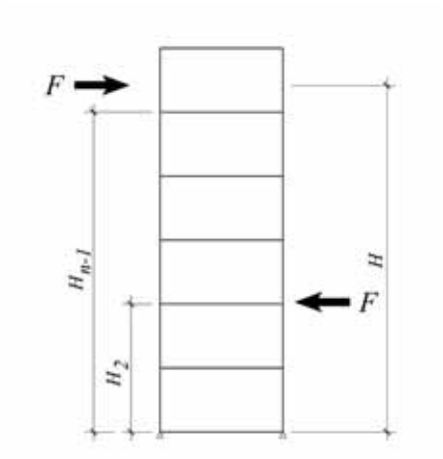

Fig. 3–25. ICD implied force distribution.

Note that for this case, tension forces can be overestimated (above the capacity-design method) using the LE+CD and ICD methods.

It should be noted that using methods other than capacity design for the VBE will lead to designs in which VBE failure is possible, although unlikely. The methods presented are intended to reasonably estimate VBE axial forces based on studies of model buildings, which are typically regular. Where structural irregularities exist, designers should consider carefully whether the LE+CD and ICD methods are sufficient.

3.5.2.5. Configuration

The high overturning forces expected in SPSW can be mitigated by the use of special configurations to distribute the overturning over multiple bays. Figure 3–27 shows four of these configurations: (a) web plate offset at one level; (b) web plate offset at each level; (c) additional web plates at certain levels acting as outriggers to deliver overturning forces to outer columns; and (d) additional web plates at certain levels acting as coupling beams between shear walls.

Designers should be aware that each of these configurations incorporates structural irregularities. All use an in-plane offset, which requires consideration of the structural overstrength in designing both the horizontal elements that transfer the seismic forces from one panel to another, as well as in the vertical elements that resist the overturning. Additionally, the configurations introduce more HBE with web plates only above or only below; these HBE are thus subject to both large axial forces and (simultaneous) large flexural forces. Additionally, where coupling or outrigger web plates are provided at a certain level, that level may have too much strength to participate in the inelastic response. Drift may then be concentrated at other levels.

Additionally, beams can be used as outriggers or couplers between walls. Figure 3–28 shows two such configurations: (a) outrigger beams that deliver overturning forces to outer

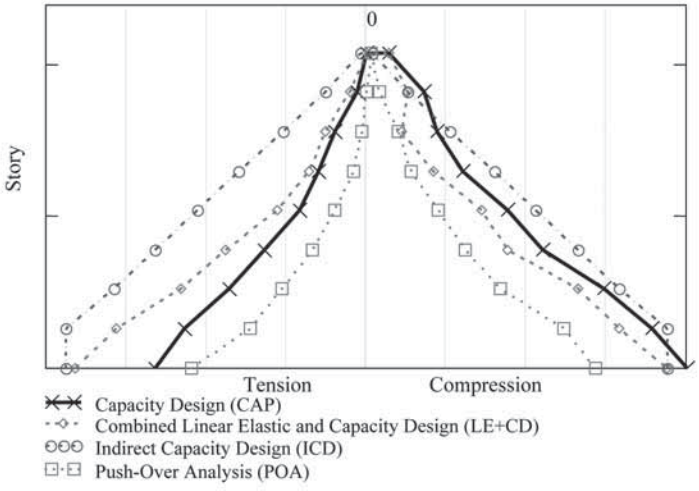

Fig. 3–26. Column axial forces.

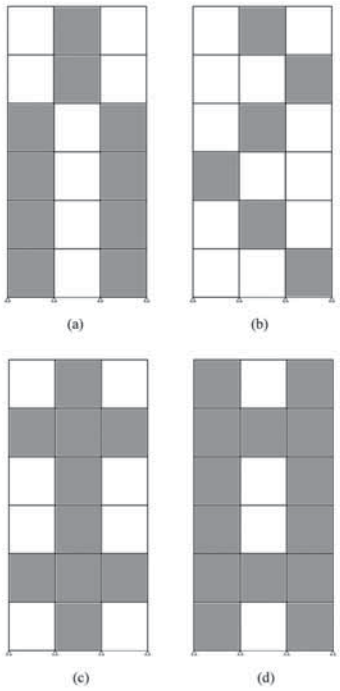

Fig. 3–27. Configurations that reduce overturning by means of web-plate location.

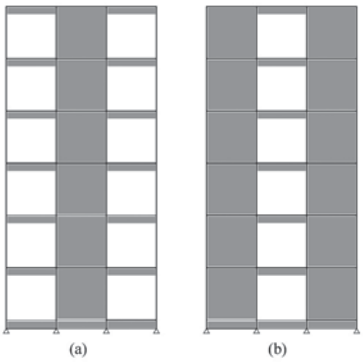

Fig. 3–28. Configurations that reduce VBE overturning forces by means of beams.

columns; and (b) coupling beams between shear walls. Beams used to distribute overturning forces should comply with the requirements of HBE. As in the case of HBE-to-VBE connections, it is preferable that a tested beam-to-column connection be used, and that designs conform to limitations in AISC 358, such as span-to-depth ratio.

3.5.2.6. Connection Design

AISC 341 contains numerous requirements pertaining to the connection of beams (HBE) to columns (VBE) in SPSW. Two of these, the strong-column/weak-beam requirement and the panel-zone strength requirement, require calculation of moments corresponding to plastic-hinge formation in the HBE. The HBE probable moment strength is combined with shear in the beam to calculate the moment at the column centerline (for the strong-column/weak-beam requirement) or at the column face (for the panel-zone strength requirement). The probable moment for each beam is

$$M_{pb}^{*} = M_{pr} + V_u e \tag{3–71}$$

where

V_p = the shear at the plastic hinge

e = the distance from the plastic hinge to the point at which moments are computed (the column centerline for the strong-column/weak-beam requirement and the column face for the panel-zone strength requirement)

M_{pr} = the probable beam moment as given in Equation 3–40, 3–41, or 3–42

For the strong-column/weak-beam requirement, the eccentricity e is

$$e = s_h \tag{3–72}$$

For the panel-zone strength requirement, the eccentricity e is

$$e = s_h - \frac{1}{2} d_c \tag{3–73}$$

where

d_c = the column depth

The plastic hinge location should be established by plastic analysis where the flexural forces due to gravity loading exceed 30 percent of the beam plastic moment. This concept may be extended to include the flexural forces due to the web-plate tension for purposes of the beam design. However, typical beams (those at levels other than the top and bottom of the SPSW) have moderate flexural demand due to web-plate tension.

As mentioned earlier, designers may wish to calculate a reduced beam flexural strength based on the axial force present in the HBE-to-VBE connection. This will permit the calculation of a lesser required plastic section modulus for the VBE.

As discussed earlier, for the strong-column/weak-beam check, designers may wish to consider both VBE to ensure that a weak-story condition does not exist. This permits utilization of the flexural strength of the VBE in tension, which is far greater due to its lower axial force. For this check, both VBE are considered, as is the axial force in each end of the HBE, and the flexural strength of the adjoining beams outside the SPSW (if rigidly connected).

The required column plastic section modulus (assuming a VBE above and below the connection) is

For LRFD

$$Z_c \geq \frac{1}{2} \frac{\sum M_{pb}^{*}}{\left[2F_{yc} - \frac{|P_{uC}| + |P_{uT}|}{A_g} \right]}$$

For ASD (3–74)

$$Z_c \geq \frac{1}{2} \frac{\sum M_{pb}^{*}}{\left[2F_{yc} - \frac{|1.5P_{aC}| + |1.5P_{aT}|}{A_g} \right]}$$

where

F_{yc} = the VBE yield strength

P_{uC} = the axial compression force in the VBE (including the effects of web-plate tension) for LRFD

P_{uT} = the axial tension force in the VBE (including the effects of web-plate tension) for LRFD

P_{aC} = the axial compression force in the VBE (including the effects of web-plate tension) for ASD

P_{aT} = the axial tension force in the VBE (including the effects of web-plate tension) for ASD

A_g = the VBE area

$\sum M_{pb}^{*}$ = sum of the expected flexural strengths of the beams framing into each VBE (i.e., each end of the HBE, plus the adjoining beams outside the SPSW, if rigidly connected)

The required column web thickness is based on the required panel-zone shear

$$R_u = \frac{\sum M^*_{pb}}{d_z} - \frac{1}{2} V_{VBE(HBE)} \tag{3–75}$$

where $V_{VBE(HBE)}$ is that calculated in Equation 3–62 and M^*_{pb} is calculated at the face of the column for the design of the panel zone (see Bruneau et al., 1997).

Note that only the shear in the VBE due to the moment-frame behavior ($V_{VBE(HBE)}$) is considered in reducing the panel zone shear, as the VBE shear due to web-plate tension ($V_{VBE(web)}$) is balanced by the corresponding force in the HBE ($P_{HBE(VBE)}$).

The panel-zone strength may be computed using either AISC 360 Equations J10–11 or J10–12 and a resistance factor of 1.0 per AISC 341 Section 9.3a. Note that J10–11 and J10–12 require that panel-zone deformations are accounted for in the analysis; in the case of SPSW, panel zone deformations do not contribute to drift to the degree they do in moment frames, and Equations J10–11 and J10–12 may be considered applicable regardless of whether the analysis includes panel-zone deformation.

The connection of the HBE web to the VBE must be designed to resist the shear in the VBE in conjunction with the axial force transferred from the VBE to the HBE. This latter force consists of both the story collector force and the inward reaction from the transverse loading on the VBE from web-plate tension. The collector force is amplified as required by ASCE 7. Equations for the two forces are given below. The vertical force is

$$R_{u(vert)} = V_{HBE} \tag{3–76}$$

The horizontal force is the greater of

$$R_{u(horiz)} \geq P_{HBE(VBE)} + \Omega_0 P_{collector} \tag{3–77}$$

and

$$R_{u(horiz)} \geq P_{HBE(VBE)} + P_{HBE(web)} \tag{3–78}$$

This is a compression force. If desired, a lower tension force may be calculated.

3.5.2.7. Web-Plate Connection Design

For high-seismic design, the web plate is assumed to reach its expected yield stress

$$\sigma = R_y F_y \tag{3–79}$$

where

$R_y F_y$ = the expected yield stress of the web-plate material

This stress is used in the equations developed previously for force per unit length at the web-plate connections to the boundary elements:

$$r_{u(HBE)} = R_y F_y \cos(\alpha)\, t_w \tag{3–80}$$

$$r_{u(VBE)} = R_y F_y \sin(\alpha)\, t_w \tag{3–81}$$

For bolted joints, the maximum spacing can be expressed as

For LRFD

$$s_x \leq \frac{R_y F_y \cos(\alpha) t_w}{\phi r_n}$$

For ASD (3–82)

$$s_x \leq \frac{\Omega R_y F_y \cos(\alpha) t_w}{1.5 r_n}$$

For LRFD

$$s_y \leq \frac{R_y F_y \sin(\alpha) t_w}{\phi r_n}$$

For ASD (3–83)

$$s_y \leq \frac{\Omega R_y F_y \sin(\alpha) t_w}{1.5 r_n}$$

where

s_x = the horizontal bolt spacing at the HBE

s_y = the vertical bolt spacing at the VBE

This spacing requirement cannot be achieved using a single line of bolts unless the web plate is reinforced for the bolted connection. This is due to the spacing requirement to preclude fracture of the web plate from occurring prior to yield. The minimum bolt spacing in a line on the connection to the HBE is

For LRFD

$$s_x \geq \frac{d_h + 1/16 \text{ in.}}{\left[1 - \dfrac{R_y F_y t_w}{\phi R_t F_u t'_w}\right]}$$

For ASD (3–84)

$$s_x \geq \frac{d_h + 1/16 \text{ in.}}{\left[1 - \dfrac{\Omega R_y F_y t_w}{1.5 R_t F_u t'_w}\right]}$$

where

d_h = the hole size measured parallel to s

t'_w = the reinforced thickness of the web plate (equal to t_w where no reinforcement is used)

R_t = ratio of expected to specified minimum tensile stress (from Section 6.2 of AISC 341)

F_u = the specified minimum tensile stress of the web-plate material

The spacing requirement for the connection to the VBE is

For LRFD

$$s_y \geq \frac{d_h + 1/16 \text{ in.}}{\left[1 - \frac{R_y F_y t_w}{\phi R_t F_u t_w'}\right]}$$

For ASD (3–85)

$$s_y \geq \frac{d_h + 1/16 \text{ in.}}{\left[1 - \frac{\Omega R_y F_y t_w}{1.5 R_t F_u t_w'}\right]}$$

It is clear that for a practical design, reinforcement of the web plate is advantageous. Although tests of unreinforced bolted web-plate connections have not shown fracture (Astaneh-Asl, 2001), such connections are difficult to make compliant with AISC 341 requirements. For both reinforced and unreinforced connections, multiple lines of bolts may be required. Although testing indicates that the strength of bolted connections of SPSW web plates is greater than that corresponding to this application of AISC 360 requirements, construction has shown that welded web-plate connections are often more practical.

For fillet-welded connections, the required weld size at the HBE can be expressed as

$$w_{HBE} = \frac{R_y F_y \cos(\alpha) t_w \sqrt{2}}{\phi 0.6 F_{EXX}\left[1 + 0.5\cos^{1.5}(\alpha)\right]}$$

For LRFD (3–86)

$$w_{HBE} = \frac{\Omega R_y F_y \cos(\alpha) t_w \sqrt{2}}{1.5\left(0.6 F_{EXX}\right)\left[1 + 0.5\cos^{1.5}(\alpha)\right]}$$

For ASD

The required weld size at the VBE can be expressed as:

$$w_{VBE} = \frac{R_y F_y \sin(\alpha) t_w \sqrt{2}}{\phi 0.6 F_{EXX}\left[1 + 0.5\sin^{1.5}(\alpha)\right]}$$

For LRFD (3–87)

$$w_{HBE} = \frac{\Omega R_y F_y \cos(\alpha) t_w \sqrt{2}}{1.5\left(0.6 F_{EXX}\right)\left[1 + 0.5\cos^{1.5}(\alpha)\right]}$$

For ASD

Typically, the angle is near 45° and the weld size required is the same at VBE and HBE connections.

As mentioned previously, welded connections should restrain the web plate from rotation in order to resist the expected plate buckling.

Chapter 4

Design Example I: Low-Seismic Design

4.1. OVERVIEW

This chapter illustrates the design of a building utilizing steel plate walls (SPW) as the lateral-load-resisting system in a zone of low seismicity (for $R = 3$ without application of the ductile-detailing requirements of AISC 341). The building will be designed for a site in downtown Chicago.

4.2. STANDARDS

The governing codes will be assumed to be the 2005 editions of ASCE 7 (including Supplement No. 1) and AISC 360. Certain design equations from AISC 341 will be used, but full compliance with that standard is not required when R is taken equal to 3.

4.3. BUILDING INFORMATION

The building footprint, size, and typical plan are shown in Figure 4–1. The building weight, W, is 20,700 kips. Plate material is ASTM A36 (F_y = 36 ksi, F_u = 58 ksi) and beam (HBE) and column (VBE) material is ASTM A992 (F_y = 50 ksi, F_u = 65 ksi).

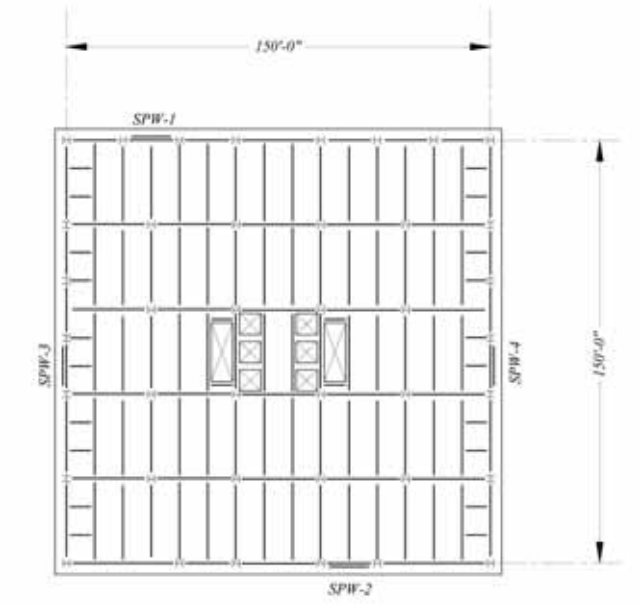

Fig. 4–1. Typical floor plan.

The building design includes four SPW panels on the perimeter. It is also common to utilize walls of the buildings core as SPW. In such a configuration, building torsion should be restrained by a supplementary perimeter system. Moment frames are a common choice for such a supplementary perimeter system. Note that for Seismic Design Categories B and C, the redundancy factor, ρ, is 1.0 regardless of configuration per ASCE 7 Section 12.3.4.1.

In order to focus on the SPW system, rather than the intricacies of the design of dual systems, the building in this design example has the SPW located on the perimeter. A, typical elevation of a SPW is shown in Figure 4–2.

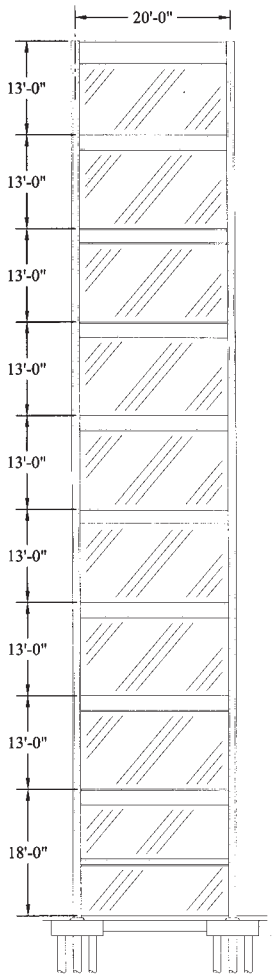

Fig. 4–2. SPW elevation.

A horizontal strut is used at mid-height of the first floor. This permits use of a VBE at the foundation level with a lower moment of inertia than would otherwise be required.

The building is located in downtown Chicago, on the corner of Wacker Drive and State Street. The seismic ground motion values are obtained from USGS maps based on the building location. In this design, the USGS web site[1] is used to obtain the information by entering the building latitude and longitude.[2] The latitude and longitude values for the site are 41.887° and −87.627°, respectively.

The soil at the site corresponds to Site Class D, reflecting the stiff soil in this location. The Building Occupancy Category is I, based on its use as an office building (ASCE 7 Table 1–1).

4.4. LOADS

For this location, the Peak Ground Acceleration (PGA) for the Maximum Considered Earthquake (MCE) is $0.0810g$, where g is the acceleration of gravity. Spectral accelerations for the MCE are $0.1618g$ at a period of 0.2 second and $0.0592g$ at a period of 1.0 second. These values are expressed as S_s and S_1, respectively:

$$S_s = 0.1618g$$

$$S_1 = 0.0592g$$

These spectral values are modified based on the site class. The modification values are selected from ASCE 7 Tables 11.4–1 and 11.4–2 based on site class and spectral acceleration. The modification vales are

$$F_a = 1.6$$

$$F_v = 2.4$$

The adjusted MCE spectral response acceleration parameters are calculated using ASCE 7 Equations 11.4–1 and 11.4–2:

$$S_{MS} = F_a S_s = 0.259g \quad (4\text{–}1)$$

$$S_{M1} = F_v S_1 = 0.142g \quad (4\text{–}2)$$

For design purposes, two-thirds of these MCE parameters are used. This reflects the assumption in ASCE 7 that there is likely to be a reserve capacity of approximately 50 percent at design level. This is equivalent to design using MCE values and a 50 percent greater response modification coefficient.

The design spectral response acceleration parameters are calculated using ASCE 7 Equations 11.4–3 and 11.4–4:

$$S_{DS} = \frac{2}{3} S_{MS} = 0.173g \quad (4\text{–}3)$$

$$S_{D1} = \frac{2}{3} S_{M1} = 0.0947g \quad (4\text{–}4)$$

These values are used to establish the building Seismic Design Category (SDC). Table 11.6–1 is used to compare S_{DS} to certain limits. Table 11.6–2 is used similarly with S_{D1}. Each table gives a SDC based on the building occupancy category and the design spectral response acceleration parameter (S_{DS} or S_{D1}). The more severe SDC obtained from the two tables is used. For this building design, the SDC is B.

The SDC is used to determine many aspects of the seismic design of the building. ASCE 7 Table 12.6–1 limits the analysis procedures that are permitted based on SDC, period, and irregularities.

For SDC B, the designer has two options. The first is to design with SPSW conforming to the requirements of AISC 341, and using a response modification coefficient R of 7. Such a design would likely have the web-plate strength governed by wind loads and the design of VBE and HBE governed by the requirements of AISC 341 based on web-plate strength. If this option is selected, the requirements in AISC 341 must be met, even if wind controls.

Alternatively, the building may be designed with SPW using a response modification coefficient $R = 3$ ("Structural System Not Specifically Detailed for Seismic Resistance") without conforming to all of the AISC 341 requirements; this latter approach will be followed in this chapter. Certain design equations from AISC 341 will be used, but the frame need not be fully compliant with the requirements of that standard. For example, the AISC 341 compactness limits will not be applied to members, and the HBE and VBE will not be designed as a rigid frame.

The equivalent lateral force procedure provided in ASCE 7 Section 12.8 will be used in this example. The building period is estimated using ASCE 7 Equation 12.8–7:

---

[1]**http://earthquake.usgs.gov/research/hazmaps/design/index.php**.

[2]The latitude and longitude of a street address can be found using one of the many mapping web sites.

$$T_a = C_T h_n{}^x$$
$$= 0.02 \times (122 \text{ ft})^{0.75} \quad (4\text{–}5)$$
$$= 0.734 \text{ sec}$$

The coefficient C_T and the exponent x are taken from ASCE 7 Table 12.8–2. The variable h_n is building height in feet.

The parameters S_{DS} and S_{D1} can be used in conjunction with ASCE 7 Equations 12.8–2 through 12.8–5 to construct a generalized spectrum, as is shown in ASCE 7 Figure 11.4–1. The spectrum for this building is shown in Figure 4–3.

For this case the building period is greater than T_s, and less than T_L (see ASCE 7 Section 11.4.5). Therefore, it is governed by ASCE 7 Equation 12.8–3. The associated seismic response coefficient, C_s, is computed based on this spectrum, the response modification coefficient, R, and the importance factor, I. For building occupancy category I, the importance factor, I, is 1.0 per ASCE 7 Table 11.5–1:

$$C_s = \frac{S_{D1}}{T_a\left(\frac{R}{I}\right)}$$
$$= \frac{0.0947g}{(0.734 \text{ sec})\left(\frac{3}{1}\right)} \quad (4\text{–}6)$$
$$= 0.0430g$$

The design base shear is calculated using ASCE 7 Equation 12.8–1:

$$V = C_s W$$
$$= 0.0430(20{,}700 \text{ kips}) \quad (4\text{–}7)$$
$$= 890 \text{ kips}$$

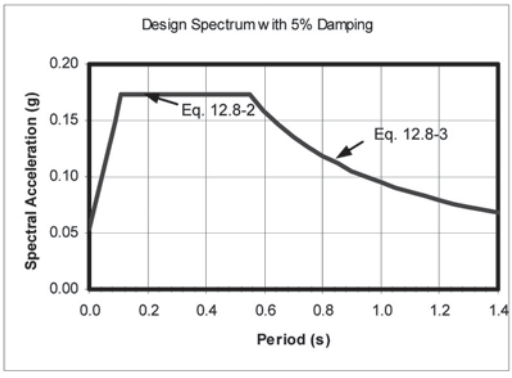

Fig. 4–3. Generalized site response spectrum.

Table 4.1. Vertical Distribution Factors and Story Forces

Level	Vertical Distribution Factor, C_{vx}	Story Force, F_x (kips)
Roof	0.225	200
Ninth Floor	0.174	155
Eighth Floor	0.152	135
Seventh Floor	0.129	115
Sixth Floor	0.107	95.2
Fifth Floor	0.0847	75.4
Fourth Floor	0.0635	56.5
Third Floor	0.0429	38.2
Second Floor	0.0238	21.2

This base shear is distributed vertically using ASCE 7 Equations 12.8–11 and 12.8–12:

$$F_x = C_{vx} V \quad (4\text{–}8a)$$

$$C_{vx} = \frac{w_x h_x{}^k}{\sum_{i=1}^{n} w_i h_i{}^k} \quad (4\text{–}8b)$$

The exponent k is interpolated for periods between 0.5 and 2.5 seconds. For this building design k is 1.12. The resulting values of C_{vx} for each level are shown in Table 4–1.

These forces are distributed horizontally based on the stiffness and location of each wall. An elastic analysis of the frames is performed both to determine this horizontal distribution and to design the frames themselves. The elastic analysis includes accidental torsion, as required by ASCE 7 Section 12.8.4.2.

The design forces for each SPW are based on this horizontal distribution of forces. Table 4–2 shows these forces.

The wind loads were found to be similar in intensity and their determination will be omitted for the sake of simplicity in presenting this example.

4.5. SPW DESIGN

The low-seismic design of SPW is intended to ensure nominally ductile performance. Design equations for the web plate are based on limited tension yielding. The design of beams and columns, which are referred to as HBE and VBE, respectively, is based on forces corresponding to the aver-

Table 4–2. Forces and Shears in Each SPW		
Level	**Frame Force (kips)**	**Frame Shear (kips)**
Roof	105	105
Ninth Floor	81.4	186
Eighth Floor	70.9	257
Seventh Floor	60.4	317
Sixth Floor	50.0	367
Fifth Floor	39.6	407
Fourth Floor	29.7	437
Third Floor	20.1	457
Second Floor	11.1	468

Table 4–3. ASTM A36 Web-Plate Design Strengths		
t_w (in.)	**ϕv_n (kips/in.)**	**ϕV_n (kips)***
0.0625	0.737	164
0.0673	0.793	176
0.0747	0.880	195
0.1046	1.23	274
0.125	1.47	327
0.1345	1.59	352
0.1875	2.21	491
0.250	2.95	654
0.3125	3.68	818
0.375	4.42	981
0.4375	5.16	1,150
0.500	5.89	1,310
0.625	7.37	1,640
*ϕV_n is calculated based upon L_{cf} = 20 ft minus 18 in.		

age web-plate tension stress. The web-plate strength is set to meet the demands corresponding to the seismic load analysis. In this design, the web-plate demands were determined in Section 4.4 using the equivalent lateral force procedure.

4.5.1. Preliminary Design

For preliminary design, as the size of HBE and VBE are not known, the web plates are assumed to resist the entire shear in the frame. As the angle of tension stress in the web plate is dependent on the section properties of the HBE and VBE, as well as on the web plate thickness and the frame dimensions, for preliminary design the angle of tension stress is assumed. Typical designs show that the angle of tension stress ranges from 30° to 55° (measured from a vertical line). The angle, α, is conservatively assumed as 30°.

Based on this angle, the design strength of web plates can be calculated using AISC 341 Equation 17–1:

$$\phi V_n = 0.90(0.42) F_y t_w L_{cf} \sin(2\alpha) \qquad (4\text{–}9)$$

where L_{cf} is the clear length of the web panel between VBE flanges.

Based on this equation and the assumed angle of tension stress, the design strength of web panels can be calculated in terms of design shear strength per unit length (ϕv_n). Assuming a value equal to the bay length (20 ft) minus 18 in., the plate design strengths in Table 4–3 can be determined, where

$$\phi v_n = 0.90(0.42)\ F_y t_w \sin(2\alpha) \qquad (4\text{–}10)$$

Using the design strengths for various plate thicknesses in ASTM A36 material from Table 4–3, preliminary plate thicknesses are selected at each level. Those sizes are presented in Table 4–4.

The design of VBE must satisfy both strength and stiffness requirements. The in-plane flexural stiffness is required to ensure that the web plate can develop sufficient tension throughout its height. This requirement is given in AISC 341 Section 17.4g

$$I_c \geq 0.00307 \frac{t_w h^4}{L} \qquad (4\text{–}11)$$

where

h = the distance between HBE centerlines

L = the distance between VBE centerlines

The required column stiffness at each level is shown in Table 4–5. For purposes of preliminary design, the beam depths at all levels are assumed to be identical, and thus the distance h is equal to the floor-to-floor height.

Note that the required moment of inertia at the first floor is very low. At this level, an intermediate HBE will be designed to reduce the height over which the VBE must resist the inward flexure due to web-plate tension.

Preliminary VBE design is based on these stiffness requirements. Strength requirements may control, but their calculation is dependent on analysis of the frame and combination with gravity loads.

Table 4–4. Preliminary Design of ASTM A36 Web Plates				
Level	**Web Plate Thickness t_w (in.)**	**Required Shear Strength V_u (kips)**	**Design Shear Strength ϕV_n (kips)**	**Demand/Capacity Ratio $\frac{V_u}{\phi V_n}$**
Ninth Floor	0.0625	105	164	0.640
Eighth Floor	0.0673	186	176	1.06
Seventh Floor	0.1046	257	274	0.938
Sixth Floor	0.125	317	327	0.969
Fifth Floor	0.125	367	327	1.12
Fourth Floor	0.1345	407	352	1.16
Third Floor	0.1875	437	491	0.890
Second Floor	0.1875	457	491	0.931
First Floor	0.1875	468	491	0.953

Table 4–5. Required Column Moment of Inertia				
Level	**Web Plate Thickness t_w (in.)**	**Panel Proportions**		**Required Column Moment of Inertia I_c (in.^{4})**
		h (in.)	**L (in.)**	
Ninth Floor	0.0625	156	240	473
Eighth Floor	0.0673	156	240	510
Seventh Floor	0.1046	156	240	792
Sixth Floor	0.125	156	240	947
Fifth Floor	0.125	156	240	947
Fourth Floor	0.1345	156	240	1,020
Third Floor	0.1875	156	240	1,420
Second Floor	0.1875	156	240	1,420
First Floor	0.1875	102	240	260

Where rigid beam-to-column connections are used, the design of HBE is dependent on flexural forces from an analysis of the frame. It should be noted, however, that flexural demands exist on the HBE based on differing web-plate tension above and below the beam. The load that the web plates are expected to exert on the HBE can be estimated as

$$w_u = \frac{V_{u(i)} - V_{u(i+1)}}{L_{cf} \tan(\alpha)} \qquad (4\text{–}12)$$

For preliminary design, a W30×108 will be used at the roof level and a W21×55 will be used at all other levels. Note that this uniform-load value is based on the assumption of an angle of tension stress of 30°. In most cases, the angle will be significantly greater, potentially permitting a reduction in this load on the beam.

Table 4–6. Preliminary Boundary Element Sections		
Level	**VBE**	**HBE**
Roof	–	W30×108
Ninth Floor	W12×96	W21×55
Eighth Floor	W12×96	W21×55
Seventh Floor	W12×120	W21×55
Sixth Floor	W12×120	W21×55
Fifth Floor	W12×120	W21×55
Fourth Floor	W12×120	W21×55
Third Floor	W12×152	W21×55
Second Floor	W12×152	W21×55
First Floor	W12×152	W10×45 (strut)

Table 4–7. Angle of Stress and Revised Web-Plate Thickness		
Level	**Angle of Stress α (°)**	**Web Plate Thickness t_w (in.)**
Ninth Floor	41.3	0.0625
Eighth Floor	41.2	0.0625
Seventh Floor	40.1	0.1046
Sixth Floor	39.7	0.1046
Fifth Floor	39.7	0.125
Fourth Floor	39.5	0.1345
Third Floor	38.6	0.1875
Second Floor	38.6	0.1875
First Floor	41.1	0.1875

The preliminary boundary element sections selected are presented in Table 4–6.

The determination of the angle of tension stress, α, is dependent on the geometric proportions of the frame, the section properties of the boundary elements, and the web-plate thickness. Once preliminary framing members are selected, a refined estimate of the angle of tension stress can be made using AISC 341 Equation 17–2:

$$\tan^4 \alpha = \frac{1+\frac{t_w L}{2A_c}}{1+t_w h\left[\frac{1}{A_b}+\frac{h^3}{360 I_c L}\right]} \qquad (4\text{–}13)$$

where

h = distance between HBE centerlines

A_b = cross-sectional area of a HBE

A_c = cross-sectional area of a VBE

I_c = moment of inertia of a VBE taken perpendicular to the direction of the web-plate line

L = distance between VBE centerlines

Web-plate thickness and boundary member sizes can be refined in this preliminary stage prior to a structural analysis of the frame. One or two iterations at this stage will permit beginning the analysis with sizes that are closer to optimal in terms of strength. Note, however, that iteration will not facilitate designs where drift is the governing criterion.

Based on the preliminary web-plate and boundary member designs, the angle of tension stress at each level is calculated. Table 4–7 presents the preliminary values of the angle of tension stress and the revised web-plate thickness based on AISC 341 Equation 17–1.

Framing member sizes are similarly revised based on the change in angle of tension stress and the change in web-plate thickness. Revised framing member sizes are presented in Table 4–8.

While such iteration can be easily performed in the preliminary design stage, designers should bear in mind that designs are subject to modification based on forces determined from an analysis of the frame. Effort in performing numerous iterations at the preliminary design stage may well be wasted. The purpose of refining the design at this stage is to reduce the number of iterations required in the analysis stage by providing more reasonable beginning sizes. This design procedure is based on the relative difficulty in revising preliminary designs (which can be done using a simple spreadsheet) and using currently available structural analysis software (which requires adaptive procedures discussed below).

4.5.2. Analysis

In order to complete the design of the HBE and VBE, design forces are required. In the preliminary design it was assumed that the entire story shear tributary to the frame was resisted by the web plate. Clearly, VBE with the flexural properties

Table 4–8. Revised Preliminary Boundary Element Sections		
Level	**VBE**	**HBE**
Roof	–	W30×108
Ninth Floor	W12×87	W21×55
Eighth Floor	W12×87	W21×55
Seventh Floor	W12×120	W21×55
Sixth Floor	W12×120	W21×55
Fifth Floor	W12×120	W21×55
Fourth Floor	W12×120	W21×55
Third Floor	W12×152	W21×55
Second Floor	W12×152	W21×55
First Floor	W12×152	W10×45 (strut)

required will participate in the resistance of the story shear if they are rigidly connected to the HBE, or if story drifts vary significantly.

At this point, it is convenient to perform an analysis to determine the portion of frame shear that is resisted by the web plate. Reduction in the required strength of the web plates could permit reduction in web-plate thickness. Changes in the boundary elements require reanalysis to confirm or modify the distribution of frame shear between the web plate and the VBE, as well as recalculation of the angle of stress in the web plate (AISC 341 Equation 17–2), as is discussed below.

The use of a computer model thus permits the iteration that is necessary to optimize the design of SPW. For this design example, the analysis was performed using an orthotropic membrane element in a mesh between the boundary elements. The membrane element is configured to represent the thin plate by rotating its local axes to align with the estimated angle of tension stress in the plate and reducing its compression stiffness to a negligible value, as explained in Section 3.3. This method of modeling gives results that reasonably match the behavior of SPW in testing, as well as the results of the more conventional strip-model method. This method is more easily implemented with currently available analysis software; comparison of the methods is presented in Chapter 3.

The orthotropic model of a SPW is shown in Figure 4–4. This model is analyzed with the forces acting on the frame.

Each iteration of analysis was used to update a spreadsheet, which was used for the following calculations:

1. Check web-plate strength versus portion of load in the plate determined by analysis (resizing would be done for strength-governed designs).

2. Recalculate the angle α based on changes in web-plate, HBE, or VBE size.

The analysis of this frame is governed by strength requirements. The sizes shown in Table 4–9 are satisfactory for both drift and strength requirements.

These member sizes were used to calculate angles of tension stress α at each level, both for constructing the model and for the capacity-design calculations that follow. These angles are shown in Table 4–10.

The analysis indicates that a portion of the shear is resisted by the columns. Table 4–11 shows the percentage of shear in the web plate at each story. This distribution of shear will be considered in the design of both the web plate and the VBE.

A second-order analysis has been performed including P–Δ effects, but not P–δ effects. To account for P–δ effects, B_1 will be applied in the calculations that follow, when appropriate.

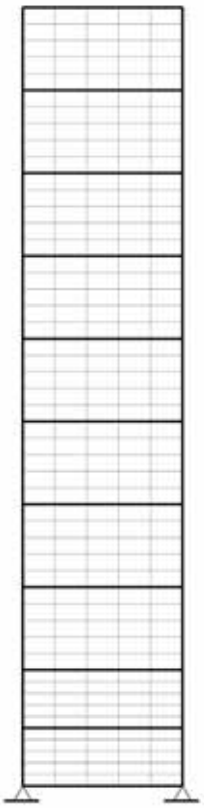

Fig. 4.4. Orthotropic model of SPW.

Table 4–9. Final Boundary Element Sections and Web Plates							
Level	Web-Plate Thickness t_w (in.)	VBE	HBE	Panel Proportions			
				h (in.)	h_c (in.)	L (in.)	L_{cf} (in.)
Roof	–	–	W27×94	–	–	–	–
Ninth Floor	0.0625	W14×132	W24×84	156	129	240	225
Eighth Floor	0.0625	W14×132	W24×84	156	132	240	225
Seventh Floor	0.1046	W14×233	W24×84	156	132	240	224
Sixth Floor	0.1046	W14×233	W24×84	156	132	240	224
Fifth Floor	0.125	W14×233	W24×84	156	132	240	224
Fourth Floor	0.1345	W14×233	W24×84	156	132	240	224
Third Floor	0.1875	W14×370	W24×84	156	132	240	222
Second Floor	0.1875	W14×370	W24×84	156	132	240	222
First Floor	0.1875	W14×370	W10×45 (strut)	102*	84.9*	240	222
*above and below the strut.							

Table 4–10. Angles of Tension Stress α	
Level	α (°)
Ninth Floor	42.6
Eighth Floor	42.6
Seventh Floor	41.6
Sixth Floor	41.6
Fifth Floor	41.2
Fourth Floor	41.0
Third Floor	40.0
Second Floor	40.0
First Floor	39.9

Table 4–11. Percentage of Story Shear Resisted by Web Plate		
Level	Percentage of Story Shear Resisted by Web Plate	Average Tension Stress in Web Plate, σ (ksi)
Ninth Floor	87.2%	13.1
Eighth Floor	78.6%	20.8
Seventh Floor	85.1%	18.8
Sixth Floor	83.4%	22.7
Fifth Floor	85.4%	22.6
Fourth Floor	83.2%	22.7
Third Floor	91.0%	19.4
Second Floor	18.0%	19.8
First Floor	68.1%	15.6

4.5.3. Design of HBE

The design of the W24×84 ASTM A992 HBE at the ninth floor will be illustrated.

HBE in SPW are subjected to significant axial forces due to the effects of web-plate tension on the VBE, as discussed in Chapter 3. They are also subject to flexural forces where web plates impart a different transverse load above and below the HBE (or are not present at all on one side, such as at the top story). Additionally, shear and moments from the deformation of the frame must be resisted, as well as any gravity loading.

The forces from web-plate tension can be calculated outside of an analysis. The axial force can be computed from the horizontal anchorage forces on the VBE above and below the HBE and flexural forces from web-plate yielding can be computed from the loading defined in Equation 3–57, using L_{cf} in place of L_h.

$$M_u = \frac{w_u L_{cf}^2}{8} + \frac{P_u L_{cf}}{4} \quad (4\text{–}14)$$

$$
\begin{aligned}
w_u &= \sigma_8 t_8 \cos^2(\alpha_8) - \sigma_9 t_9 \cos^2(\alpha_9) \\
&= (20.8 \text{ ksi})(0.0625 \text{ in.})\cos^2(42.6^\circ) \\
&\quad -(13.1 \text{ ksi})(0.0625 \text{ in.})\cos^2(42.6^\circ) \\
&= 0.244 \text{ kips/in.} \qquad (4\text{–}15)
\end{aligned}
$$

$$
\begin{aligned}
L_{cf} &= L - d_c \\
&= 240 \text{ in.} - 14.7 \text{ in.} \\
&= 225 \text{ in.}
\end{aligned}
$$

From a secondary beam supported at midspan

$$
\begin{aligned}
P_u &= 35.0 \text{ kips} \\
M_u &= \frac{(0.244 \text{ kips/in.})(225 \text{ in.})^2}{8} \\
&\quad + \frac{(35.0 \text{ kips})(225 \text{ in.})}{4} \qquad (4\text{–}16) \\
&= 3{,}510 \text{ kip-in.}
\end{aligned}
$$

The shear in the HBE is

$$
V_u = \frac{35.0 \text{ kips}}{2} + \frac{w_g + w_u}{2} L_{cf} \qquad (4\text{–}17)
$$

$$
\begin{aligned}
w_g &= 0 \text{ kips/in.} \\
V_u &= \frac{35.0 \text{ kips}}{2} + \frac{(0.244 \text{ kips/in.})(225 \text{ in.})}{2} \\
&= 45.0 \text{ kips}
\end{aligned}
$$

The axial force in the HBE is

$$
P_{HBE} = P_{HBE(VBE)} \pm \frac{1}{2} P_{HBE(web)} \qquad (4\text{–}18)
$$

$$
\begin{aligned}
P_{HBE(VBE)} &= \sum \frac{1}{2} \sigma \sin^2(\alpha) t_w h_c \qquad (4\text{–}19) \\
&= \frac{1}{2} [(13.1 \text{ ksi}) \sin^2(42.6^\circ) \\
&\quad \times (0.0625 \text{ in.})(129 \text{ in.}) + (20.8 \text{ ksi}) \\
&\quad \times \sin^2(42.6^\circ)(0.0625 \text{ in.})(132 \text{ in.})] \\
&= 63.5 \text{ kips}
\end{aligned}
$$

$$
\begin{aligned}
P_{HBE(web)} &= \frac{1}{2} \begin{bmatrix} \sigma_i t_i \sin(2\alpha_i) L_{cf_i} \\ -\sigma_{i+1} t_{i+1} \sin(2\alpha_{i+1}) L_{cf_{i+1}} \end{bmatrix} \qquad (4\text{–}20) \\
&= \frac{1}{2} [(20.8 \text{ ksi})(0.0625 \text{ in.}) \\
&\quad \times \sin(2 \times 42.6^\circ)(225 \text{ in.}) - (13.1 \text{ ksi}) \\
&\quad \times (0.0625 \text{ in.}) \sin(2 \times 42.6^\circ)(225 \text{ in.})] \\
&= 54.0 \text{ kips}
\end{aligned}
$$

No additional axial force is transmitted through the HBE. This force can be divided equally on either side of the HBE, so half of $P_{HBE(web)}$ will be used in design. On the left side (adjacent to the VBE in tension) the connection force is

$$
P_u = 63.5 \text{ kips} + \frac{1}{2}(54.0 \text{ kips}) = 90.5 \text{ kips}
$$

On the right side (adjacent to the VBE in compression) the connection force is

$$
P_u = 63.5 \text{ kips} - \frac{1}{2}(54.0 \text{ kips}) = 36.5 \text{ kips}
$$

Both forces are compressive, thus P_u = 90.5 kips is more critical. Based on this force, the moment-magnification factor B_1 is calculated for the W24×84 HBE as:

$$
B_1 = \frac{C_m}{1 - \frac{P_u}{P_{e1}}} \geq 1.0 \qquad (4\text{–}21)
$$

$$
C_m = 1.0
$$

$$
KL = 1(240 \text{ in.}) = 240 \text{ in.}
$$

$$
\begin{aligned}
P_{e1} &= \frac{\pi^2 EI}{(KL)^2} \qquad (4\text{–}22) \\
&= \frac{\pi^2 (29{,}000 \text{ ksi})(2{,}370 \text{ in.}^4)}{(240 \text{ in.})^2} \\
&= 11{,}800 \text{ kips}
\end{aligned}
$$

$$
\begin{aligned}
B_1 &= \frac{1.0}{1 - \left(\frac{90.5 \text{ kips}}{11{,}800 \text{ kips}} \right)} \geq 1.0 \qquad (4\text{–}23) \\
&= 1.01 \geq 1.0; \text{ use } 1.01
\end{aligned}
$$

Since B_1 = 1.01, P–δ effects increase the moments above those calculated previously. Therefore,

$$
\begin{aligned}
P_r &= P_u = 90.5 \text{ kips} \\
M_r &= B_1 M_{nt} + B_2 M_{lt} \approx B_1 M_u \\
&= 1.01(3{,}510 \text{ kip-in.}) \\
&= 3{,}550 \text{ kip-in.}
\end{aligned}
$$

Check Compactness

Compactness will be checked using AISC 360 to determine which design strength equations may be used. There is no restriction on the element slenderness in this design.

For the W24×84 HBE in flexure,

$$
\frac{b_f}{2t_f} \leq 0.38 \sqrt{\frac{E}{F_y}} = 9.15 \qquad (4\text{–}24)
$$

$$
b_f / 2t_f = 5.86 < 9.15
$$

$$\frac{h}{t_w} \le 3.76\sqrt{\frac{E}{F_y}} = 90.6 \qquad (4\text{–}25)$$

$$h/t_w = 45.9 < 90.6$$

The section is compact in flexure.

In compression,

$$\frac{b_f}{2t_f} \le 0.56\sqrt{\frac{E}{F_y}} = 13.5 \qquad (4\text{–}26)$$

$$b_f/2t_f = 5.86 < 13.5$$

The flanges are nonslender in compression.

$$\frac{h}{t_w} \le 1.49\sqrt{\frac{E}{F_y}} = 35.9 \qquad (4\text{–}27)$$

$$h/t_w = 45.9 > 35.9$$

The web is slender in compression.

Check Shear Strength

$$\frac{h}{t_w} \le 2.24\sqrt{\frac{E}{F_y}} = 54.0$$

$$\phi = 1.0$$

$$\phi_v V_n = \phi_v 0.6 F_y A_w \qquad (4\text{–}28)$$

$$= 1.0(0.6)(50\text{ ksi})(24.1\text{ in.})(0.470\text{ in.})$$

$$= 340\text{ kips}$$

$$\phi_v V_n > V_u = 45.0\text{ kips} \quad \textbf{o.k.}$$

Check Combined Compression and Flexure

$$KL/r_x = 1(240\text{ in.})/(9.79\text{ in.}) = 24.5$$

$$KL/r_y = 1(120\text{ in.})/(1.95\text{ in.}) = 61.5$$

Minor-axis buckling controls:

$$Q = Q_s Q_a$$

$$Q_s = 1.0$$

Using AISC 360 Equation E7–17 with f conservatively taken equal to F_y,

$$b_{e\,web} = 1.92t\sqrt{\frac{E}{F_y}}\left[1 - \frac{0.34}{(b/t)}\sqrt{\frac{E}{F_y}}\right]$$

$$= 1.92(0.470)\sqrt{\frac{29{,}000}{50}}\left[1 - \frac{0.34}{(48.0)}\sqrt{\frac{29{,}000}{50}}\right]$$

$$= 18.0\text{ in.}$$

$$h = d - 2k_{des} = 24.1\text{ in.} - 2(1.27\text{ in.}) = 21.6\text{ in.}$$

$$A_{eff} = A_g - (h - b_e)t_w$$

$$= 24.7\text{ in.}^2 - (21.6\text{ in.} - 18.0\text{ in.})(0.470\text{ in.})$$

$$= 23.0\text{ in.}^2$$

$$Q_a = A_{eff}/A = 23.0\text{ in.}^2/24.7\text{ in.}^2 = 0.931$$

$$Q = Q_s Q_a = 1.0(0.931) = 0.931$$

$$F_e = \frac{\pi^2 E}{\left[\frac{KL}{r}\right]^2} \qquad (4\text{–}29)$$

$$= \frac{\pi^2(29{,}000\text{ ksi})}{(61.5)^2}$$

$$= 75.7\text{ ksi}$$

$$> 0.44QF_y = 20.5$$

Use AISC 360 Equation E7–2:

$$F_{cr} = Q\left[0.658^{\frac{QF_y}{F_e}}\right]F_y \qquad (4\text{–}30)$$

$$= 0.931\left[0.658^{\frac{0.931(50\text{ ksi})}{75.7\text{ ksi}}}\right](50\text{ ksi})$$

$$= 36.0\text{ ksi}$$

$$\phi_c P_n = \phi_c F_{cr} A_g \qquad (4\text{–}31)$$

$$= 0.90(36.0\text{ ksi})(24.7\text{ in.}^2)$$

$$= 800\text{ kips}$$

$$P_c = \phi_c P_n = 800\text{ kips}$$

$$P_r/P_c = 90.5\text{ kips}/800\text{ kips} = 0.113$$

For the flexural strength, the limiting unbraced length is taken from AISC Manual Table 3–2:

$$L_p = 6.89\text{ ft} = 82.7\text{ in.}$$

$$L_r = 20.3\text{ ft} = 244\text{ in.}$$

$$L_b = 120\text{ in.}$$

Since $L_p < L_b < L_r$, inelastic lateral-torsional buckling controls.

Conservatively using $C_b = 1.0$,

$$\phi_b M_p = 840\text{ kip-ft} = 10{,}100\text{ kip-in.}$$

$$\phi_b M_r = 515\text{ kip-ft} = 6{,}180\text{ kip-in.}$$

The flexural strength is obtained by linear interpolation:

$$M_c = \phi_b M_p - (\phi_b M_p - \phi_b M_r)\left(\frac{L_b - L_p}{L_r - L_p}\right) \quad (4\text{–}32)$$

$$= 9{,}190 \text{ kip-in.}$$

$$M_r / M_c = 3{,}550 \text{ kip-in.} / 9{,}190 \text{ kip-in.}$$

$$= 0.386$$

As $P_r/P_c < 0.2$, use Equation H1–1b:

$$\frac{P_r}{2P_c} + \frac{M_r}{M_c} = 0.443 < 1.0 \quad \textbf{o.k.} \quad (4\text{–}33)$$

4.5.4. Design of VBE

The design of the W14×132 VBE at the eighth floor will be illustrated. The total factored gravity load in this VBE is 103 kips.

VBE in SPW are subject to high axial forces due to overturning from levels above. These axial forces are concurrent with flexural demands from two sources. The first source is the deformation of the column due to uneven story drifts. The second source is the tension stress in the web plate, which exerts an inward force on the VBE. This force acts on the column in compression in the direction opposite of the frame shear and on the column in tension in the direction of the frame shear. Both of these sources of flexural forces are represented in the analytical model.

VBE in SPW are designed to resist forces corresponding to the average stress in the wall.

The axial compression force in the VBE includes the effects of the web plate at the eighth and ninth floors, and the shear V_u from the HBE at the ninth floor and the roof. The resulting compressive force is

$$E = \sum \frac{1}{2} \sigma \sin(2\alpha) t_w h_c + \sum V_u \quad (4\text{–}34)$$

The sum of seismic shears (ΣV_u) should include all of the beams above. The seismic shear in the HBE is

$$V_u = \frac{w_u}{2} L_{cf} \quad (4\text{–}35)$$

Thus, the compressive force is

$$E = \sum \frac{1}{2} \sigma \sin(2\alpha) t_w h_c + \sum \left[\frac{w_u}{2} L_{cf}\right] \quad (4\text{–}36)$$

The resulting compressive force is

$$E = \frac{1}{2}\begin{bmatrix}(13.1 \text{ ksi}) \sin(2 \times 42.6^\circ) \\ \times (0.0625 \text{ in.})(129 \text{ in.}) + (20.8 \text{ ksi}) \\ \times \sin(2 \times 42.6^\circ)(0.0625 \text{ in.})(132 \text{ in.})\end{bmatrix} + \frac{(0.444 \text{ kips/in.})(225 \text{ in.})}{2} + \frac{(0.244 \text{ kips/in.})(225 \text{ in.})}{2}$$

$$= 216 \text{ kips}$$

With the additional 103 kips of gravity load, P_u = 319 kips.

Based on this force, the moment-magnification factor B_1 is calculated for the W14×132 VBE as:

$$B_1 = \frac{C_m}{1 - \frac{P_u}{P_e}} \geq 1.0 \quad (4\text{–}37)$$

$$C_m = 1.0 \quad (4\text{–}38)$$

$$KL = 1(156 \text{ in.}) \quad (4\text{–}39)$$

$$= 156 \text{ in.}$$

$$P_{e1} = \frac{\pi^2 EI}{(KL)^2} \quad (4\text{–}40)$$

$$= \frac{\pi^2 (29{,}000 \text{ ksi})(1{,}530 \text{ in.}^4)}{(156 \text{ in.})^2}$$

$$= 18{,}000 \text{ kips}$$

$$B_1 = \frac{1.0}{1 - \left(\frac{319 \text{ kips}}{18{,}000 \text{ kips}}\right)} \geq 1.0 \quad (4\text{–}41)$$

$$= 1.02 \geq 1.0; \text{ use } 1.02$$

The axial tension force is calculated based on the shear in the beams and the stress in the web plates:

$$E = \sum \frac{1}{2} \sigma \sin(2\alpha) t_w h_c - \sum \left[\frac{w_u}{2} L_{cf}\right] \quad (4\text{–}42)$$

$$= \frac{1}{2}[(13.1 \text{ ksi}) \sin(2 \times 42.6^\circ) \times (0.0625 \text{ in.})(129 \text{ in.}) + (20.8 \text{ ksi}) \times \sin(2 \times 42.6^\circ)(0.0625 \text{ in.})(132 \text{ in.})] - \frac{(0.444 \text{ kips/in.})(225 \text{ in.})}{2} - \frac{(0.244 \text{ kips/in.})(225 \text{ in.})}{2}$$

$$= 60.7 \text{ kips}$$

The gravity load exceeds this tensile force.

The flexural force is the sum of the effects of web tension and that of frame behavior. The flexure from web tension is

$$M_{VBE(web)} = \sigma \sin^2(\alpha) t_w \left(\frac{h_c^2}{12}\right) \quad (4\text{–}43)$$

$$= (20.8 \text{ ksi}) \sin^2(42.6^\circ)(0.0625 \text{ in.}) \times (132 \text{ in.})^2 / 12$$

$$= 865 \text{ kip-in.}$$

The moment from column deformation is taken from the model. This force includes some of the effects of web-plate tension; for simplicity of the design process, that portion of the force is accounted for twice. In order to separate the two sources of flexure, separate modeling of the frame is required.

$$M_{VBE(frame)} = 1{,}510 \text{ kip-in.}$$

$$M_u = M_{VBE(frame)} + M_{VBE(web)} \quad (4\text{–}44)$$

$$= 1{,}510 \text{ kip-in.} + 865 \text{ kip-in.}$$

$$= 2{,}380 \text{ kip-in.}$$

Since $B_1 = 1.02$, P-δ effects increase the moments above those calculated previously. Therefore,

$$P_r = P_u = 319 \text{ kips}$$

$$M_r = B_1 M_{nt} + B_2 M_{lt} \approx B_1 M_u \quad (4\text{–}45)$$

$$= 1.02 \text{ (2,380 kip-in.)}$$

$$= 2{,}430 \text{ kip-in.}$$

The shear in the VBE is the sum of the effect of web tension and the portion of shear not resisted by the web plate.

$$V_{VBE(web)} = \frac{1}{2} \sigma \sin^2(\alpha) t_w h_c \quad (4\text{–}46)$$

$$= \frac{1}{2}(20.8 \text{ ksi}) \times \sin^2(42.6^\circ)(0.0625 \text{ in.})(132 \text{ in.})$$

$$= 39.3 \text{ kips}$$

The analysis shows that 78.6 percent of the shear is in the web plate (see Table 4–11). It is assumed that the remaining shear is shared (see Table 4–2) equally by the two VBE:

$$V_{VBE(frame)} = \frac{1}{2}(1 - 0.786)(186 \text{ kips})$$

$$= 20.0 \text{ kips}$$

The total shear in the VBE is thus:

$$V_{VBE} = V_{VBE(frame)} + V_{VBE(web)} \quad (4\text{–}47)$$

$$= 20.0 \text{ kips} + 39.3 \text{ kips}$$

$$= 59.3 \text{ kips}$$

Check Compactness

For the W14×132 VBE in flexure,

$$\frac{b_f}{2t_f} \le 0.38\sqrt{\frac{E}{F_y}} = 9.15 \quad (4\text{–}48)$$

$$b/2t_f = 7.15 < 9.15$$

$$\frac{h}{t_w} \le 1.49\sqrt{\frac{E}{F_y}} = 35.9 \quad (4\text{–}49)$$

$$h/t_w = 17.7 < 35.9$$

The section is compact in flexure.

In compression,

$$\frac{b_f}{2t_f} \le 0.56\sqrt{\frac{E}{F_y}} = 13.5$$

$$\frac{b_f}{2t_f} = 5.86 < 13.5$$

$$\frac{h}{t_w} \le 1.49\sqrt{\frac{E}{F_y}} = 35.9$$

$$\frac{h}{t_w} = 17.7 < 35.9$$

The section is not slender in compression.

Check Shear Strength

$$\frac{h}{t_w} \le 2.24\sqrt{\frac{E}{F_y}} = 54.0$$

$$\phi_v = 1.0$$

$$\phi_v V_n = \phi_v 0.6 F_y A_w \quad (4\text{–}50)$$

$$= 1.0(0.6)(50 \text{ ksi})(14.7 \text{ in.})(0.645 \text{ in.})$$

$$= 284 \text{ kips}$$

$$\phi_v V_n > V_u = 59.3 \text{ kips} \quad \textbf{o.k.}$$

Check Combined Compression and Flexure

By inspection, the compression strength is governed by minor-axis buckling.

$$KL/r_y = 1(156 \text{ in.})/(3.76 \text{ in.}) = 41.5$$

$$F_e = \frac{\pi^2 E}{\left[\frac{KL}{r}\right]^2} \quad (4\text{–}51)$$

$$= \frac{\pi^2 (29{,}000 \text{ksi})}{\left(41.5\right)^2}$$

$$= 166 \text{ ksi} > 0.44F_y = 22.0 \text{ ksi}$$

Use Equation E3–2:

$$F_{cr} = \left[0.658^{\frac{F_y}{F_e}}\right] F_y \quad (4\text{–}52)$$

$$= \left[0.658^{\frac{50 \text{ ksi}}{166 \text{ ksi}}}\right] (50 \text{ ksi})$$

$$= 44.1 \text{ ksi}$$

$$\phi_c P_n = \phi_c F_{cr} A_g \quad (4\text{–}53)$$

$$= 0.90(44.1 \text{ ksi})(38.8 \text{ in.}^2)$$

$$= 1{,}540 \text{ kips}$$

$$P_c = \phi_c P_n = 1{,}540 \text{ kips}$$

$$P_r / P_c = 319 \text{ kips}/1{,}540 \text{ kips} = 0.207$$

For the flexural strength, the limiting unbraced length is taken from AISC Manual Table 3–2:

$$L_p = 13.3 \text{ ft} = 160 \text{ in.}$$

$$L_b = 156 \text{ in.}$$

Since $L_b < L_p$, lateral-torsional buckling does not control. The flexural strength is

$$M_c = \phi_b M_n \quad (4\text{–}54)$$

$$= \phi_b F_y Z_x$$

$$= 0.90(50 \text{ ksi})(234 \text{ in.}^3)$$

$$= 10{,}500 \text{ kip-in.}$$

$$M_r / M_c = 2{,}430 \text{ kip-in.} / 10{,}500 \text{ kip-in.}$$

$$= 0.231$$

As $P_r / \phi P_c > 0.2$, use Equation H1–1a:

$$\frac{P_r}{P_c} + \frac{8}{9}\left(\frac{M_r}{M_c}\right) = 0.412 < 1.0 \quad \textbf{o.k.}$$

Check Combined Tension and Flexure

By inspection, tension will not control the design over compression. When tension and flexure does control, see AISC Specification Section H1.2.

4.5.5. Connection of Web Plate to Boundary Elements

Because the design of web plates utilizes a strength based on spreading of yielding over some portion of the plate, it is necessary to preclude fracture of the web-plate connections at local areas of higher stress. Thus, the web plate welds will be sized so that web-plate tension yielding will occur prior to weld fracture.

Note that the factor R_y, which is used to determine the expected yield strength, is not used here in this low-seismic design example. While R_y is strictly a material property and is not related to the type of loading, some judgment must be applied in considering the numerous variables that affect the reliability of this aspect of the connection design. In this example, and because the seismic response modification factor R is taken equal to 3, it is considered sufficiently reliable to compare the specified minimum yield strength of the web plate (F_y) with the specified minimum weld strength (F_{EXX}), reduced by the resistance factor. While it is probable that the actual web-plate yield strength is significantly greater than the specified minimum, it is also likely that the weld strength is greater than its specified minimum, and the resistance factor of 0.75 provides an adequate margin of safety.

For fillet-welded connections, the required total weld size at the HBE can be expressed as

$$w_{HBE} = \frac{F_y \cos(\alpha) t_w \sqrt{2}}{\phi 0.6 F_{EXX}\left[1 + 0.5\cos^{1.5}(\alpha)\right]} \quad (4\text{–}55)$$

The required total weld size at the VBE can be expressed as

$$w_{VBE} = \frac{F_y \sin(\alpha) t_w \sqrt{2}}{\phi 0.6 F_{EXX}\left[1 + 0.5\sin^{1.5}(\alpha)\right]} \quad (4\text{–}56)$$

These weld sizes are the total required. In this case, two parallel welds are used to resist the web-plate tension (as shown in Figure 4–5), and the overlap of the web plate and the fish plate is small. Thus, the two welds are assumed to share the force equally, and the sum of the two weld sizes must equal or exceed the total required weld size calculated above. Table 4–12 shows the total required fillet weld size at each level for F_y = 36 ksi and F_{EXX} = 70 ksi, as well as the size of each weld for the two parallel welds.

Figure 4–5 shows a connection detail for the 3⁄16-in. web plate to the VBE at the first floor. In this case, two 1⁄8-in. fillet welds are used.

At the foundation, the 3⁄16-in. web plate must be anchored to the grade beam. Here a WT is used to span between anchors.

Table 4–12. Required Fillet Weld Size						
Level	**Web Plate Thickness t_w (in.)**	**Angle of Stress α (°)**	**Weld Size at HBE (in.)**		**Weld Size at VBE (in.)**	
			Total	**Two Welds Each**	**Total**	**Two Welds Each**
Ninth Floor	0.0625	42.6	0.0565	equal to t_w	0.0535	equal to t_w
Eighth Floor	0.0625	42.6	0.0565	equal to t_w	0.0535	equal to t_w
Seventh Floor	0.1046	41.6	0.0955	equal to t_w	0.0883	equal to t_w
Sixth Floor	0.1046	41.6	0.0955	equal to t_w	0.0883	equal to t_w
Fifth Floor	0.125	41.2	0.115	equal to t_w	0.105	equal to t_w
Fourth Floor	0.1345	41.0	0.124	⅛	0.113	⅛
Third Floor	0.1875	40.0	0.174	⅛	0.155	⅛
Second Floor	0.1875	40.0	0.174	⅛	0.155	⅛
First Floor	0.1875	39.9	0.174	⅛	0.155	⅛

The shear and tension on each anchor rod must be considered. The shear on each anchor rod is

$$v_u = \frac{1}{2} F_y \sin(2\alpha) t_w s \qquad (4\text{–}57)$$
$$= \frac{1}{2}(36 \text{ ksi}) \sin\left(2 \times 39.9^\circ\right)(3/16 \text{ in.}) s$$
$$= 3.32 \text{ kips/in.} \times s$$

The tension on each anchor rod is

$$t_u = F_y \cos^2(\alpha) t_w s \qquad (4\text{–}58)$$
$$= 36 \text{ ksi} \times \cos^2\left(39.9^\circ\right)(3/16 \text{ in.}) \times s$$
$$= 3.97 \text{ kips/in.} \times s$$

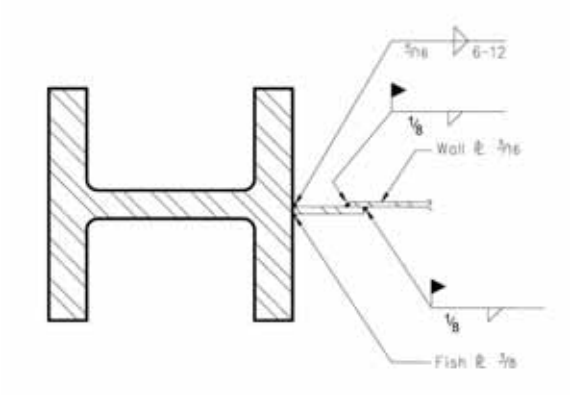

Fig. 4–5. Connection of 3⁄16 in. web plate.

Assuming a 10-in. spacing, each anchor must resist 33.2 kips of shear and 39.7 kips of tension. Figure 4–6 shows the base connection.

Alternatively, a steel beam can be provided as the HBE at the bottom. This beam would connect to the bottom VBE on either side of the SPW.

4.5.6. Connection of HBE to VBE

The connection of the W24×84 HBE to the W14×132 VBE at the ninth floor will be designed. A single-plate shear con-

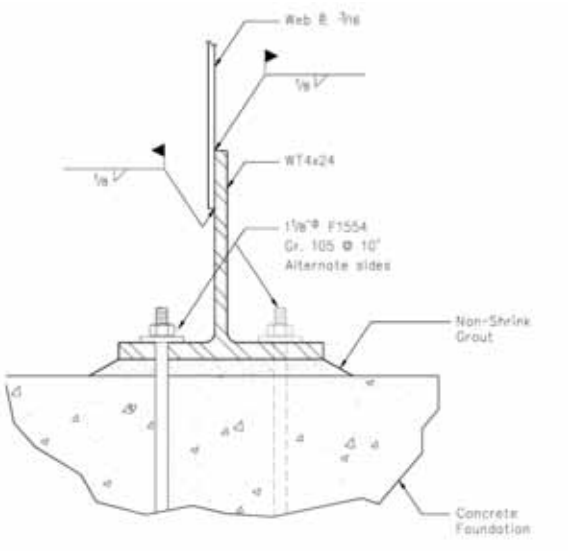

Fig. 4–6. Connection of 3⁄16 in. web plate at base.

nection will be designed to resist the combined shear and axial force. This connection is shown in Figure 4–7.

Try a ½-in. × 5-in. plate 21 in. deep with seven ⅞-in.-diameter ASTM A325X bolts in STD holes. The horizontal edge distance is 2½ in., the vertical edge distance is 1½ in., and the bolts are spaced at 3 in.

Required Strength

The connection will be designed considering the collector forces, the shear in the column, and the end forces calculated for the HBE. The vertical force component is due only to the HBE:

$$V_u = 45.0 \text{ kips}$$

The horizontal compression force at the end of the HBE is

$$N_{HBE} = 95.1 \text{ kips}$$

This force is partly due to the collector and partly due to the inward reaction of the VBE. The collector portion is that caused by the difference in web forces above and below the HBE ($P_{HBE(web)}$, Equation 4–20).

The horizontal force (compression or tension) at the end of the collector is half the frame force given in Table 4–2, since it is transferred at both ends of the collector

$$N_{Coll} = 81.4 \text{ kips}/2 = 40.7 \text{ kips}$$

This force is larger than half of $P_{HBE(web)}$, which results from a condition where the web plate above the beam is less heavily stressed than was assumed in the design of the HBE, and

$$\frac{1}{2}P_{HBE(web)} = \frac{1}{2}(54.0 \text{ kips}) = 27.0$$

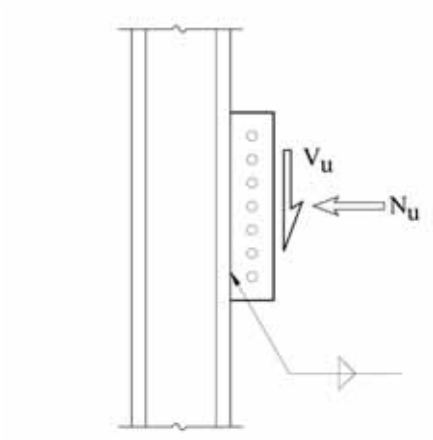

Fig. 4–7. Single-plate connection of HBE to VBE.

more of the force in the web plate below is being delivered through the collector. Thus, N_{coll} is more critical in this case.

When the collector is in tension, the collector force N_{Coll} is subtracted from the inward reaction of the VBE ($P_{HBE(VBE)}$, Equation 4–19), resulting in a small compression force.

$$N_u = P_{HBE(VBE)} - N_{Coll}$$
$$= 63.5 \text{ kips} - 40.7 \text{ kips} = 22.8 \text{ kips}$$

When the collector is in compression, the collector force is added to the inward reaction of the VBE ($P_{HBE(VBE)}$, Equation 4–19).

$$N_u = N_{Coll} + P_{HBE(VBE)}$$
$$= 40.7 \text{ kips} + 63.5 \text{ kips} = 104 \text{ kips}$$

Because both conditions result in compression, this axial compression force governs the design of the shear plate.

Check Plate Yielding

An elliptical interaction approach will be used, with

$$\left(\frac{V_u}{\phi_y V_n}\right)^2 + \left(\frac{N_u}{\phi_c N_n}\right)^2 \le 1.0$$

$$\phi_y V_n = 1.00(0.6)F_y tL \quad (4\text{–}59)$$
$$= 1.00(0.6)(36 \text{ ksi})(½ \text{ in.})(21 \text{ in.})$$
$$= 216 \text{ kips}$$

For this short compression element, $Kl/r < 25$ and $F_{cr} = F_y$. Thus,

$$\phi_c N_n = 0.90\, F_y tL \quad (4\text{–}60)$$
$$= 0.90(36 \text{ ksi})(½ \text{ in.})(21 \text{ in.})$$
$$= 340 \text{ kips}$$

$$\left(\frac{45.0 \text{ kips}}{216 \text{ kips}}\right)^2 + \left(\frac{104 \text{ kips}}{340 \text{ kips}}\right)^2 = 0.137 \le 1.0 \quad \textbf{o.k.}$$

Check Plate Rupture

While shear rupture can occur, rupture is not applicable for the horizontal compression component. Conservatively, the following interaction will be checked.

$$\left(\frac{V_u}{\phi_n V_n}\right)^2 + \left(\frac{N_u}{\phi_c N_n}\right)^2 \le 1.0$$

$$\phi_n V_n = 0.75(0.6)\, F_u A_{nv} \quad (4\text{–}61)$$

$$A_{nv} = A_g - n(d_b + \tfrac{1}{8}\text{ in.})(t) \quad (4\text{–}62)$$

$$= (\tfrac{1}{2}\text{ in.})(21\text{ in.}) - (7)(\tfrac{7}{8}\text{ in.} + \tfrac{1}{8}\text{ in.})(\tfrac{1}{2}\text{ in.})$$

$$= 7.00\text{ in.}^2$$

$$\phi_n V_n = 0.75(0.6)(58\text{ ksi})(7.00\text{ in.}^2)$$

$$= 183\text{ kips}$$

$$\left(\frac{45.0\text{ kips}}{183\text{ kips}}\right)^2 + \left(\frac{104\text{ kips}}{340\text{ kips}}\right)^2 = 0.154 \le 1.0 \quad \textbf{o.k.}$$

Check Bolt Shear

The resultant force on the bolt group is

$$\sqrt{V_u^2 + N_u^2} = \sqrt{(45.0\text{ kips})^2 + (104\text{ kips})^2} = 113\text{ kips} \quad (4\text{–}63)$$

The design strength of the bolt group is

$$\phi R_n = \phi n F_{nv} A_b = 0.75(7)(60\text{ ksi})\left[\frac{\pi}{4}(\tfrac{7}{8}\text{ in.})^2\right] = 189\text{ kips} > 113\text{ kips} \quad \textbf{o.k.} \quad (4\text{–}64)$$

Check Bolt Bearing

The beam web and plate are of similar thickness, but the plate is ASTM A36 material, while the beam is ASTM A992 material. Therefore, bearing on the plate is more critical. For the vertical component, at the bottom bolt,

$$1.2L_c = 1.2[1\tfrac{1}{2}\text{ in.} - (\tfrac{15}{16}\text{ in.})/2] = 1.24\text{ in.}$$

$$2.4d_b = 2.4(\tfrac{7}{8}\text{ in.}) = 2.10\text{ in.} > 1.2L_c$$

Tearout controls and

$$\phi r_n = \phi 1.2 L_c t F_u \quad (4\text{–}65)$$

$$= 0.75(1.24\text{ in.})(\tfrac{1}{2}\text{ in.})(58\text{ ksi})$$

$$= 27.0\text{ kips}$$

For the remaining bolts

$$1.2L_c = 1.2(3\text{ in.} - \tfrac{15}{16}\text{ in.})$$

$$= 2.48\text{ in.}$$

$$2.4d_b = 2.10\text{ in.} < 1.2L_c$$

Bearing controls and

$$\phi r_n = \phi 2.4 d_b t F_u \quad (4\text{–}66)$$

$$= 0.75(2.10\text{ in.})(\tfrac{1}{2}\text{ in.})(58\text{ ksi})$$

$$= 45.7\text{ kips}$$

For the bolt group,

$$\phi R_{nv} = 27.0\text{ kips} + 6\ (45.7\text{ kips})$$

$$= 301\text{ kips}$$

For the horizontal component, all bolts have $2.4d_b > 1.2L_c$ and

$$\phi R_{nn} = 7(45.7\text{ kips})$$

$$= 320\text{ kips}$$

Therefore,

$$\left(\frac{V_u}{\phi R_{nv}}\right)^2 + \left(\frac{N_u}{\phi R_{nn}}\right)^2 \le 1.0$$

$$\left(\frac{45.0\text{ kips}}{301\text{ kips}}\right)^2 + \left(\frac{104\text{ kips}}{320\text{ kips}}\right)^2 = 0.128 \le 1.0 \quad \textbf{o.k.}$$

Check Block Shear Rupture

As with plate rupture, block shear rupture is not applicable for the horizontal compression component. Additionally, with a horizontal edge distance of 2½ in., and a vertical edge distance of 1½ in., the block shear rupture check for the vertical component will exceed the check previously made for shear rupture. Thus, it does not control.

Weld Size

The fillet welds are selected as 5⁄16-in. fillet welds to equal 5⁄8 times t_p. This develops the strength of the plate.

The shear plate connection satisfies all of the checks and therefore is acceptable.

4.5.7. Design of Intermediate Strut at First Floor

The intermediate strut at the first floor is subjected to an axial force. This force can be determined in the same way as the HBE axial force based on the stress in the web plate.

$$P_{strut} = \sum \tfrac{1}{2}\sigma \sin^2(\alpha) t_w h_c \quad (4\text{–}67)$$

$$= \frac{1}{2}[(15.6\text{ ksi})\sin^2(39.9^\circ) \times (0.1875\text{ in.})(84.9\text{ in.}) + (15.6\text{ ksi}) \times \sin^2(39.9^\circ)(0.1875\text{ in.})(84.9\text{ in.})]$$

$$= 102\text{ kips}$$

Try a W10×45.

Check Compactness

$$\frac{b_f}{2t_f} \le 0.56\sqrt{\frac{E}{F_y}} = 13.5 \qquad (4\text{–}68)$$

$b/2t_f = 6.47 < 13.5$

$$\frac{h}{t_w} \le 1.49\sqrt{\frac{E}{F_y}} = 35.9 \qquad (4\text{–}69)$$

$h/t_w = 22.5 < 35.9$

The section is not slender in compression.

Check Compression

$KL/r_x = 1(240 \text{ in.})/(4.32 \text{ in.}) = 55.6$

$KL/r_y = 1(240 \text{ in.})/(2.01 \text{ in.}) = 119$

Minor-axis buckling controls.

$$F_e = \frac{\pi^2 E}{\left[\frac{KL}{r}\right]^2} \qquad (4\text{–}70)$$

$$= \frac{\pi^2(29{,}000 \text{ ksi})}{(119)^2}$$

$$= 20.2 \text{ ksi} < 0.44F_y = 22.0 \text{ ksi}$$

Use Equation E3–3:

$$F_{cr} = 0.877F_e \qquad (4\text{–}71)$$

$$= 0.877(20.2 \text{ ksi})$$

$$= 17.7 \text{ ksi}$$

$$\phi_c P_n = \phi_c F_{cr} A_g \qquad (4\text{–}72)$$

$$= 0.90(17.7 \text{ ksi})(13.3 \text{ in.}^2)$$

$$= 212 \text{ kips}$$

$\phi_c P_n > P_u = 102$ kips **o.k.**

The intermediate strut is acting as a stiffener and therefore must have a minimum transverse stiffness, as defined by Equation 3–7.

$$I_{st} \ge at_w^3 j \qquad (4\text{–}73)$$

where

a = spacing between transverse stiffeners

h = length of stiffener

$j = 2.5(h/a)^2 - 2 \ge 0.5$

$$= 2.5\left(\frac{240 \text{ in.} - 17.9 \text{ in.}}{84.9 \text{ in.}}\right)^2 - 2 = 15.1 \ge 0.5$$

$I_{st} \ge (84.9 \text{ in.})(0.1875 \text{ in.})^3(15.1)$

$= 8.45 \text{ in.}^4$

$I_y = 53.4 \text{ in.}^4 \ge 8.45 \text{ in.}^4$ **o.k.**

The W10×45 is adequate.

Chapter 5

Design Example II: High-Seismic Design

5.1. OVERVIEW

This chapter illustrates the design of a building utilizing Special Plate Shear Walls (SPSW) in a zone of high seismicity (for R = 7 with application of the ductile detailing requirements of AISC 341). The example building used in Chapter 4 will be redesigned assuming a site in downtown San Francisco.

5.2. STANDARDS

The design will again be governed by the 2005 editions of ASCE 7 (including Supplement No. 1) and AISC 360. Additionally, as will be seen below, the seismic design category of the structure (and use of $R > 3$) will necessitate use of AISC 341. Concrete elements (to the extent that they are addressed in this example) are required to conform to ACI 318.

5.3. BUILDING INFORMATION

The building footprint and size are identical to that used in the previous design example. The typical plan is shown in Figure 5–1. The building weight and material grades are as given in Chapter 4.

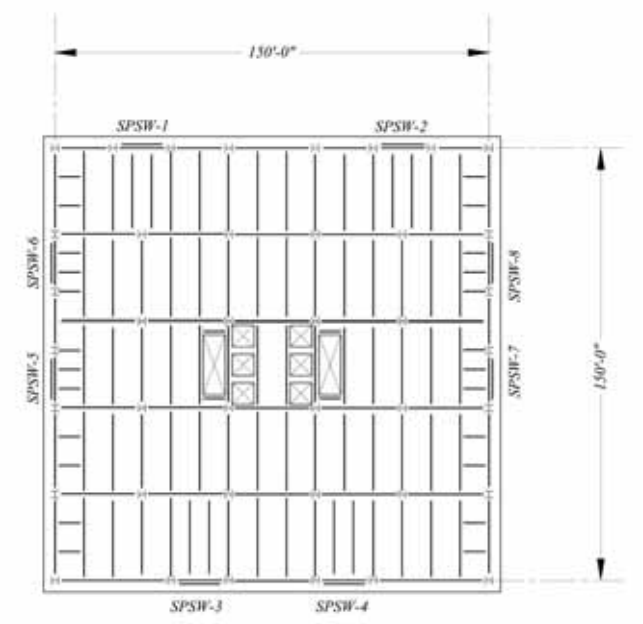

Fig. 5–1. Typical floor plan.

The building design includes eight SPSW panels on the perimeter so that the prescriptive requirements of ASCE 7 Section 12.3.4.2 are met, and the redundancy factor, ρ, may be taken as 1.0. The length of each wall panel has been selected to comply with the requirements of this provision.

It is also common to utilize walls of the building core as SPSW. In such a configuration, building torsion should be restrained by a supplementary perimeter system in order to avoid an extreme torsional irregularity (ASCE 7 Table 12.3–1). Moment frames are a common choice for such a supplementary perimeter system, and a perimeter moment frame with a SPSW core is an excellent choice for buildings over 160 ft tall, where ASCE 7 requires that a dual system be used.

In order to focus on the SPSW system, rather than the intricacies of the design of dual systems or the calculation of the redundancy factor, the building in this design example has the SPSW located on the perimeter. A typical elevation of a SPSW is shown in Figure 5–2. Note that the adjacent

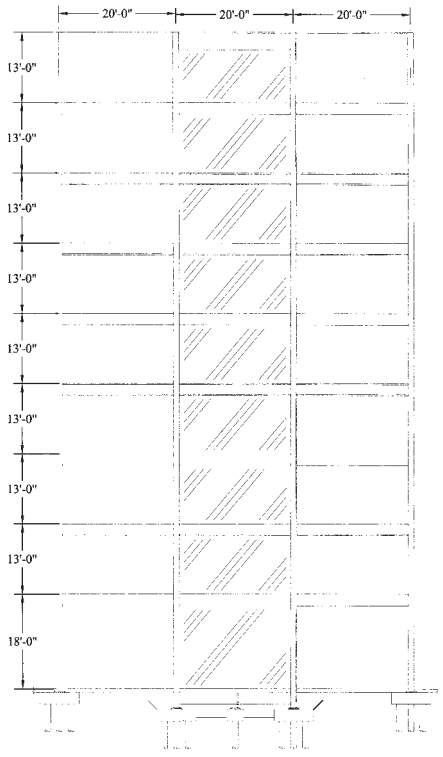

Fig. 5–2. SPSW elevation.

bays are also modeled, as the reduction in overturning forces due to the flexure of the adjoining beams is instrumental in limiting the story drift within allowable limits for this building.

Unlike the previous design example in Chapter 4, the design does not include a horizontal strut at mid-height of the first floor. Were such a strut used, see Chapter 4, except that the design should be based on the web plate achieving its expected yield stress.

The building is located in downtown San Francisco, on the corner of Montgomery and Market Streets. The seismic ground motion values are obtained from USGS maps based on the building location. In this design, the USGS web site[1] is used to obtain the information by entering the building latitude and longitude.[2] The latitude and longitude values for the site are 37.789° and –122.402°, respectively.

The soil at the site corresponds to Site Class D, reflecting the stiff soil in this location. The building occupancy category is I, based on its use as an office building (ASCE 7 Table 1–1).

5.4. LOADS

For this location, the Peak Ground Acceleration (PGA) for the Maximum Considered Earthquake (MCE) is $0.7062g$, where g is the acceleration of gravity. Spectral accelerations for the MCE are $1.7035g$ at a period of 0.2 second and $0.8501g$ at a period of 1.0 second. These values are expressed as S_s and S_1, respectively:

$$S_s = 1.7035g$$

$$S_1 = 0.8501g$$

These spectral values are modified based on the site class. The modification values are selected from ASCE 7 Tables 11.4–1 and 11.4–2 based on site class and spectral acceleration. The modification values are

$$F_a = 1.0$$

$$F_v = 1.5$$

The adjusted MCE spectral response acceleration parameters are calculated using ASCE 7 Equations 11.4–1 and 11.4–2:

$$S_{MS} = F_a S_s = 1.70g \quad (5\text{–}1)$$

$$S_{M1} = F_v S_1 = 1.28g \quad (5\text{–}2)$$

For design purposes, two-thirds of these MCE parameters are used. This reflects the assumption in ASCE 7 that there is likely to be a reserve capacity of approximately 50 percent at design level. This is equivalent to using MCE values and a 50 percent greater response modification coefficient.

The design spectral response acceleration parameters are calculated using ASCE 7 Equations 11.4–3 and 11.4–4:

$$S_{DS} = \frac{2}{3} S_{MS} = 1.13g \quad (5\text{–}3)$$

$$S_{D1} = \frac{2}{3} S_{M1} = 0.853g \quad (5\text{–}4)$$

These values are used to establish the building Seismic Design Category (SDC). ASCE 7 Table 11.6–1 is used to compare S_{DS} to certain limits. ASCE 7 Table 11.6–2 is used similarly with S_{D1}. Each table gives a SDC based on the building occupancy category and the design spectral response acceleration parameter (S_{DS} or S_{D1}). The more severe SDC obtained from the two tables is used. For this building design, the SDC is D.

The SDC is used to determine many aspects of the seismic design of the building. ASCE 7 Table 12.6-1 limits the analysis procedures that are permitted based on SDC, period, and irregularities.

For SDC D, it must be determined whether the building period is greater than 3.5 times T_s, the period that separates the constant-acceleration range from the period-sensitive range of the seismic response spectrum. Buildings with such long periods are not permitted to be designed using the equivalent lateral force procedure. The building period is estimated using ASCE Equation 12.8–7.

$$T_a = C_T h_n^x = 0.02 \times (122 \text{ ft})^{0.75} = 0.734 \text{ sec} \quad (5\text{–}5)$$

The coefficient C_T and the exponent x are taken from ASCE 7 Table 12.8–2. The variable h_n is building height in feet.

The period value T_s is calculated based on S_{DS} and S_{D1}:

$$T_s = \frac{S_{D1}}{S_{DS}} = \frac{0.853}{1.13} = 0.755 \text{ sec} \quad (5\text{–}6)$$

---

[1] **http://earthquake.usgs.gov/research/hazmaps/design/index.php**

[2] The latitude and longitude of a street address can be found using one of the many mapping web sites.

The building period, expressed in terms of T_s is

$$T_a = 0.972\ T_s < 3.5\ T_s \tag{5–7}$$

Thus, T_a is within the limit for which use of the equivalent lateral force procedure is permitted.

For SDC D, it must be determined whether the building has any of the following irregularities: Type 1 (a or b) in ASCE 7 Table 12.3–1, or Types 1 (a or b), 2, or 3 in ASCE 7 Table 12.3–2. It is assumed that the building will be designed so as to avoid all of these irregularities, and therefore the use of the equivalent lateral force procedure per ASCE 7 Section 12.8 is permitted in ASCE 7 Table 12.6–1. Alternatively, a modal analysis procedure can be used and avoidance of those irregularities need not be assumed, although a regular structure is preferable, where possible.

The parameters S_{DS} and S_{D1} can be used in conjunction with ASCE 7 Equations 12.8–2 through 12.8–5 to construct a generalized spectrum, as is shown in ASCE 7 Figure 11.4–1. The spectrum for this building is shown in Figure 5–3.

As the building period is less than T_s, it is within the constant acceleration range governed by ASCE 7 Equation 12.8–2. The associated seismic response coefficient, C_s, is computed based on this spectrum, the response modification coefficient, R, and the importance factor, I. For building occupancy category I, the importance factor, I, is 1.0 per ASCE 7 Table 11.5–1.

$$\begin{aligned} C_s &= \frac{S_{DS}}{R/I} \\ &= \frac{1.13g}{7/1} \\ &= 0.161g \end{aligned} \tag{5–8}$$

The design base shear is calculated using ASCE 7 Equation 12.8–1:

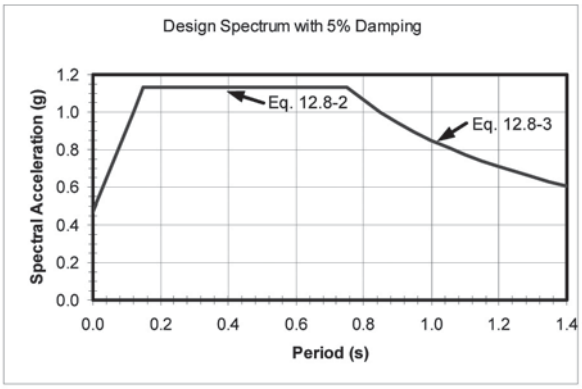

Fig. 5–3. Generalized site response spectrum.

$$\begin{aligned} V &= C_s W \\ &= 0.161\ (20{,}700\ \text{kips}) \\ &= 3{,}330\ \text{kips} \end{aligned} \tag{5–9}$$

This base shear is distributed vertically using ASCE 7 Equations 12.8-11 and 12.8–12:

$$F_x = C_{vx} V \tag{5–10a}$$

$$C_{vx} = \frac{w_x h_x^{\,k}}{\sum_{i=1}^{n} w_i h_i^{\,k}} \tag{5–10b}$$

The exponent k is interpolated for periods between 0.5 and 2.5 seconds. For this building design k is 1.12. The resulting values of C_{vx} for each level are shown in Table 5–1.

These forces are distributed horizontally based on the stiffness and location of each wall. An elastic analysis of the frames is performed both to determine this horizontal distribution and to design the frames themselves. The elastic analysis includes accidental torsion, as required by ASCE 7 Section 12.8.4.2.

The design forces for each SPSW are based on this horizontal distribution of forces. Table 5–2 shows these forces.

For purposes of this design example, it is assumed that wind loads are smaller than seismic loads and do not affect the required strength of the SPSW.

5.5. SPSW DESIGN

The high-seismic design of SPSW is intended to ensure ductile performance based on tension yielding of the web plate. The design of beams and columns, which are referred to as HBE and VBE, respectively, is based on forces corresponding to the web-plate strength. The web-plate strength is set to meet the demands corresponding to the seismic load analysis. In this design, the web-plate demands were determined in Section 5.4 using the equivalent lateral force procedure.

Reduced Beam Section (RBS) moment connections will be used for all HBE-to-VBE connections. For simplicity, the reduced flexural strength will be set to two-thirds of the unreduced beam expected strength for all beams, and the hinge location will be set at $d_b/2$ from the column face.

5.5.1. Preliminary Design

For preliminary design, as the size of HBE and VBE are not known, the web plates are assumed to resist the entire shear in the frame. As the angle of tension stress in the web plate is dependent on the section properties of the HBE and VBE, as well as on the web-plate thickness and the frame dimensions, for preliminary design an angle of tension stress is assumed. Typical designs show that the angle of tension stress ranges

Table 5–1. Vertical Distribution Factors and Story Forces

Level	Vertical Distribution Factor	Story Force (kips)
Roof	0.225	749
Ninth Floor	0.174	579
Eighth Floor	0.152	506
Seventh Floor	0.129	430
Sixth Floor	0.107	356
Fifth Floor	0.0847	282
Fourth Floor	0.0635	211
Third Floor	0.0429	143
Second Floor	0.0238	79.3

Table 5–2. Forces and Shears in Each SPSW

Level	Frame Force (kips)	Frame Shear (kips)
Roof	197	197
Ninth Floor	152	349
Eighth Floor	133	482
Seventh Floor	113	595
Sixth Floor	93.5	689
Fifth Floor	74.0	763
Fourth Floor	55.4	818
Third Floor	37.5	855
Second Floor	20.8	876

from 30° to 55° (measured from a vertical line). The angle, α, is conservatively assumed as 30°.

Based on this angle, the design strength of web plates of unit length can be calculated using AISC 341 Equation 17–1:

$$\phi V_n = 0.90(0.42)F_y t_w L_{cf} \sin(2\alpha) \qquad (5\text{–}11)$$

where L_{cf} is the clear length of the web panel between VBE flanges.

Based on this equation and the assumed angle of tension stress, the design strength of web panels can be calculated in terms of design shear strength per unit length (ϕv_n). Assuming a value equal to the bay length (20 ft) minus 18 in., the plate design strengths in Table 5–3 can be determined, where

$$\phi v_n = 0.90(0.42)F_y t_w \sin(2\alpha) \qquad (5\text{–}12)$$

It should be noted that web plates thinner than ¼ in. are typically considered much less practical than thicker plates. Fabricators must obtain them in rolls and flatten them for use in SPSW. Nevertheless, it is not recommended to overdesign SPSW web plates, as the capacity-design requirements of AISC 341 may make such designs impractical.

Using the design strengths for various plate thicknesses in ASTM A36 material from Table 5–3, preliminary plate thicknesses are selected at each level. Those sizes are presented in Table 5–4.

The design of VBE must satisfy both strength and stiffness requirements. The in-plane flexural stiffness is required to ensure that the web plate can develop sufficient tension throughout its height. This requirement is given in AISC 341 Section 17.4g:

$$I_c \geq 0.00307 \frac{t_w h^4}{L} \qquad (5\text{–}13)$$

where

h = the distance between HBE centerlines

L = the distance between VBE centerlines

The required column stiffness at each level is shown in Table 5.5. For purposes of preliminary design, the beam depths at all levels are assumed to be identical, and thus the distance h is equal to the floor-to-floor height.

Preliminary VBE design is based on these stiffness requirements. Strength requirements may control, but their calculation is dependent on analysis of the frame and combination with gravity loads.

With rigid beam-to-column connections, the design of HBE is likewise dependent on flexural forces from an analysis of the frame. It should be noted, however, that flexural demands exist on the HBE when the web-plate thickness differs above and below the beam. As the preliminary web-plate thickness may be changed as the design is refined, it is not necessary to compute those demands at this stage. Nevertheless, except at the roof, the maximum difference in plate thickness can be used to estimate the demands. For a maximum difference in plate thickness of 1/16 in., the load that the web plates are expected to exert on the HBE can be estimated as

Table 5–3. Web Plate Design Strengths		
t_w (in.)	ϕv_n (kips/in.)	ϕV_n (kips)*
0.0625	0.737	164
0.0673	0.793	176
0.0747	0.840	195
0.1046	1.23	274
0.125	1.47	327
0.1345	1.59	352
0.1875	2.21	491
0.250	2.95	654
0.3125	3.68	818
0.375	4.42	981
0.4375	5.16	1,150
0.500	5.89	1,310
0.625	7.37	1,640
*ϕV_n is calculated based upon L_{cf} = 20 ft minus 18 in.		

Table 5–4. Preliminary Design of Web Plates

Level	Web Plate Thickness t_w (in.)	Required Shear Strength V_u (kips)	Design Shear Strength ϕV_n (kips)	Demand/ Capacity Ratio $\frac{V_u}{\phi V_n}$
Ninth Floor	0.0747	197	195	1.01
Eighth Floor	0.125	349	327	1.07
Seventh Floor	0.1875	482	491	0.982
Sixth Floor	0.250	595	654	0.910
Fifth Floor	0.250	689	654	1.05
Fourth Floor	0.3125	763	818	0.933
Third Floor	0.3125	818	818	1.00
Second Floor	0.3125	855	818	1.05
First Floor	0.375	866	981	0.893

$$w_u = R_y F_y (t_i - t_{i+1}) \cos^2(\alpha) \quad (5\text{–}14)$$

$$= 1.3(36 \text{ ksi})(1/16 \text{ in.}) \cos^2(30°)$$

$$= 2.19 \text{ kips/in. or } 26.3 \text{ kips/ft}$$

R_y is given in AISC 341 Table I-6-1.

For preliminary design, a W27×94 will be used at all levels. Note that this uniform-load value is based on the assumption of an angle of tension stress of 30°. In most cases, the angle will be significantly greater, potentially permitting a reduction in this load on the beam.

For the roof beam, no counterbalancing web plate above exists, and the entire flexural force from the web plate must be resisted by the beam.

The preliminary boundary element sections selected are presented in Table 5.6.

The determination of the angle of tension stress, α, is dependent on the geometric proportions of the frame, the section properties of the boundary elements, and the web-plate thickness. Once preliminary framing members are selected, a refined estimate of the angle of tension stress can be made using AISC 341 Equation 17–2:

$$\tan^4 \alpha = \frac{1 + \frac{t_w L}{2A_c}}{1 + t_w h \left[\frac{1}{A_b} + \frac{h^3}{360 I_c L} \right]} \quad (5\text{–}15)$$

where

h = distance between HBE centerlines

A_b = cross-sectional area of a HBE

A_c = cross-sectional area of a VBE

I_c = moment of inertia of a VBE taken perpendicular to the direction of the web-plate line

L = distance between VBE centerlines

Web-plate thickness and boundary member sizes can be refined in this preliminary stage prior to a structural analysis of the frame. One or two iterations at this stage will permit beginning the analysis with sizes that are closer to optimal in terms of strength. Note, however, that iteration will not facilitate designs where drift is the governing criterion.

Based on the preliminary web-plate and boundary member designs, the angle of tension stress at each level is calculated. Table 5.7 presents the preliminary values of the angle of tension stress and the revised web-plate thickness based on AISC 341 Equation 17–1.

Framing member sizes are similarly revised based on the change in angle of tension stress and the change in web-plate thickness. Revised framing member sizes are presented in Table 5.8.

While such iteration can be easily performed in the preliminary design stage, designers should bear in mind that designs are subject to modification based on forces determined from an analysis of the frame. Effort in performing numerous iterations at the preliminary design stage may well be

Table 5–5. Required Column Moment of Inertia

Level	Web-Plate Thickness t_w (in.)	Panel Proportions		Required Column Moment of Inertia I_c (in.^{4})
		h (in.)	L (in.)	
Ninth Floor	0.0747	156	240	566
Eighth Floor	0.125	156	240	947
Seventh Floor	0.1875	156	240	1,420
Sixth Floor	0.250	156	240	1,890
Fifth Floor	0.250	156	240	1,890
Fourth Floor	0.3125	156	240	2,370
Third Floor	0.3125	156	240	2,370
Second Floor	0.3125	156	240	2,370
First Floor	0.375	216	240	10,400

Table 5–6. Preliminary Boundary Element Sections

Level	VBE	HBE
Roof	–	W27×94
Ninth Floor	W14×132	W27×94
Eighth Floor	W14×132	W27×94
Seventh Floor	W14×132	W27×94
Sixth Floor	W14×193	W27×94
Fifth Floor	W14×193	W27×94
Fourth Floor	W14×605	W27×94
Third Floor	W14×605	W27×94
Second Floor	W14×605	W27×94
First Floor	W14×605	W27×94

Table 5–7. Angle of Stress and Revised Web-Plate Thickness

Level	Angle of Stress α (°)	Web Plate Thickness t_w (in.)
Ninth Floor	42.5	0.0625
Eighth Floor	41.5	0.125
Seventh Floor	40.7	0.1875
Sixth Floor	39.9	0.1875
Fifth Floor	39.9	0.250
Fourth Floor	38.7	0.250
Third Floor	38.7	0.3125
Second Floor	38.7	0.3125
First Floor	35.6	0.3125

Table 5–8. Revised Preliminary Boundary Element Sections

Level	VBE	HBE
Roof	–	W27×102
Ninth Floor	W14×159	W21×62
Eighth Floor	W14×159	W21×62
Seventh Floor	W14×159	W21×62
Sixth Floor	W14×193	W21×62
Fifth Floor	W14×193	W24×84
Fourth Floor	W14×605	W21×62
Third Floor	W14×605	W21×62
Second Floor	W14×605	W27×84
First Floor	W14×605	W27×102

wasted. The purpose of refining the design at this stage is to reduce the number of iterations required in the analysis stage by providing more reasonable beginning sizes. This design procedure is based on the relative difficulty in revising preliminary designs (which can be done using a simple spreadsheet) and using currently available structural analysis software (which requires adaptive procedures discussed below).

5.5.2. Analysis

In order to complete the design of the HBE and VBE, design forces are required. In the preliminary design it was assumed that the entire story shear tributary to the frame was resisted by the web plate. Clearly, VBE with the flexural properties required will participate in the resistance of the story shear.

At this point, it is convenient to perform an analysis to determine the portion of frame shear that is resisted by the web plate. Reduction in the required strength of the web plates could permit reduction in web-plate thickness, which in turn reduces the strength and stiffness requirements on the boundary elements. Changes in the boundary elements require reanalysis to confirm or modify the distribution of frame shear between the web plate and the VBE, as well as recalculation of the angle of stress in the web plate (AISC 341 Equation 17–2), as is discussed below.

Table 5–9. Final Boundary Element Sections and Web Plates							
Level	Web-Plate Thickness t_w (in.)	VBE	HBE	Panel Proportions			
				h (in.)	h_c (in.)	L (in.)	L_{cf} (in.)
Roof	–	–	W30×108	–	–	–	–
Ninth Floor	0.0673	W14×283	W27×94	156	126	240	223
Eighth Floor	0.1046	W14×283	W27×94	156	129	240	223
Seventh Floor	0.125	W14×283	W27×94	156	129	240	223
Sixth Floor	0.1345	W14×398	W30×108	156	129	240	222
Fifth Floor	0.1875	W14×398	W27×94	156	126	240	222
Fourth Floor	0.1875	W14×665	W30×116	156	129	240	218
Third Floor	0.250	W14×665	W27×94	156	126	240	218
Second Floor	0.250	W14×665	W27×94	156	129	240	218
First Floor	0.250	W14×665	W30×108	216	189	240	218

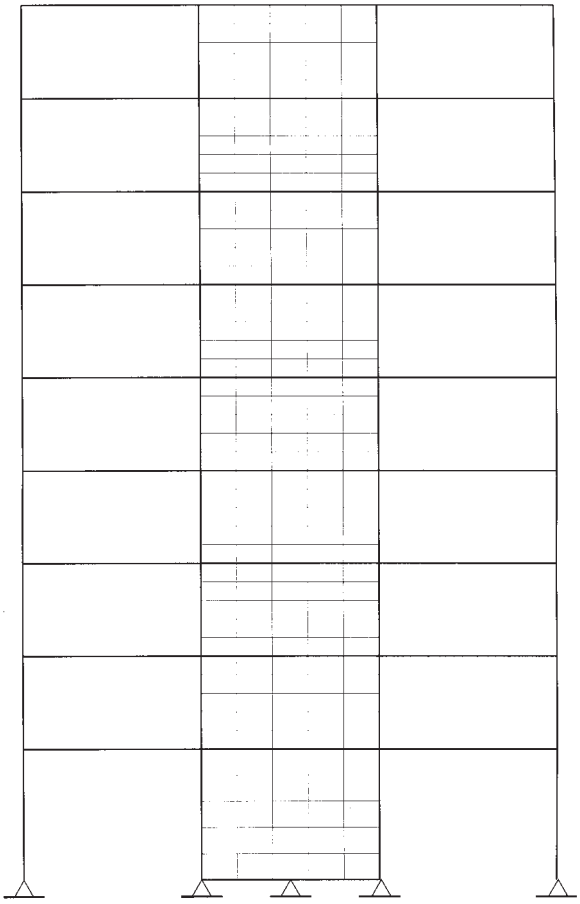

Fig. 5–4. Orthotropic model of SPSW.

The use of a computer model thus permits the iteration that is necessary to optimize the design of SPSW. For this design example, the analysis was performed using an orthotropic membrane element in a mesh between the boundary elements. The membrane element is configured to represent the thin plate by rotating its local axes to align with the estimated angle of tension stress in the plate and reducing its compression stiffness to a negligible value, as explained in Section 3.3. This method of modeling gives results that reasonably match the behavior of SPSW in testing, as well as the results of the more conventional strip-model method. This method is more easily implemented with currently available analysis software; comparison of the methods is presented in Chapter 3.

The orthotropic model of a SPSW is shown in Figure 5–4. This model is analyzed with the forces acting on the frame.

Each iteration of analysis was used to update a spreadsheet, which was used for the following calculations:

1. Check web-plate strength versus portion of load in the plate determined by analysis (resizing would be done for strength-governed designs).

2. Check HBE strength versus flexural forces from gravity loads, web-plate yielding, and axial forces from VBE (due to web-plate yielding).

3. Check VBE strength versus forces from gravity, web-plate yielding, and forces from HBE (due to gravity loads, web-plate yielding, and plastic-hinge formation).

Table 5–10. Angles of Tension Stress α	
Level	**α (°)**
Ninth Floor	43.0
Eighth Floor	41.9
Seventh Floor	41.5
Sixth Floor	41.3
Fifth Floor	40.8
Fourth Floor	40.3
Third Floor	40.1
Second Floor	39.4
First Floor	37.2

Table 5–11. Percentage of Story Shear Resisted by Web Plate	
Level	**Percentage of Story Shear Resisted by Web Plate**
Ninth Floor	44.8
Eighth Floor	59.0
Seventh Floor	63.9
Sixth Floor	57.9
Fifth Floor	66.2
Fourth Floor	68.4
Third Floor	69.4
Second Floor	70.0
First Floor	66.8

4. Recalculate the angle α based on changes in web-plate, HBE, or VBE size.

The analysis indicates this frame is governed by drift limits for most of the frame. In calculating the drift, the forces should be determined using the building period established by analysis, rather than the approximate period. The strength of the web plates can be checked using this calculated period, or a coefficient multiplied by the approximate period, whichever is less (see ASCE 7 Section 12.8.2). The sizes shown in Table 5–9 are satisfactory for both drift and strength requirements.

These member sizes were used to calculate angles of tension stress α at each level using Equation 5–15 (AISC 341 Equation 17–2). The angle of stress is used both for constructing the model and for the capacity-design calculations that follow. These angles are shown in Table 5.10.

The analysis indicates that a portion of the shear is resisted by the columns. Table 5.11 shows the percentage of shear in the web plate at each story. This distribution of shear will be considered in the design of both the web plate and the VBE.

A second-order analysis has been performed including P-Δ effects, but not P-δ effects. To account for P-δ effects, B_1 will be applied in the calculations that follow, when appropriate.

5.5.3. Design of HBE

The design of the W27×94 HBE at the ninth floor will be illustrated.

HBE in SPSW are subjected to significant axial forces due to the effects of web-plate tension on the VBE, as discussed in Chapter 3. They are also subject to flexural forces where web plates are of different thickness above and below the HBE (or are not present at all on one side, such as at the top story). Additionally, shear and moments from the deformation of the frame must be resisted, as well as any gravity loading.

The forces from web-plate tension can be calculated outside of an analysis using capacity-design methods as discussed in Chapter 3. The axial force can be computed from the horizontal anchorage forces on the VBE above and below the HBE and flexural forces from web-plate yielding can be computed from the loading defined in Equation 3–57.

$$M_u = \frac{w_u L_h^2}{8} + P_u\left(\frac{L}{3} - \frac{d_c}{2} - \frac{d_b}{2}\right) \tag{5–16}$$

$$w_u = R_y F_y [t_8 \cos^2(\alpha_8) - t_9 \cos^2(\alpha_9)] \tag{5–17}$$

$$= 1.3(36\text{ ksi})[(0.1046\text{ in.})\cos^2(41.9°) - (0.0673\text{ in.})\cos^2(43.0°)$$

$$= 1.03\text{ kips/in.}$$

For the W27×94 HBE and W14×283 VBE,

$$L_h = L - 2s_h = L - 2[\tfrac{1}{2}(d_c + d_b)] \tag{5–18}$$

$$= 240\text{ in.} - 2[\tfrac{1}{2}(16.7\text{ in.} + 26.9\text{ in.})]$$

$$= 196\text{ in.}$$

From two secondary beams supported at the third points:

$$P_u = 23.3\text{ kips} \tag{5–19}$$

$$M_u = \frac{(1.03\text{ kips/in.})(196\text{ in.})^2}{8} + 23.3\text{ kips}\left(\frac{240\text{ in.}}{3} - \frac{16.7\text{ in.}}{2} - \frac{26.9\text{ in.}}{2}\right)$$

$$= 6{,}300\text{ kip-in.}$$

The axial force in the HBE is

$$P_{HBE} = P_{HBE(VBE)} \pm \frac{1}{2} P_{HBE(web)} \quad (5\text{–}20)$$

$$P_{HBE(VBE)} = \sum \frac{1}{2} R_y F_y \sin^2(\alpha) t_w h_c \quad (5\text{–}21)$$

$$= \frac{1}{2}(1.3)(36 \text{ ksi}) \times \begin{bmatrix} \sin^2(43.0^\circ)(0.0673 \text{ in.})(126 \text{ in.}) \\ +\sin^2(41.9^\circ)(0.1046 \text{ in.})(129 \text{ in.}) \end{bmatrix}$$

$$= 233 \text{ kips}$$

$$P_{HBE(web)} = \frac{1}{2} R_y F_y \left[t_i \sin(2\alpha_i) - t_{i+1} \sin(2\alpha_{i+1}) \right] L_{cf} \quad (5\text{–}22)$$

$$= \frac{1}{2}(1.3)(36 \text{ ksi})(223 \text{ in.}) \times \begin{bmatrix} (0.1046 \text{ in.})\sin(2 \times 41.9^\circ) \\ -(0.0673 \text{ in.})\sin(2 \times 43.0^\circ) \end{bmatrix}$$

$$= 192 \text{ kips}$$

No additional axial force is transmitted through the HBE. This force can be divided equally on either side of the HBE, so half of $P_{HBE(web)}$ will be used in design. On the left side (adjacent to the VBE in tension) the connection force is

$$P_u = 233 \text{ kips} + \frac{1}{2}(192 \text{ kips}) = 329 \text{ kips}$$

On the right side (adjacent to the VBE in compression) the connection force is

$$P_u = 233 \text{ kips} - \frac{1}{2}(192 \text{ kips}) = 137 \text{ kips}$$

Both forces are compressive, thus $P_u = 329$ kips is more critical. Based on this force, the moment-magnification factor B_1 is calculated for the W27×94 HBE as:

$$B_1 = \frac{C_m}{1 - \frac{P_u}{P_{e1}}}$$

$$C_m = 1.0$$

$$KL = 1(240 \text{ in.}) = 240 \text{ in.}$$

$$P_{e1} = \frac{\pi^2 EI}{(KL)^2} = \frac{\pi^2 (29{,}000 \text{ ksi})(3{,}270 \text{ in.}^4)}{(240 \text{ in.})^2} = 16{,}300 \text{ kips}$$

$$B_1 = \frac{1.0}{1 - \left(\frac{329 \text{ kips}}{16{,}300 \text{ kips}} \right)} \geq 1.0$$

$$= 1.02 \geq 1.0; \text{ use } 1.02$$

Since $B_1 = 1.02$, P-δ effects increase the moments above those calculated previously. Therefore,

$$P_r = P_u = 329 \text{ kips}$$

$$M_r = B_1 M_{nt} + B_2 M_{lt} \approx B_1 M_u$$

$$= 1.02(6{,}300 \text{ kip-in.})$$

$$= 6{,}430 \text{ kip-in.}$$

The shear in the HBE is

$$V_u = \frac{2M_{pr}}{L_h} + P_u + \frac{w_g + w_u}{2}(L_{cf}) \quad (5\text{–}23)$$

The probable beam flexural strength, M_{pr}, upon which the shear V_u is based is the strength of the reduced beam section, amplified by the material overstrength factor R_y and a factor 1.1 to account for strain hardening. The reduced beam section is here assumed to have two-thirds the plastic section modulus of the W27×94 HBE.

$$M_{pr} = 1.1 R_y F_y Z_{RBS} \quad (5\text{–}24)$$

$$= 1.1 R_y F_y (\tfrac{2}{3} Z_x)$$

$$= 1.1(1.1)(50 \text{ ksi})(\tfrac{2}{3})(278 \text{ in.}^3)$$

$$= 11{,}200 \text{ kip-in.}$$

where

Z_{RBS} = the plastic section modulus of the reduced beam section.

As discussed in Chapter 3, axial forces present in the HBE at the connections may be used to calculate a reduced flexural strength at the plastic hinge (and thus a reduced value of V_u).

$$P_y = F_y A_g$$

$$= 50 \text{ ksi } (27.7 \text{ in.}^2)$$

$$= 1{,}390 \text{ kips}$$

At the left side,

$$P_u / P_y = 329 \text{ kips} / 1{,}390 \text{ kips} = 0.237$$

$$P_u / P_y > 0.2$$

$$M^*_{pr} = \frac{9}{8}(1.1 R_y F_y Z_{RBS}) \left[1 - \frac{P_{u\,HBE}}{P_y} \right]$$

$$= 9{,}620 \text{ kip-in.}$$

At the right side,

$$P_u / P_y = 137 \text{ kips} / 1{,}390 \text{ kips} = 0.0986$$

$$P_u / P_y < 0.2$$

$$M_{pr}^{*} = \left(1.1R_yF_yZ_{RBS}\right)\left[1-\frac{1}{2}\left(\frac{P_{u\ HBE}}{P_y}\right)\right]$$
$$= 10,700 \text{ kip-in.}$$

Continuing with the calculation of V_u, there is no distributed gravity loading on the beam:

$$w_g = 0 \text{ kips/in.}$$
$$V_u = \frac{(10,700 \text{ kip-in.} + 9,620 \text{ kip-in.})}{196 \text{ in.}} + 23.3 \text{ kips} + (1.03 \text{ kips/in.})(223 \text{ in.})/2$$
$$= 242 \text{ kips}$$

Note that neglecting the axial force in the HBE would have resulted in a calculated V_u of 252 kips.

Check Compactness

$$\frac{b_f}{2t_f} \le 0.30\sqrt{\frac{E}{F_y}} = 7.22 \qquad (5\text{–}25)$$
$$\frac{b}{2t_f} = 6.70 < 7.22$$

$$C_a = \frac{P_u}{\phi_b P_y} \qquad (5\text{–}26)$$
$$= 329 \text{ kips}/0.90(1,390 \text{ kips})$$
$$= 0.263$$

$$\frac{h}{t_w} \le 1.12\sqrt{\frac{E}{F_y}}\left[2.33 - C_a\right] \text{ for } C_a > \frac{1}{8} \qquad (5\text{–}27)$$

$$1.12\sqrt{\frac{E}{F_y}}\left[2.33 - C_a\right] = 55.6 \qquad (5\text{–}28)$$

$h/t_w = 49.5 < 55.6$

The W27×94 meets the applicable seismic compactness requirements.

Check Lateral Bracing

$$L_b \le 0.086 r_y E/F_y \qquad (5\text{–}29)$$
$$0.086\ r_y\ E/F_y = 0.086(2.12 \text{ in.})(29,000 \text{ ksi})/(50 \text{ ksi})$$
$$= 106 \text{ in.}$$
$$L_b = 80 \text{ in.} < 106 \text{ in.} \quad \textbf{o.k.}$$

The required strength of the lateral brace is 2 percent of the flange strength:

$$P_{br} = 0.02\ F_y\ b_f\ t_f \qquad (5\text{–}30)$$
$$= 0.02(50 \text{ ksi})(10.0 \text{ in.})(0.745 \text{ in.})$$
$$= 7.45 \text{ kips}$$

The required stiffness of lateral bracing is determined from Equation A–6-8:

$$\beta_{br} = \frac{1}{\phi}\left[\frac{10M_rC_d}{L_bh_o}\right] \qquad (5\text{–}31)$$

where

$$\phi = 0.75$$
$$M_r = R_yF_yZ_x$$
$$= 1.1(50 \text{ ksi})(278 \text{ in.}^3)$$
$$= 15,300 \text{ kip-in.}$$
$$C_d = 1.0$$
$$h_o = d - t_f \qquad (5\text{–}32)$$
$$= 26.9 \text{ in.} - 0.745 \text{ in.}$$
$$= 26.2 \text{ in.}$$

$$\beta_{br} = \frac{1}{0.75}\left[\frac{10(16,500 \text{ kips})1.0}{(80 \text{ in.})(26.2 \text{ in.})}\right] \qquad (5\text{–}33)$$
$$= 97.3 \text{ kips/in.}$$

The lateral bracing elements (the secondary beams framing into the HBE at the third points) are designed to resist the calculated force and provide the required stiffness. The design of these elements is not shown here.

Check Shear Strength

$$\frac{h}{t_w} \le 2.24\sqrt{\frac{E}{F_y}} = 54.0$$
$$\phi_v = 1.0$$

$$\phi_vV_n = \phi_v0.6F_yA_w \qquad (5\text{–}34)$$
$$= 1.0(0.6)(50 \text{ ksi})(26.9 \text{ in.})(0.490 \text{ in.})$$
$$= 395 \text{ kips}$$
$$\phi V_n > V_u = 242 \text{ kips} \quad \textbf{o.k.}$$

Check Combined Compression and Flexure

KL/r_x = 1(240 in.)/(10.9 in.) = 22.0

KL/r_y = 1(80 in.)/(2.12 in.) = 37.7

Minor-axis buckling controls.

$$F_e = \frac{\pi^2 E}{\left[\frac{KL}{r}\right]^2} \tag{5–35}$$

$$= \frac{\pi^2 (29{,}000 \text{ ksi})}{(37.7)^2}$$

$$= 201 \text{ ksi} > 0.44F_y = 22.0 \text{ ksi}$$

Use AISC 360 Equation E3–2:

$$F_{cr} = \left[0.658^{\frac{F_y}{F_e}}\right] F_y \tag{5–36}$$

$$= \left[0.658^{\frac{50 \text{ ksi}}{201 \text{ ksi}}}\right](50 \text{ ksi})$$

$$= 45.1 \text{ ksi}$$

$$\phi_c P_n = \phi_c F_{cr} A_g \tag{5–37}$$

$$= 0.90(45.1 \text{ ksi})(27.7 \text{ in.}^2)$$

$$= 1{,}120 \text{ kips}$$

$P_c = \phi_c P_n$ = 1,120 kips

P_r/P_c = 329 kips/1,120 kips = 0.294

For the flexural strength, the limiting unbraced length is taken from AISC Manual Table 3–2:

L_p = 7.49 ft = 89.9 in.

L_b = 80 in.

Since $L_b < L_p$, lateral-torsional buckling does not control. The flexural strength is

$$M_c = \phi_b M_n = \phi_b F_y Z_x \tag{5–38}$$

$$= 0.90(50 \text{ ksi})(278 \text{ in.}^3)$$

$$= 12{,}500 \text{ kip-in.}$$

M_r/M_c = 6,430 kip-in. /12,500 kip-in.

= 0.514

As $P_r/P_c > 0.2$, use Equation H1-1a:

$$\frac{P_r}{P_c} + \frac{8}{9}\left(\frac{M_r}{M_c}\right) = 0.751 < 1.0 \quad \textbf{o.k.} \tag{5–39}$$

Check Moment of Inertia

The required moment of inertia is

$$I_{HBE} \geq 0.003 \frac{(\Delta t_w) L^4}{h} \tag{5–40}$$

$$= 0.003(0.1046 \text{ in.} - 0.0673 \text{ in.})(240 \text{ in.})^4/(156 \text{ in.})$$

$$= 2{,}380 \text{ in.}^4$$

I_x = 3,270 in.^{4} > 2,380 in.^{4} **o.k.**

Check Web Thickness

$$t_{w\,HBE} \geq \frac{t_w R_y F_y}{F_{y\,HBE}} \tag{5–41}$$

$$\geq (0.1046 \text{ in.})(1.3)(36 \text{ ksi})/(50 \text{ ksi})$$

$$\geq 0.0979 \text{ in.}$$

t_w = 0.490 in. > 0.0979 in. **o.k.**

5.5.4. Design of VBE

The design of the W14×283 VBE at the eighth floor will be illustrated.

VBE in SPSW are subject to high axial forces due to overturning from levels above. These axial forces are concurrent with significant flexural demands from two sources. The first source is the deformation of the rigid frame of which the VBE (columns) form a part (VBE and HBE in SPSW are required to form rigid frames). The second source is the tension stress in the web plate, which exerts an inward force on the VBE. This force acts on the column in compression in the direction opposite of the frame shear and on the column in tension in the direction of the frame shear. Both of these sources of flexural forces are represented in the analytical model.

VBE in SPSW must be designed to resist forces corresponding to the expected yield strength of the wall. The analysis of the wall is based on loads corresponding to the base shear, not the strength of web plate provided. Accordingly, the member forces from the analysis must be increased to a level corresponding to the web-plate strength for SPSW.

Chapter 3 provides methods for calculating the estimated forces (which are substantially higher than the forces corresponding to the design base shear). For this example, the capacity-design method will be used to determine the axial forces in the VBE.

The axial compression force in the VBE includes the effects of the web plate at the eighth and ninth floors and the shear V_u from the HBE at the ninth floor and the roof. The resulting compressive force is

$$E_m = \sum \frac{1}{2} R_y F_y \sin(2\alpha) t_w h + \sum V_u \qquad (5\text{–}42)$$

The sum of seismic shears (ΣV_u) should include all of the beams above. The seismic shear in the HBE is

$$V_u = \frac{2M_{pr}}{L_h} + \frac{w_u}{2} L_{cf} \qquad (5\text{–}43)$$

In the case of the adjoining rigidly connected beams outside the SPSW bay, their upward force due to frame behavior can be taken as

$$V_u = 2\,M_{pr}/L_h \qquad (5\text{–}44)$$

assuming rigid connections at each end of the beam. Thus, the compressive force is

$$E_m = \sum \frac{1}{2} R_y F_y \sin(2\alpha)\, t_w h_c + \sum \left[\frac{2M_{pr\ HBE}}{L_h} + \frac{w_u}{2} L_{cf} \right] - \sum \left[\frac{2M_{pr\ Adj}}{L_h} \right] \qquad (5\text{–}45)$$

where

$M_{pr\,Adj}$ = the expected flexural strength of the adjoining beams

For simplicity, the seismic shears adjusted for the axial force present in the compression case will be given as follows:

$$\Sigma V_u = 242 \text{ kips} + 348 \text{ kips} - 88.7 \text{ kips} - 179 \text{ kips}$$

$$= 322 \text{ kips}$$

These are for the ninth floor beam, roof beam, and adjoining beams, respectively. The determination of such values was previously illustrated for the ninth floor HBE (for which V_u = 242 kips in the above calculation).

In the tension case

$$\Sigma V_u = -70.0 \text{ kips} - 34.0 \text{ kips} - 88.7 \text{ kips} - 179 \text{ kips}$$

$$= -372 \text{ kips}$$

The resulting compressive force is

$$E_m = \frac{1}{2}(1.3)(36 \text{ ksi}) \times \begin{bmatrix} \sin(2\times 43.0^\circ)(0.0673 \text{ in.})(126 \text{ in.}) \\ +\sin(2\times 41.9^\circ)(0.1046 \text{ in.})(129 \text{ in.}) \end{bmatrix} + 322 \text{ kips} = 834 \text{ kips}$$

With the additional 103 kips of gravity load (and the contribution of 0.2 $S_{DS}D$), the total axial force, P_u = 938 kips. Based on this force, the moment-magnification factor B_1 is calculated for the W14×283 VBE as:

$$B_1 = \frac{C_m}{1 - \left(\frac{P_u}{P_E} \right)} \geq 1.0 \qquad (5\text{–}46)$$

$$C_m = 1.0 \qquad (5\text{–}47)$$

$$KL = 1(156 \text{ in.}) = 156 \text{ in.} \qquad (5\text{–}48)$$

$$P_{e1} = \frac{\pi^2 EI}{(KL)^2}$$

$$P = \frac{\pi^2 (29{,}000 \text{ ksi})(3{,}840 \text{ in.}^4)}{(156 \text{ in.})^2} = 45{,}100 \text{ kips} \qquad (5\text{–}49)$$

$$B_1 = \frac{1.0}{1 - \left(\frac{938 \text{ kips}}{45{,}100 \text{ kips}} \right)} \geq 1.0 = 1.02 \geq 1.0; \text{ use } 1.02 \qquad (5\text{–}50)$$

The axial tension force is calculated based on the expected strength of the beams and web plates:

$$E_m = \sum \frac{1}{2} R_y F_y \sin(2\alpha)\, t_w h_c + \sum \frac{2M_{pr}}{L_h} - \sum \frac{w_u}{2} L_{cf} \qquad (5\text{–}51)$$

$$E_m = \frac{1}{2}(1.3)(36 \text{ ksi}) \times \begin{bmatrix} \sin(2\times 43.0^\circ)(0.0673 \text{ in.})(126 \text{ in.}) \\ +\sin(2\times 41.9^\circ)(0.1046 \text{ in.})(129 \text{ in.}) \end{bmatrix} - 372 \text{ kips} = 140 \text{ kips}$$

Next, VBE flexural forces (shear and moment) must be calculated. The most accurate method of establishing VBE flexural forces, outside a nonlinear analysis, is to model the VBE as a continuous member on multiple supports. This method is illustrated in Chapter 3. In this design example, the flexural forces will be estimated story by story, assuming fixed ends for the VBE. The contributions of web-plate tension and HBE plastic hinging will be estimated separately and combined.

The flexure from web tension at the connection is

$$M_{VBE(web)} = R_y F_y \sin^2(\alpha) t_w \left(\frac{h_c^2}{12} \right) = 1.3(36 \text{ ksi}) \sin^2(41.9^\circ)(0.1046 \text{ in.}) \times (129 \text{ in.})^2 / 12 = 3{,}030 \text{ kip-in.} \qquad (5\text{–}52)$$

The moment from HBE plastic hinging is calculated based on the flexural strength of the adjoining beams (reduced due to the axial force present). The moment in the VBE segment at the connection from HBE plastic hinging is one-half the flexural strength of the two beams at the connection (the HBE and the adjoining beam, which is rigidly connected in this design). The stain-hardening factor of 1.1 and the material overstrength factor of 1.1 will not be used here; they will be used in a similar check (for strong-column/weak-beam) in which the resistance factor is not used.

The condition at the VBE in compression is evaluated here, as it will control the design.

$$M_{VBE(HBE)} = \frac{1}{2}\sum M_{pb} \tag{5–53}$$

$$M_{pb} = M_{pr}/(1.1R_y) + V_u s_h \tag{5–54}$$

From the W27×94:

$$M_{pb} = \frac{(11{,}200 \text{ kip-in.})}{1.1(1.1)} + (242 \text{ kips})\left[\tfrac{1}{2}(16.7 \text{ in.} + 26.9 \text{ in.})\right] = 14{,}500 \text{ kip-in.}$$

The adjoining beam, a W24×68 in a 20-ft bay, does not have a web plate, and thus its shear is much lower. Its flexural strength is reduced only by the collector force, not by the inward VBE reaction due to web-plate tension.

$$P_u = \frac{1}{2} P_{HBE(web)} = \frac{1}{2}(192 \text{ kips}) = 96.0 \text{ kips}$$

$$P_u/P_y = 96.0 \text{ kips}/1{,}010 \text{ kips} = 0.0950$$

$$P_u/P_y < 0.2$$

$$M_{pr}^{*} = (1.1R_yF_yZ)\left[1 - \frac{1}{2}\left(\frac{P_{u\,HBE}}{P_y}\right)\right] = 10{,}200 \text{ kip-in.}$$

$$M_{pb} = \frac{(10{,}200 \text{ kip-in.})}{1.1(1.1)} + (88.7 \text{ kips})\left[\tfrac{1}{2}(16.7 \text{ in.} + 23.7 \text{ in.})\right] = 10{,}200 \text{ kip-in.}$$

$$M_{VBE(HBE)} = \frac{1}{2}\sum M_{pb} = \frac{1}{2}(14{,}500 \text{ kip-in.} + 10{,}200 \text{ kip-in.}) = 12{,}400 \text{ kip-in.}$$

$$M_u = M_{VBE(web)} + M_{VBE(HBE)} \tag{5–55}$$

$$= 3{,}030 \text{ kip-in.} + 12{,}400 \text{ kip-in.}$$

$$= 15{,}400 \text{ kip-in.}$$

In the middle of the VBE, the flexural forces from the HBE plastic hinging are much lower than at the connection. As these forces dominate over the flexural forces due to web-plate tension, the condition at middle of the VBE will not be explicitly evaluated.

Since $B_1 = 1.03$, P-δ effects increase the moments above those calculated previously. Therefore,

$$P_r = P_u = 938 \text{ kips}$$

$$M_r = B_1M_{nt} + B_2M_{lt} \approx \mathrm{B}_1M_u$$

$$= 1.02(15{,}400 \text{ kip-in.})$$

$$= 15{,}700 \text{ kip-in.}$$

The shear in the VBE is the sum of the effect of web tension and the portion of shear not resisted by the web plate.

$$V_{VBE(web)} = \frac{1}{2}R_yF_y \sin^2(\alpha)t_wh_c \tag{5–56}$$

$$= \frac{1}{2}(1.3)(36 \text{ ksi}) \times \sin^2(41.9^\circ)(0.1046 \text{ in.})(129 \text{ in.}) = 141 \text{ kips}$$

The shear due to HBE hinging can be approximated as

$$V_{VBE(HBE)} = \sum \frac{1}{2}\left(\frac{M_{pc}}{h_c}\right) = \frac{\frac{1}{2}(12{,}400 \text{ kip-in.} + 15{,}400 \text{ kip-in.})}{(129 \text{ in.})} = 108 \text{ kips}$$

The analysis shows that the 59.0 percent of the shear is in the web plate (see Table 5–11), and 9.50 percent in the adjacent bays modeled. It is assumed that the remaining shear is shared equally by the two VBE:

$$V_{VBE(HBE)} \geq \frac{1}{2}(1 - 0.590 - 0.0950)(349 \text{ kips}) \geq 55.0 \text{ kips}$$

The total shear is

$$V_u = V_{VBE(HBE)} + V_{VBE(web)} \tag{5–57}$$

$$= 108 \text{ kips} + 141 \text{ kips}$$

$$= 249 \text{ kips}$$

Check Compactness

$$\frac{b_f}{2t_f} \le 0.30\sqrt{\frac{E}{F_y}} = 7.22 \quad (5\text{–}58)$$

$$b/2t_f = 3.89 < 7.22$$

$$C_a = \frac{P_u}{\phi_b P_y} \quad (5\text{–}59)$$

$$= 938 \text{ kips} / 0.90(50 \text{ ksi})(83.3 \text{ in.}^2)$$

$$= 0.250$$

$$\frac{h}{t_w} \le 1.12\sqrt{\frac{E}{F_y}}\left[2.33 - C_a\right] \text{ for } C_a > \frac{1}{8} \quad (5\text{–}60)$$

$$1.12\sqrt{\frac{E}{F_y}}\left[2.33 - C_a\right] = 56.1$$

$$h/t_w = 8.84$$

The W14×283 meets the applicable seismic compactness requirements.

Check Shear Strength

$$\frac{h}{t_w} \le 2.24\sqrt{\frac{E}{F_y}} = 54.0$$

$$\phi_v = 1.0$$

$$\phi_v V_n = \phi_v 0.6\, F_y A_w \quad (5\text{–}61)$$

$$= 1.0(0.6)(50 \text{ ksi})(16.7 \text{ in.})(1.29 \text{ in.})$$

$$= 646 \text{ kips}$$

$$\phi_v V_n > V_u = 249 \text{ kips} \quad \textbf{o.k.}$$

Check Combined Compression and Flexure

By inspection, the compression strength is governed by minor-axis buckling.

$$KL/r_y = (1)(156 \text{ in.})/(4.17 \text{ in.}) = 37.4$$

$$F_e = \frac{\pi^2 E}{\left[\frac{KL}{r}\right]^2} \quad (5\text{–}62)$$

$$= \frac{\pi^2 (29{,}000 \text{ ksi})}{(37.4)^2}$$

$$= 205 \text{ ksi} > 0.44F_y = 22.0$$

Use Equation E3–2:

$$F_{cr} = \left[0.658^{\frac{F_y}{F_e}}\right]F_y \quad (5\text{–}63)$$

$$= \left[0.658^{\frac{50 \text{ ksi}}{205 \text{ ksi}}}\right](50 \text{ ksi})$$

$$= 45.1 \text{ ksi}$$

$$\phi_c P_n = \phi_c F_{cr} A_g \quad (5\text{–}64)$$

$$= 0.90(45.1 \text{ ksi})(83.3 \text{ in.}^2)$$

$$= 3{,}380 \text{ kips}$$

$$P_c = \phi_c P_n = 3{,}380 \text{ kips}$$

$$P_r/P_c = 938 \text{ kips} / 3{,}380 \text{ kips} = 0.278$$

For the flexural strength, the limiting unbraced length is taken from AISC Manual Table 3–2:

$$L_p = 14.7 \text{ ft} = 176 \text{ in.}$$

$$L_b = 156 \text{ in.}$$

Since $L_b < L_p$, lateral-torsional buckling does not control. The flexural strength is

$$M_c = \phi_b M_n \quad (5\text{–}65)$$

$$= \phi_b F_y Z_x$$

$$= 0.90(50 \text{ ksi})(542 \text{ in.}^3)$$

$$= 24{,}400 \text{ kip-in.}$$

$$M_r/M_c = 15{,}700 \text{ kip-in.} / 24{,}400 \text{ kip-in.}$$

$$= 0.643$$

As $P_u/\phi P_n > 0.2$, use Equation H1-1a:

$$\frac{P_u}{\phi P_n} + \frac{8M_u}{9\phi M_n} = 0.850 < 1.0 \quad \textbf{o.k.}$$

Check Combined Tension and Flexure

By inspection, tension will not control the design over compression. When tension and flexure does control, see AISC Specification Section H1.2.

5.5.5. Connection of Web Plate to Boundary Elements

AISC 341 requires that such connections be designed for the expected strength of the plate. As discussed in Chapter 3, these forces are dependent on the angle of tension stress α. The strength of fillet welds is also dependent on this angle.

Table 5–12. Required Fillet Weld Size for SPSW1						
Level	Web-Plate Thickness t_w (in.)	Angle of Stress α (°)	Wed Size at HBE (in.)		Weld Size at VBE (in.)	
			Total	Two Welds Each	Total	Two Welds Each
Ninth Floor	0.0673	43.0	0.0788	equal to t_w	0.0752	equal to t_w
Eighth Floor	0.1046	41.9	0.124	equal to t_w	0.115	equal to t_w
Seventh Floor	0.125	41.5	0.149	equal to t_w	0.137	equal to t_w
Sixth Floor	0.1345	41.3	0.160	1/8	0.147	1/8
Fifth Floor	0.1875	40.8	0.224	1/8	0.204	1/8
Fourth Floor	0.1875	40.3	0.225	1/8	0.202	1/8
Third Floor	0.250	40.1	0.301	3/16	0.269	3/16
Second Floor	0.250	39.4	0.303	3/16	0.266	3/16
First Floor	0.250	37.2	0.309	3/16	0.257	3/16

For fillet-welded connections, the required total weld size at the HBE can be expressed as

$$w_{(HBE)} = \frac{R_y F_y \cos(\alpha) t_w \sqrt{2}}{\phi 0.6 F_{EXX}\left[1 + 0.5\cos^{1.5}(\alpha)\right]} \qquad (5\text{–}66)$$

The required total weld size at the VBE is

$$w_{(VBE)} = \frac{R_y F_y \sin(\alpha) t_w \sqrt{2}}{\phi 0.6 F_{EXX}\left[1 + 0.5\sin^{1.5}(\alpha)\right]} \qquad (5\text{–}67)$$

These weld sizes are the total required. In this case, two parallel welds are used to resist the web-plate tension (as shown in Figure 5–5), and the overlap of the web plate and fish plate is small. Thus, the two welds are assumed to share the force equally, and the sum of the two weld sizes must equal or exceed the total required weld size calculated above. Table 5–12 shows the total required fillet weld size at each level for F_y = 36 ksi and F_{EXX} = 70 ksi, as well as the size of each weld for the two parallel welds.

Figure 5–5 shows a connection detail for the ¼-in. web plate to the VBE at the first floor. In this case, two 3/16-in. welds are used.

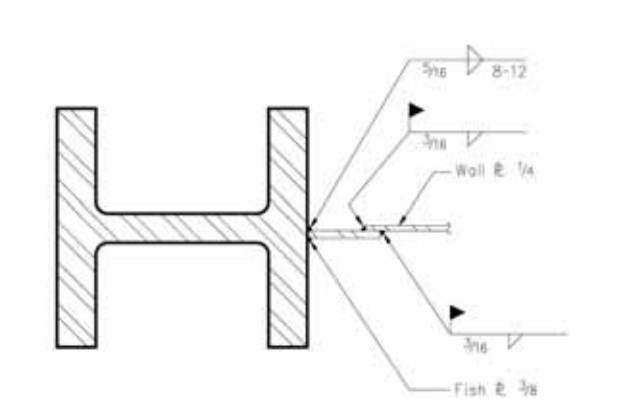

Fig. 5–5. Connection of ¼ in. web plate to VBE.

5.5.6. Connection of HBE to VBE

The connection of the W27×94 HBE to the W14×283 VBE at the ninth floor will be designed. The connection is an RBS moment connection, as described in AISC 358. This connection utilizes complete-joint-penetration groove welds to connect the beam flanges and web to the column flange. It thus satisfies the flexural-strength and detailing requirement of AISC 341 Section 17.4b.

Check Strong-Column/Weak-Beam

As discussed in Chapter 3, the strong-column/weak-beam check is performed considering both VBE, each end of the HBE, and the adjoining beams outside the SPSW.

$$\Sigma M_{pc}^* \geq \Sigma M_{pb}^* \qquad (5\text{–}68)$$

$$M_{pb}^* = M_{pr} + V_u s_h \qquad (5\text{–}69)$$

From the W27×94 at the VBE in compression:

M_{pb}^* = (10,700 kip-in.)

+ (242 kips)[½(16.7 in. + 26.9 in.)]

= 16,000 kip-in.

From the W27×94 at the VBE in tension:

$$M_{pb}^* = (9{,}620 \text{ kip-in.}) + (34.0 \text{ kips})[\tfrac{1}{2}(16.7 \text{ in.} + 26.9 \text{ in.})] = 10{,}400 \text{ kip-in.}$$

For the adjoining W24×68 beam:

$$M_{pb}^* = 10{,}200 \text{ kip-in.}$$

$$\Sigma M_{pb}^* = 16{,}000 \text{ kip-in.} + 10{,}400 \text{ kip-in.} + 2(10{,}200 \text{ kip-in.}) = 46{,}800 \text{ kip-in.}$$

The VBE flexural strength is reduced considering the axial force. This axial force is calculated based on the expected strength of the web plate and beam above. For the VBE in compression:

$$\Sigma M_{pcC}^* = 2(F_y - P_u/A_g)Z_x = 2(50 \text{ ksi} - 938 \text{ kips}/83.3 \text{ in.}^2)(542 \text{ in.}^3) = 42{,}000 \text{ kip-in.} \quad (5\text{–}70)$$

For the VBE in tension:

$$\Sigma M_{pcT}^* = 2(F_y - P_u/A_g)Z = 2(50 \text{ ksi} - 72.0 \text{ kips}/83.3 \text{ in.}^2)(542 \text{ in.}^3) = 53{,}300 \text{ kip-in.} \quad (5\text{–}71)$$

$$\Sigma M_{pc}^* = 42{,}000 \text{ kip-in.} + 53{,}300 \text{ kip-in.} = 95{,}300 \text{ kip-in.}$$

$\Sigma M_{pc}^* > \Sigma M_{pb}^*$ **o.k.**

Note that the check would not work at the VBE in compression if each VBE were considered separately.

Panel-Zone Check

The minimum web thickness is

$$t \geq \frac{d_z + w_z}{90} \quad (5\text{–}72)$$

$$= \begin{bmatrix} 26.9 \text{ in.} - (2 \times 0.745 \text{ in.}) \\ + 16.7 \text{ in.} - (2 \times 2.07 \text{ in.}) \end{bmatrix} / 90$$

$$= 0.422 \text{ in.}$$

$t_{wc} = 1.29$ in. **o.k.**

The required panel-zone shear strength is

$$R_u = \frac{\sum \left[M_{pb}^* + V_p \left(\frac{d_b}{2} \right) \right]}{d_z} \quad (5\text{–}73)$$

$$R_u = \begin{bmatrix} 10{,}700 \text{ kip-in.} + 10{,}200 \text{ kip-in.} \\ + (242 \text{ kips})(26.9 \text{ in.}/2) \\ + (88.7 \text{ kips})(26.9 \text{ in.}/2) \end{bmatrix} / [26.9 \text{ in.} - (2 \times 0.745 \text{ in.})]$$

$$= 998 \text{ kips}$$

This shear may be reduced considering the shear in the VBE corresponding to HBE hinging. This shear is at least

$$\frac{1}{2} V_{VBE(HBE)} = \frac{1}{2} \times 107 \text{ kips} = 53.5 \text{ kips}$$

$$R_u = 998 \text{ kips} - 53.5 \text{ kips} = 945 \text{ kips}$$

This force need not exceed the expected strength of the connected flanges (a W27×94 and a W24×68):

$$R_u \leq \sum 1.1 R_y F_y b_{fb} t_{fb} \quad (5\text{–}74)$$

$$= 1.1(1.1)(50 \text{ ksi})(10.0 \text{ in.})(0.745 \text{ in.}) + 1.1(1.1)(50 \text{ ksi})(8.97 \text{ in.})(0.585 \text{ in.})$$

$$= 768 \text{ kips}$$

Thus, $R_u = 768$ kips

The panel-zone shear strength check is performed neglecting the axial force due to web-plate yielding in the beam:

$$\phi R_n = 1.0 \times 0.6 F_{yc} d_c t_{wc} \left[1 + \frac{3 b_{cf} t_{cf}^2}{d_b d_c t_w} \right] \quad (5\text{–}75)$$

$$= \begin{bmatrix} 1.0(0.6)(50 \text{ ksi})(16.7 \text{ in.})(1.29 \text{ in.}) \\ \times 1 + \dfrac{3(16.1 \text{ in.})(2.07 \text{ in.})^2}{(26.9 \text{ in.})(16.7 \text{ in.})(1.29 \text{ in.})} \end{bmatrix}$$

$$= 866 \text{ kips}$$

$\phi R_n > R_u$ **o.k.**

Check Flange Local Bending

The required strength can be calculated either by computing the moment at the column face or simply by using 1.1 times the expected strength of the beam flange. The strength of the flange is the lower of the two.

$$R_u \leq 1.1 R_y F_y b_{fb} t_{fb} \quad (5\text{–}76)$$

$$= 1.1(1.1)(50 \text{ ksi})(10.0 \text{ in.})(0.745 \text{ in.})$$

$$= 451 \text{ kips}$$

$$\phi R_n = \phi 6.25 t_f^2 F_y \quad (5\text{–}77)$$
$$= 0.90(6.25)(2.07\text{ in.})^2(50\text{ ksi})$$
$$= 1{,}210\text{ kips}$$
$$\phi R_n > R_u \quad \textbf{o.k.}$$

Check Web Yielding

$$\phi R_n = \phi(5k + N) t_w F_y \quad (5\text{–}78)$$
$$= 1.00\begin{bmatrix}5(2.67\text{ in.})\\ +0.745\text{ in.}\end{bmatrix}(1.29\text{ in.})(50\text{ ksi})$$
$$= 909\text{ kips}$$
$$\phi R_n > R_u \quad \textbf{o.k.}$$

Check Web Crippling

$$\phi R_n = \phi 0.80 t_w^2 \left[1 + 3\left(\frac{N}{d}\right)\left(\frac{t_w}{t_f}\right)^2\right]\sqrt{\frac{EF_y t_f}{t_w}} \quad (5\text{–}79)$$
$$= 0.75(0.80)(1.29\text{ in.})^2\left[1 + 3\left(\frac{0.745\text{ in.}}{16.7\text{ in.}}\right)\left(\frac{1.29\text{ in.}}{2.07\text{ in.}}\right)^2\right]$$
$$\times\sqrt{\frac{29{,}000\text{ ksi}(50\text{ ksi})(2.07\text{ in.})}{1.29\text{ in.}}}$$
$$= 1{,}600\text{ kips}$$
$$\phi R_n > R_u \quad \textbf{o.k.}$$

Check Web Connection

The connection of the HBE web to the VBE must resist the combined effects of the shear (V_u) and the compression ($P_{u\,HBE}$) in the HBE at the connection. These are combined using the von Mises yield criterion, and a required connection area is computed. At the left end:

$$3(V_u/A)^2 + (P_{u\,HBE}/A)^2 \le (\phi F_y)^2 \quad (5\text{–}80)$$

$$A \ge \frac{\sqrt{3V_u^2 + P_{u\,HBE}^2}}{\phi F_y} \quad (5\text{–}81)$$
$$A \ge \frac{\sqrt{3(242\text{ kips})^2 + (137\text{ kips})^2}}{0.90(50\text{ ksi})}$$
$$= 9.80\text{ in.}^2$$

At the other end,

$$A \ge \frac{\sqrt{3(34.0\text{ kips})^2 + (329\text{ kips})^2}}{0.9(50\text{ ksi})}$$
$$= 7.43\text{ in.}^2$$

The web area is

$$13.2\text{ in.}^2 - 2(1\text{ in.})(0.490\text{ in.}) = 12.2\text{ in.}^2 > A \quad \textbf{o.k.}$$

5.5.7. VBE Splices and Base Connection

The VBE is spliced at the fourth and sixth floors. The seismic tension forces on these splices, and on the anchorage at the base plate, is calculated using capacity-design procedures, as discussed in Chapter 3.

Check VBE Splice at Sixth Floor

The splices of VBE are required to comply with Section 8.4 of AISC 341. The required strength is calculated based on the expected strength of the SPSW above, in combination with dead loads and the vertical component of seismic acceleration.

The SPSW component is calculated using Equation 3–61 at the story mid-height:

$$E_m = \sum\frac{1}{2} R_y F_y \sin(2\alpha) t_w h_c + \sum\left[\frac{2M_{pr}}{L_h} - \frac{w_u}{2} L_{cf}\right] \quad (5\text{–}82)$$

This component will be given as E_m = 936 kips.

The dead load effect on the column is subtracted from the seismic load, and the vertical component of seismic acceleration is added to it. The resulting axial force is

$$P_u = 0.9D - E_m - 0.2\,S_{DS} \quad (5\text{–}83)$$

This axial force will be given as 792 kips.

The required flexural and shear strengths of the splice are computed in the same way as for the eighth-floor VBE. The forces, however, are calculated at the splice location, rather than at the beam-to-column connection. The required flexural strength is

$$M_u = M_{VBE(HBE)} + M_{VBE(web)} \quad (5\text{–}84)$$
$$M_{VBE(web)} = R_y F_y \sin^2(\alpha) t_w \left(\frac{h_c^2}{24}\right)$$
$$M_u = \frac{1}{2}(8{,}410\text{ kip-in.}) + 3{,}030\text{ kip-in.}$$
$$= 7{,}240\text{ kip-in.}$$

The component of shear from web-plate tension is negligible if the splice is located near the center of the clear height. The shear is due mainly to the frame behavior:

$$V_{VBE(HBE)} = 107\text{ kips}$$

The flanges and web will be joined by complete joint penetration welds. The strength is thus that of the smaller section, and the connection is satisfactory.

Check Base Connection

The required tension strength is computed based on the design strength of the web plates above

$$E_m = \sum \frac{1}{2} R_y F_y \sin(2\alpha)\, t_w h_c + \sum \left[\frac{2M_{pr}}{L_h} - \frac{w_u}{2} L_{cf} \right]$$

This component will be given as E_m = 3,630 kips.

A portion of the dead load effect on the column is subtracted from the seismic load, and the vertical component of seismic acceleration is added to it. The resulting axial force is

$$P_u = 0.9D - E_m - 0.2\, S_{DS} \quad (5\text{–}85)$$

This axial force will be given as 3,370 kips.

The required flexural strength of the base HBE RBS connection is computed based on a fixed-end condition in the HBE, both for frame-type flexure and for web-plate tension. For frame-type flexure, the moment corresponding to the required VBE flexural strength at the level above is used so that the inflection point can be at least at column mid-height. The moment due to web-plate tension is simply the fixed-end moment.

$$M_u = M_{VBE(HBE)} + M_{VBE(web)} \quad (5\text{–}86)$$

$$M_{VBE(web)} = R_y F_y \sin^2(\alpha) t_w \left(\frac{h_c^2}{12} \right)$$

$$M_u = 4{,}440 \text{ kip-in.} + 14{,}500 \text{ kip-in.} = 18{,}900 \text{ kip-in.}$$

Although not required by AISC 341, it is preferable that a strong-column/weak-beam condition be maintained here.

$$(F_y - P/A)\, Z_{(VBE)} < 1.1\, R_y\, F_y\, Z_{(HBE)} \quad (5\text{–}87)$$

$$Z_{(HBE)} \le (F_y - P/A)\, Z_{(VBE)} / 1.1\, R_y\, F_y = 621 \text{ in.}^3$$

A W30×108 will be used. Note that the RBS will not be used at this level, since the rotational demand is small. The moment at the hinge is

$$M_u' = M_u\, L_{cf} / L \quad (5\text{–}88)$$

$$L_{cf} = L - 2\,[\tfrac{1}{2}\, d_c + \tfrac{1}{2}\, d_{bc}] \quad (5\text{–}89)$$

$$= 240 \text{ in.} - [21.6 \text{ in.} + 29.8 \text{ in.}]$$

$$= 189 \text{ in.}$$

$$M_u = 18{,}900 \text{ kip-in. } (189 \text{ in.}/240 \text{ in.})$$

$$= 14{,}900 \text{ kip-in.}$$

$$\phi M_n = \phi F_y Z_x \quad (5\text{–}90)$$

$$= 0.90(50 \text{ ksi})(346 \text{ in.}^3)$$

$$= 15{,}600 \text{ kip-in.}$$

$$\phi M_n > M_u \quad \textbf{o.k.}$$

The required shear strength is computed the same as for the VBE at the eighth floor:

$$V_{VBE} = V_{VBE(HBE)} + V_{VBE(web)} \quad (5\text{–}91)$$

$$V_{VBE(HBE)} = \left[\left(1.1\, R_y F_y Z_{(HBE)}\right) + \left(\frac{1}{2} \sum M_{pb}^* \right) \right] / h_c$$

where

ϕM_{pb}^* = the moments at the column centerline at the second floor due to HBE hinging

= 83.0 kips + 428 kips

= 511 kips

The shear and flexure are resisted by connection to the steel grade beam connecting the two VBE at the base.

In order to reduce the required flexural strength due to web-plate tension, the beam will be connected to a pile at mid-span, thus reducing the span to ten feet. Note that the flexure in the HBE caused by tension in the web plate is not additive with the flexure due to web-plate tension on the VBE transmitted to the HBE.

The tension in the VBE is resisted by twelve 2¼-in. ASTM F1554 Grade 105 anchors, which will transfer the tension into the pile cap.

Chapter 6

Design of Openings

6.1. OVERVIEW

Openings are often required in SPW and SPSW. Where SPW or SPSW are used in the building core, openings often must be provided to allow entry to stairs or elevators, or for the passage of ducts. This chapter provides a general treatment of the design of openings in the web plate of SPSW. A design example is included to illustrate the procedure.

AISC 341 requires that HBE and VBE be provided around openings to anchor the web-plate tension unless testing has been performed to justify use of unreinforced openings. See Chapter 2 for a description of testing of a SPSW with unreinforced perforations by Vian and Bruneau (2005). These special HBE and VBE are termed Local Boundary Elements (LBE) here. Vertical LBE are required to extend the full story height from HBE to HBE, and horizontal LBE are required to extend the full bay width from VBE to VBE. These horizontal LBE thus reduce the required moment of inertia, and required flexural strength due to web-plate tension of the VBE.

The internal forces in the LBE can be complicated to compute. Each LBE imposes reactions on adjoining LBE due to the loading caused by the diagonal tension in the web plate. Additionally, the VBE impose reactions on the horizontal LBE, which act as horizontal struts. Where vertical LBE occur at every level, they may also act as struts. Such LBE should be designed to meet the criteria for struts described in Chapter 3, in addition to the requirements given in this chapter. The local overturning at the opening creates forces on the HBE above and below the opening. Figure 6–1 shows some of these effects diagrammatically. Note that complete free-body-diagrams would require also showing the moments at the end of each member. These have been omitted in Figure 6–1 for clarity.

This chapter illustrates the design of an opening in the SPSW of Chapter 5. The same process can be used with the SPW of Chapter 4 with σ used in place of $R_y F_y$.

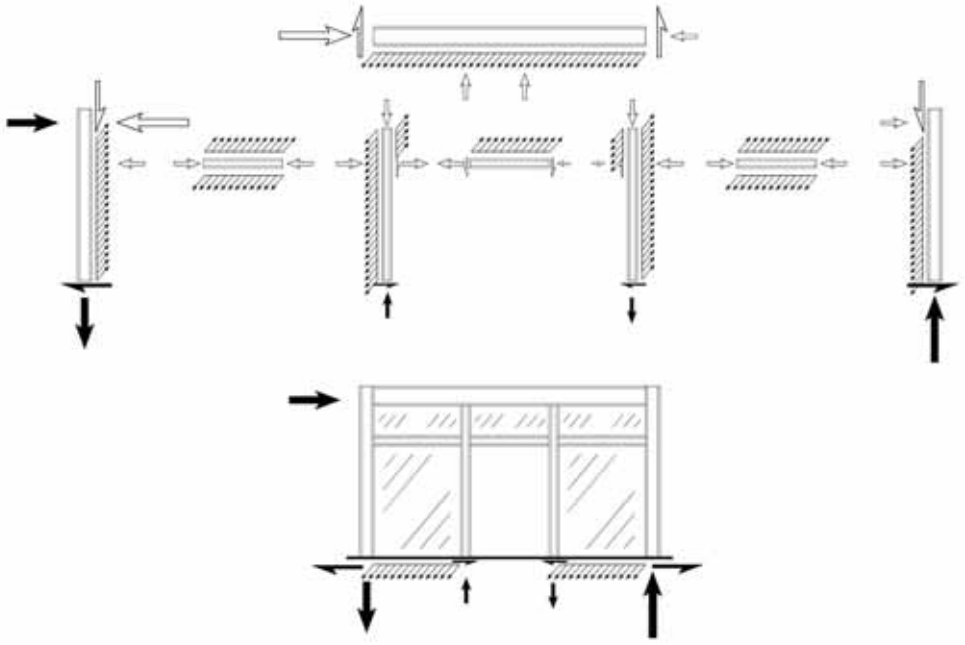

Fig. 6–1. SPSW with opening (moments at ends of HBE, VBE, and LBE not shown for clarity).

6.2. DESIGN PROCEDURE

The design of SPSW with openings is similar to the typical design of SPSW (that is, the design of SPSW without openings). Web plates are sized to provide the required strength, and the forces on boundary elements are computed based on the web-plate strength and the computed angle of tension stress, α. A preliminary design may be performed with an assumed angle of tension stress, followed by a final design with the angle calculated using the actual sizes of the boundary elements.

Typically, a design will have already been performed of the SPSW without openings. The introduction of openings and LBE will not require redesign of VBE, although reductions in VBE flexural forces may permit use of a smaller section. HBE above and below the opening must be redesigned, however, due to the local overturning demands, and the web plate must be redesigned due to the reduced horizontal length, as well as a possible significant change to the angle of tension stress. Where the design is governed by drift, the introduction of large openings should be included in the analysis in which drift is calculated.

Push-over analysis can be useful in the determination of forces on the LBE. The push-over analysis of a SPSW is essentially the same with and without openings. In this chapter, capacity-design methods are developed and presented.

6.2.1. Preliminary Design

The preliminary design involves selecting web plates for strength and estimating the required strength of the LBE based on the expected strength of each of the web-plate panels.

At horizontal sections of SPSW with openings, the web plates on either side of the opening must be thicker than would otherwise be required in order to provide a strength and stiffness equivalent to that of a solid panel without openings for resisting shear in the SPSW. Typically, providing the same total area of web plate will result in similar strength and stiffness. Where the resulting panels are of slender proportions, this may not be the case. At sections of the SPSW at the same floor level immediately above and below the opening, web plates are provided that are thinner than those on either side of the opening (i.e., the web plates are the same thickness as would be provided if there were no opening).

Figure 6–2 shows a SPSW panel with an opening. Web plate panels are numbered in the figure, and segments of the LBE are given letter designations. Four types of LBE are designated; the forces acting on the others are similar, as discussed below. Equations corresponding to this configuration also may be used for door-type openings as shown in Figure 6–1, where panels 6, 7, and 8 in Figure 6–2 do not exist and panels 4 and 5 extend to the HBE below.

If the required thickness of the web plate without an opening is t_1, at the level of the opening (web plates 4 and 5 in Figure 6–2), the web plates provided are of thickness t_2:

$$t_2 = t_1\left(\frac{L_{cf}}{L_1 + L_3}\right) \qquad (6\text{–}1)$$

A web plate with the smallest thickness satisfying this criterion should be used. Said another way, a discontinuity in web-plate strength should be avoided. This proportioning will lead to a more even distribution of tension yielding in the panels. Note that the increased thickness of the web plates across the section with the opening will tend to offset the effect of the opening on drift.

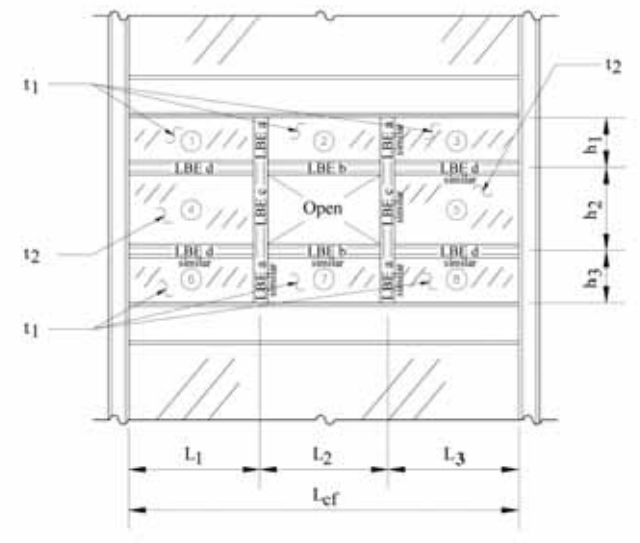

Fig. 6–2. SPSW with opening.

6.2.2. Determination of Forces on Local Boundary Elements

LBE are provided around the opening to permit the web plates to yield in tension. These boundary elements are designed for the forces corresponding to web-plate tension yielding. In the preliminary design of SPSW, the stiffness criterion of AISC 341 Section 17.4g is used to obtain a preliminary VBE design. In the case of the design of LBE at openings, the spans may be very small, in which case the stiffness criterion is likely trivial, and the preliminary design is typically based on required strength. The stiffness of the vertical and horizonal LBE should meet the required moment of inertia for boundary elements given in Chapter 3. This may control the design for larger openings. As is the case for SPSW without openings, struts may be used to tie LBE to the VBE and

HBE in order to reduce the required moment of inertia (and required flexural strength) of the LBE.

As the boundary elements have not been sized, an assumption must be made for preliminary design concerning the angle of tension stress in each portion. For simplicity, the angle can be assumed as 45° in every web plate for preliminary design.

Based on this assumption, the preliminary design forces on the LBE are computed. The shear force per unit length on the interfaces with boundary elements is

$$v_u = \frac{1}{2} R_y F_y \sin(2 \times 45^\circ) t_w = \frac{1}{2} R_y F_y t_w \quad (6\text{–}2)$$

This force acts as a distributed axial load in the LBE.

The distributed transverse force acting on the LBE is

$$w_u = R_y F_y \sin^2(45^\circ) t_w = \frac{1}{2} R_y F_y t_w \quad (6\text{–}3)$$

The LBE also impose reactions on each other. In addition, the VBE of SPSW react against the horizontal LBE. Figure 6–3 shows the free-body diagrams for the LBE for the forces due to web-plate tension acting directly on them; additional forces due to the reactions of adjoining LBE are not shown. The loading is shown pushing the wall to the right. For simplicity, the opening is taken as symmetrical in the bay (L_3 = L_1), and thus there are only four types of LBE ("a," "b," "c," and "d" as labeled in Figure 6–3). Each of the top four diagrams ("a," "b," "c," and "d") shows the distributed load on the corresponding LBE and how it is resisted in the SPSW. Diagram "e" shows the distributed loading on the VBE. Diagram "f" shows the designations for web plates and LBE, as well as their dimensions.

LBE "a" typically serves only to transmit axial force to the HBE above and below the level with the opening. Distributed loading from the adjoining web plates on each side counterbalances, and there is no net loading due to web-plate tension in the fully yielded condition.

LBE "b" has significant transverse and axial distributed loading because a web plate is present on only one side. The transverse load becomes tension in LBE "c," while the axial load is dragged through to LBE "d," where all of it is typically resisted by web plates 4 and 5.

LBE "c" likewise has significant transverse and axial distributed loading because a web plate is present on only one side. The transverse load becomes compression in LBE "d." The axial load is transmitted to LBE "a," which deliver it to the HBE above and below.

LBE "d" has significant transverse and axial distributed loading because web plates of different thickness are present above and below. The net transverse load is resisted by compression in LBE "c" and the VBE. The net axial load is the counterbalancing force for the axial force developed in LBE "b." Where these two forces are not equal, the difference acts as an applied force on the VBE.

The VBE has significant transverse and axial distributed loading as well. The transverse loading is resisted by LBE "d," as well as by the HBE. A portion of it counterbalances the transverse force in LBE "c;" the remainder must be transmitted to LBE "b." The axial force is transmitted to the VBE below.

From Figure 6–3, it is clear that each LBE is subjected to forces from multiple panels. The following equations give the shear and transverse loads on each of the four types of LBE, and the resulting internal forces and reactions. Dimensions and thicknesses are as shown in Figure 6–2. For simplicity, the depths of LBE are neglected in the equations. This is reasonable, as long as the LBE web is at least as strong as the adjoining plate, and the vertical LBE are assumed not to participate in resisting any of the story shear.

LBE "a"

The distributed transverse load is

$$w_u = 0$$

The distributed axial load is

$$v_u = 0$$

The shear reaction is

$$V_u = 0$$

The moment is

$$M_u = 0$$

The axial compression force is the reaction from LBE "c:"

$$N_u = \frac{1}{4} R_y F_y t_2 h_2 \quad (6\text{–}4)$$

Note that two of the LBE labeled "a" are in tension.

In the out-of-plane direction, it is recommended that the vertical members (the continuous members comprising LBE "a" at each end and LBE "c" in the middle) be designed to meet the stiffness criterion for stiffeners discussed in Chapter 3 (Equation 3–7). For this member the required out-of-plane moment of inertia is

$$I \geq L_1 t_2^3 j \quad (6\text{–}5)$$

where

$$j = 2.5(\Sigma h/L_1)^2 - 2 \geq 0.5$$

where

$$\Sigma h = h_1 + h_2 + h_3$$

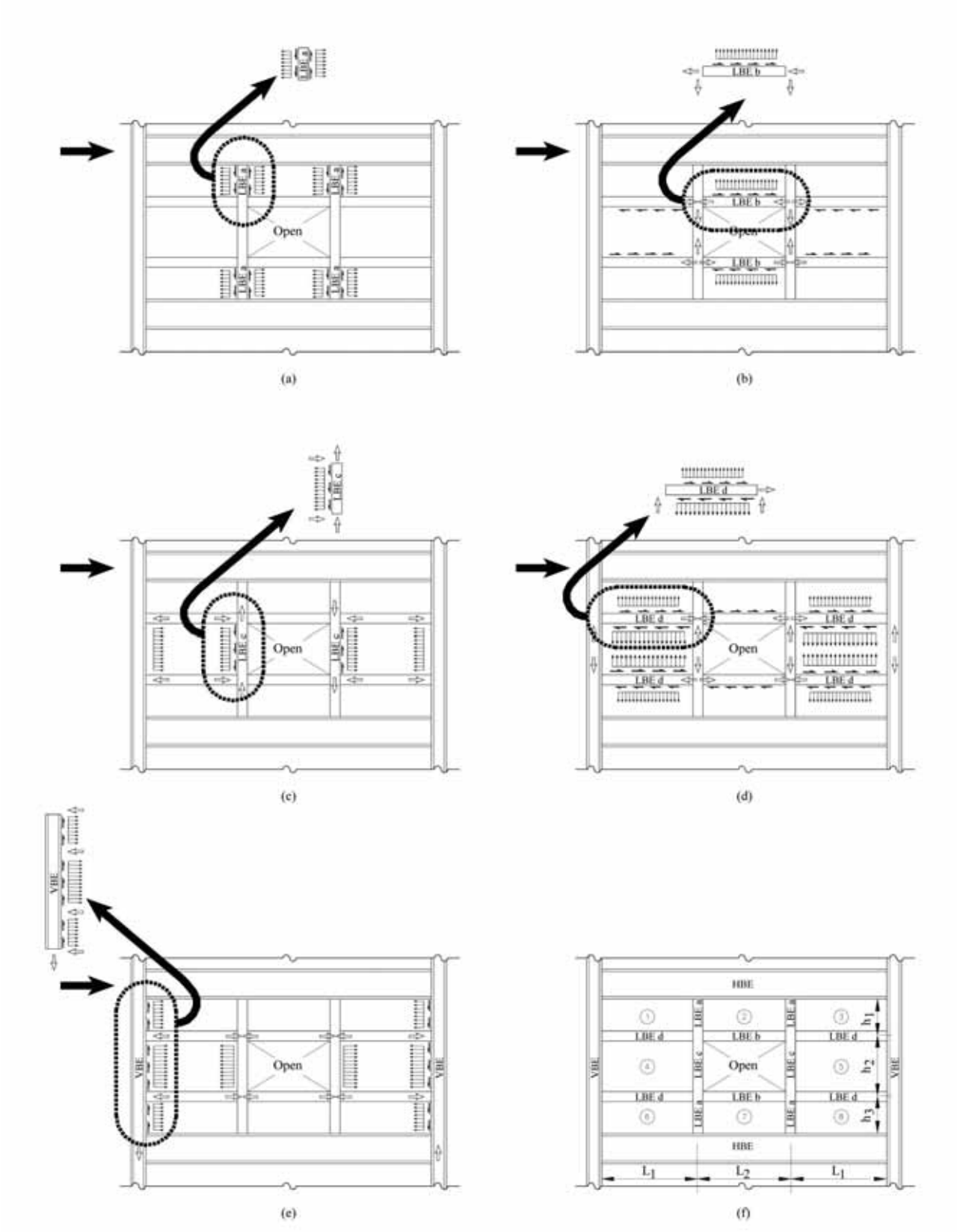

Fig. 6–3. Forces acting on boundary elements in SPSW with opening.

LBE "b"

The distributed transverse load is

$$w_u = \frac{1}{2} R_y F_y t_1 \tag{6–6}$$

The distributed axial load is

$$v_u = \frac{1}{2} R_y F_y t_1 \tag{6–7}$$

The shear reaction is

$$V_u = w_u L_2/2 \tag{6–8}$$

The simple-span moment is

$$M_u = w_u L_2^2/8 \tag{6–9}$$

Alternatively, rigid connections may be used, thus reducing this moment to $w_u L_2^2/12$.

The axial force at the left end is

$$N_{u\,L} = \frac{1}{4} R_y F_y \left[t_1 L_2 - t_1 h_1\right] \tag{6–10}$$

This connection may be in tension or compression. For the LBE d on the right side (between panels 3 and 5), the two terms are additive and the connection is in compression. The axial compression at the right end is

$$N_{u\,R} = \frac{1}{4} R_y F_y \left[t_1 L_2 + t_1 h_1\right] \tag{6–11}$$

The required moment of inertia for a simple span[1] is

$$I \geq 0.01 \left(\frac{t_1 L_2^{\,4}}{h_1} \right) \tag{6–12}$$

Note that, if the member has rigid end connections, the coefficient may be reduced to 0.00307.

LBE "c"

The distributed transverse load is

$$w_u = \frac{1}{2} R_y F_y t_2 \tag{6–13}$$

The distributed axial load is

$$v_u = \frac{1}{2} R_y F_y t_2 \tag{6–14}$$

The shear reaction is

$$V_u = w_u h_2/2 \tag{6–15}$$

The fixed-end moment (the vertical LBE is continuous) is

$$M_u = w_u h_2^2/12 \tag{6–16}$$

The axial force at the top is

$$N_{u\,top} = \frac{1}{4} R_y F_y \left[t_1 \left(L_2 + L_1\right) - t_2 \left(h_2 + L_1\right)\right] \tag{6–17}$$

The axial force at the bottom is

$$N_{u\,bot} = \frac{1}{4} R_y F_y \left[t_1 \left(L_2 + L_1\right) + t_2 \left(h_2 - L_1\right)\right] \tag{6–18}$$

The required moment of inertia is

$$I \geq 0.00307 \left(\frac{t_2 h_2^{\,4}}{L_1} \right) \tag{6–19}$$

LBE "d"

The distributed transverse load is

$$w_u = \frac{1}{2} R_y F_y \left(t_2 - t_1\right) \tag{6–20}$$

The distributed axial load is

$$v_u = \frac{1}{2} R_y F_y \left(t_2 - t_1\right) \tag{6–21}$$

The shear reaction is

$$V_u = w_u L_1/2 \tag{6–22}$$

The simple-span moment is

$$M_u = w_u L_1^2/8 \tag{6–23}$$

Alternatively, rigid connections may be used, thus reducing this moment to $w_u L_2^2/12$.

The axial compression force at the right end is

$$N_{u\,R} = \frac{1}{4} R_y F_y \left[t_1 \left(h_1 - L_2\right) + t_2 h_2\right] \tag{6–24}$$

For the similar member on the right side of SPSW (between panels 3 and 5), all three terms are positive.

$$N_{u\,sim} = \frac{1}{4} R_y F_y \left[t_1 \left(h_1 + L_2\right) + t_2 h_2\right] \tag{6–25}$$

The axial compression force at the left end is

$$N_{u\,L} = \frac{1}{4} R_y F_y \left[t_1 \left(h_1 - 2L_1 - L_2\right) + t_2 \left(h_2 + 2L_1\right)\right] \tag{6–26}$$

[1]The coefficient 0.01 is extrapolated from the requirement of AISC 341 Section 17.4g, which corresponds to a VBE that is continuous from story to story.

This reaction is mainly due to the VBE being pulled in by the web plate. Where the horizontal area of the thicker web plates ($2t_2L_1$) do not match the area of the thinner web plates (t_1 [$2L_1$+ L_2]), this reaction will also include some additional shear that the VBE must resist at the elevation of the weaker section of the wall.

The required in-plane moment of inertia for a simple span is based on the difference between web-plate thicknesses:

$$I \geq 0.01\left(\frac{(t_2 - t_1)L_1^4}{h_2}\right) \tag{6–27}$$

Note that, if the member has rigid end connections, the coefficient may be reduced to 0.00307.

In the out-of-plane direction, it is recommended that LBE "d" be designed to meet the stiffness criterion for stiffeners discussed in Chapter 3 (Equation 3–7):

$$I \geq h_2 t_2^3 j \tag{6–28}$$

where

$$j = 2.5(L_1/h_2)^2 - 2 \geq 0.5$$

It is recommended that similar (or identical) sections be used for LBE "b" and "d."

6.2.3. Final Design

For final design, the angle of tension stress is computed for each panel, and a more exact calculation is made of the forces on the local boundary elements.

The angle of tension stress is calculated using Equation 3–1:

$$\tan^4 \alpha = \frac{1 + \dfrac{t_w L}{2A_c}}{1 + t_w h\left[\dfrac{1}{A_b} + \dfrac{h^3}{360 I_c L}\right]} \tag{6–29}$$

where

h = distance between horizontal member centerlines

A_b = average cross-sectional area of the horizontal members bounding the panel

A_c = average cross-sectional area of a vertical members bounding the panel

I_c = average moment of inertia of the vertical members bounding the panel taken perpendicular to the direction of the web-plate line

L = distance between vertical member centerlines

t_w = thickness of the web plate

The LBE are typically much smaller than the VBE and HBE. For purposes of calculating the angle of stress, average values of the section properties are used.

For panel 2, the vertical LBE bounding the plate are stiffened by the presence of adjacent web plates (in panels 1 and 3), and thus the moment of inertia of LBE "a" is not relevant. Additionally, the flexibility of LBE "b" may affect the angle of tension stress. For panels 1 and 2, the moment of inertia of LBE "a" is effectively increased by the adjacent web plate (in panel 2). Thus, for panels 1, 2, and 3, the applicability of Equation 6–29 is compromised. The same applies to panels 6, 7, and 8. Designers may choose to calculate the angle based on a single panel encompassing the three (ignoring the presence of the two LBE "a"). For this purpose, the panel proportion limits of AISC 341 Section 17.2b should not be applied. Designers may also wish to adapt Equation 6–29 to reflect the increased effective column stiffness. In that case, use of an average angle of stress for the three panels is recommended.

If the calculated angle is within 5° of the assumed value (45°) for every panel, the recalculation of LBE forces will not yield significantly different results. If the angles are significantly different, the following equations can be used to check the designs of the LBE:

LBE "a"

The distributed transverse load is

$$w_u = R_y F_y t_1[\sin^2(\alpha_1) - \sin^2(\alpha_2)] \tag{6–30}$$

$$= 0 \text{ for } \alpha_1 = \alpha_2$$

where

α_i = the angle of web-plate tension stress calculated of web plate i

The distributed axial load is

$$v_u = \frac{1}{2} R_y F_y t_1 \left[\sin(2\alpha_1) - \sin(2\alpha_2)\right] \tag{6–31}$$
$$= 0 \text{ for } \alpha_1 = \alpha_2$$

In most cases, these forces w_u and v_u are negligible; they are zero for cases when the average angle is used for the bounding panels. The shear reaction is

$$V_u = w_u h_1/2 \tag{6–32}$$

$$= 0 \text{ for } \alpha_1 = \alpha_2$$

The moment (assuming simple connections) is

$$M_u = w_u h_1^2/8 \tag{6–33}$$

$$= 0 \text{ for } \alpha_1 = \alpha_2$$

The axial compression force at the top is

$$N_{u\ top} = \frac{1}{4} R_y F_y \left[t_1 h_1 \left(\sin(2\alpha_2) - \sin(2\alpha_1) \right) + t_2 h_2 \right] \quad (6\text{–}34)$$
$$= \frac{1}{4} R_y F_y t_2 h_2 \text{ for } \alpha_1 = \alpha_2$$

The axial compression force at the bottom is

$$N_{u\ bot} = \frac{1}{4} R_y F_y \left[t_1 h_1 \left(\sin(2\alpha_1) - \sin(2\alpha_2) \right) + t_2 h_2 \right] \quad (6\text{–}35)$$
$$= \frac{1}{4} R_y F_y t_2 h_2 \text{ for } \alpha_1 = \alpha_2$$

LBE "b"

The distributed transverse load is

$$w_u = R_y F_y t_1 \cos^2(\alpha_2) \quad (6\text{–}36)$$

The distributed axial load is

$$v_u = \frac{1}{2} R_y F_y t_1 \sin\left(2\alpha_2\right) \quad (6\text{–}37)$$

The shear reaction is

$$V_u = w_u L_2/2 \quad (6\text{–}38)$$

The moment (assuming simple connections) is

$$M_u = w_u L_2^2/8 \quad (6\text{–}39)$$

The axial force at the ends is

$$N_u = V_{u(a)} \pm \frac{1}{2} v_u L_2 + \frac{1}{4} R_y F_y t_1 h_1 \sin^2\left(\alpha_1\right) \quad (6\text{–}40)$$

The connection at the left is in tension and the connection at the right is in compression.

The required moment of inertia is the same as was calculated in the preliminary design.

LBE "c"

The distributed transverse load is

$$w_u = R_y F_y t_2 \sin^2(\alpha_4) \quad (6\text{–}41)$$

The distributed axial load is

$$v_u = \frac{1}{2} R_y F_y t_2 \sin\left(2\alpha_4\right) \quad (6\text{–}42)$$

The shear reaction is

$$V_u = w_u h_2/2 \quad (6\text{–}43)$$

The moment (assuming fixed connections) is

$$M_u = w_u h_2^2/12 \quad (6\text{–}44)$$

The axial force at the ends is

$$N_u = V_{u(d)} - V_{u(b)} \pm \frac{1}{2} v_u h_2 \quad (6\text{–}45)$$

The required moment of inertia is the same as was calculated in the preliminary design.

LBE "d"

The distributed transverse load is

$$w_u = R_y F_y \left[t_2 \cos^2(\alpha_4) - t_1 \cos^2(\alpha_1) \right] \quad (6\text{–}46)$$

The distributed axial load is

$$v_u = \frac{1}{2} R_y F_y \left[t_2 \sin\left(2\alpha_4\right) - t_1 \sin\left(2\alpha_1\right) \right] \quad (6\text{–}47)$$

The shear reaction is

$$V_u = w_u L_1/2 \quad (6\text{–}48)$$

The moment (assuming simple connections) is

$$M_u = w_u L_1^2/8 \quad (6\text{–}49)$$

The axial compression force at the right end is

$$N_{u\,R} = \frac{1}{2} R_y F_y \left[\begin{array}{l} t_1 h_1 \sin^2\left(\alpha_1\right) \\ + t_2 h_2 \sin^2\left(\alpha_4\right) - \frac{1}{2} t_2 L_2 \sin\left(2\alpha_4\right) \end{array} \right] \quad (6\text{–}50)$$

The axial compression force at the left end is

$$N_{u\,L} = N_{u\,R} - v_u L_1 \quad (6\text{–}51)$$

Where the angle of tension stress α does not range more than 10°, the average value of α may be used in the design of the LBE without significant loss of accuracy. This will simplify the calculations considerably.

The horizontal LBE are normally designed as individual members supported out-of-plane by the vertical LBE, a single member composed of LBE "a" at the top, LBE "c" in the center, and LBE "a" (similar) at the bottom. This vertical LBE is then designed with an unbraced length of the clear height of the story between HBE.[2] Furthermore, the vertical LBE must be designed to provide adequate bracing for compression forces in the horizontal HBE per Appendix 6 of AISC 360.

This condition qualifies as "nodal bracing." The required strength for nodal bracing of a column is given by AISC 360 Equation A–6–3:

$$P_{br} = 0.01 P_u \quad (6\text{–}52)$$

[2]Under some conditions, such as a tall story in a short SPSW bay, it is advantageous to have the horizontal LBE be continuous instead.

The required stiffness for nodal bracing of a column is given by AISC 360 Equation A–6–4:

$$\beta_{br} = \frac{10.7 P_u}{L_b} \tag{6–53}$$

The maximum compression force is in LBE "d" between panels 3 and 5, due to the combination of the shear from panel 2 being dragged to panel 5 and the vertical LBE and the VBE on either side of panels 3 and 5 imposing their reactions from the transverse (horizontal) component of the web-plate tension. The required bracing force and stiffness is thus calculated using this force:

$$P_u = N_{u(d)} \tag{6–54}$$
$$= \frac{1}{2} R_y F_y \begin{bmatrix} t_1 h_1 \sin^2(\alpha_1) \\ + t_2 h_2 \sin^2(\alpha_4) + \frac{1}{2} t_2 L_2 \sin(2\alpha_4) \end{bmatrix}$$

The vertical LBE is designed with this force applied in the out-of-plane direction at the points of connection with the horizontal LBE.[3] Out-of-plane stiffness must be compared to the required stiffness of AISC 360 Equation A–6–4 (Equation 6–53). This requirement may govern over that of Equation 6–5.

While the above bracing requirements also apply to the VBE, they are trivial for VBE in most if not all cases.

6.2.4. Web-Plate Shear Strength

The shear strength of the SPSW with the opening should be verified. The available shear strength, $\phi_v V_n$ (LRFD) or V_n/Ω_v (ASD), is determined using the nominal strength and ϕ_v = 0.90 or Ω_v = 1.67.

Above the opening, the nominal shear strength is

$$V_n = 0.42 F_y t_1 [2L_1 \sin(2\alpha_1) + L_2 \sin(2\alpha_2)] \tag{6–55}$$
$$= 0.42 F_y t_1 [2L_1 + L_2] \sin(2\alpha_1) \text{ for } \alpha_1 = \alpha_2$$

At the level of the opening, the nominal shear strength is

$$V_n = 0.42 F_y t_2 [2L_1 \sin(2\alpha_4)] \tag{6–56}$$

Below the opening, the nominal shear strength is

$$V_n = 0.42 F_y t_1 [2L_1 \sin(2\alpha_6) + L_2 \sin(2\alpha_7)] \tag{6–57}$$
$$= 0.42 F_y t_1 [2L_1 + L_2] \sin(2\alpha_6) \text{ for } \alpha_6 = \alpha_7$$

Note that the equations above assume a symmetrical placement of the opening ($L_3 = L_1$). For asymmetric openings, the shear strength equations can be modified by using $L_1 + L_3$ in lieu of the term $2L_1$.

The available shear strength must be at least as large as the required shear strength of the SPSW in the analysis. Additionally, to minimize the shear strength required of the VBE, the nominal shear strengths should be approximately equal. It is not recommended to use the same thickness for all panels of the SPSW at the floor level of the opening, as yielding would then be concentrated in the two panels adjacent to the opening, creating larger ductility demands on those panels and additional shear demands on the VBE.

6.2.5. Design of VBE

The VBE at the level of the opening can be redesigned considering the decreased height between horizontal members for flexure due to web-plate tension [as shown in Figure 6–3(f)]. This has the effect of drastically reducing the required moment of inertia based on AISC 341 Section 17.4g. It also reduces the moment due to the transverse loading from the web plate in tension.

Where the openings are not repeated at every level, this redesign need not be performed, as the required VBE section will be governed by other levels. Indeed, the VBE size in this case will usually be dictated by the demands at other levels in the tier.

Where a large additional shear is imposed on the VBE, the VBE should be checked for connection limit states as well as shear and bending.

6.2.6. Design of HBE

The overturning of the panels around the opening is resisted by the HBE above and below the opening. The reactions from members LBE "a" create a couple on each HBE, adding to the required flexural strength, as is shown in Figure 6–4.

The moment caused by this couple is

$$M_u = N_{u(a)} L_1 L_2 / L_{cf} \tag{6–58}$$

where

$N_{u(a)}$ = the reaction on the HBE from LBE "a"

This moment is added to the moment calculated based on the web plate tension above and below the HBE and any frame flexural moment. See Chapter 3 for the computation of these other sources of moment.

---

[3]Applying this maximum force at two locations overestimates the effect slightly. It is legitimate to apply a lower force at one of the locations:

$$P_u = \frac{1}{2} R_y F_y \left[t_1 h_3 \sin^2(\alpha_6) + t_2 h_2 \sin^2(\alpha_4) - \frac{1}{2} t_2 L_2 \sin(2\alpha_4) \right]$$

6.3. DESIGN EXAMPLE

The procedure described above will be applied to an opening in a SPSW. The bay dimension and story height are similar to those for the seventh floor in Chapter 5.

$$L_{cf} = 223 \text{ in.}$$

$$h_c = 129 \text{ in.}$$

It is assumed that the web plate has been designed for strength without an opening. The one-story-high by one-story-wide panel will be redesigned for a window opening symmetrically placed in the center.

The original web plate design is a 0.125-in.-thick ASTM A36 plate. Figure 6–5 shows the design, including the sizes of the web plates above and below the story under consideration.

An opening with L_2 = 80 in. and h_2 = 72 in. will be introduced into this web plate. Thus, $L_1 = L_3$ = 71.5 in. and $h_1 = h_3$ = 28.5 in. Roughly one-third of the horizontal web plate length is thus removed by the opening.

$$0.125 \text{ in. } [223 \text{ in.}/(223 \text{ in.} - 80 \text{ in.})] = 0.195 \text{ in.}$$

Therefore, instead of the 0.125-in. web plate, web plates 0.1875 in. thick will be used on either side of the opening.

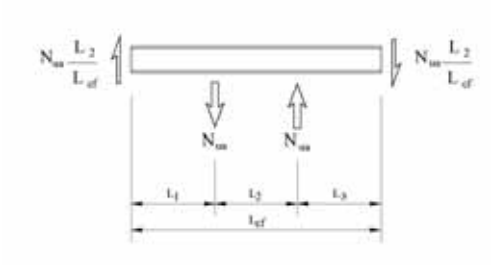

Fig. 6–4. Forces from LBE on HBE above opening (similar on HBE below opening).

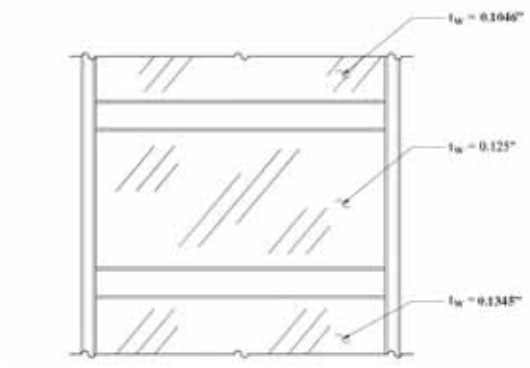

Fig. 6–5. SPSW panel without opening.

Above and below the level of the opening, the 0.125 in. thickness originally designed will be used. In this way, the panel have similar demand-capacity ratios and yielding of all of the individual web plates will be promoted without placing large shear demands on the VBE.

Local boundary elements will be provided extending from HBE to HBE and from VBE to VBE, as required by Section 17.2c of AISC 341. Figure 6–6 shows the modified panel with the opening and web-plate thickness.

A preliminary design of the SPSW is performed using the procedures described in this chapter. Required strengths of the LBE are calculated based on the web-plate expected yield stress.

LBE "a"

The distributed transverse load is

$$w_u = 0$$

The distributed axial load is

$$v_u = 0$$

The shear reaction is

$$V_u = 0$$

The moment is

$$M_u = 0$$

The axial compression force is the reaction from LBE "c:"

$$N_u = \frac{1}{4} R_y F_y t_2 h_2$$
$$= \frac{1}{4}(1.3)(36 \text{ ksi})(0.1875 \text{ in.})(72 \text{ in.})$$
$$= 158 \text{ kips}$$

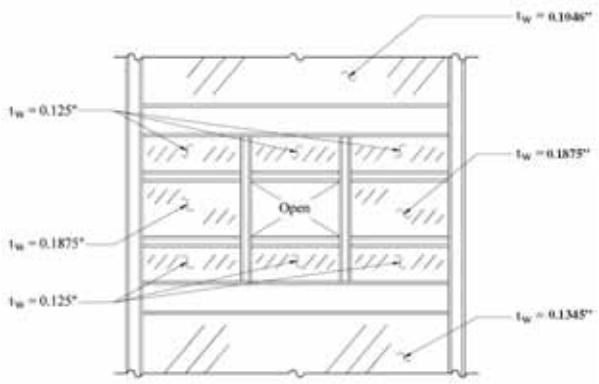

Fig. 6–6. SPSW panel with opening.

The required out-of-plane moment of inertia is

$$I \geq L_1 t_2^3 j$$

$$j = 2.5(\Sigma h/L_1)^2 - 2 \geq 0.5$$

$$\Sigma h = h_1 + h_2 + h_3 = 129 \text{ in.}$$

$$j = 2.5(129 \text{ in.}/72 \text{ in.})^2 - 2 = 6.03$$

$$I \geq (71.5 \text{ in.})(0.1875 \text{ in.})^3(6.03)$$

$$\geq 2.84 \text{ in.}^4$$

LBE "b"

The distributed transverse load is

$$w_u = \frac{1}{2} R_y F_y t_1$$
$$= \frac{1}{2}(1.3)(36 \text{ ksi})(0.125 \text{ in.})$$
$$= 2.93 \text{ kips/in.}$$

The distributed axial load is

$$v_u = \frac{1}{2} R_y F_y t_1$$
$$= \frac{1}{2}(1.3)(36 \text{ ksi})(0.125 \text{ in.})$$
$$= 2.93 \text{ kips/in.}$$

The shear reaction is

$$V_u = w_u L_2/2$$

$$= (2.93 \text{ kips/in.})(80 \text{ in.})/2$$

$$= 117 \text{ kips}$$

The required in-plane moment of inertia for pinned ends is

$$I \geq 0.01\left(\frac{t_1 L_2^{\,4}}{h_1}\right)$$
$$= 0.01(0.125 \text{ in.})(80 \text{ in.})^4/(28.5 \text{ in.})$$
$$= 1{,}800 \text{ in.}^4$$

The required in-plane moment of inertia for fixed ends is

$$I \geq 0.00307\left(\frac{t_1 L_2^{\,4}}{h_1}\right)$$
$$= 0.00307(0.125 \text{ in.})(80 \text{ in.})^4/(28.5 \text{ in.})$$
$$= 552 \text{ in.}^4$$

Fixed ends will be used. The moment is

$$M_u = w_u L_2^2/12$$

$$= (2.93 \text{ kip/in.})(80 \text{ in.})^2/12$$

$$= 1{,}560 \text{ kip-in.}$$

The axial force at the left end is

$$N_{u\,L} = \frac{1}{4} R_y F_y \left[t_1 L_2 - t_1 h_1\right]$$
$$= \frac{1}{4}(1.3)(36 \text{ ksi})(0.125 \text{ in.})(80 \text{ in.} - 28.5 \text{ in.})$$
$$= 75.3 \text{ kips}$$

The axial compression at the right end is

$$N_{u\,R} = \frac{1}{4} R_y F_y \left[t_1 L_2 + t_1 h_1\right]$$
$$= \frac{1}{4}(1.3)(36 \text{ ksi})(0.125 \text{ in.})(80 \text{ in.} + 28.5 \text{ in.})$$
$$= 159 \text{ kips}$$

LBE "c"

The distributed transverse load is

$$w_u = \frac{1}{2} R_y F_y t_2$$
$$= \frac{1}{2}(1.3)(36 \text{ ksi})(0.1875 \text{ in.})$$
$$= 4.39 \text{ kips/in.}$$

The distributed axial load is

$$v_u = \frac{1}{2} R_y F_y t_2$$
$$= \frac{1}{2}(1.3)(36 \text{ ksi})(0.1875 \text{ in.})$$
$$= 4.39 \text{ kips/in.}$$

The shear reaction is

$$V_u = w_u h_2/2$$

$$= (4.39 \text{ kips/in.})(72 \text{ in.})/2$$

$$= 158 \text{ kips}$$

The fixed-end moment is

$$M_u = w_u h_2^2/12$$

$$= (4.39 \text{ kips/in.})(72 \text{ in.})^2/12$$

$$= 1{,}900 \text{ kip-in.}$$

Table 6–1. Calculated Angles of Stress		
Panel Designation	**Panel Thickness (in.)**	**Angles of stress α (°)**
1	0.125	44.7
2	0.125	45.2
3	0.125	44.7
4	0.1875	42.7
5	0.1875	42.7
6	0.125	45.0
7	0.125	45.7
8	0.125	45.0

The axial force at the top is

$$N_{u\ top} = \frac{1}{4} R_y F_y \left[t_1 \left(L_2 + L_1 \right) - t_2 \left(h_2 + L_1 \right) \right]$$
$$= \frac{1}{4}(1.3)(36\text{ ksi}) \begin{bmatrix} (0.125\text{ in.})(80\text{ in.} + 71.5\text{ in.}) \\ -(0.1875\text{ in.})(72\text{ in.} + 71.5\text{ in.}) \end{bmatrix}$$
$$= -93.2 \text{ kips (the minus sign signifies tension)}$$

The axial force at the bottom is

$$N_{u\ bot} = \frac{1}{4} R_y F_y \left[t_1 \left(L_2 + L_1 \right) + t_2 \left(h_2 - L_1 \right) \right]$$
$$= \frac{1}{4}(1.3)(36\text{ ksi}) \begin{bmatrix} (0.125\text{ in.})(80\text{ in.} + 71.5\text{ in.}) \\ +(0.1875\text{ in.})(72\text{ in.} - 71.5\text{ in.}) \end{bmatrix}$$
$$= 223 \text{ kips (compression)}$$

The required moment of inertia is

$$I \geq 0.00307 \left(\frac{t_2 {h_2}^4}{L_1} \right)$$
$$= 0.00307(0.1875\text{ in.})(72\text{ in.})^4 / (71.5\text{ in.})$$
$$= 216\text{ in.}^4$$

LBE "d"

The distributed transverse load is

$$w_u = \frac{1}{2} R_y F_y \left(t_2 - t_1 \right)$$
$$= \frac{1}{2}(1.3)(36\text{ ksi})(0.1875\text{ in.} - 0.125\text{ in.})$$
$$= 1.46 \text{ kips/in.}$$

The distributed axial load is

$$v_u = \frac{1}{2} R_y F_y \left(t_2 - t_1 \right)$$
$$= \frac{1}{2}(1.3)(36\text{ ksi})(0.1875\text{ in.} - 0.125\text{ in.})$$
$$= 1.46 \text{ kips/in.}$$

The shear reaction is

$$V_u = w_u L_1/2$$
$$= (1.46\text{ kips/in.})(71.5\text{ in.})/2$$
$$= 52.2 \text{ kips}$$

Fixed ends will be used. The moment is

$$M_u = w_u {L_1}^2/12$$
$$= (1.46\text{ kips/in.})(71.5\text{ in.})^2/12$$
$$= 622 \text{ kip-in.}$$

The axial compression force at the right end is

$$N_{u\ R} = \frac{1}{4} R_y F_y \left[t_1 \left(h_1 - L_2 \right) + t_2 h_2 \right]$$
$$= \frac{1}{4}(1.3)(36\text{ ksi}) \begin{bmatrix} (0.125\text{ in.})(28.5\text{ in.} - 80\text{ in.}) \\ +(0.1875\text{ in.})(72\text{ in.}) \end{bmatrix}$$
$$= 93.6 \text{ kips}$$

For the similar member on the right side of SPSW (between panels 3 and 5), all three terms are positive.

$$N_{sim} = \frac{1}{4} R_y F_y \left[t_1 \left(h_1 + L_2 \right) + t_2 h_2 \right]$$
$$= \frac{1}{4}(1.3)(36\text{ ksi}) \begin{bmatrix} (0.125\text{ in.})(28.5\text{ in.} + 80\text{ in.}) \\ +(0.1875\text{ in.})(72\text{ in.}) \end{bmatrix}$$
$$= 317 \text{ kips}$$

The axial compression force at the left end is

$$N_{u\ L} = \frac{1}{4} R_y F_y \left[t_1 \left(h_1 - 2L_1 - L_2 \right) + t_2 \left(h_2 + 2L_1 \right) \right]$$
$$= \frac{1}{4}(1.3)(36\text{ ksi}) \begin{bmatrix} (0.125\text{ in.})[28.5\text{ in.} - 2(71.5\text{ in.}) - 80\text{ in.}] \\ +(0.1875\text{ in.})[72\text{ in.} + 2(71.5\text{ in.})] \end{bmatrix}$$
$$= 187 \text{ kips}$$

The required in-plane moment of inertia for fixed ends is

$$I \geq 0.00307 \frac{(t_2 - t_1){L_1}^4}{h_2}$$
$$= \frac{0.00307(0.1875\text{ in.} - 0.125\text{ in.})(71.5\text{ in.})^4}{72\text{ in.}}$$
$$= 69.6\text{ in.}^4$$

The required out-of-plane moment of inertia is

$$I \geq h_2 t_2^3 j \qquad (6\text{–}59)$$

$$j = 2.5(L_1/h_2)^2 - 2 \geq 0.5$$

$$= 2.5(71.5 \text{ in.}/72 \text{ in.})^2 - 2$$

$$= 0.465 \geq 0.5; \text{ use } 0.5$$

$$I \geq (72 \text{ in.})(0.1875 \text{ in.})^3(0.5)$$

$$= 0.237 \text{ in.}^4$$

Based on these required strengths, preliminary sizes of LBE are determined. For simplicity, only one section is used: W14×43 for both the vertical and horizontal LBE.

Using this size, the angle of tension stress is calculated in each of the eight panels using Equation 6–25. Table 6–1 shows the calculated angles.

Without the opening, the angle of tension stress was calculated as 41.5°. The web-plate design shear strength is 327 kips. The required web-plate shear strength is 308 kips, which is 63.9 percent of the 482-kip required shear strength for the seventh story.

The web-plate shear strength above the opening is

$$V_n = 0.42F_y t_1 \left[2L_1 \sin(2\alpha_1) + L_2 \sin(2\alpha_2)\right] \qquad (6\text{–}60)$$

$$= 0.42(36 \text{ ksi})(0.125 \text{ in.}) \begin{bmatrix} 2(71.5 \text{ in.}) \sin(2\times 44.7°) \\ +(80 \text{ in.}) \sin(2\times 45.2°) \end{bmatrix}$$

$$= 421 \text{ kips}$$

The web-plate shear strength at the level of the opening is

$$V_n = 0.42F_y t_2 [2L_1 \sin(2\alpha_4)] \qquad (6\text{–}61)$$

$$= 0.42 \text{ (36 ksi)(0.1875 in.) [2(71.5 in.) sin(2 × 42.7°)]}$$

$$= 404 \text{ kips}$$

The web-plate shear strength below the opening is

$$V_n = 0.42F_y t_1 \left[2L_1 \sin(2\alpha_6) + L_2 \sin(2\alpha_7)\right] \qquad (6\text{–}62)$$

$$= 0.42(36 \text{ ksi})(0.125 \text{ in.}) \begin{bmatrix} 2(71.5 \text{ in.}) \sin(2\times 45.0°) \\ +(80 \text{ in.}) \sin(2\times 45.7°) \end{bmatrix}$$

$$= 421 \text{ kips}$$

Based upon the least of these, the design shear strength is

$$\phi_v V_n = 0.9(404 \text{ kips})$$

$$= 364 \text{ kips} > V_u = 308 \text{ kips} \quad \textbf{o.k.}$$

The web plates provided therefore are adequate.

Note that the strength at the section at the opening is slightly reduced because the increase in thickness is slightly lesser in proportion than the decrease in width. Thus, an additional shear is imposed on the VBE. The shear force transmitted to the VBE is

$$V_u = 421 \text{ kips} - 404 \text{ kips}$$

$$= 17.0 \text{ kips}$$

This additional shear is more than offset by the fact that the horizontal LBE reduce the span of the VBE in resisting the transverse loading due to web-plate tension.

The reactions on the HBE above and below are equal to the axial force in LBE "a." Thus,

$$N_{ua} = 158 \text{ kips}$$

These forces are used in the design of the HBE, in conjunction with the distributed loading due to the unbalanced web-plate tension and the flexural forces from frame behavior.

Chapter 7

Discussion of Special Considerations

7.1. OVERVIEW

This chapter addresses some additional practical issues that must be considered in the design and construction of steel plate shear walls.

7.2. MATERIAL SPECIFICATIONS

Materials used for web plates in steel plate shear walls must behave in a manner consistent with the assumptions used in their design. Additionally, designers will find some materials permit more practical designs. For high-seismic design ($R > 3$), materials are limited to those listed in Section 6.1 of AISC 341.

Among the characteristics required by AISC 341 for steel materials expected to undergo significant inelastic strain are a known expected strength, high ductility, relatively high toughness, and weldability. In addition, it is desirable to use a material with a low yield strength and a low material overstrength (i.e., a low factor R_y, the ratio of the expected and specified minimum yield strength of the material).

The material used for web plates in high-seismic design of steel plate shear walls must have a known expected yield strength ($R_y F_y$) so that web-plate connections can be designed properly. In addition to the web-plate connections, the design forces for boundary elements depend on the expected strength of the web-plate material in high-seismic design.

In order to permit use of the design equations, it is necessary for web plates to be sufficiently ductile to accommodate nonuniform yielding, starting from localized initial yield to a more uniform state of stress. For high-seismic design, web plates must be able to reach uniform yielding across their entire area. Thus, a material with a large inelastic strain capacity is needed. The list of materials in AISC 341 is based, in part, on a 20 percent elongation capacity in a 2-in. gage length.

It is desirable to use a web-plate material that is relatively low in strength, especially where designs are controlled by drift. For low- to mid-rise SPSW buildings, use of thicker web plates generally aids construction, especially at the top floors where story shears are low. Thus, material with yield strength of 30, 33, or 36 ksi present advantages over 50 ksi material. Note that AISC 341 does not permit material with specified minimum yield stress greater than 50 ksi to be used for web plates in high-seismic design, unless testing is performed to justify it.

A low deviation of expected yield stress from the specified minimum yield stress (i.e., a low factor R_y) reduces the strength required of elements adjoining the web plate. In some cases, considerable savings could be realized by specifying a range of yield strength more limited than that permitted by the ASTM specification, provided that the plate material is readily available. The availability of steel with such special requirements should be confirmed prior to specification. Designers may wish to give alternative combinations of web-plate thickness and measured yield strength in order to achieve the required strength and limit unnecessary (and costly) overstrength without specifying material that is difficult to obtain. For example, a designer could specify a web plate of 5⁄16-in. thickness and a measured yield strength between 30 and 36 ksi, with an alternative of 1⁄4-in. thickness and a measured yield strength between 38 and 45 ksi, provided the change in stiffness is not detrimental.

Of the materials listed in Section 6.1 of AISC 341, a suitable and often-used material for web plates is ASTM A36. ASTM A709 could also be suitable. Primarily used in bridge design, ASTM A709 Grade 36 is available in thicknesses similar to that of A36 because it is simply ASTM A36 with additional bridge-related requirements. ASTM A572 and A588 (“weathering steel”) are also permissible, although their higher specified minimum yield stress (42 or 50 ksi for A572; 50 ksi for A588) makes them less desirable.

Other materials may also be appropriate based on the criteria used to select those listed in Section 6.1 of AISC 341. ASTM A1011 SS[1] is especially suitable for use in SPSW. It is available in low-strength grades (Grade 30 and 33) and has good weldability. It provides a high inelastic deformation capacity (25 percent for Grade 30 material between 0.097 and 0.230 in. thickness). This material has been used in the design of SPSW (Eatherton, 2004). ASTM A1011 HSLAS Grade 55 is allowed by AISC 341, but it is not suitable for SPSW because of its higher strength and lower inelastic strain capacity. ASTM A1011 CS and A1011 DS both typically provide good elongation capacity and a low yield strength. However, the mechanical properties

[1]This material was previously covered by ASTM 570 SS.

Table 7–1. Suitable ASTM Materials for SPSW Web Plates

ASTM Designation		Specified Minimum Yield Stress F_y (ksi)	Specified Minimum Tensile Stress F_u (ksi)	Minimum Elongation in 2 in. Gage Length[7] (%)	Listed in AISC 341?	R_y, Ratio of Expected to Specified Minimum Yield Stress
A36		36	58	23	Yes	1.3
A529 Gr. 50		50	70	21	Yes	Not Defined
A572	Gr. 42	42	60	24	Yes	Not Defined
	Gr. 50	50	65	21	Yes	1.1
A588		50	70	21	Yes	1.1
A709	Gr. 36	36	58	23	Yes	Not Defined
	Gr. 50	50	65	21	Yes	Not Defined
A1011	CS	(30–50)[1]	Not Defined	(25)[1]	No	Not Defined
	DS	(30–45)[1]	Not Defined	(28)[1]	No	Not Defined
	SS Gr. 30	30	49	25[2]; 24[3]; 21[4]	No	Not Defined
	SS Gr. 33	33	52	23[2]; 22[3]	No	Not Defined
	SS Gr. 36 Type 1	36	53	22[2]; 21[3]	No	Not Defined
	SS Gr. 36 Type 2	36	58	21[2]; 20[3]	No	Not Defined
	SS Gr. 40	40	55–80	21[2]; 20[3]	No	Not Defined
	HSLAS Gr. 45 Class 1	45	60	25[5]; 23[6]	No	Not Defined
	HSLAS Gr. 45 Class 2	45	55	25[5]; 23[6]	No	Not Defined
	HSLAS Gr. 50 Class 1	50	65	22[5]; 20[6]	No	Not Defined
	HSLAS Gr. 50Class 2	50	60	22[5]; 20[6]	No	Not Defined

[1] Denotes nonmandatory, typical value. Designers must verify the actual yield strength of the material.
[2] Value for thickness between 0.097 and 0.230 in.
[3] Value for thickness between 0.064 and 0.097 in.
[4] Value for thickness between 0.025 and 0.064 in.
[5] Value for thickness above 0.097 in.
[6] Value for thickness up to 0.097 in.
[7] Using test method given in ASTM A370.

listed for these materials by ASTM (and in Table 7–1) are nonmandatory. Designers wishing to employ ASTM A1011 CS or A1011 DS should specify testing of material provided to meet the desired yield strength, and, at a minimum, an elongation capacity of 20 percent in a 2-in. gage length per ASTM A370.

Table 7–1 lists the various materials that may be considered for SPSW web plates and their relevant characteristics. All of these materials are hot-formed and have suitable weldability. For many of the materials listed in Table 7–1, designers must either investigate the expected yield stress of the material for the selected grade, or specify a maximum to be established using ASTM A370.

The materials listed in Table 7–1 are produced in a range of thicknesses. For SPSW, the thickness range between 0.0593 in. and ⅝ in. is most relevant. The production of the materials in Table 7–1 in that thickness range is listed in Table 7–2.

Provided that the material is available, testing of web-plate material can offer significant advantages. If a permitted range of yield stress is specified for the web plates for a specific project, with a minimum yield strength above the ASTM specified minimum for the material but below the expected yield strength R_yF_y, the required strength of connections and boundary elements can be significantly reduced. For example, if the web-plate material in Chapter 5 could

Table 7–2. Commonly Produced Thicknesses of Materials Suitable for Web Plates in SPSW

Web-Plate Thickness (in.)	Standard Gage or Fractional Thickness (in.) if no Standard Gage is Applicable	ASTM Designation																	
		A36	A529 Gr. 50	A572 Gr. 42	A572 Gr. 50	A588	A709 Gr. 36	A709 Gr. 50	A1011 CS	A1011 DS	A1011 SS Gr. 30	A1011 SS Gr. 33	A1011 SS Gr. 36 Type 1	A1011 SS Gr. 36 Type 2	A1011 SS Gr. 40	A1011 HSLAS Gr. 45 Class 1	A1011 HSLAS Gr. 45 Class 2	A1011 HSLAS Gr. 50 Class 1	A1011 HSLAS Gr. 50 Class 2
0.0593	16								•	•	•	•	•	•	•	•	•	•	•
0.0625	1/16	•																	
0.0673	15								•	•	•	•	•	•	•	•	•	•	•
0.0747	14	•							•	•	•	•	•	•	•	•	•	•	•
0.0897	13								•	•	•	•	•	•	•	•	•	•	•
0.1046	12	•							•	•	•	•	•	•					
0.1196	11								•	•	•	•	•	•					
0.125	1/8	•																	
0.1345	10	•							•	•	•	•	•	•					
0.1495	9								•	•	•	•	•	•					
0.1644	8								•	•	•	•	•	•					
0.1793	7								•	•	•	•	•	•					
0.1875	3/16	•	•	•	•	•	•	•			•	•	•	•					
0.1943	6										•	•	•	•					
0.2092	5										•	•	•	•					
0.2242	4										•	•	•	•					
0.2391	3										•	•	•	•					
0.250	1/4	•	•	•	•	•	•	•											
0.3125	5/16	•	•	•	•	•	•	•											
0.375	3/8	•	•	•	•	•	•	•											
0.4375	7/16	•	•	•	•	•	•	•											
0.500	1/2	•	•	•	•	•	•	•											
0.625	5/8	•	•	•	•	•	•	•											

have been designed with material having a specified minimum yield stress of 40 ksi and a maximum of 46 ksi (instead of using F_y equal to 36 ksi and $R_y F_y$ equal to 46.8 ksi) the seismic load effects on connections and boundary elements would have been reduced by 12 percent because of the corresponding reduction in thickness required. For structures with elements designed to control drift this reduction may be of minor consequence; for structures with elements designed for strength, the savings would more than offset the costs of testing in many cases. The authors recommend that if testing is used to establish material properties, at least one test be performed for each heat of steel used for web plates and that the feasibility of testing and other special specification requirements be confirmed early in the design phase.

7.3. SERVICEABILITY

The design examples in Chapters 4 and 5 addressed the design of SPW and SPSW, respectively, in order to meet the strength and performance requirements for the loading specified in ASCE 7. For most building applications, it is also desirable to investigate the serviceability performance of the system under the more moderate service loading that it is likely to undergo.

There are no codified criteria for the required performance at serviceability loads. This aspect of design requires discussion with the building owner or user, as the performance requirements are subjective and must be considered in the context of potential added cost. For further guidance on serviceability design criteria, see AISC Design Guide 3, *Serviceability Design Considerations for Steel Buildings,* Second Edition (West and Fisher, 2003).

7.3.1. Buckling of Web Plates: Attachments

The buckling behavior of the web plate presents a number of serviceability considerations that are unique to SPSW. Slender web plates are likely to buckle under low levels of lateral loading. Extremely slender web plates may buckle before construction is complete. While this is consistent with the strength and stiffness assumptions in the SPSW design equations, the transverse displacement associated with buckling may affect any attachments to the wall. Architectural walls surrounding web plates must therefore provide sufficient clearance to accommodate this displacement.

The expected buckling of web plates makes attachment of nonstructural items to them problematic. It is best to avoid attachments to web plates and provide an architectural wall on either side of the web plate.

7.3.2. Loading at Buckling of Web Plate

Designers may wish to calculate the level of loading that theoretically corresponds to buckling of the web plate, and make sure that the interested parties understand and accept that web-plate buckling will be part of the performance under such loading. The critical buckling stress can be calculated using an expression derived by Timoshenko and Woinowsky-Kreiger (1959).

$$\tau_{cr} = \frac{\pi^2 E}{12(1-\upsilon^2)(s_1/t)^2} \qquad (7\text{–}1a)$$

where

s_1 = the smaller spacing between stiffeners

τ_{cr} = the critical buckling shear

υ = Poisson's ratio

The limiting plate thickness is

$$t_{cr} = \frac{2s_1}{\pi}\sqrt{\frac{3(1-v^2)\tau}{E}} \qquad (7\text{–}1b)$$

Plates of this thickness or thicker will yield in shear. Thinner plates will experience shear buckling at stress levels below that of shear yielding.

For the building in Chapter 4, the most slender web plates are at the top of the building, where the critical buckling stress is 6 psi—less than 1 percent of the design shear strength. This level of shear stress corresponds to a wind speed of approximately 10 miles per hour. While the role of numerous additional sources of lateral resistance may be important at low levels of loading, it is clear that buckling of the web plate should be anticipated in the service life of the building.

7.4. CONFIGURATION

Designers may find that it is difficult to satisfy many of the requirements of AISC 341 for SPSW in bays 30 ft long or longer. The design requirements for HBE, especially at the top level, make longer spans unattractive. Designers may wish to introduce a series of vertical struts as discussed in Chapter 3; alternatively, shorter bays can be designed to provide very high strength. Shorter bays, however, may lead to increased axial forces in VBE, as well as increased drift. As discussed in Chapter 3, reduction of axial forces in VBE by use of special configurations can be advantageous, both for control of drift and for the required strength of those elements.

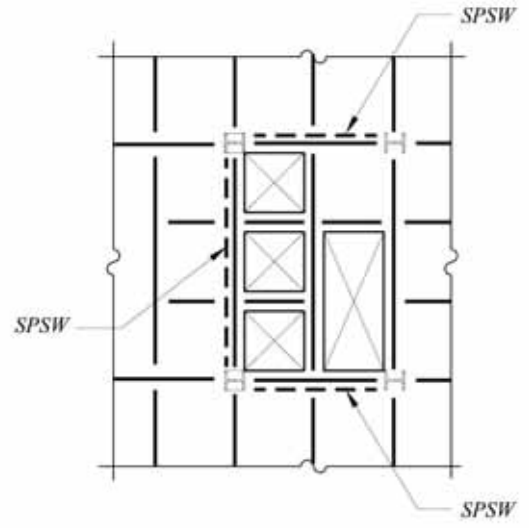

Fig. 7–1. Intersecting orthogonal SPSW.

The design examples in this Design Guide use SPW or SPSW at the building perimeter. This is done for simplicity of illustration of the design method. In many building applications it is convenient to locate shear walls at the elevator and stair locations at the building core. This provides less torsional resistance than location of the shear walls at the perimeter. Frequently, a perimeter moment frame is used at the building perimeter to reduce building torsion when shear walls in the building core resist the majority of the lateral loads.

Orthogonal shear walls located at the building core will often intersect, sharing the VBE. Figure 7–1 shows a plan with intersecting SPSW at a building core.

This condition complicates the design of the SPSW in two ways. First, the VBE must meet the transverse stiffness requirement of AISC 341 Section 17.4g (Equation 3–22). Wide-flange shapes may require additional plates to form box sections to meet this requirement. Alternatively, columns may be made of built-up box sections or HSS. Figure 7–2 shows some alternative VBE sections; designers should consider the added flexibility of thin plates in bending. It should be noted that no such configurations have been tested, although some applications have employed intersecting SPSW.

The second way in which intersecting orthogonal SPSW complicate the design is that VBE must be designed for simultaneous seismic loading in each orthogonal direction. While it is unlikely that the two SPSW will reach their peak overturning moments simultaneously, SPSW are expected to show significant ductility, and the forces in elements cannot be added using elastic methods, such as with the square root of the sum of the squares (SRSS), or combining 100 percent of the force from one direction of loading with 30 percent of the force from loading in the orthogonal direction. FEMA 356 recommends combining 100 percent of the displacement in one direction of loading with 30 percent of the displacement in the orthogonal direction. This method accounts for the expected ductility of the system.

7.5. CONSTRUCTION

The construction of buildings with SPSW generally does not present extraordinary challenges. Many have been built using standard techniques of structural steel detailing, fabrication, and erection.

7.5.1. Bolted Construction

The use of bolted steel web plates presents some construction challenges, in addition to the design challenges discussed in Chapter 3. Bolted joints of web plates may require welded reinforcement in order to permit close bolt spacing while maintaining a design that is governed by web-plate yielding rather than rupture at the net section. Reinforcement also reduces the number of bolts required, which otherwise might necessitate multiple rows of bolts at every joint.

Of more concern is the difficulty in aligning the large number of bolts required for each web plate. Even if web-plate splices within each story are shop welded, each web plate is likely to have dozens of bolts, possibly more than 100. Erection tolerance for out-of-plumbness of VBE columns is likely to lead to conditions of bolt-hole misalignment.

While bolted construction is often faster for erection, for web plates in steel plate shear walls, its advantages in this respect are not ensured.

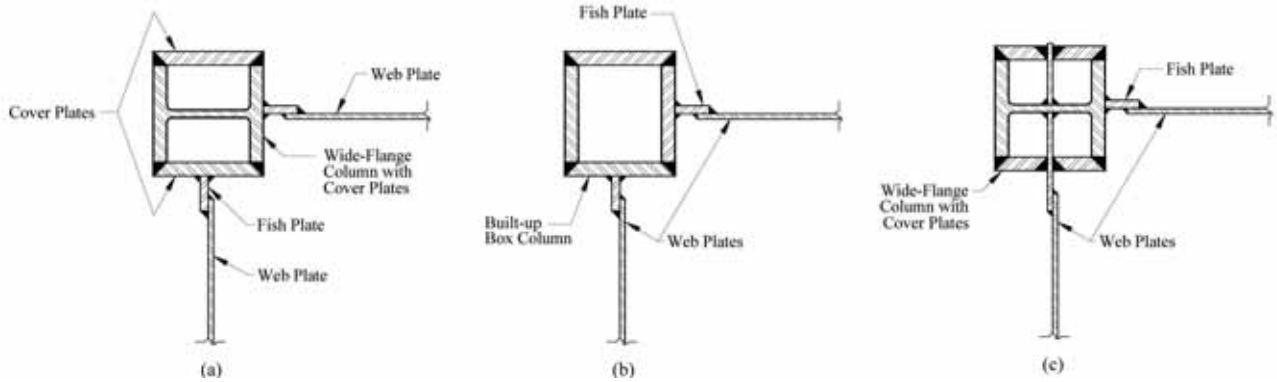

Fig. 7–2. Alternative VBE sections.

7.5.2. Welded Construction

The use of welded construction is generally preferred for the web plates in steel plate shear walls. Fillet welds at the perimeter of web plates can typically be sized for a single pass (5⁄16 in. or less, depending upon welding position).

Where gage material with thickness of 1⁄8 in. or less is used for web plates, welding in the vertical position may be difficult. Field welds of web plates to VBE fish plates may be difficult to achieve without melting through the thin material. Alternative details have been used in such cases, including only welding the edge of the web plates to the fish plates (i.e., without the other weld at the edge of the fish plate).

In applications with smaller SPW or SPSW, such as low-rise buildings, the welding may be done in the shop and the entire assembly erected in one piece. For larger applications, some field splicing is necessary. In those cases, designers may wish to pay special attention to the qualification of welders for these procedures. Adequate demonstration of qualification should be part of the quality assurance plan, as required by Section 18 of AISC 341.

As with all welds in the seismic load resisting system, AISC 341 has requirements for the minimum filler metal toughness rating. These requirements are given in Section 7.3, including a Charpy V-notch toughness of 20 ft-lb at 0 °F. This requirement applies to the welded connections of the web plate, as well as to the welded connections and splices of VBE, HBE and collectors and chords of diaphragms.

The moment connections of HBE to VBE in SPSW require "demand critical welds." These have a minimum Charpy V-notch toughness of 40 ft-lb at 70 °F, in addition to the requirements above. This toughness is established using testing and qualification procedures described in Appendix X to AISC 341.

7.5.3. Sequence and Speed of Erection

SPW and SPSW are built similarly to braced frames: columns and beams are erected, followed by the infill web plates. Prior to the connection of the web plates, some temporary means is used to stabilize and plumb the structure.

In some cases, designers have taken precautions to prevent large dead-load forces from accumulating in multi-story shear walls, with the goal of precluding buckling of the web plate prior to the application of a significant lateral load (Astaneh-Asl, 2001). However, this may not be necessary, as it has been suggested that an initially slightly buckled plate is not detrimental to the lateral seismic performance. As discussed above, the level of lateral loading at which web-plate buckling can be expected is fairly low. Also, as discussed in Chapters 2 and 3, the shear-buckling strength of the web plates contributes very little to the overall strength and stiffness of the system. For these reasons, there is no requirement to prevent web-plate buckling from occurring under dead loads, and designers need not place any special requirements on sequence of erection or connection of elements.

Erection can thus be fairly rapid, although welding of web plates and of HBE-to-VBE connections may continue for some time after erection of the frame is complete.

7.5.4. Connection of Other Elements

While web plates in SPW and SPSW are fairly resistant to the propagation of cracks that develop at the connections of plates to boundary elements during their inelastic response at large ductilities, it is nevertheless recommended that no attachments from other building systems, such as mechanical ducts or partitions, be made to them. This is primarily due to the expected buckling of the web plate and the effect that might have on the supported item, but also to prevent the initiation of mid-plate cracking, a condition that has not been investigated to date.

While partition framing can easily run past the web plate, large panels on the building interior can pose a significant obstacle to the optimal routing of mechanical, electrical, and plumbing systems. This can be especially obtrusive where SPW or SPSW are located surrounding the building core where these systems converge and are routed vertically.

The perforated web-plate shear wall shown in Figure 2–18 offers an approach that allows for penetration of the shear wall by other building systems. Another test from the same series (shown in Figure 2–19) likewise permits penetration (Vian and Bruneau, 2004). This web plate provides openings at the upper corners. In order to permit web-plate tension yielding to occur at these locations, the curved stiffener must be designed as an arch and anchored to the VBE and HBE flanges.

7.5.5. Retrofit Applications

SPW and SPSW can be considered for many retrofit applications. If the structure to be retrofit is a moment frame, it may already meet many of the requirements for SPSW frames. Frames should meet the proportioning requirements of AISC 341 Section 17.2b. The introduction of a web plate will reduce the flexural demands on the frame by significantly reducing drift, while increasing the axial forces. Frames that meet the strong-column/weak-beam requirement of Section 17.4a of AISC 341 before the addition of the web plate may not once the axial forces due to web-plate tension in the column are considered.

The flexibility of the VBE may limit the maximum web-plate thickness that can be introduced. These limitations should be investigated at the outset of considering use of a SPSW retrofit. The maximum web-plate thickness based on column flexibility is based on Section 17.4g of AISC 341 (Equation 3–22):

$$t_w \leq \frac{326LI_c}{h^4} \qquad (7\text{–}2)$$

Where this requirement precludes the use of SPSW, designers may consider strengthening the boundary elements or using stiffened or composite steel plate walls that would ensure pure shear yielding of the web plate, which would not impose these flexural forces on the VBE. Alternatively, horizontal struts may be used to reduce the required moment of inertia of VBE, as discussed in Chapter 3.

The maximum web-plate thickness may also be governed by the flexural strength or stiffness of the beams. For structures designed as moment frames, typical beams will have significant flexural strength and may be able to support web-plate tension stresses across their spans (considering the offsetting effects of the web plate above the beam).

At the top level, where there is no web plate above to offset the tension stress pulling the beam down, it may not be possible to provide a web plate of realistic thickness. Designers may need to strengthen the beam. Designers may also wish to consider three alternatives at this level.

First, the top-level web plate of the SPSW frame may be designed as a stiffened or composite steel plate wall, thus eliminating the transverse load imposed on the top HBE by web-plate tension. While this would theoretically impose the flexural forces on the next HBE (which would have an unstiffened web plate below, and a stiffened web-plate above); the yielding of that lower beam due to this effect requires the web plate above to yield in tension as well, and thus the beam can be designed as if the web plate above were unstiffened.

Second, designers may consider reducing the required flexural strength of the beam by the introduction of a significant opening across the beam span. The local overturning moments at the boundary elements at either side of the opening may be very large, and this approach may not be viable if the required strength of the wall is large at this level.

Third, a series of vertical struts may be included in the SPSW so that the top HBE is supported at mid-span, and its reaction at this location, combined with the reactions of all the intermediate HBE, accumulate in the series of struts and offset the upward mid-span reaction of the bottom HBE. This concept is described in Chapter 3.

7.6. FIRE PROTECTION

The International Building Code (ICC, 2000) requires differing levels of fire protection for members of the steel structure, depending on their role in the support of gravity loads. There are requirements for beams, as well as requirements for the "structural frame" as defined in a footnote to Table 601. These latter requirements are typically more stringent.

Web plates in SPW and SPSW typically are not considered part of the structural frame, which is defined as follows:

The structural frame shall be considered to be the columns and girders, beams, trusses and spandrels having direct connection to the columns and bracing members designed to carry gravity loads.

Neither the HBE nor the VBE depend on the web plate for resistance to gravity loading. The web plate, as discussed previously, is a slender member with little or no resistance to compression; it can typically be expected to have buckled under self-weight or during the application of dead loads. The web plate therefore is not considered part of the structural frame and thus is not required to be fireproofed unless it is part of a fire-rated separation or shaft. Under those circumstances, a fire-resistant assembly can be provided on one side of the web plate. The partition on the opposite side would not be required to be fire resistant. If it is desired to use fire protection directly on a web plate, such an assembly should be tested to determine its fire resistance or fire engineered to ensure proper performance. For further guidance on the design of SPW and SPSW for fire resistance, see AISC Design Guide 19, *Fire Resistance of Structural Steel Framing* (Ruddy et al., 2003).

7.7. FUTURE RESEARCH AND TOOLS

This Design Guide has been written based on the research available to date and commonly used analysis tools. Because this is a new system, the supporting research is expected to increase rapidly before this Design Guide is updated. The authors have provided design recommendations that are intended to provide reliable performance. At times, the recommendations have been made anticipating that they may later be revised (typically relaxed) based on future testing and analysis. It is also expected that nonlinear analysis tools currently available can demonstrate that a particular design that does not conform to some of the recommendations nevertheless can achieve the desired performance. Specific items that are the subject of ongoing investigation include:

- The stiffness criterion for HBE proposed in Chapter 3.
- The stiffness criterion for VBE in AISC 341.
- The applicability of the strain-hardening factor of 1.1 in various HBE-to-VBE connection calculations.
- Use of the full HBE plastic moment in conjunction with full web yielding in VBE design.
- Calculation of the angle α (as required by AISC 341) versus use of an assumed angle of 45°.
- The location of the HBE plastic hinge for calculating VBE moments.
- Calculation of VBE required flexural strength based on a simple span due to hinging at each end.

Bibliography and References

ACI (2005), ACI 318-05*, Building Code Requirements for Structural Concrete*, American Concrete Institute, Farmington Hills, MI.

AISC (2005a), ANSI/AISC 341-05, *Seismic Provisions for Structural Steel Buildings*, American Institute of Steel Construction Inc., Chicago, IL.

AISC (2005b), ANSI/AISC 360-05, *Specification for Structural Steel Buildings*, American Institute of Steel Construction Inc., Chicago, IL.

AISC (2005c), ANSI/AISC 358-05, *Prequalified Connections for Special and Intermediate Steel Moment Frames for Seismic Applications*, American Institute of Steel Construction Inc., Chicago, IL.

ASCE (2005), SEI/ASCE 7-05, *Minimum Design Loads for Buildings and Other Structures* (including Supplement No. 1), American Society of Civil Engineers, Reston, VA.

ASTM (1998), A 653/A 653M-98, *Standard Specification for Steel Sheet, Zinc-Coated (Galvanized) Zinc-Iron Alloy-Coated (Galvannealed) by the Hot-Dip Process*," American Society for Testing and Materials, Philadelphia, PA.

ASTM (1997), A 336/A 336M-97, *Standard Specification for Commercial Steel Sheet, Carbon, Cold-Rolled*, American Society for Testing and Materials, Philadelphia, PA.

ATC (1992), *Guidelines for Seismic Testing of Components of Steel Structures*, Report 24, Applied Technology Council.

Aoyama, H. and Yamamoto, Y. (1984), "Aseismic Strengthening of Existing RC Buildings by Steel Panel Shear Walls with Rims," *Transactions*, Vol. 6, pp. 733–740, Japan Concrete Institute.

Astaneh-Asl, A. (2003), "Chapter 10: Steel Shear Walls," *Design of Steel Composite Structures, Including Seismic Effects*, Department of Civil and Environmental Engineering, University of California, Berkeley.

Astaneh-Asl, A. (2001), "Seismic Behavior and Design of Steel Shear Walls," *Steel Technical Information and Product Services Report*, Structural Steel Educational Council, Moraga, CA.

Astaneh-Asl, A. (2002), "Seismic Behavior and Design of Composite Steel Plate Shear Walls," *Steel Technical Information and Product Services Report*, Structural Steel Educational Council, Moraga, CA.

Astaneh-Asl, A. and Zhao, Q. (2002), "Cyclic Behavior of Steel Shear Wall Systems," *Proceedings of the Annual Stability Conference*, Structural Stability Research Council, Seattle, WA.

Astaneh-Asl, A. and Zhao, Q. (2001), "Cyclic Tests of Steel Shear Walls," *Report Number UCB/CE-Steel-01/01*, August, Department of Civil and Environmental Engineering, University of California, Berkeley.

Baldelli, J.A. (1983), "Steel Shear Walls for Existing Buildings," AISC *Engineering Journal*, Second Quarter, pp. 70–77.

Basler, K. (1961), "Strength of Plate Girders in Shear," ASCE *Journal of the Structural Division*, Vol. 87, No. 7, pp. 150–180.

Behbahanifard, M., Grondin, G., and Elwi, A. (2003), "Experimental and Numerical Investigation of Steel Plate Shear Walls," *Structural Engineering Report No. 254*, Department of Civil and Environmental Engineering, University of Alberta, Edmonton, Alberta, Canada.

Berman, J.W. and Bruneau, M. (2003a), "Plastic Analysis and Design of Steel Plate Shear Walls," ASCE *Journal of Structural Engineering*, Vol. 129, No. 11, pp. 1448–1456.

Berman, J.W. (2005), private correspondence.

Berman, J.W. and Bruneau, M. (2003b), "Experimental Investigation of Light-Gauge Steel Plate Shear Walls for the Seismic Retrofit of Buildings," *Technical Report MCEER-03-0001*, Multidisciplinary Center for Earthquake Engineering Research, Buffalo, NY.

Berman, J.W. and Bruneau, M. (2004), "Steel Plate Shear Walls are not Plate Girders," AISC *Engineering Journal*, Third Quarter, pp. 95–106.

Bruneau, M., Berman, J., López-Garcia, D., and Vian, D. (2005), "Steel Plate Shear Wall Buildings: Design Requirements and Research," *Proceedings of 2005 North American Steel Construction Conference*, Montreal, Canada.

Bruneau, M. and Bhagwager, T. (2002), "Seismic Retrofit of Flexible Steel Frames Using Thin Infill Panels," *Engineering Structures*, Vol. 24, No. 4, pp. 443–453.

Bruneau, M., Uang, C.M., and Whittaker, A. (1997), *Ductile Design of Steel Structures*, McGraw-Hill, New York.

CSA (2001), CAN/CSA S16-01, *Limit States Design of Steel Structures*, Canadian Standards Association, Willowdale, Ontario, Canada.

CSA (1994), CAN/CSA S16-94, *Limit States Design of Steel Structures*, Canadian Standards Association, Willowdale, Ontario, Canada.

CSA (1978), CAN/CSA S16.1-M78, *Steel Structures for Buildings Limit States Design*, Canadian Standards Association, Willowdale, Ontario, Canada.

CSI (1997), *SAP2000 Reference Manual*, Computers and Structures, Inc., Berkeley, CA.

Caccese, V., Elgaaly, M., and Chen, R. (1993), "Experimental Study of Thin Steel-Plate Shear Walls Under Cyclic Load," ASCE *Journal of Structural Engineering*, Vol. 119, No. 2, pp. 573–587.

Çelebi, M. (1997), "Response of Olive View Hospital to Northridge and Whittier Earthquakes," ASCE *Journal of Structural Engineering*, Vol. 123, No. 4, pp. 389–396.

Chen, W.F., Goto, Y., and Liew, J.Y.R. (1996), S*tability Design of Semi-Rigid Frames*, John Wiley & Sons, New York.

Cook, N.E. (1983), "Strength of Flexibly-Connected Steel Frames Under Load-Histories," PhD Dissertation, University of Colorado–Boulder, Boulder, CO.

Dafalias, Y.F. and Popov, E.P. (1976), "Plastic Internal Variables Formalism of Cyclic Plasticity," ASCE *Journal of Applied Mechanics*, Vol. 43, pp. 645–651.

Dean, R.G., Cannon, T.J., and Poland, C.D. (1977), "Unusual Structural Aspects of the H.C. Moffitt Hospitals," *Proceedings of the Structural Engineers Association of California 46th Convention*, Coronado, CA, pp. 32–73.

Driver, R.G. and Grondin, G.Y. (2001), "Steel Plate Shear Walls: Now Performing on the Main Stage," *Modern Steel Construction*, September, AISC, Chicago.

Driver, R.G., Grondin, G.Y., Behbahanifard, M., and Hussain, M.A. (2001), "Recent Developments and Future Directions in Steel Plate Shear Wall Research," *Proceedings of the North American Steel Construction Conference,* Ft. Lauderdale, FL, May.

Driver, R.G., Kulak, G. L., Elwi, A. E., and Kennedy, D.J.L. (1998a), "Cyclic Tests of Four-Story Steel Plate Shear Wall," ASCE *Journal of Structural Engineering*, Vol. 124, No. 2, pp. 112–120.

Driver, R.G., Kulak, G. L., Elwi, A. E., and Kennedy, D.J.L. (1998b), "FE and Simplified Models of Steel Plate Shear Wall," ASCE *Journal of Structural Engineering*, Vol. 124, No. 2, pp. 121–130.

Driver, R.G., Kulak, G.L., Kennedy, D.J.L., and Elwi, A.E. (1997), "Finite Element Modelling of Steel Plate Shear Walls," *Proceedings of the Structural Stability Research Council Annual Technical Session*, Toronto, Canada, pp. 253–264.

Driver, R.G., Kulak, G.L., Kennedy, D.J.L., and Elwi, A.E. (1997), "Seismic Behaviour of Steel Plate Shear Walls," *Structural Engineering Report No. 215*, Department of Civil Engineering, University of Alberta, Edmonton, Alberta, Canada.

Driver, R.G., Kulak, G.L., Kennedy, D.J.L., and Elwi, A.E. (1996), "Seismic Performance of Steel Plate Shear Walls Based on a Large-Scale Multi-Storey Test," *Proceedings of the 11th World Conference on Earthquake Engineering*, Acapulco, Mexico, Paper 1876, p. 9.

Driver, R.G., Kulak, G.L., Kennedy, D.J.L., and Elwi, A.E. (1995), "Large-Scale Test on a Four Storey Steel Plate Shear Wall Subjected to Idealized Quasi-Static Earthquake Loading," *Proceedings of the 7th Canadian Conference on Earthquake Engineering*, Canadian Association for Earthquake Engineering, Montreal, Canada, pp. 657–664.

Eatherton, M. (2005), Senior Design Engineer, GFDS Engineers, San Francisco, personal communication.

Eatherton, M. and Johnson, K. (2004), "High-End Residence using Steel Plate Shear Walls in Woodside, California," *Proceedings of the SEAOC 2004 Convention: 75th Anniversary Celebration*, Monterey, CA, pp. 19–29.

Elgaaly, M. (1998), "Thin Steel Plate Shear Walls Behavior and Analysis," *Thin Walled Structures*, Elsevier, Vol. 32, Nos. 1–3, pp. 151–180.

Elgaaly, M., Caccese, V., and Du, C. (1993), "Post-Buckling Behavior of Steel-Plate Shear Walls Under Cyclic Loads," ASCE *Journal of Structural Engineering*, Vol. 119, No. 2, pp. 588–605.

Elgaaly, M. and Liu, Y. (1997), "Analysis of Thin-Steel-Plate Shear Walls," ASCE *Journal of Structural Engineering*, Vol. 123, No. 11, pp. 1487–1496.

FEMA (2004), FEMA 450, *NEHRP Recommended Provisions for Seismic Regulations for New Buildings and Other Structures*, Building Seismic Safety Council for the Federal Emergency Management Agency, Washington, DC.

FEMA (2001a), FEMA 369, *NEHRP Recommended Provisions for Seismic Regulations for New Buildings and Other Structures, Part 1–Provisions*, Building Seismic Safety Council for the Federal Emergency Management Agency, Washington, DC.

FEMA (2001b), FEMA 369, *NEHRP Recommended Provisions for Seismic Regulations for New Buildings and Other Structures, Part 2–Commentary*, Building Seismic Safety Council for the Federal Emergency Management Agency, Washington, DC.

FEMA (2000a), FEMA 350, *Recommended Seismic Design Criteria for New Steel Moment-Frame Buildings*, Building Seismic Safety Council for the Federal Emergency Management Agency, Washington, DC.

FEMA (2000b), FEMA 356, *Prestandard and Commentary for the Seismic Rehabilitation of Buildings*, Building Seismic Safety Council for the Federal Emergency Management Agency, Washington, DC.

FEMA (1997), FEMA 302, *NEHRP Recommended Provisions for Seismic Regulations for New Buildings and Other Structures, Part 1–Provisions*, Building Seismic Safety Council for the Federal Emergency Management Agency, Washington, DC.

Fujitani, H., Yamanouchi, H., Okawa, I. Sawai, N., Uchida, N., and Matsutani, T. (1996), "Damage and Performance of Tall Buildings in the 1995 Hyogoken Nanbu Earthquake," *Proceedings of 67th Regional Conference (in conjunction with ASCE Structures Congress XIV)*, Council on Tall Building and Urban Habitat, Chicago, pp. 103–125.

Glotman, M. (2005), Structural Engineer, Glotman Simpson, Vancouver, Canada, personal communication.

Goto, Y., Suzuki, S., and Chen, W.F. (1991), "Analysis of Critical Behavior of Semi-Rigid Frames With or Without Load Histories in Connections," *International Journal of Solids and Structures*, Vol. 27, No. 4, pp. 467–483.

Hitaka, T. and Matsui, C. (2003), "Experimental Study of Steel Shear Walls with Slits," ASCE *Journal of Structural Engineering*, Vol. 129, No. 5, pp. 586–595.

Hooper, J. (2005), Principal and Director of Earthquake Engineering, Magnusson Klemencic Associates, Seattle, personal communication.

Innovation (2002), "Building His Profession," *Innovation: Journal of the Association of Professional Engineers and Geoscientists of British Columbia*, pp. 14–16, October.

International Code Council (2000), *International Building Code*, Building Officials and Code Administrators International (BOCA), International Conference of Building Officials (ICBO) and Southern Building Code Congress International (SBCCI), 3rd printing.

Kennedy, D.J.L., Kulak, G.L., and Driver, R.G. (1994), "Discussion of 'Post-Buckling Behavior of Steel-Plate Shear Walls Under Cyclic Loads' by M. Elgaaly, V. Caccese and C. Du," ASCE *Journal of Structural Engineering*, Vol. 120, No. 7, pp. 2250–2251.

Kuhn, P., Peterson, J.P., and Levin, L.R. (1952), "A Summary of Diagonal Tension, Part 1—Methods of Analysis," *Tech. Note 2661*, National Advisory Committee for Aeronautics, Langley Aeronautical Laboratory, Langley Field, VA.

Kulak, G.L., Kennedy, D.J.L., and Driver, R.G. (1994), "Discussion of 'Experimental Study of Thin Steel-Plate Shear Walls Under Cyclic Load' by V. Caccese, M. Elgaaly and R. Chen," ASCE *Journal of Structural Engineering*, Vol. 120, No. 10, pp. 3072–3073.

Kulak, G.L., Kennedy, D.J.L., Driver, R.G., and Medhekar, M.S. (1999), "Behavior and Design of Steel Plate Shear Walls," *Proceedings of the North American Steel Construction Conference*, Toronto, Canada, pp. 11–20.

Kulak, G.L., Kennedy, D.J.L., Driver, R.G., and Medhekar, M.S. (2001), "Steel Plate Shear Walls: An Overview," AISC *Engineering Journal,* First Quarter, Vol. 38, pp. 50–62.

Lee, S.C. and Yoo, C.H. (1998), "Strength of Plate Girder Web Panels Under Pure Shear," ASCE *Journal of Structural Engineering*, Vol. 124, No. 2, pp. 184–194.

Lubell, A.S. (1997), "Performance of Unstiffened Steel Plate Shear Walls Under Cyclic Quasi-static Loading," M.S. Thesis, Department of Civil Engineering, University of British Columbia, Vancouver, British Columbia, Canada.

Lubell, A.S., Prion, H.G.L., Ventura, C.E., and Rezai, M. (2000), "Unstiffened Steel Plate Shear Wall Performance Under Cyclic Loading," ASCE *Journal of Structural Engineering*, Vol. 126, No. 4, pp. 453–460.

Marsh, C., Ajam, W., and Ha, H. (1988), "Finite Element Analysis of Postbuckled Shear Webs," ASCE *Journal of Structural Engineering*, Vol. 114, No. 7, pp. 1571–1587.

Martinez-Romero, E. (2003), "Construcción Compuesta En Edificios Altos," *VII Simposio Internacional De Estructuras De Acero, Veracruz*, Ver. Mexico.

MathWorks (1999), *MatLab Function Reference*, The MathWorks, Natick, MA.

Mimura, H. and Akiyama, H. (1977), "Load-Deflection Relationship of Earthquake-Resistant Steel Shear Walls with a Developed Diagonal Tension Field," *Transactions of the Architectural Institute of Japan,* Vol. 260, pp. 109–114, October, (in Japanese).

Mo, Y.L. and Perng, S.F. (2000), "Seismic Performance of Framed Shearwalls Made of Corrugated Steel," *Proceedings of the 6th ASCCS International Conference on Steel Concrete Composite Structures*, Los Angeles, CA, March 22–24, pp. 1057–1064.

Montgomery, C.J., Medhekar, M. (2001), Discussion on "Unstiffened Steel Plate Shear Wall Performance Under Cyclic Load," ASCE *Journal of Structural Engineering*, Vol. 127, No. 8, pp. 973–973.

Naeim, F. and Lobo, R. (1994), "Performance of Nonstructural Components During the January 17, 1994 Northridge Earthquake: Case Studies of Six Instrumented Multistory Buildings," *Proceedings of the ATC-29-1 ATC-29-1 Seminar on Seismic Design, Retrofit, and Performance of Nonstructural Components, Applied Technology Council*, Redwood City, CA.

Nakashima, M. (2005), Professor, Division of Seismic Resistant Structures, Disaster Prevention Research Institute, Kyoto University, Kyoto, Japan, personal communication.

Nakashima, M., Fujiwara, T., Suzuki, Y., Bruneau, M., Iwai, S., and Kitahara, A. (1995), "Damage to Engineered Buildings from the 1995 Great Hanshin Earthquake," *Journal of Natural Disaster Sciences*, Vol. 16, No. 20, pp. 71–78.

OSHPD (1995), "Northridge Earthquake: A Report to the Hospital Building Safety Board on the Performance of Hospitals," Office of Statewide Health Planning and Development, Facilities Development Division, Sacramento, CA.

Porter, D.M., Rockey, K.C., and Evans, H.R. (1975), "The Collapse Behavior of Plate Girders Loaded in Shear," *The Structural Engineer*, Vol. 53, No. 8, August, London, England.

Rezai, M. (1999), "Seismic Behaviour of Steel Plate Shear Walls by Shake Table Testing," PhD Dissertation, Department of Civil Engineering, University of British Columbia, Vancouver, Canada.

Rezai, M., Ventura, C. E., and Prion, H.G.L. (2000), "Numerical Investigation of Thin Unstiffened Steel Plate Shear Walls," *Proceedings of the12th World Conference on Earthquake Engineering*, Aukland, New Zealand, February.

Roberts, T.M. and Sabouri-Ghomi, S. (1992), "Hysteretic Characteristics of Unstiffened Perforated Steel Plate Shear Walls," *Thin-Walled Structures,* Vol. 14, No. 2, pp. 139–151

Roberts, T.M. and Sabouri-Ghomi, S. (1991), "Hysteretic Characteristics of Unstiffened Plate Shear Panels," *Thin-Walled Structures*, Vol. 12, No. 2, pp. 145–162.

Roberts, T.M. and Shahabian, F. (2001), "Ultimate Resistance of Slender Web Panels to Combined Bending, Shear and Patch Loading," *Journal of Constructional Steel Research,* Vol. 57, pp. 779–790.

Robinson, K. and Ames, D. (2000), "Steel Plate Shear Walls—Library Seismic Upgrade," *Modern Steel Construction*, Vol. 40, No. 1, pp. 56–60.

Ruddy, J.L., Marlow, J.P., Ioannides, S.A., and Alfawakhiri, F. (2003), AISC Design Guide No. 19, *Fire Resistance of Structural Steel Framing*, AISC, Chicago, IL.

Sabouri-Ghomi, S. and Roberts, T.M. (1992), "Nonlinear Dynamic Analysis of Steel Plate Shear Walls Including Shear and Bending Deformations," *Engineering Structures*, Vol. 14, No. 5, pp. 309–317.

Schumacher, A., Grondin, G.Y., and Kulak, G.L. (1999), "Connection of Infill Panels in steel Plate Shear Walls," *Canadian Journal of Civil Engineering,* NRC Research Press, Vol. 26, No. 5, pp. 549–563.

Schumacher, A., Grondin, G.Y., and Kulak, G.L. (1997), "Connection of Infill Panels in Steel Plate Shear Walls," *Structural Engineering Report No. 217*, Department of Civil and Environmental Engineering, University of Alberta, Edmonton, Alberta, Canada.

Seilie, I.F., Hooper, J. (2005), "Steel Plate Shear Walls: Practical Design and Construction," *Modern Steel Construction*, Vol. 45, No. 4, pp. 37–43.

Shishkin, J.J., Driver, R.G., and Grondin, G.Y. (2005), "Analysis of Steel Plate Shear Walls Using Conventional Engineering Software," *Proceedings of the 33rd Annual General Conference of the Canadian Society for Civil Engineering*, Toronto, Ontario, June 2–4.

Sugii, K. and Timler, P. A. (1988), "Design Procedures Development, Analytical Verification and Cost Evaluation of Steel Plate Shear Wall Structures," *Technical Report No. 98-01*, Earthquake Engineering Research Facility, Department of Civil Engineering, University of British Columbia, Canada.

Sugii, K. and Yamada, M. (1996), "Steel Panel Shear Walls With and Without Concrete Covering," *Proceedings of the 11th World Conference on Earthquake Engineering*, Acapulco, Mexico, Paper No. 403.

Takahashi, Y., Takemoto, Y., Takeda, T., and Takagi, M. (1973), "Experimental Study on Thin Steel Shear Walls and Particular Bracings Under Alternative Horizontal Load," *Preliminary Report, IABSE Symposium on Resistance and Ultimate Deformability of Structures Acted on by Well Defined Repeated Loads*, Lisbon, Portugal, pp. 185–191.

Thorburn, L.J., Kulak, G.L., and Montgomery, C.J. (1983), "Analysis of Steel Plate Shear Walls," *Structural Engineering Report No. 107*, Department of Civil Engineering, University of Alberta, Edmonton, Alberta, Canada.

Timler, P.A. (1988), "Design Procedures Development, Analytical Verification and Cost Evaluation of Steel Plate Shear Wall Structures," *Technical Report No. 98-01*, Earthquake Engineering Research, Facility, Department of Civil Engineering, University of British Columbia, Canada.

Timler P.A. and Kulak G.L. (1983), "Experimental Study of Steel Plate Shear Walls," *Structural Engineering Report No. 114*, Department of Civil Engineering, University of Alberta, Edmonton, Alberta, Canada.

Timler, P.A. and Ventura, C.E. (1999), "Economical Design of Steel Plate Shear Walls from a Consulting Engineer's Perspective," *Proceedings of the North American Steel Construction Conference*, Toronto, Canada, pp. 36-1–36-18.

Timler, P.A., Ventura, C.E., Prion, H., and Anjam R. (1998), "Experimental and Analytical Studies of Steel Plate Shear Walls as Applied to the Design of Tall Buildings," *The Structural Design of Tall Buildings,* Vol. 7, No. 3, pp. 233–249.

Timoshenko, S. and Woinowsky-Krieger, S. (1959), *Theory of Plates and Shells*, 2nd ed., McGraw-Hill, New York.

Tromposch, E.W. and Kulak, G.L. (1987), "Cyclic and Static Behaviour of Thin Panel Steel Plate Shear Walls," *Structural Engineering Report No. 145*, Department of Civil Engineering, University of Alberta, Edmonton, Alberta, Canada.

Troy, R.G. and Richard, R.M. (1988), "Steel Plate Shear Walls," *Engineering Review*, No. 1, pp. 35–39.

Vian, D. and Bruneau, M. (2004), "Testing of Special LYS Steel Plate Shear Walls," *Proceedings of the 13th World Conference on Earthquake Engineering*, Vancouver, British Columbia, Canada, Paper No. 978.

West, M.A. and Fisher, J.M. (2003), AISC Design Guide No. 3, *Serviceability Design Considerations for Steel Buildings*, Second Edition, AISC, Chicago, IL.

Wagner, H. (1931), "Flat Sheet Metal Girders with Very Thin Metal Webs, Part I—General Theories and Assumptions," *Technical Memo. No. 604*, National Advisory Committee for Aeronautics.

Wosser, T.D. and Poland, C.D. (2003), "Degenkolb Engineers," *Journal of Structural Design of Tall and Special Buildings*, Vol. 12, pp. 227–244.

Xue, M. and Lu, L.W. (1994), "Interaction of Infilled Steel Shear Wall Panels with Surrounding Frame Members," *Proceedings of the Structural Stability Research Council Annual Technical Session,* Bethlehem, PA, pp. 339–354.

Yamaguchi, T., et al. (1998), "Seismic Control Devices Using Low-Yield-Point Steel," *Nippon Steel Technical Report No. 77,* pp. 65–72, (available at http://www.nsc.co.jp/gikai/en/contenthtml/n78 /n78.html).

Yang, T.Y. and Whittiker, A. (2002), "MCEER Demonstration Hospitals—Mathematical Models and Preliminary Results," *Technical Report*, Multidisciplinary Center for Earthquake Engineering Research, University at Buffalo, Buffalo, NY.

Yokoyama, T., Kajiyama, Y., and Komuro, H. (1978), *Structural Scheme of Nippon Building B-Wing*, (in Japanese).

Zhao, Q. and Astaneh-Asl, A. (2002), "Cyclic Tests of Steel Shear Walls," *Report Number UCB/CE-Steel-2002-01*, Department of Civil and Environmental Engineering, University of California, Berkeley.